THE SYNTHESIS, CHARACTERIZATION, AND ANALYSIS OF POLYNORBORNENES CONTAINING VARIOUS ORGANOMETALLIC SPECIES

A Thesis

submitted to the Graduate Faculty

in Partial Fulfilment of the Requirements

for the Degree of Master of Science

Molecular and Macromolecular Sciences

Department of Chemistry

Faculty of Science

University of Prince Edward Island

Christopher L. Rock

Charlottetown, Prince Edward Island

May 2013

CONDITIONS FOR THE USE OF THE THESIS

The author has agreed that the Library, University of Prince Edward Island, may make this thesis freely available for inspection. Moreover, the author has agreed that permission for extensive copying of this thesis for scholarly purposes may be granted by the professor or professors who supervised the thesis work recorded herein or, in their absence, by the Chair of the Department or the Dean of the Faculty in which the thesis work was done. It is understood that due recognition will be given to the author of this thesis and to the University of Prince Edward Island in any use of the material in this thesis. Copying or publication or any other use of the thesis for financial gain without approval by the University of Prince Edward Island and the authors' written permission is prohibited.

Requests for permission to copy or to make any other use of material in this thesis in whole or in part should be addressed to:

Nola Etkin
Chair of the Department of Chemistry
Faculty of Science
University of Prince Edward Island
550 University Avenue, Charlottetown, PE
Canada C1A 4P3

PERMISSION TO USE POSTGRADUATE THESIS

Title of thesis: THE SYNTHESIS, CHARACTERIZATION, AND ANALYSIS OF POLYNORBORNENES CONTAINING VARIOUS ORGANOMETALLIC SPECIES

Name of Author: Christopher L. Rock

Department: Chemistry

Degree: Master of Science Year: 2013

In presenting this thesis in partial fulfillment of the requirements for a postgraduate degree from the University of Prince Edward Island, I agree that the Libraries of this University may make this thesis freely available for inspection and give permission to add an electronic version of the thesis to the Digital Repository at the University of Prince Edward Island. Moreover the author agrees that permission for extensive copying of this thesis for scholarly purposes may be granted by the professor or professors who supervised my thesis work, or, in their absence, by the Chair of the Department or the Dean of the Faculty in which my thesis work was done. It is understood any copying or publication or use of this thesis or parts thereof for financial gain shall not be allowed without my written permission. It is also understood that due recognition shall be given to me and to the University of Prince Edward Island in any scholarly use which may be made of any material in my thesis.

Signature: _____

Date: July 31st, 2013

University of Prince Edward Island

Faculty of Science

Charlottetown

CERTIFICATION OF THESIS WORK

We, the undersigned, certify that Christopher Rock, BSc, candidate for the degree of Master of Science has presented a thesis with the following title: "The synthesis, characterization, and analysis of polynorbornenes containing various organometallic species", that the thesis is acceptable in form and content, and that a satisfactory knowledge of the field covered by the thesis was demonstrated by the candidate through an oral examination held on July 29, 2013.

Examiners: Dr Alaa Abd-El-Aziz _____

Dr Nola Etkin _____

Dr Brian Wagner _____

Dr Rabin Bissessur _____

Dr Charles Carragher _____

Dr Russ Kerr – Chair _____

Date _____

Abstract

This thesis describes the synthetic strategies for the incorporation of a number of metal species into a series of polynorbornenes, as well as their characterization and thermal analysis. This was accomplished through the synthesis of new monometallic norbornene compounds containing chromium and iron, which was either neutral or cationic, as well as new bimetallic norbornenes containing chromium and cobalt in addition to neutral iron. A series of polymers were developed using Grubbs' 2nd generation catalyst and their thermal properties determined. From there, these properties were compared to a series of copolymers and block copolymers, which were synthesized using the same norbornene structure that was utilized for the homopolymers. All compounds and polymers were characterized utilizing a combination of ^{1}H NMR, ^{13}C NMR, several two dimensional NMR techniques, solid state NMR, and scanning electron microscopy. The molecular weight of the polymer synthesised in Chapter Four was determined through GPC, which was not possible for the other polymers due to insolubility. Thermal properties were determined through TGA and DSC. Further work in this area would include conversion of these materials into ceramics and a series of mechanical, conductive, and magnetic tests on both the polymers and the ceramics formed. Additional work would also explore varying the ratio of metals in the copolymers, as well as introducing other metals into the materials.

Acknowledgements

I must begin by thanking my supervisor of the past 4 years, Dr. Abd-El-Aziz, for the amazing opportunity that he has given me and all of the unwavering support that he has provided. I am especially glad that he was so supportive and encouraging during the whole process behind transferring to UPEI. Thank you to my co-supervisor, Dr. Etkin, who got me acclimated to the lab and the department, as well as Dr. Bissessur and Dr. Wagner. Thank you to Steven Scully for all his help with the NMR, Dr. Lacroix for his help with SEM, Dr. Patrick at UBC for running the X-ray crystallography, Dr. Werner-Zwanzinger at Dalhousie for the solid state NMR, Dr. Stephan at the University of Toronto for the GPC data, and Michael Cowper for his help with the thermal analysis.

Extra special thank you to all of the current and prior members of all of the lab groups at both UBC and UPEI (Michael, Inan, Jessica, Liz, Mason, Sibel, Sapphire, Diana, Patrick, Cory, Roger, Jordan, Lydia, Wen, and Addison) for all the fun times, encouragement, help, and advice, plus all the professors at UBC-O (Steve, Kevin, and Paul in particular) for the grand journey that was my undergraduate experience. Thank you for preparing me for this degree and the next.

Outside of school, I need to thank all the awesome people who kept me sane during the whole process, whether it was at football, taekwon-do, jiu-jitsu, or whatever, especially the islanders who made me feel so welcome.

Finally, I need to thank my family, who made all of this possible. I cannot describe what it means to have you and for you to be there to support my dreams, no matter what.

They'll tell you 'failure is not an option'

That is ridiculous

Failure is always an option

Failure is the most readily available option at all times

But it's a choice

You can choose to fail

Or you can choose to succeed

~Chael Sonnen~

Table of Contents

List of Schemes

List of Figures

List of Tables

List of Symbols and Abbreviations

°C	degrees Celsius
^{13}C NMR	carbon-13 nuclear magnetic resonance spectroscopy
^{1}H NMR	proton nuclear magnetic resonance spectroscopy
2D	two dimensional
COSY	correlation spectroscopy
Cp	cyclopentadienyl ring
Cy	cyclohexane
cm	centimetres
δ	NMR chemical shift in parts per million downfield from a standard
d	doublet
d_6	6 deuterium atoms
DCC	N,N'-dicyclohexylcarbodiimide
DCM	dichloromethane
DCU	dicyclohexylurea
dd	doublet of doublets
DI	deionized
DMAP	4-dimethylaminopyridine
DMF	N,N'-dimethylformamide
dt	doublet of triplets
g	grams
HSQC	heteronuclear single bond quantum coherence spectroscopy
Hz	Hertz (s^{-1})

J	coupling constant (in spectroscopy, Hz)
L	litre
M	molar (mol/L)
m	multiplet
Mes	mesitylene
min.	minute
mL	millilitre
mmol	millimoles
M_w	molecular weight
N_2	nitrogen gas
NMR	nuclear magnetic resonance
Nu	nucleophile
ORTEP	oak ridge thermal elipsoid plot
PDI	polydispersity index
ppm	parts per million
q	quartet
ROMP	ring opening metathesis polymerization
rt	room temperature
s	singlet
t	triplet
THF	tetrahydrofuran

Chapter One: Introduction

1.1 Scope of present work

This thesis discusses the incorporation of metals into polynorbornenes. Chapter Two focuses on the development of three monometallic polynorbornenes, each containing a different metal atom or ion. Chapter Three focuses on the copolymerization of those three monomers, using a number of combinations of the monomers and techniques for combination. Chapter Four focuses on the development of a chromium-iron bimetallic monomer and its polymerization. The purpose of developing these compounds is to create materials with a high metal content, in order to determine their possible magnetic or conductive properties. It would then be possible for these compounds to be utilized as precursors to ceramics or metallic nanoparticles.

1.2 Ferrocene

Initially synthesized in 1951, ferrocene became the first of a classification of compounds to exhibit a "sandwich structure" (Figure 1.1), with aromatic rings bound through multiple atoms in the planes both above and below the metal centre[1,2]. Speculation as to the exact structure of this compound was ended with complete structural characterization in 1952[2,3].

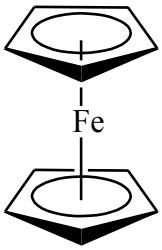

Figure 1.1: The structure of ferrocene.

One of the most interesting characteristics of ferrocene is its ability to undergo a number of different reactions on the cyclopentadienyl (Cp) rings, similar to metal-free organic aromatics, without disturbing the overall structure.

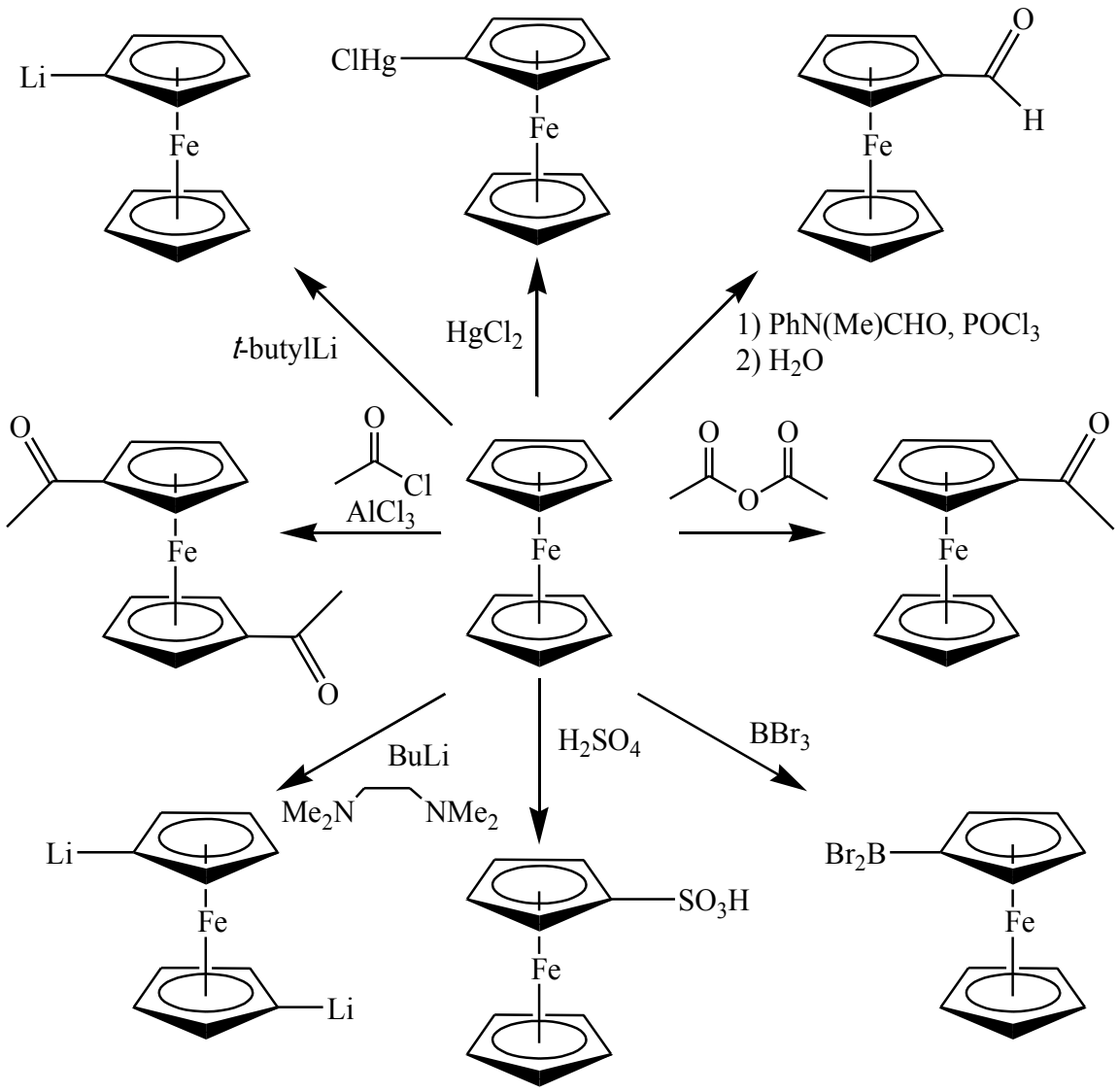

Figure 1.2: Selected reactions of ferrocene[4-7].

This ability to undergo a large variety of functionalizations has allowed ferrocene to be incorporated into many larger molecules, without the need for advanced organometallic chemical reactions[2,3]. The first ferrocene containing polymer was developed by Arimoto and Haven via vinyl ferrocene in 1955[8]. Since then, there have been many examples of ferrocene being incorporated into polymeric materials in both the backbone and the side

chain[9-11]. This work has been undertaken due to ferrocene's relative thermal stability, as well as its ability to stand up to many different forms of radiation[1,8,10,12]. Additionally, with ferrocene being diamagnetic, characterization of any materials containing it can be performed very simply through standard nuclear magnetic resonance (NMR) techniques.

1.3 η^6-arene- η^5-cyclopentadienyl iron(II)

A considerable amount of work performed by the Abd-El-Aziz group has focused on the use of an η^6-arene- η^5-cyclopentadienyl iron(II) hexafluorophosphate, due to its ability to activate the arene towards further substitution, which is significantly more difficult when working with the metal free analogues[13-34]. These compounds can be synthesized through a simple ligand exchange of ferrocene, where a single Cp ring can be replaced with an arene with a number of different functional groups attached. This was first accomplished by Nesmeyanov in 1963 utilizing aluminum chloride in the presence of aluminum powder, which prevents the oxidation of the ferrocene[35]. Depending on the arene used, these reactions can be done neat but decalin is the solvent of choice when this is not possible.

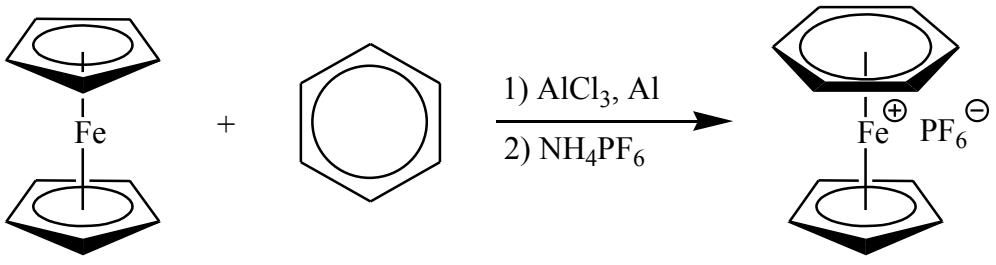

Figure 1.3: Ligand exchange of ferrocene with benzene to form η^6-benzene- η^5-cyclopentadienyl iron(II) hexafluorophosphate.

The use of halogenated arenes in this reaction allows for further reactivity of the compounds, through the use of metal-mediated nucleophilic aromatic substitution reactions.

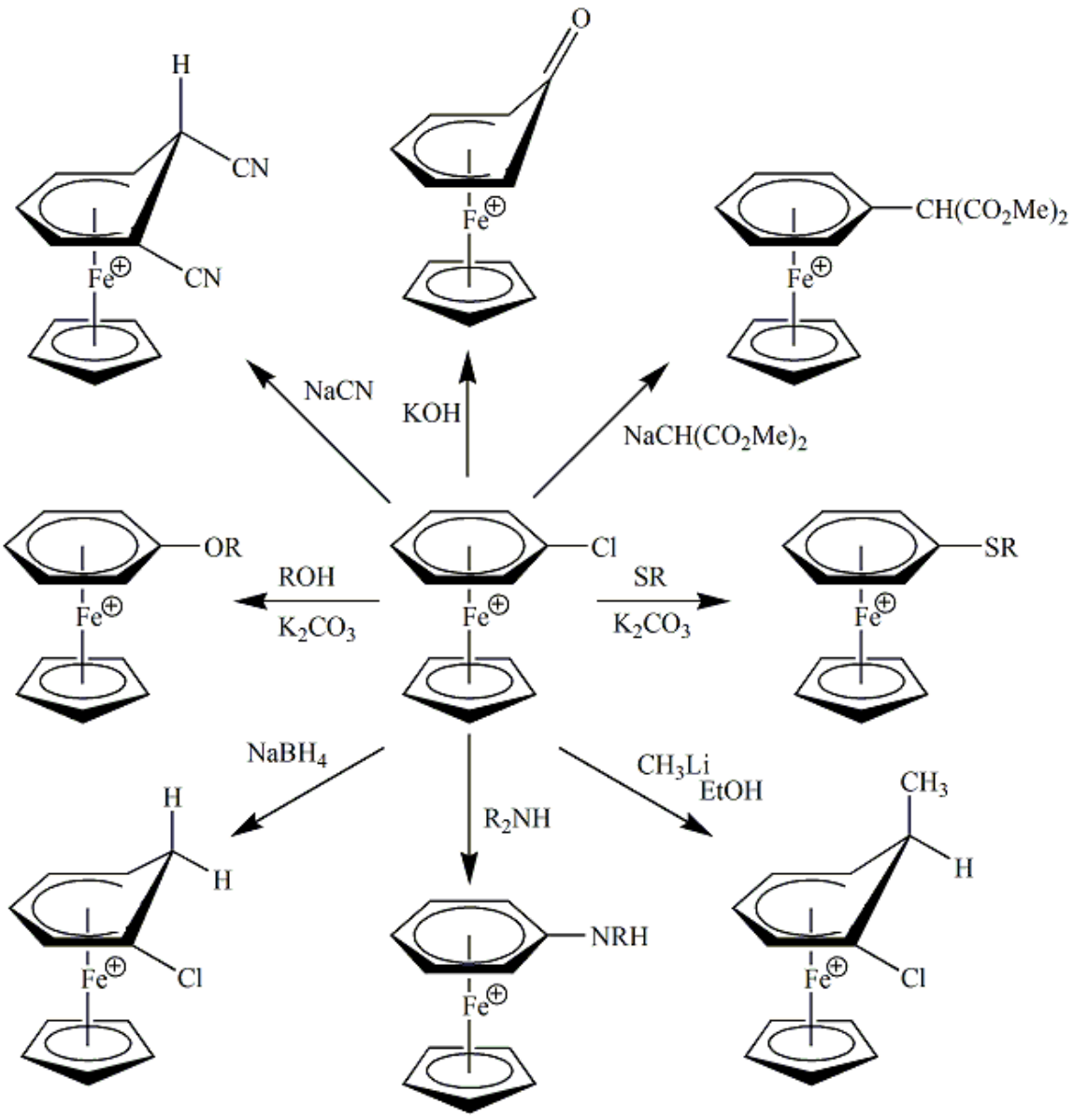

Figure 1.4: Examples of the reactivity of the η^6-benzene- η^5-cyclopentadienyl iron(II) with various nucleophiles[6].

The ability of these complexes to undergo substitution is a direct result of the electron withdrawing ability of the bound metal, which activates the halogen towards substitution[36,37]. The mechanism of this reaction is shown in Figure 1.5, where the reaction is assisted through the addition of a weak, non-nucleophilic base such as potassium carbonate.

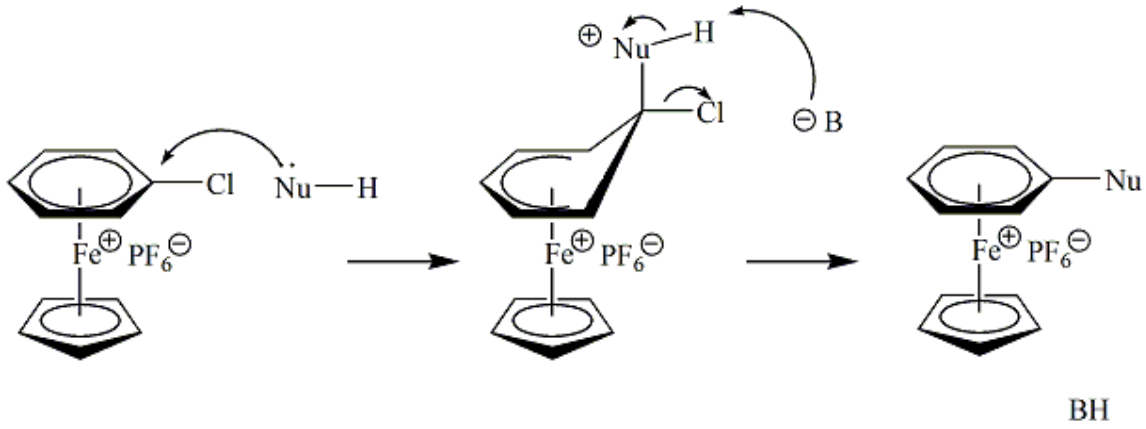

Figure 1.5: Mechanism of nucleophilic substitution of η^6-chlorobenzene- η^5-cyclopentadienyl iron(II)[6].

As with ferrocene, the cationic iron species is diamagnetic, allowing for easy characterization through standard NMR techniques[15]. However, this type of compound does pose other challenges, as it is incapable of withstanding column chromatography on silica gel, resulting in the decomposition of the material, which precludes this as a possible technique for purification[38]. Additionally, these compounds show some instability towards heat and light, producing the need for greater caution during synthesis and purification.

1.4 η^6-arene chromium tricarbonyls

The first direct synthesis of an η^6-arene chromium tricarbonyl directly from the metal carbonyl and a free arene was performed in 1958[39-41]. These early reactions were performed in refluxing diglyme or decalin, high boiling point solvents that would not interact with either of the reagents, similar to the Nesmeyanov reaction for the synthesis of the cationic iron complex (Figure 1.3). Since this time, there have been repeated attempts to improve on this basic reaction, as it typically would need high temperatures for extended periods of time in order to produce significant yields. Increased yields have been found when a modification to the metal carbonyl was performed, with replacing three of the carbonyl ligands with other ligands such as pyridine[42] or acetonitrile[43], as they are more labile under arene coordination reaction conditions. One of the most successful methods used an η^6-naphthalene ligand as a chromium tricarbonyl transfer agent, as it would sublime during the reaction[44,45]. Additionally, the use of higher boiling point ethers was explored, with *n*-butyl ether or dioxane, along with a small amount of THF, becoming the solvent system of choice[46-48].

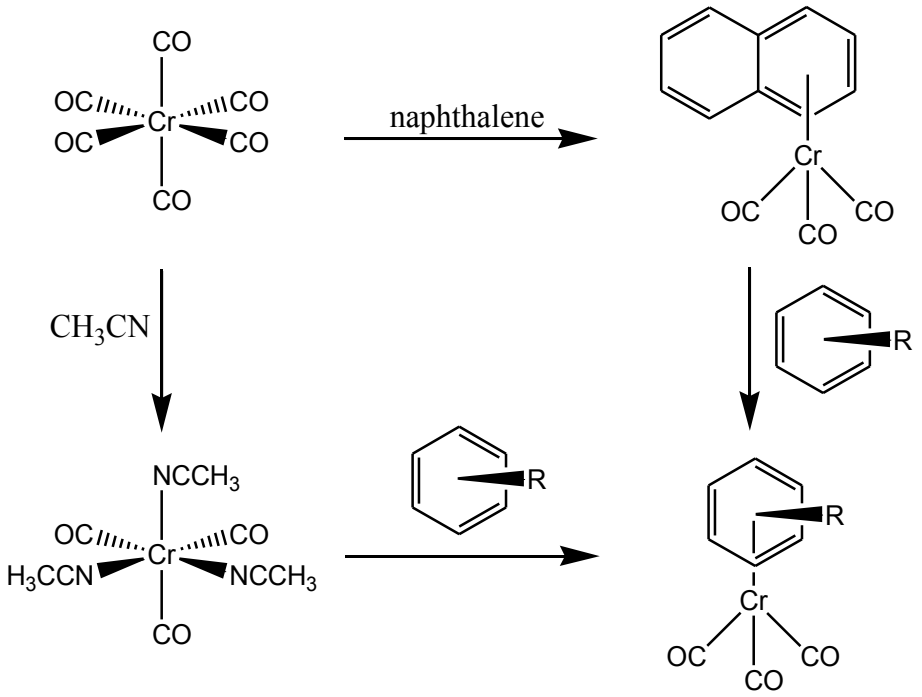

Figure 1.6: Alternate routes for the synthesis of an η^6-arene chromium tricarbonyl.

It has been shown that coordination of a large variety of substituted arenes, including those containing functional groups such as amines[49,50], alcohols[51], aldehydes[52,53], or even ferrocene[54] directly bound to the arene, are possible under these reaction conditions. The chromium tricarbonyl moiety shows sensitivity to oxidizing reagents but can withstand a large variety of reaction conditions, making it very useful for integration into larger compounds.

1.5 Norbornenes and ring opening metathesis polymerization

Norbornene, or bicyclo[2.2.1]hept-2-ene, is a highly strained bicyclic compound that is often used to form polymeric materials. It is a useful system due to its ability to undergo polymerization via a number of different mechanisms: radical, cationic, vinyl, or ring

opening polymerization[55]. Each type causes different properties to be exhibited in the resulting materials.

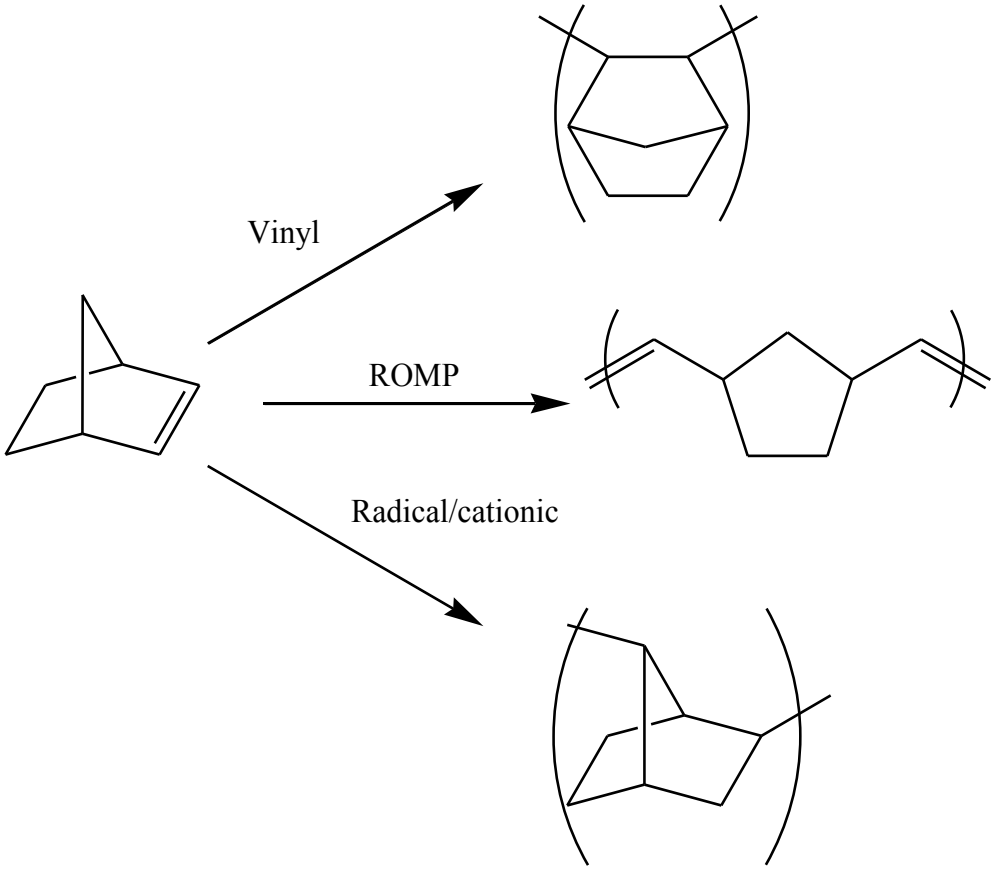

Figure 1.7: Different reaction types for producing polynorbornenes.

This thesis focuses on the use of ring-opening metathesis polymerization (ROMP) due to its ability to be highly controlled, its well understood mechanism, and its lack of interaction with other functional groups present in the compounds. The ROMP reaction mechanism involves the formation of a metalocyclobutane ring via the [2+2] interaction between the metal alkylidene and the norbornene alkene. As seen in Scheme 1.1, the polymer chain is propagated *via* the formation of a new metal alkylidene with the first group attached.

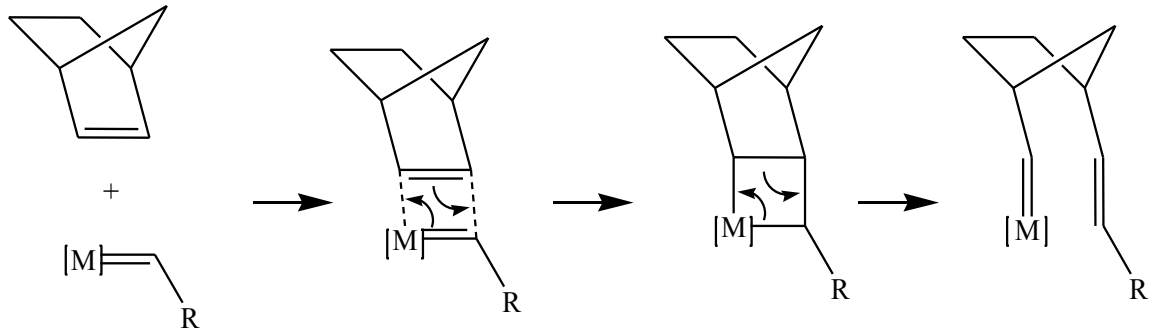

Scheme 1.1: Mechanism for ROMP.

Catalysts capable of performing this type of reaction are typically capable of performing other metathesis type reactions, such as ring closing metathesis and cross metathesis. To prevent these from occurring after the completion of the chain propagation, a vinyl ether is added to the reaction, which is itself partially incorporated into the polymer, resulting in an end-cap, as well as converting the metathesis active alkylidene into an inactive carbene[56].

There are a number of different ROMP catalysts available, based on either ruthenium, molybdenum, or tungsten[57]. This thesis works exclusively with the ruthenium based Grubbs' 2nd generation catalyst, which has been proven to have high functional group tolerance[58] and the capability of polymerizing norbornenes containing carboxylic acids[59], amino acids[60], esters[13,14], and ethers, among other groups[61,62].

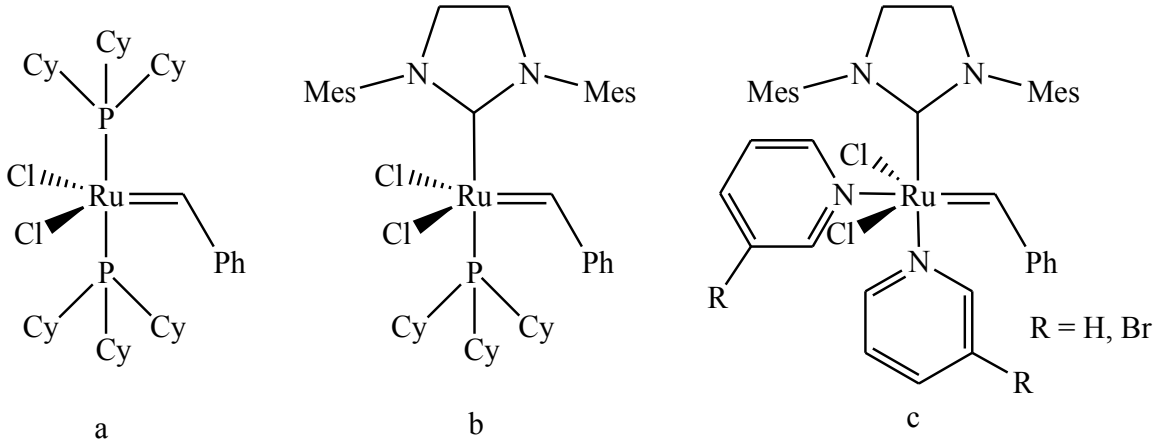

Figure 1.8: Grubbs' Catalysts a) 1st b) 2nd c) 3rd.

1.6 Metal containing polymers

Some of the earliest metal containing polymers were reported in the 1930's[63,64]. The majority of this early work focused on coordination polymers until the characterization of ferrocene in 1952[2,3]. This led to the creation of a new branch of chemistry, organo-transiton metal polymers. The polymerization of vinyl ferrocene was first reported in 1955 by Arimoto and Haven[65]. Subsequent work was undertaken in this area in the 1960's and 1970's by Hayes, George[66-68], Pittman[69], and Carraher. Pittman and Carraher in particular worked extensively to include a large variety of transition metals into polymers, including manganese, chromium, tungsten, cobalt, zirconium, hafnium, tin, and lead[70-87]. Work done by Manners in the late 1990's utilized ring opening polymerization of metallocenophanes[88-90] to form a new ferrocene-silicon copolymer. The Abd-El-Aziz group began work in the incorporation of the η^6-arene- η^5-cyclopentadienyl iron(II) moiety described in Section 1.3 into polymers. This was

initially done through condensation polymerization reactions[14,27], which incorporate the metal into the backbone of the polymer. Subsequently, this resulted in the development of polymers with the metal species contained in the side chain[17,21,23,28], which was typically performed through the polymerization of one of two groups: a methacrylate or a norbornene. Continuing work in this area has led to the development of a series of bimetallic polymers that include cobalt in addition to either the ferrocene or cationic iron species. This was accomplished through the binding of dicobalt octacarbonyl across the pi-system of a triple bond[33,34]. Compounds of this nature have been converted into ceramics by Tang and have shown interesting magnetic properties[91].

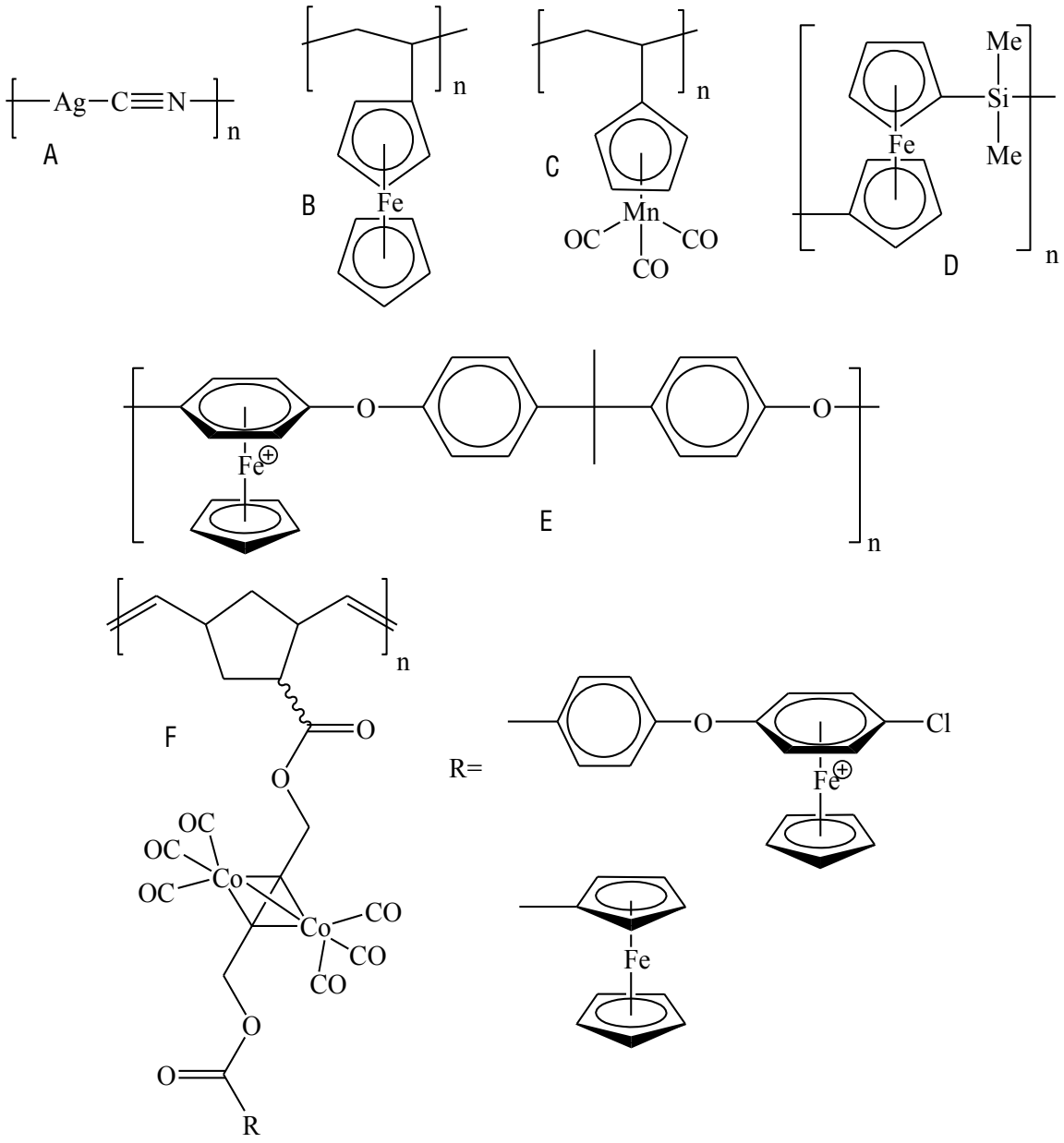

Figure 1.9: A brief history of organometallic polymers by A) West B) Arimoto and Haven C) Pittman D) Manners E-F) Abd-El-Aziz.

1.7 Materials and Instrumentation

All materials were purchased from Sigma-Aldrich, Alfa Aesar, or Fisher Scientific and used without further purification. All solvents were HPLC grade. Unless otherwise noted, all NMR was collected on a Bruker Advance Spectrometer with a gradient field probe at 300 MHz for ^{1}H and 75 MHz for ^{13}C. All spectra are references to residual solvents, reported in ppm, and coupling constants are reported in Hz. Thermogravimetric analysis was performed at high resolution on a TA Instruments TGAQ500 with a heating rate of 10 °C/min and the gas flow (either N_2 or air) was 60 mL/min. Differential scanning calorimetry was performed on a TA Instruments DSCQ100 with a heating rate of 10 °C/min with a 50 mL/min. flow of nitrogen. Scanning electron microscopy was performed on a Hitachi TM3000 SEM and the samples were coated with a 300 Å layer of gold/palladium using a Denton Desk II Cold Sputter via a 40 mA current for 75 seconds in order to facilitate electron beam focusing. Solid state NMR was performed at Dalhousie University on a Bruker Advance NMR spectrometer using a probe head for rotors of a 4 mm diameter at 100 MHz for ^{13}C by Dr. Ulrike Werner-Zwanzinger. Full experimental conditions are included in the appendix. Gel permeation chromatography was performed at the University of Toronto on a series of three 7.8 x 300 mm Waters Styragel HR SE THF columns with a Waters 2707 Autosampler and a Waters 2414 Refractive Index Detector by Dr. Doug Stephen.

2.1 **Synthesis of η^6-arene-η^5-cyclopentadienyl iron(II) containing polynorbornenes**

The first step in the synthesis of a norbornene containing the η^6-arene-η^5-cyclopentadienyl iron(II) species is to perform a ligand exchange on ferrocene. Chlorobenzene was chosen as it has only a single site at which nucleophilic substitution can occur, despite requiring a slightly longer and higher temperature reaction in order to displace the chlorine[34]. As with most chlorinated arenes for this reaction, chlorobenzene also acted as the solvent and 2.3 was formed using previously published methods[36].

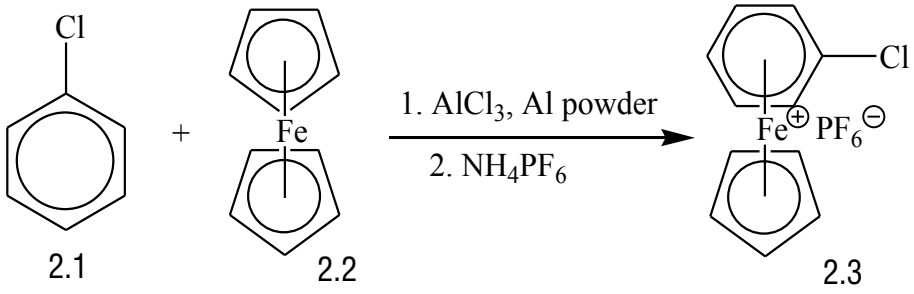

Scheme 2.1: Synthesis of 2.3.

As shown previously, these compounds can undergo nucleophilic substitution in the presence of aromatic alcohols. This reaction is also assisted by the presence of the non-nucleophilic base, K_2CO_3, which facilitates the deprotonation of the alcohols. As seen in Scheme 2.2, it is possible to substitute the chlorine with 4-hydroxybenzyl alcohol, performed through the modification of literature procedures[29].

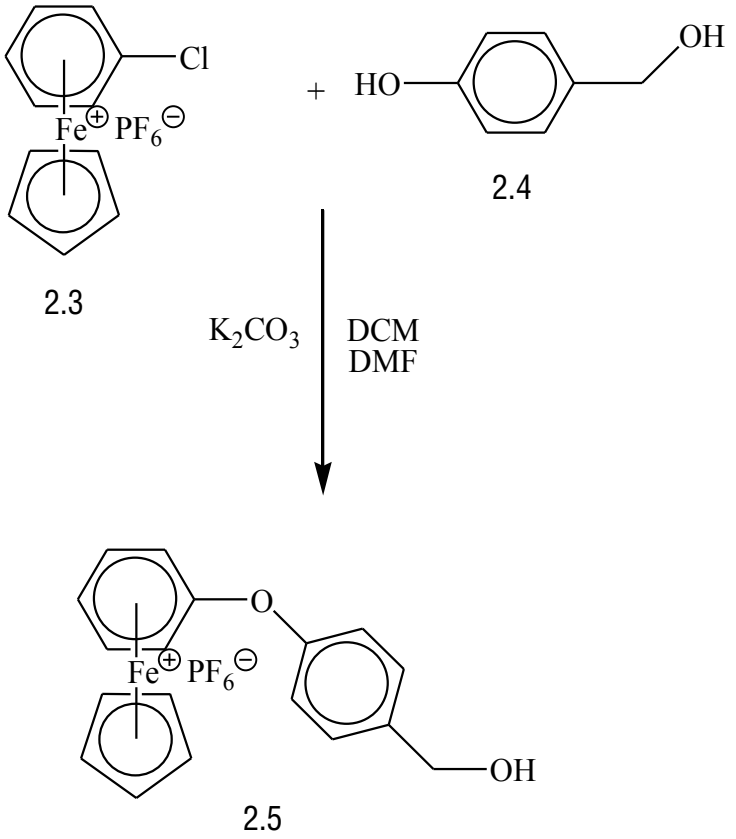

Scheme 2.2: Nucleophilic substitution to form 2.5.

The ^{1}H NMR of 2.5 shows the incorporation of the new, metal free arenes clearly at 7.56 and 7.34 ppm. It can be seen that there is no reaction between 2.3 and the benzylic position alcohol, based on its lack of an upfield shift of the benzylic protons, as well as their continued coupling to the alcohol proton.

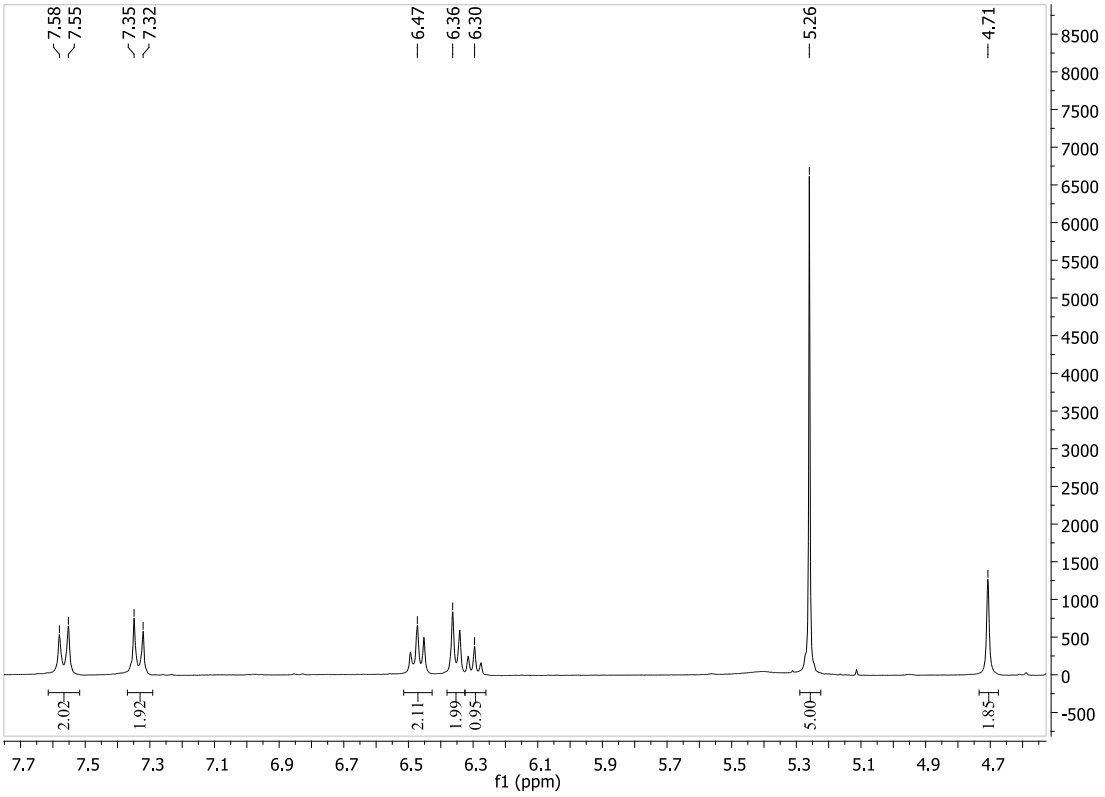

Figure 2.1: Portion of the ^{1}H NMR spectrum of 2.5.

From here, it is now possible to react the free alcohol with the carboxylic acid of 5-norbornene-2-carboxylic acid (2.6). This esterification was accomplished using N,N'-dicyclohexylcarbodiimide (DCC) and 4-dimethylaminopyride (DMAP), a non-nucleophilic nitrogen base. Reagents of this type were first utilized by Steglich in 1978 and for the purpose of simplicity, this reaction will be referred to as a Steglich esterification[92]. One of the most notable features of this reaction is the formation of dicyclohexyl urea (DCU) as a by-product. This white solid is partially soluble in most solvents but will crystallize out of solution at low temperatures, allowing for removal *via* simple filtration, although this step may need to be repeated several times.

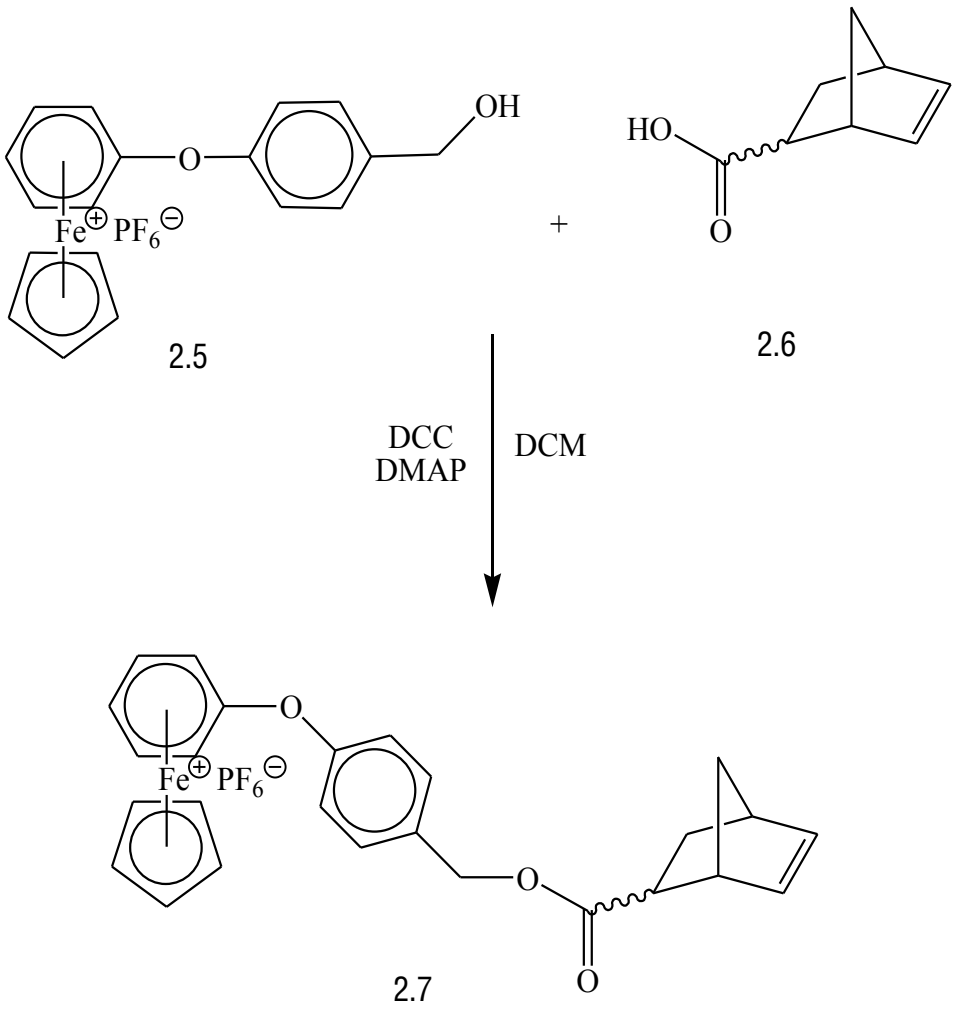

Scheme 2.3: Steglich esterification to form 2.7.

Successful incorporation of the norbornene is evidenced by the appearance of the olefinic protons at 6 ppm. It can also be seen that, based on the integration of these signals, there is an approximately 2:1 ratio of isomers within the sample, with the *endo* form being the more predominant. There is also an upfield shift of the benzylic protons as a result of the formation of an ester, as well as the formation of two signals due to the two isomeric forms present (Figure 2.2)

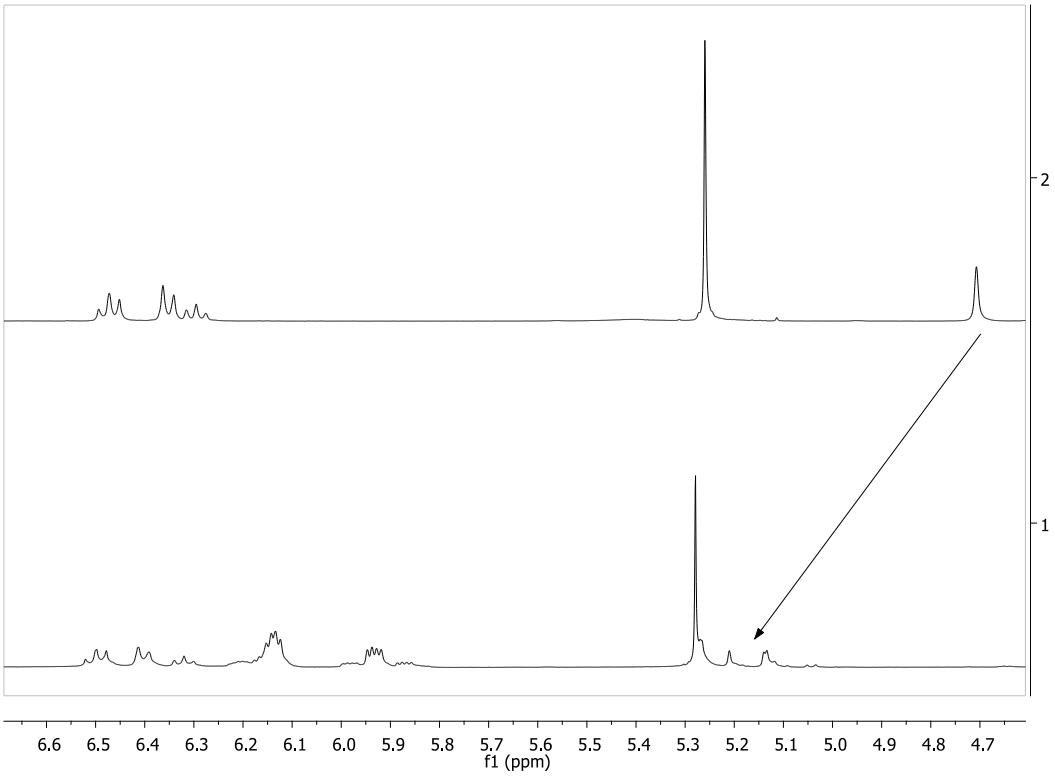

Figure 2.2: ^{1}H NMR of 2.5 (top) and 2.7 (bottom), showing the upfield shift and dual signals in the benzylic position as a result of esterification.

In order to simplify the assignment of NMR signals, a single isomeric form of 2.7 was synthesized. The simplest method for doing this was the removal of the *endo* isomer of 2.6 through an iodolactionization reaction and then performing an esterification with 2.5[93]. This allowed for the full assignment of signals for the single isomer.

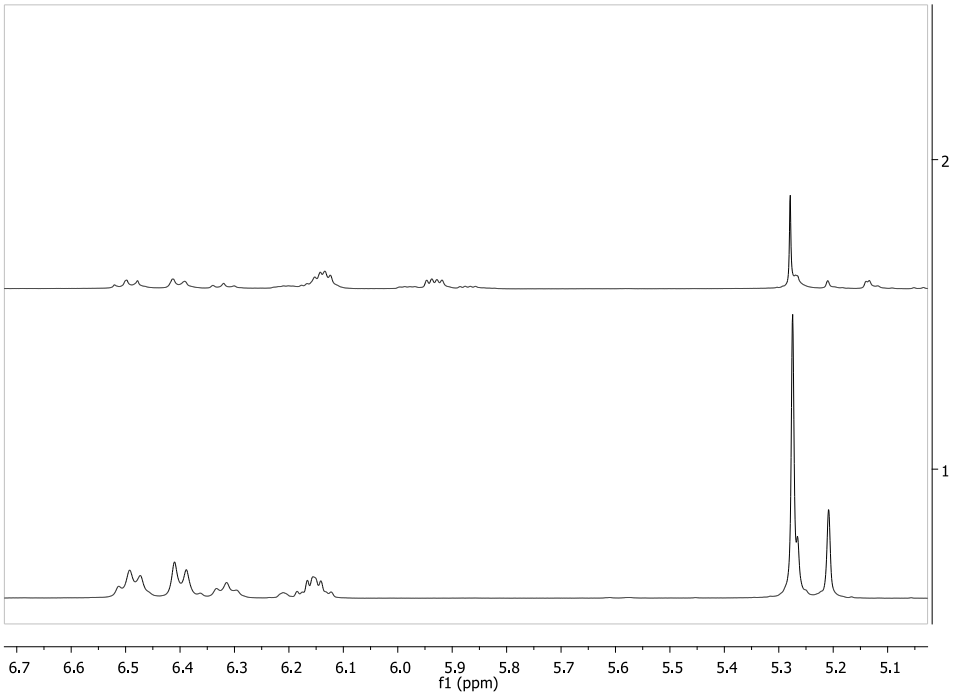

Figure 2.3: Section of the ^{1}H NMR of 2.7 (top) and 2.7-*exo* (bottom).

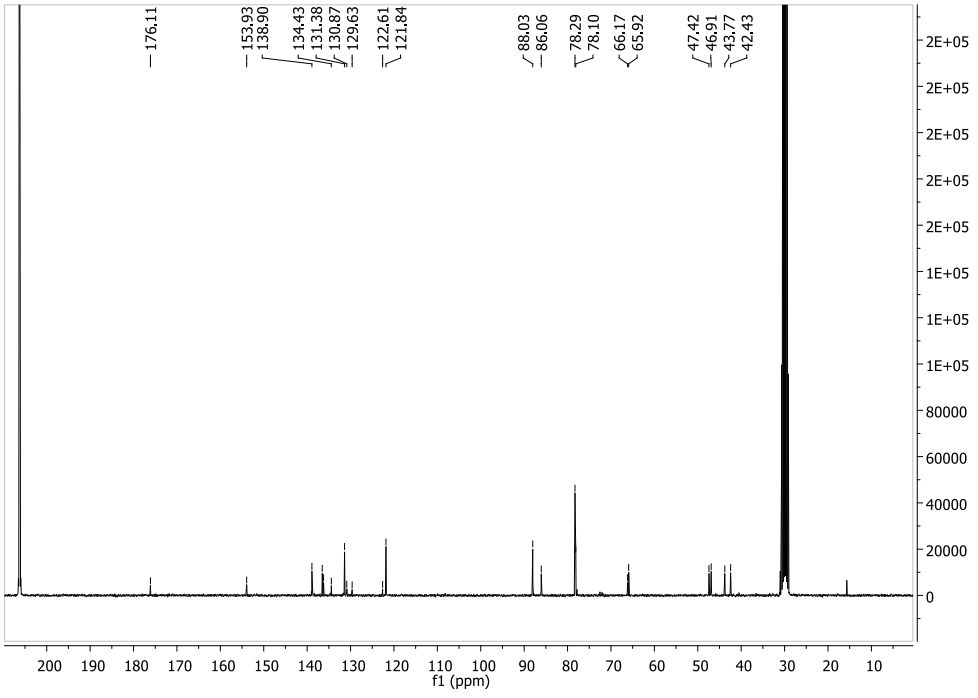

Figure 2.4: ^{13}C NMR of 2.7-*exo*.

Full signal assignment for 2.7-*exo* was accomplished through both COSY and HSQC NMR.

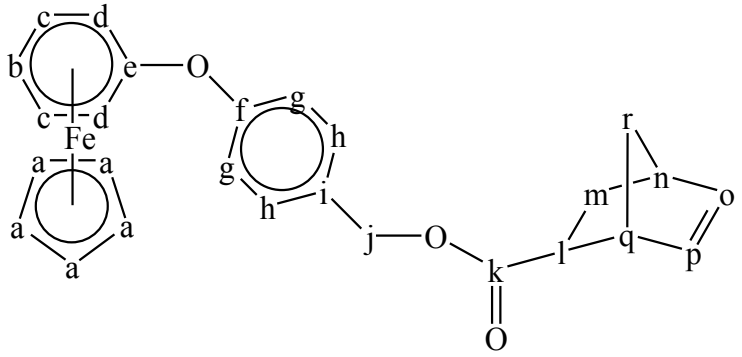

Figure 2.5: Atom labels for 2.7-*exo*. Charges and the counter anion were omitted for clarity.

Table 2.1: NMR assignments for *2.7-exo*.

Label	^{1}H NMR δ	^{13}C NMR δ
a	5,27	78.3
b	6.32	86.1
c	6.40	78.1
d	6.49	88.3
e	-	153.9
f	-	136.2
g	7.39	121.8
h	7.62	131.4
i	-	134.4
j	5.21	65.9
k	-	176.1
l	1.95	31.0
m	2.29	43.8
n	2.95	42.4
o	6.15	136.5
p	6.15	138.9
q	3.05	47.4
r	1.56-1.28	46.9

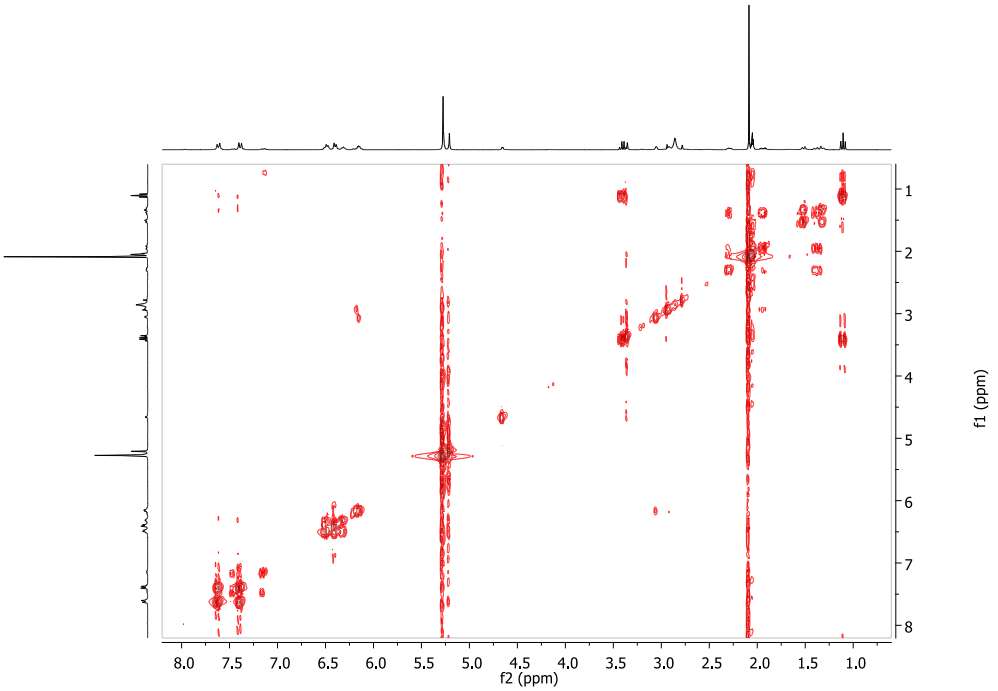

Figure 2.6: COSY NMR of 2.7-*exo*.

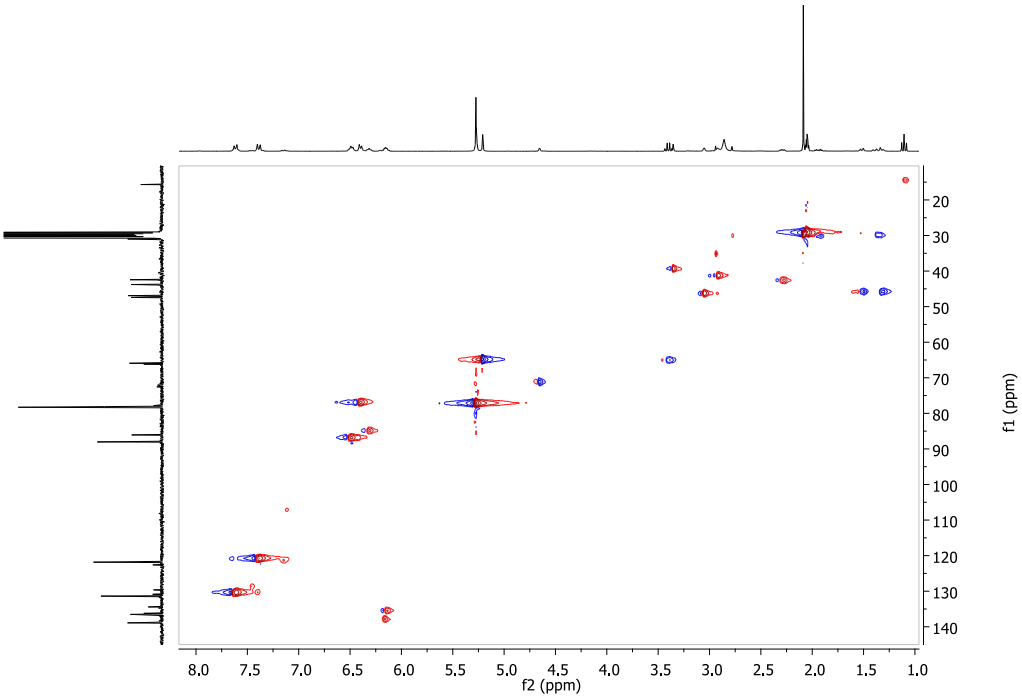

Figure 2.7: HSQC NMR of 2.7-*exo*.

Polymerization of 2.7 was carried out using a 20:1 ratio of monomer to catalyst, in dry THF under an atmosphere of N_2. Sometime during this 30 min., the polymer became insoluble in the reaction solvent and precipitated out of solution as a jelly-like material, all in one piece. Despite the polymer no longer being in solution, 5 mL of ethyl vinyl ether was injected in order to kill the catalyst and to end-cap the polymers that may have remained dissolved in the THF. Once the solvent was removed via under high vacuum, polymer 2.8 was isolated as a beige-brown chunky solid, that became jelly-like with the addition of more solvent and was completely insoluble in all solvents tried, with the exception of being partially soluble in acetonitrile. This allowed for solution NMR to be run in CD_3CN, as seen in Figure 2.8.

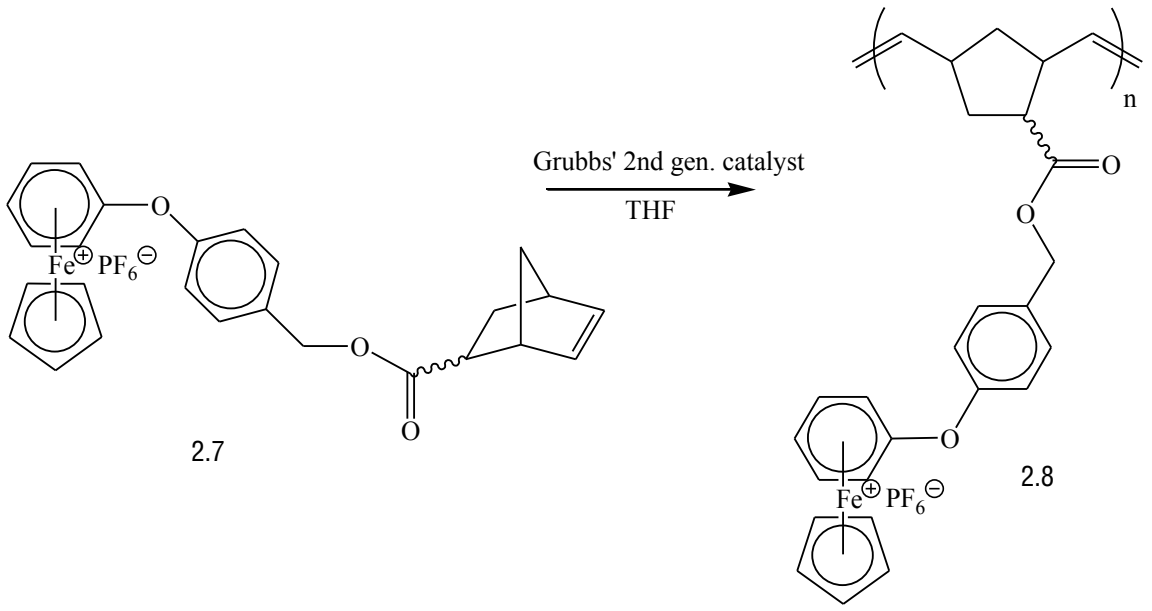

Scheme 2.4: Polymerization of 2.7 to form polymer 2.8.

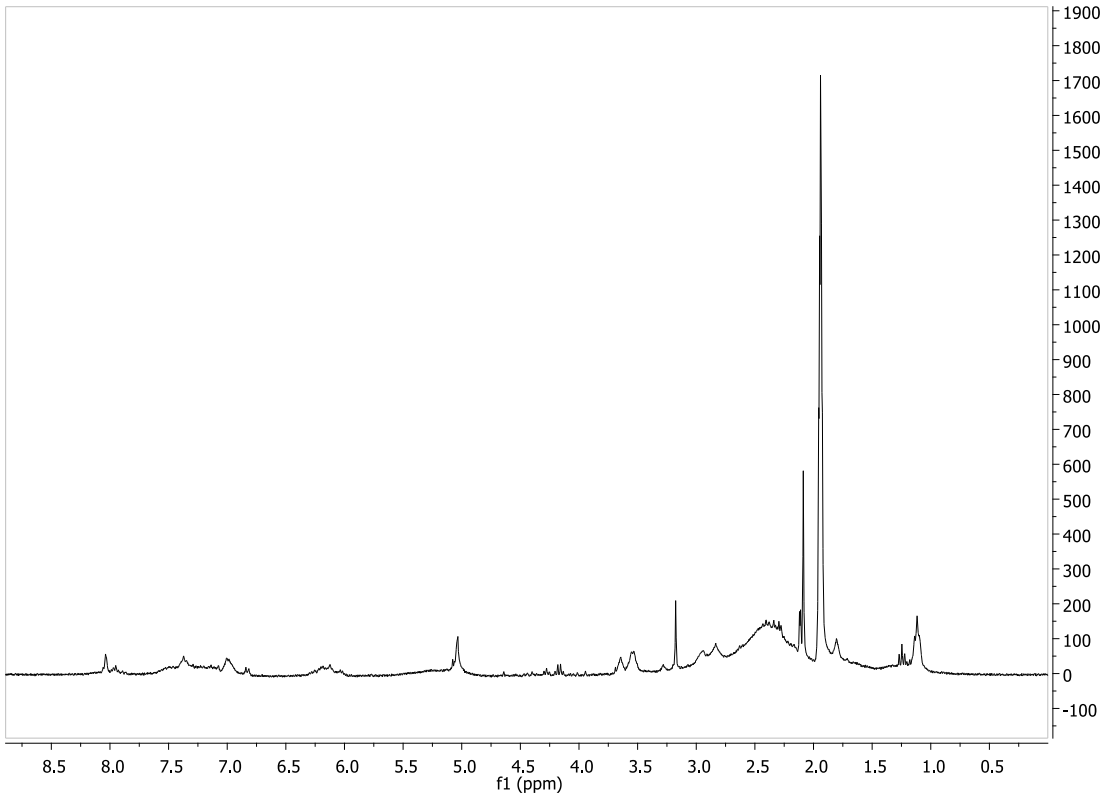

Figure 2.8: ^{1}H NMR spectrum of polymer 2.8.

The proton spectrum of 2.8 showed the characteristic broadening of peaks as a result of polymer formation. The Cp of the iron complex can still be seen at approximately 5.0 ppm, while the metal bound aromatics (6.2 ppm) and metal free aromatics (7.0-7.5 ppm) are also observable. The sharper peaks present in the lower end of the spectrum are a result of the cyclopentane rings that make up the polymer backbone. There are still sharp peaks observed, indicating oligomers rather than polymers have been formed, however, it is very likely that only the lowest molecular weight compounds were soluble, with the largest polymers remaining in the solid state and not observable in the spectrum.

In order to observe the surface morphology of the polymer, it was examined under a scanning electron microscope (SEM). It can been seen clearly in Figure 2.9 that underneath the surface, the polymer is very globular and, despite a smooth coat, these globules can be seen along the surface of the polymer as well.

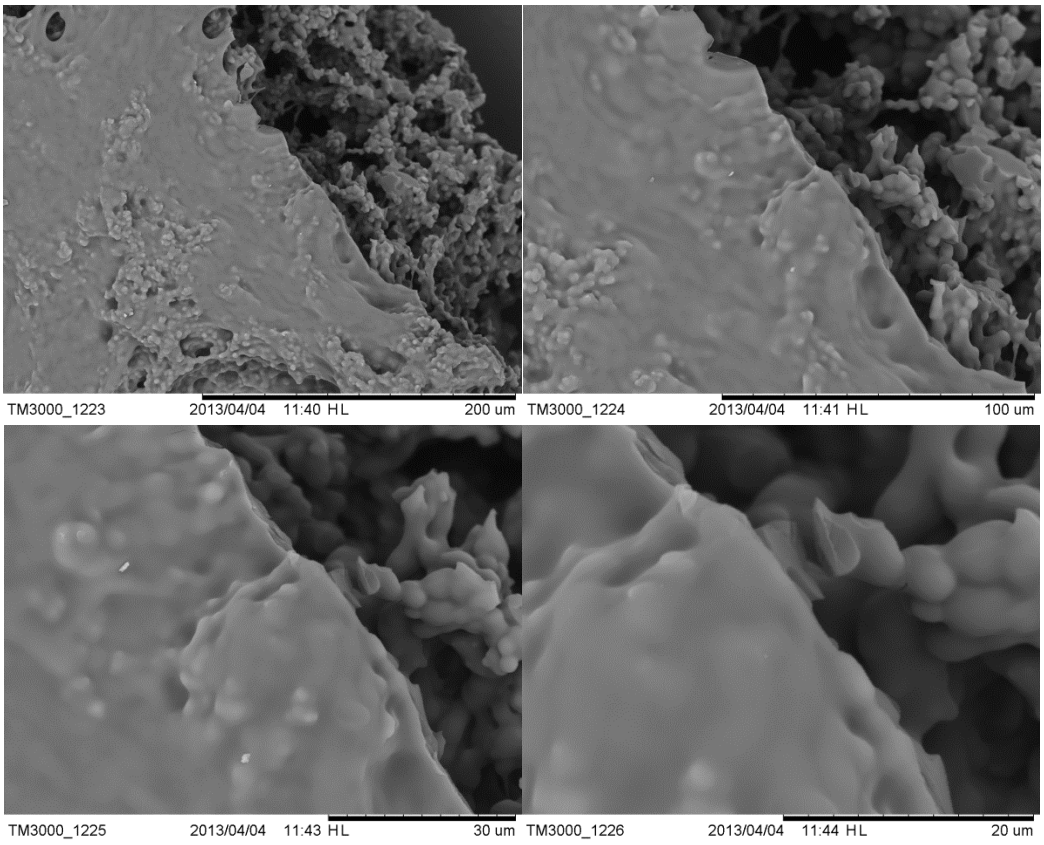

Figure 2.9: SEM images of polymer 2.8 at 500 x (top left), 1000 x (top right), 2000 x (bottom left), and 4000 x magnification (bottom right).

2.2 Synthesis of ferrocene containing polynorbornenes

In order to incorporate the ferrocene moiety into a larger molecule, it must first be functionalized. This is accomplished through a simple acylation reaction utilizing acetic anhydride (2.9) in order to form acetyl ferrocene (2.10). Reaction with iodine and pyridine, followed by a solution of sodium hydroxide, results in the formation of carboxylic acid ferrocene (2.11), which is much more suitable for incorporation into a larger compound[6].

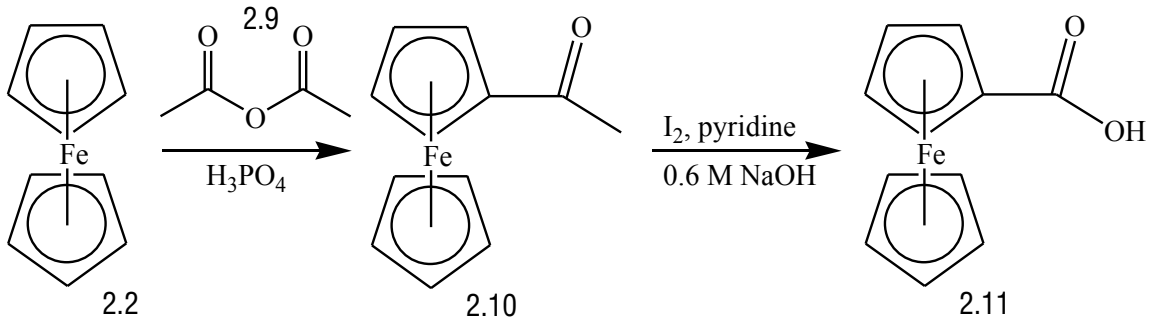

Scheme 2.5: Synthesis of carboxylic acid ferrocene (2.11) from ferrocene (2.2).

From here, it was now possible to include the norbornene functional group into the compound. The synthesis of this compound was previously reported by Schrock[94], however with limited characterization and utilizing a different synthetic scheme. As with the formation of 2.7, this was performed using the Steglich esterification conditions. However, unlike the compounds containing the cationic iron species, the ferrocene is robust enough to withstand purification via column chromatography on silica gel, using a 3:2 mixture of diethyl ether to hexanes as the mobile phase.

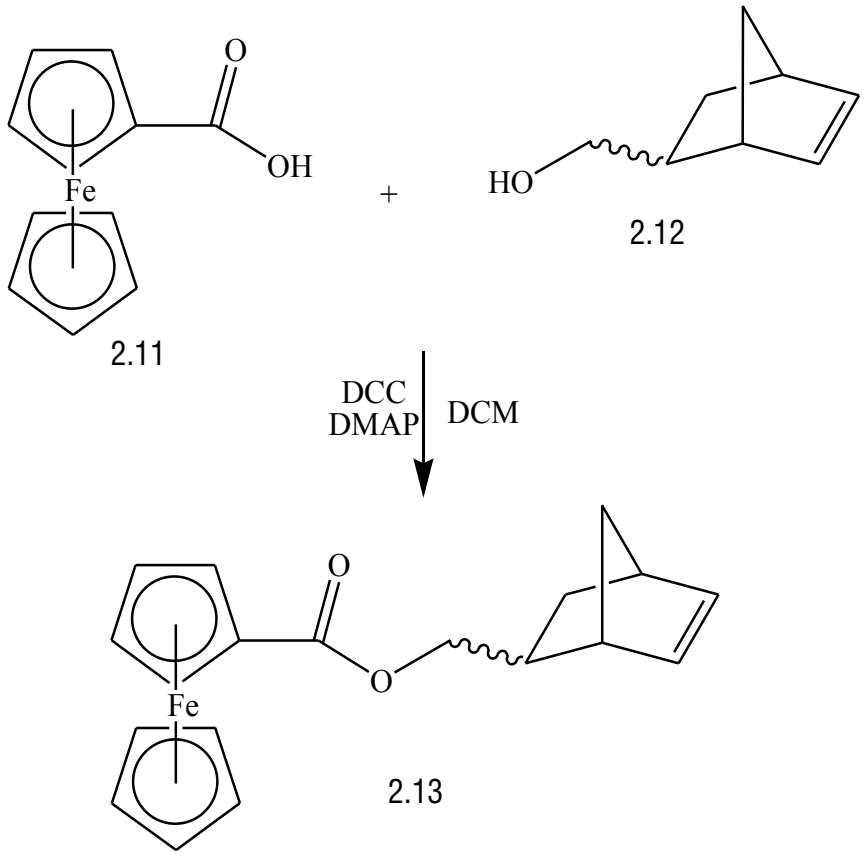

Scheme 2.6: Steglich esterification to form 2.13.

Analysis of the ^{13}C NMR shows there to be very little distinction between the two isomers, with regards to the signals due to the ferrocene. There is only a slight broadening of the singlet due to the Cp ring on the ^{1}H NMR. This is shown clearly by the single carbon signal correlating to the Cp signal in the HSQC NMR in Figure 2.10.

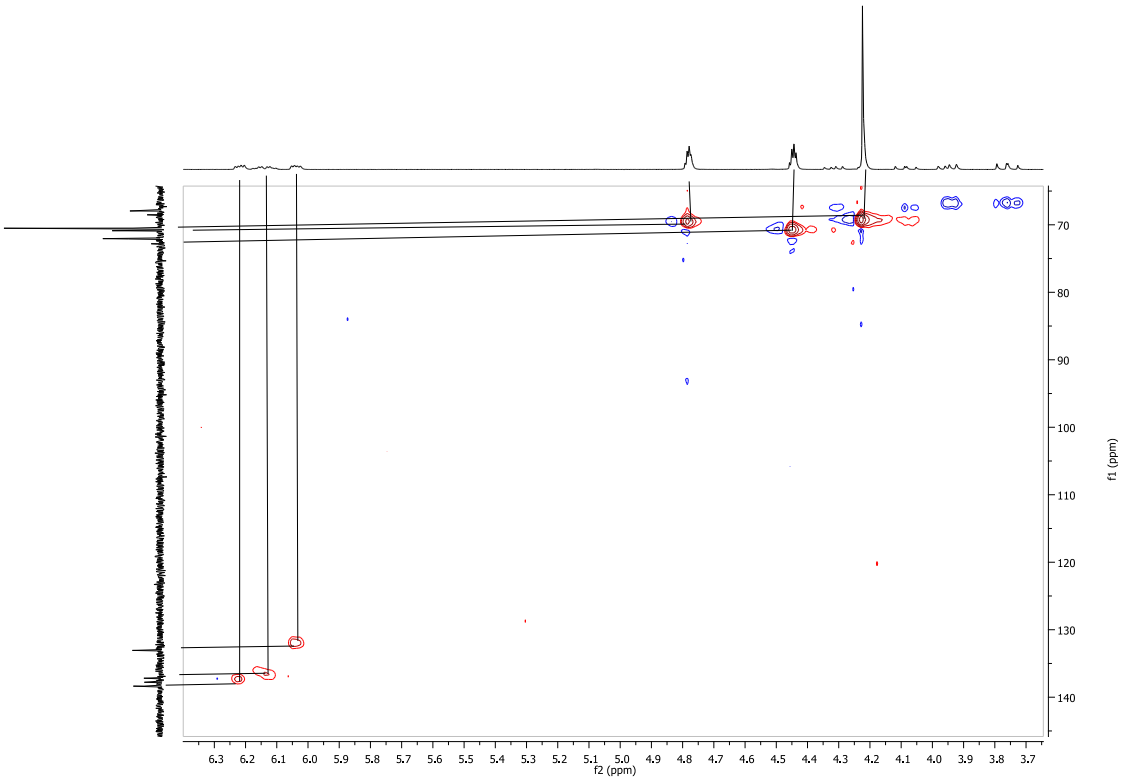

Figure 2.10: Section of the HSQC NMR spectrum of 2.13.

However, there is clear indication of both isomers when examining the resonances due to the olefinic hydrogens, as well as evidence for complete incorporation due to the slight downfield shift of the signals (from a range of 6.11-5.91 ppm to 6.24 to 6.01 ppm) in the ^{1}H NMR (see Figure 2.11). Integration of these signals shows that the two forms are in an approximately 2:1 *endo* to *exo* ratio, which was much lower than previously reported[94].

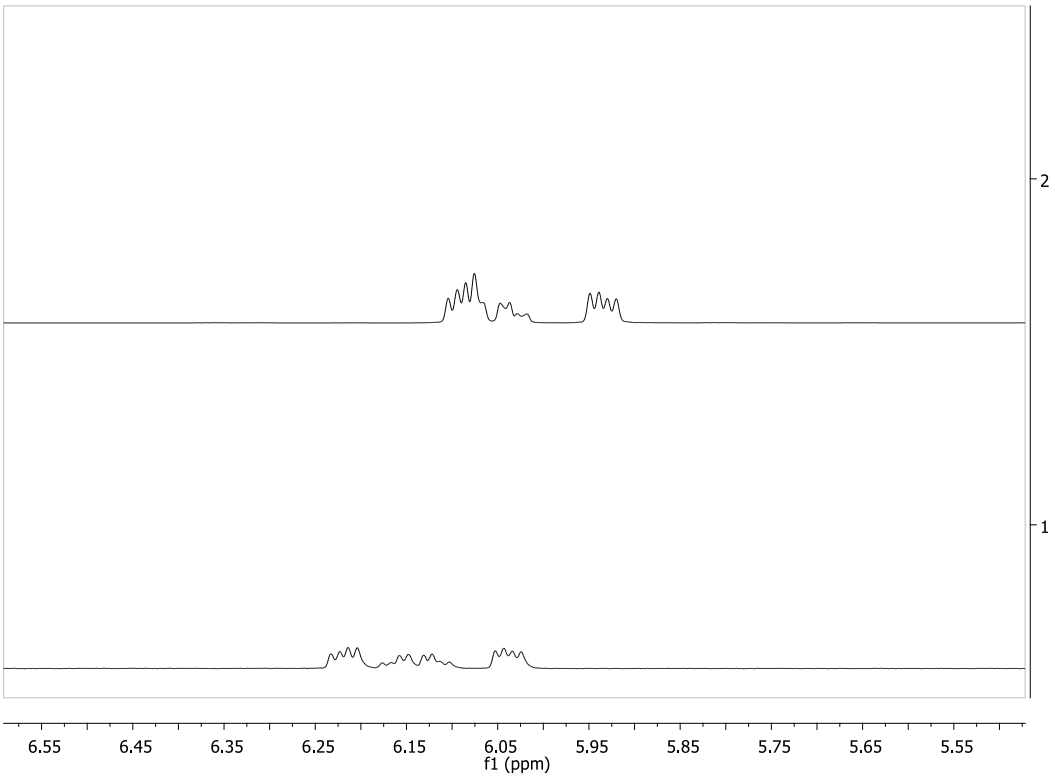

Figure 2.11: Section of the ^{1}H NMR spectra of stock 2.12 (top) and 2.13 (bottom).

Unlike the compounds synthesized using 5-norbornene-2-carboxylic acid (2.6), it was not possible to obtain only a single isomer of compound 2.13. However, it is possible to assign several of the ^{1}H and ^{13}C signals in the structure, as seen in Figure 2.12.

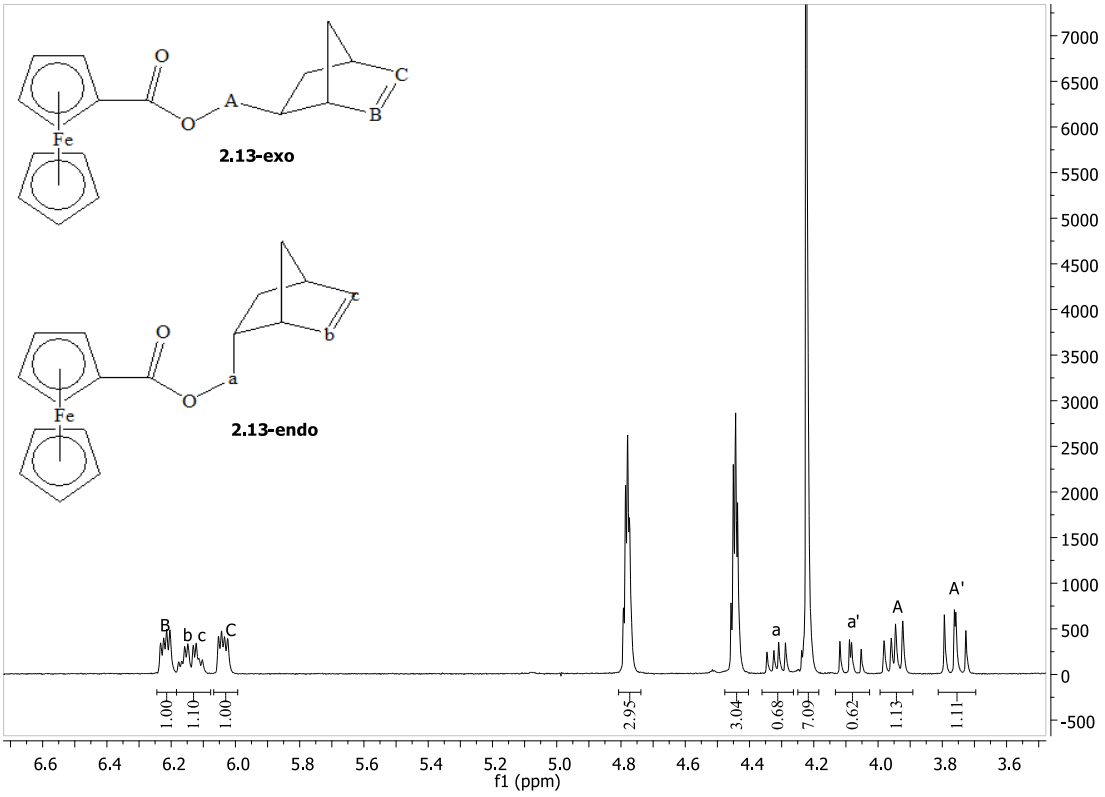

Figure 2.12: Assignment of several of the ^{1}H NMR spectrum signals due to the different isomers of 2.13.

These assignments were made based on two notable correlations found in the 2D NMR performed on 2.13. First, there is clear coupling between the olefinic proton signals and the protons directly attached to the bridge of the bicycle (Figure 2.13 label A). Second, the coupling seen between the diastereotopic protons α to the ester and the proton in the contrary endo/exo position on the 2-position of the bicycle (Figure 2.13 label B).

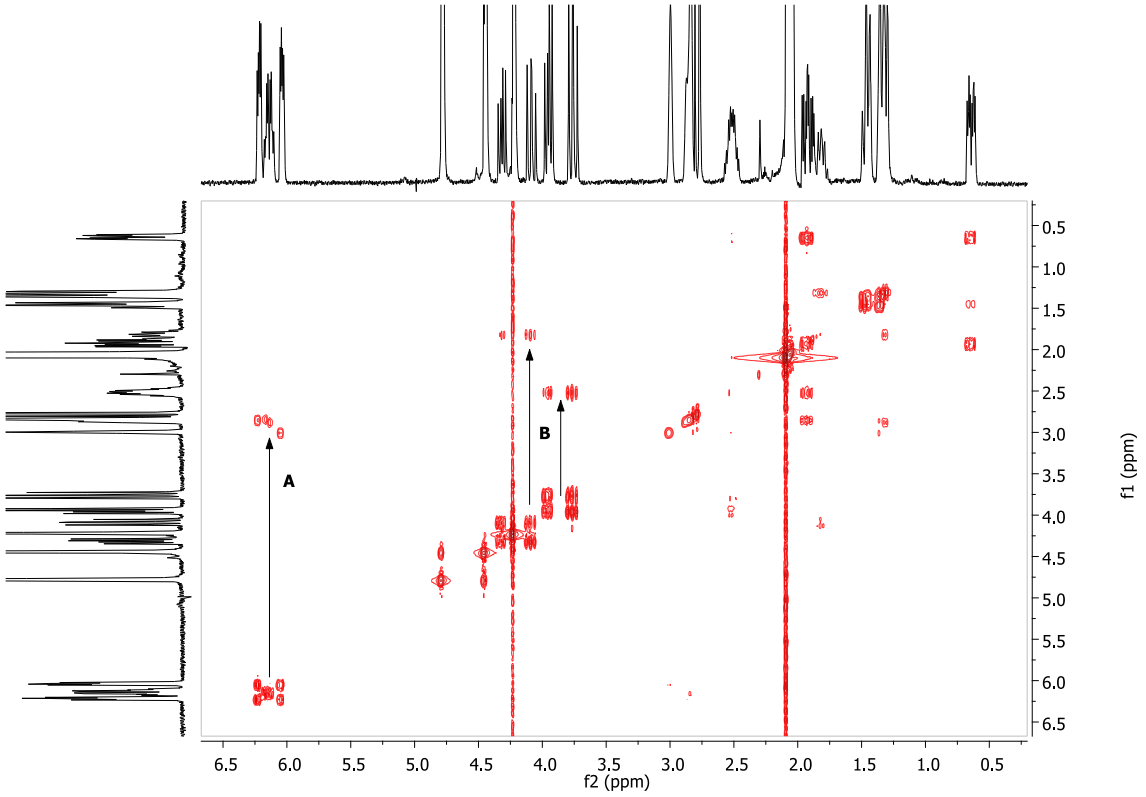

Figure 2.13: COSY NMR spectrum of 2.13.

It can be proven that the protons α to the ester are diastereotopic based on the HSQC. As can be seen in the boxes label A and B in Figure 2.14, both proton signals correspond to a single ^{13}C signal, at 68.52 ppm for the *exo* isomer and 67.95 for the *endo*.

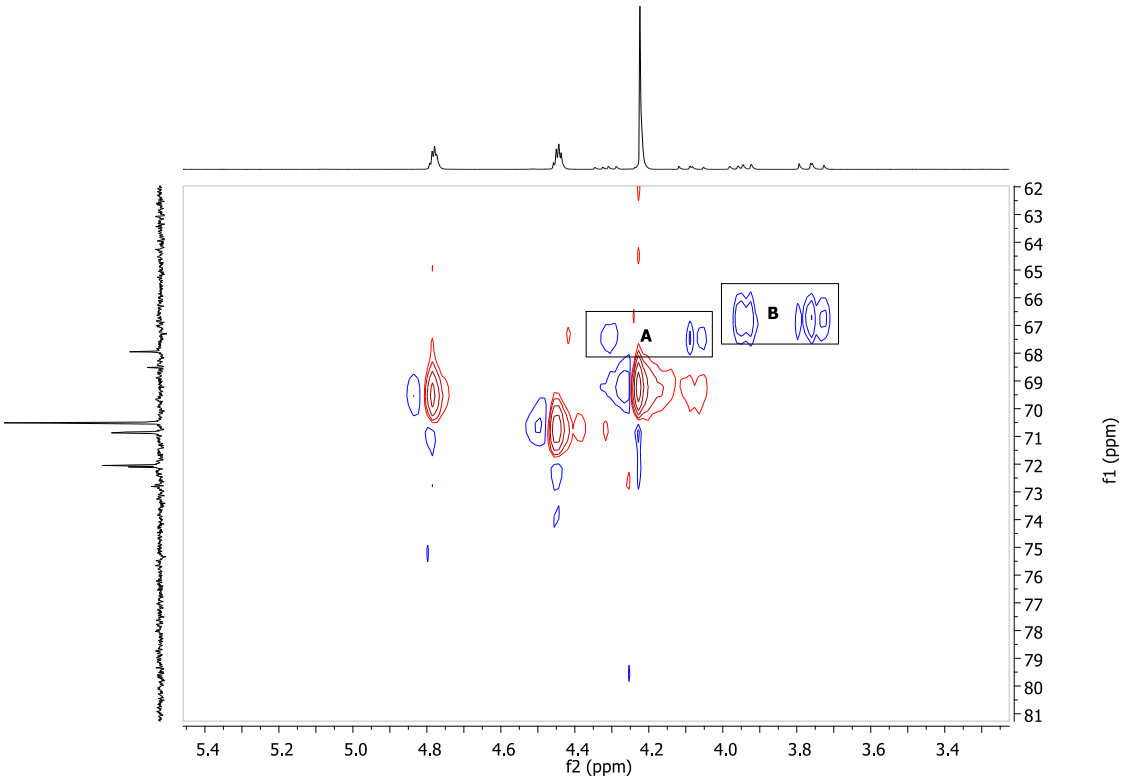

Figure 2.14: Section of the HSQC NMR spectrum of 2.13 highlighting the diastereotopic protons.

The previously reported polymerization of 2.13 was carried out using a molybdenum catalyst and produced oligomers of approximately 15 units[94]. Polymerization of 2.13 was again carried out using a 20:1 ratio of monomer to Grubbs' catalyst in dry, degassed THF under an atmosphere of N_2. After the addition of ethyl vinyl ether to end-cap the polymers and to kill the catalyst, the solvent was removed and polymer 2.14 was collected as a dark red rubber-like material. The high yield of this reaction indicates that some amount of solvent was trapped by the polymer, despite continued attempts to remove it under high vacuum.

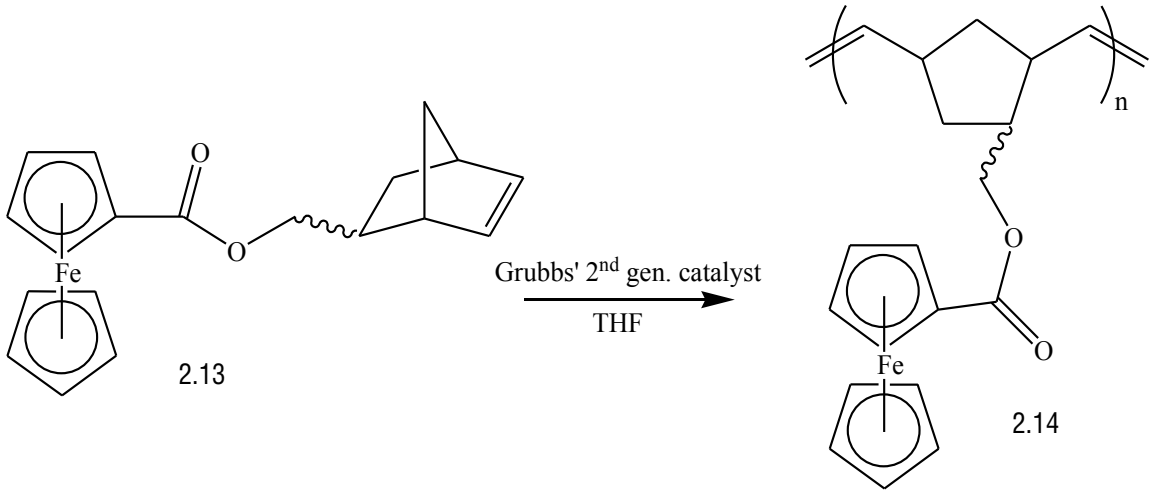

Scheme 2.7: Polymerization of 2.13 to form polymer 2.14.

Unlike polymer 2.8, 2.14 had very limited solubility in any of the available lab solvents, despite vigorous attempts to assist in getting the compound into solution. Gel permeation chromatography (GPC) run on the soluble portion yielded a M_w of 231 421 and a polydispersity index (PDI) of 1.72, indicating the formation of much larger polymers than previously reported[94]. This lack of solubility precluded performing solution NMR, so this sample was run in the solid state. As seen in Figure 2.15, there is a large peak at 70.1 ppm, representative of the ferrocene carbons, indicating that there was retention of the ferrocene moiety throughout the polymerization, though this was to be expected, due to the robustness of the compound.

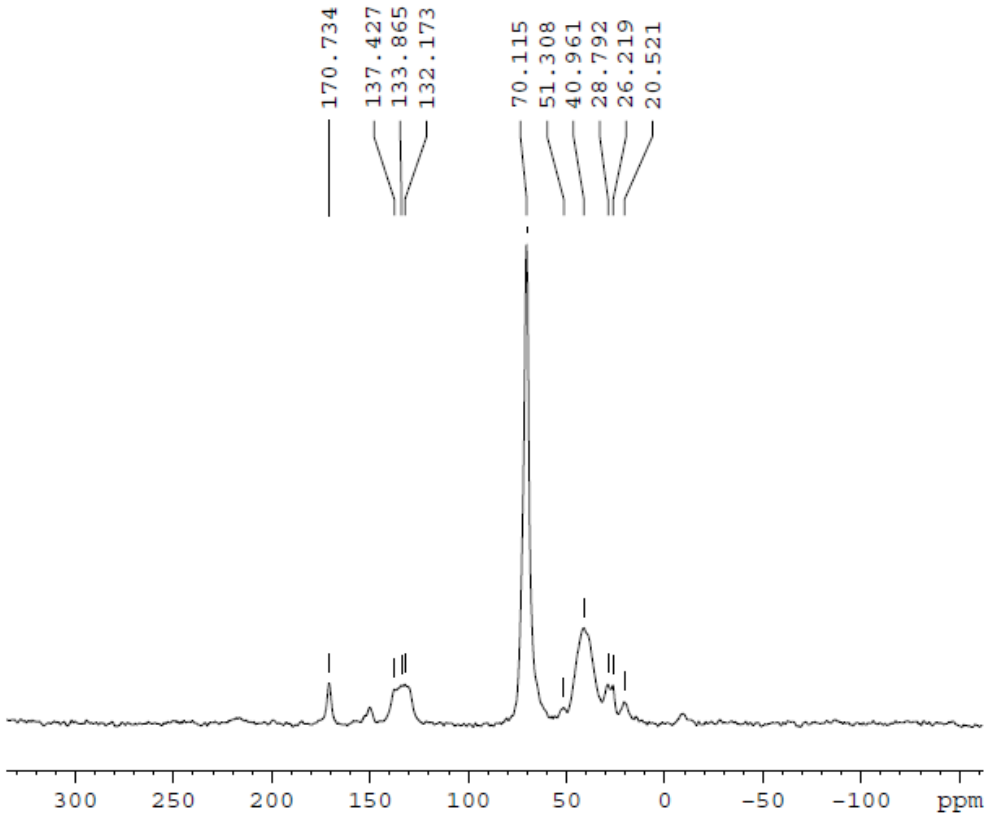

Figure 2.15: Solid state NMR spectrum of polymer 2.14.

Observation of 2.14 under a SEM revealed a highly folded surface structure, with the polymer being very thin, appearing similar to cellophane. Unlike 2.8, however, the surface of the polymer was very smooth.

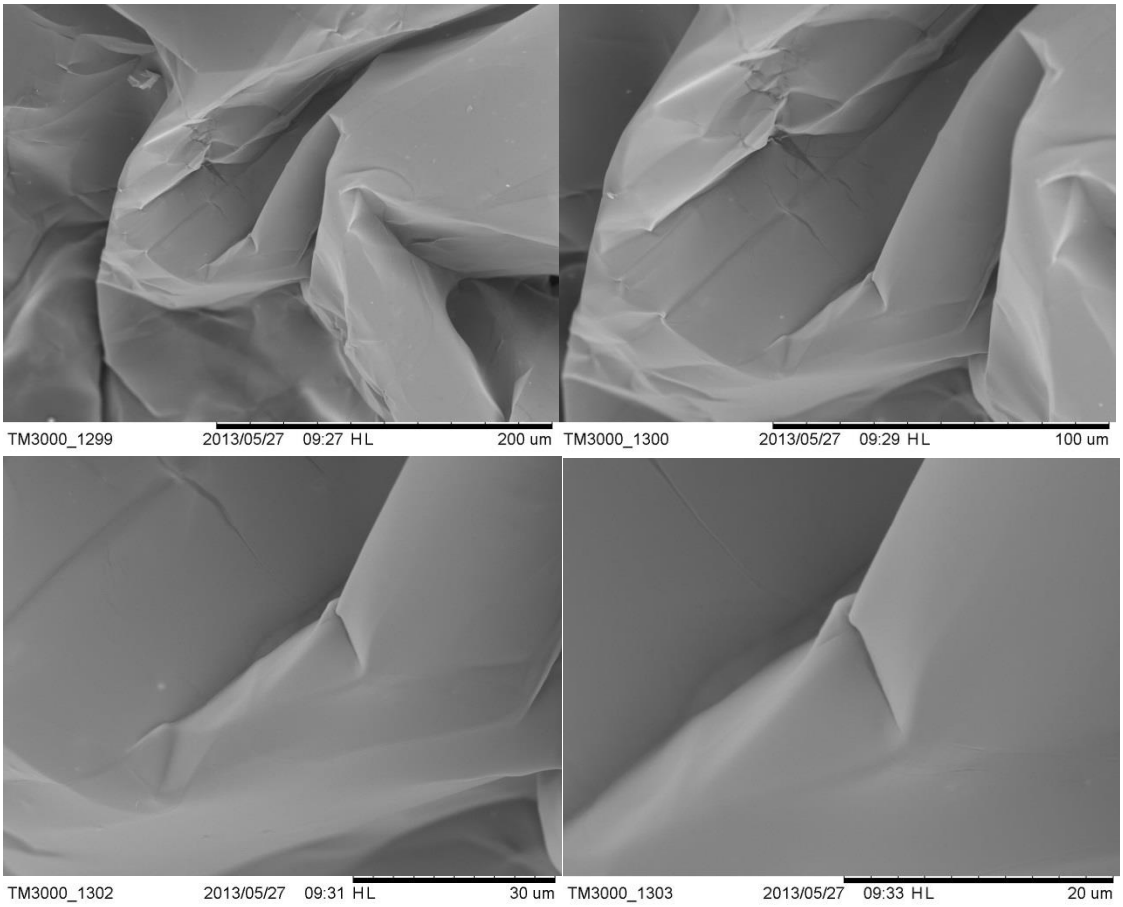

Figure 2.16: SEM images of polymer 2.14 at 500 x (top left), 1000 x (top right), 2000 x (bottom left), and 4000 x magnification (bottom right).

2.3 **Synthesis of η^6-arene chromium tricarbonyl containing polynorbornenes**

Unlike the previous two polymers, where functionalization of the metal bound aromatics was performed post-complexation to the metal, it was more practical to incorporate the necessary functional groups prior to this step. For this reason, benzyl alcohol (2.16) was selected as the appropriate arene, as it would allow for further functionalization very easily under reaction conditions previously utilized. It was determined that a

modification of literature procedures resulted in the best yield for this reaction, with refluxing in a solution of THF and 1,4-dioxane for a period of 5 days producing the best results[95,96].

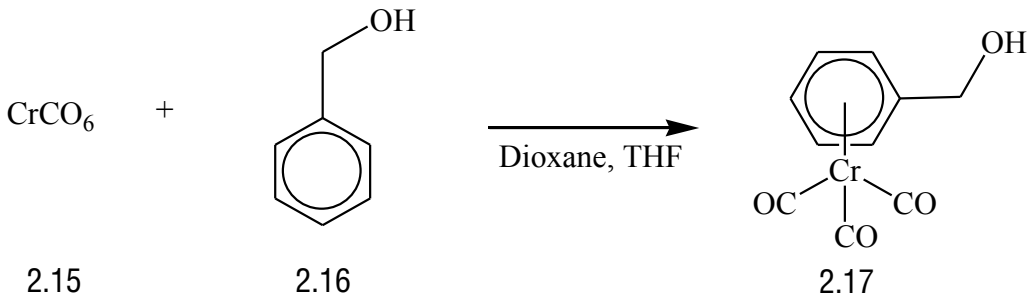

2.15 2.16 2.17

Scheme 2.8: Synthesis of 2.17 via arene coordination.

As seen in the ^{1}H NMR (Figure 2.17) and ^{13}C NMR (Figure 2.18) spectra, there is a dramatic upfield shift in the aromatic signals as a result of coordination to chromium, resulting in the proton signals moving from 8 to between 5.7 and 5.5 ppm and the carbon signals moving from 150 to between 95 and 93 ppm. Additionally, the signal resulting from the chromium bound carbonyls can be clearly seen at 234 ppm in the ^{13}C NMR spectrum.

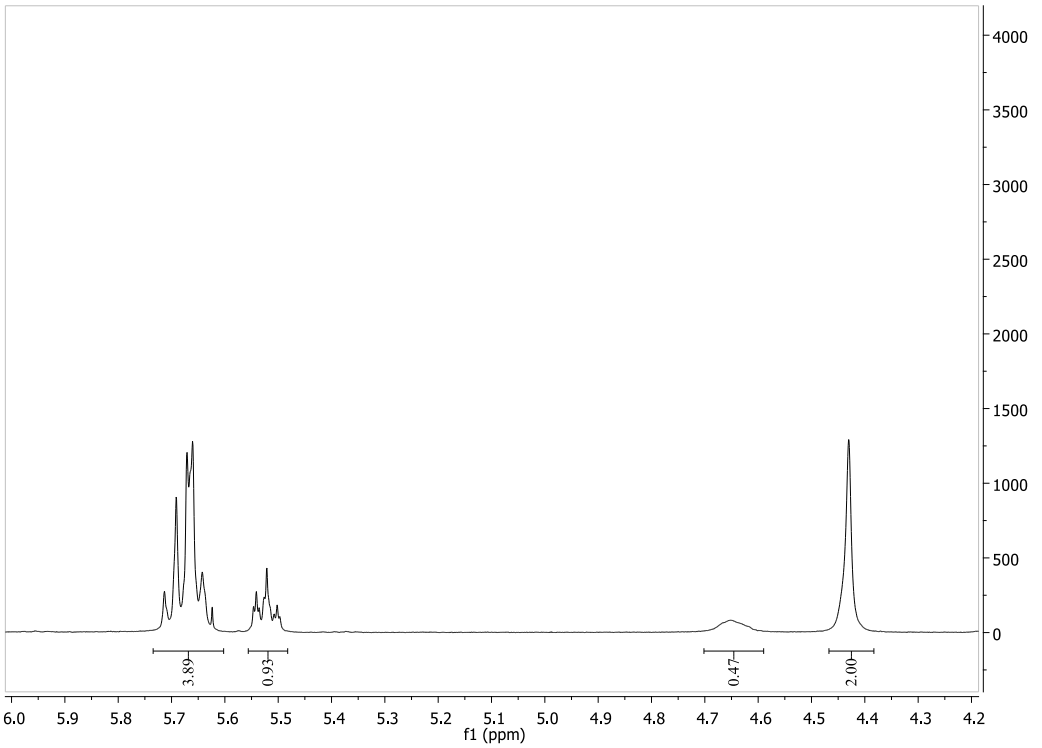

Figure 2.17: Section of the ^{1}H NMR spectrum of 2.17.

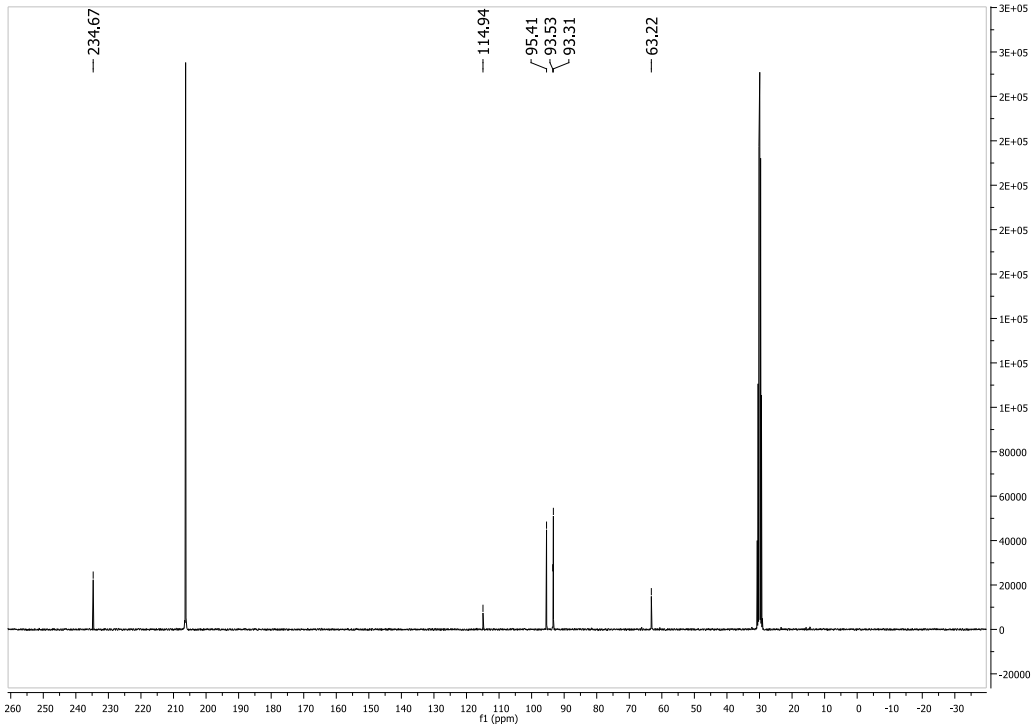

Figure 2.18: ^{13}C NMR spectrum of 2.17.

As with the formation of 2.7, the norbornene functional group is incorporated into the compound through a Steglich esterification with 2.6. Like the ferrocene based compounds, the chromium is capable of withstanding purification on silica gel. Again using a 3:2 mixture of diethyl ether to hexanes as the mobile phase and silica as the solid phase, it was possible to isolate 2.18 as a green, oil-like material.

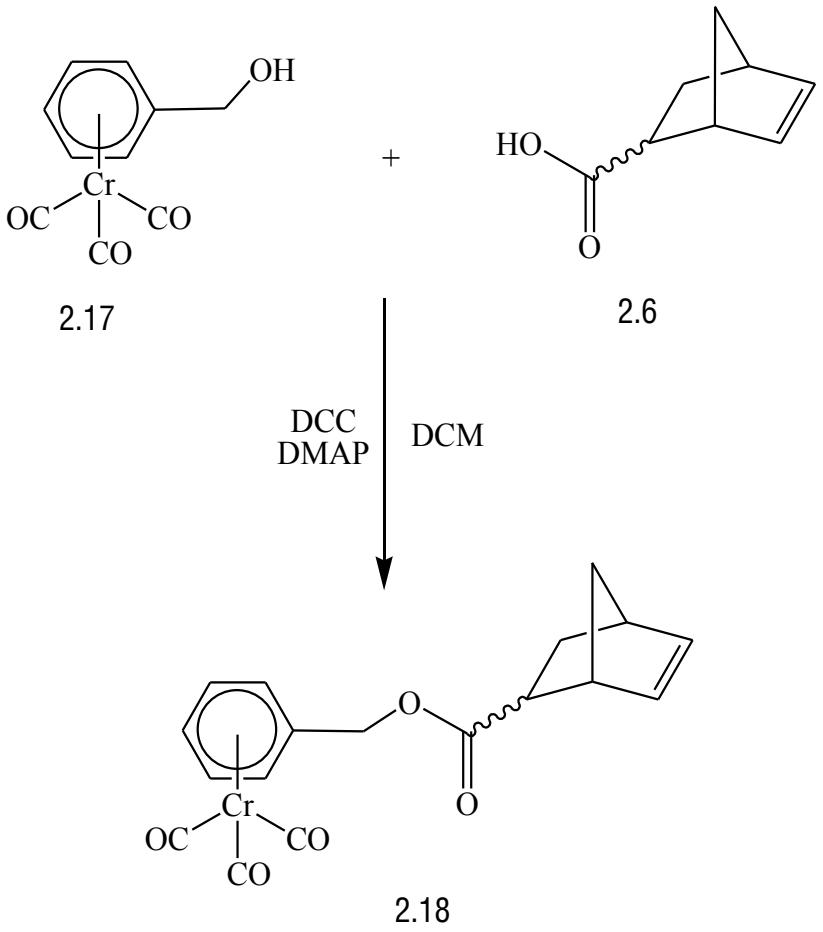

Scheme 2. 9: Steglich esterification to form 2.18.

As with 2.7, the presence of the two isomeric forms makes interpretation of the NMR spectra very difficult. It is seen that both forms are present, due to the very small differences in the signals due to the chromium bound carbonyls (Figure 2.19), as well as the multiple olefinic and benzylic proton signals (Figure 2.20).

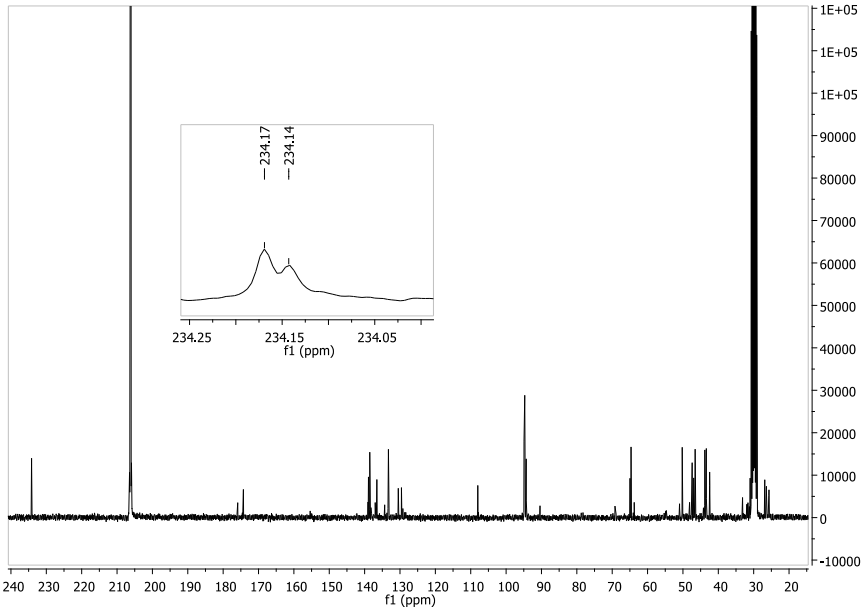

Figure 2.19: ^{13}C NMR spectrum of 2.18, with an inset showing the metal bound carbonyl signals of the two isomers.

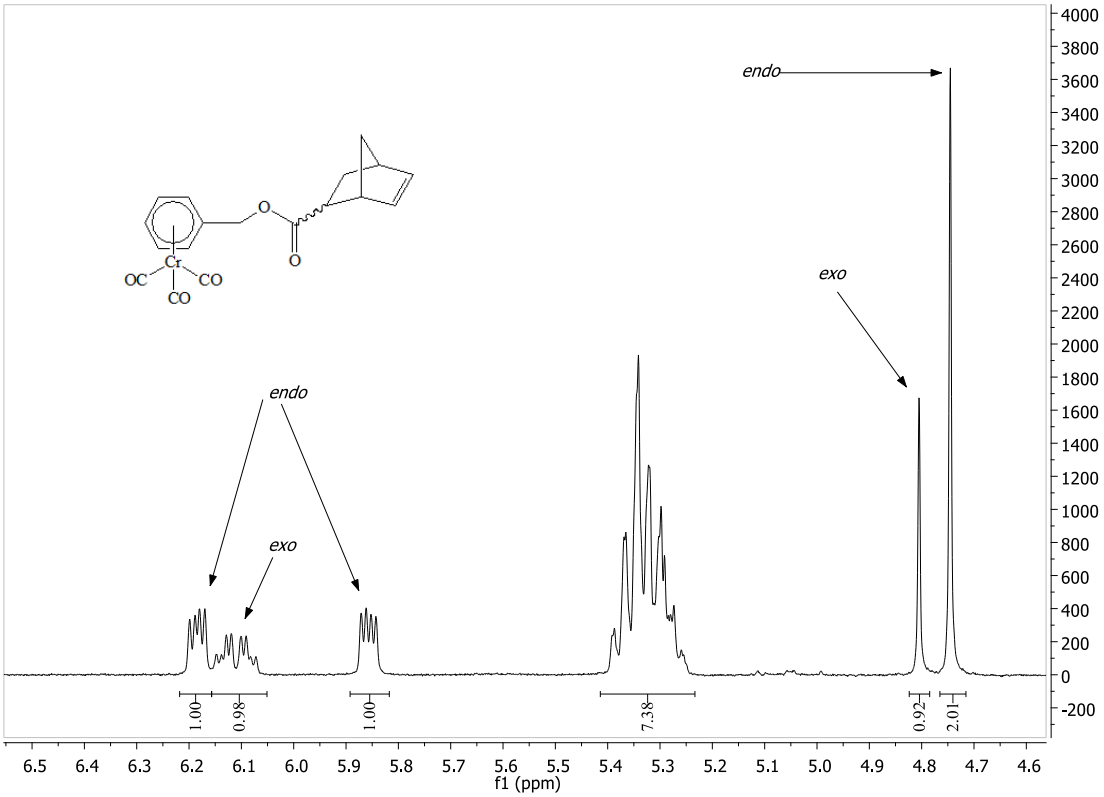

Figure 2.20: Section of the ^{1}H NMR spectrum of 2.18.

As with **2.7**, it was possible to isolate a single isomer of **2.18** by replicating the reaction with only a single isomer of **2.6** present[92]. This allowed for a full characterization of all signals in the compound.

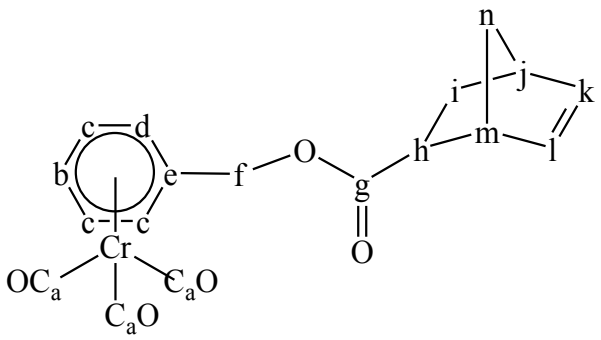

Figure 2.21: Atom labels for **2.18-*exo***.

Table 2.2: NMR assignments for **2.18-*exo***.

Label	^{1}H NMR δ	^{13}C NMR δ
a	-	234.11
b	5.64	94.40
c	5.70	94.73
d	5.75	94.92
e	-	107.83
f	4.92	64.95
g	-	175.84
h	1.93	30.97
i	2.30	43.63
j	3.08	46.94
k	6.15	136.51
l	6.15	138.89
m	2.92	42.43
n	1.55-1.25	47.37

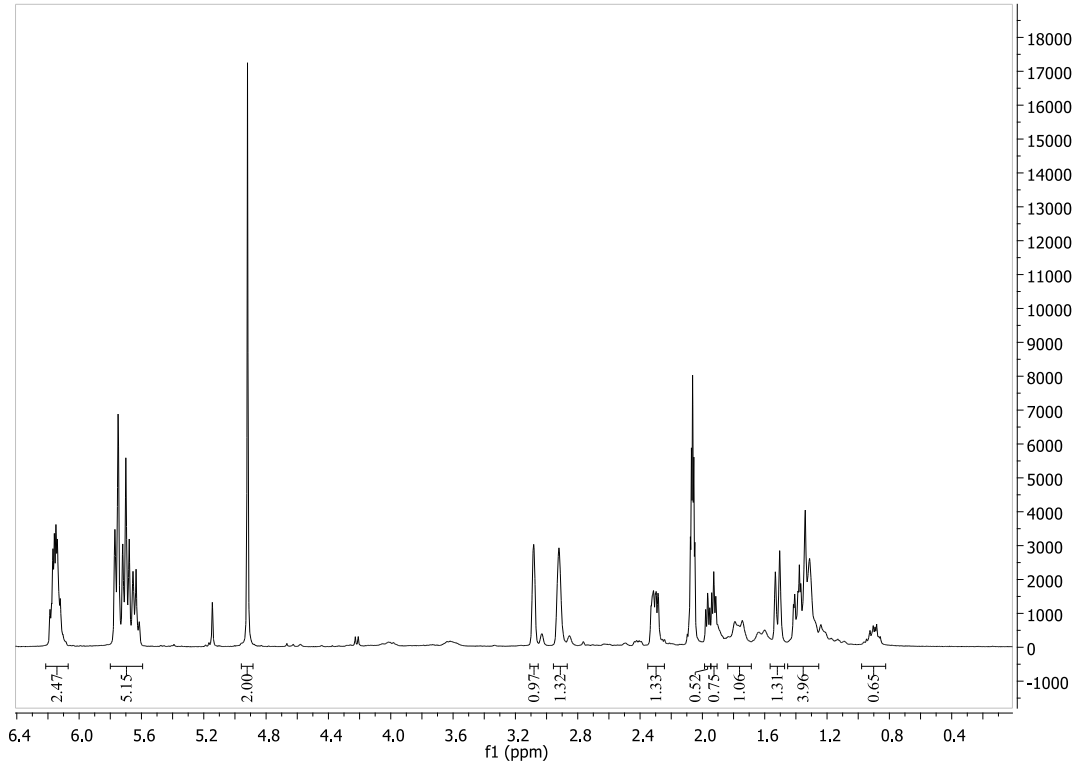

Figure 2.22: ^{1}H NMR spectrum of 2.18-*exo.*

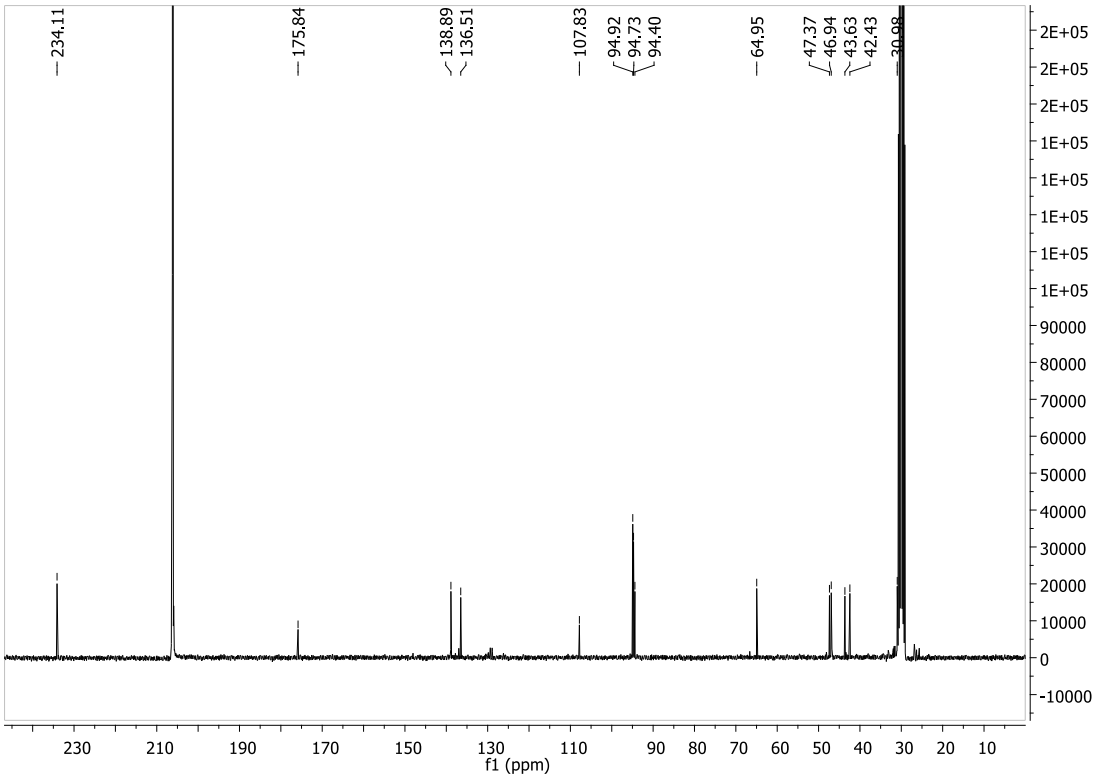

Figure 2.23: ^{13}C NMR spectrum of 2.18-*exo*.

Full assignment of the complex signals as a result of the norbornene was accomplished through both COSY and HSQC NMR. As noted in Figure 2.24, clear correlations between the olefinic protons and the protons located at the bridge of the bicycle are seen (label A, Figure 2.24), at 3.09 (signal j in Table 2.2) and 2.92 ppm (signal m). Signal m also shows correlation to both the doublet of triplets (dt) at 1.90 ppm (signal h) and the broad signal from 1.55 to 1.25 ppm (signal n), representing the *endo* proton in the 2 position in the bicyclic ring and the methylene in the single bridge of the compound, respectively. Signal j shows coupling to the bridge protons but lacks any other correlations, notably signal i. However, there are clear correlations between signal i and signal h, completing the signal assignments.

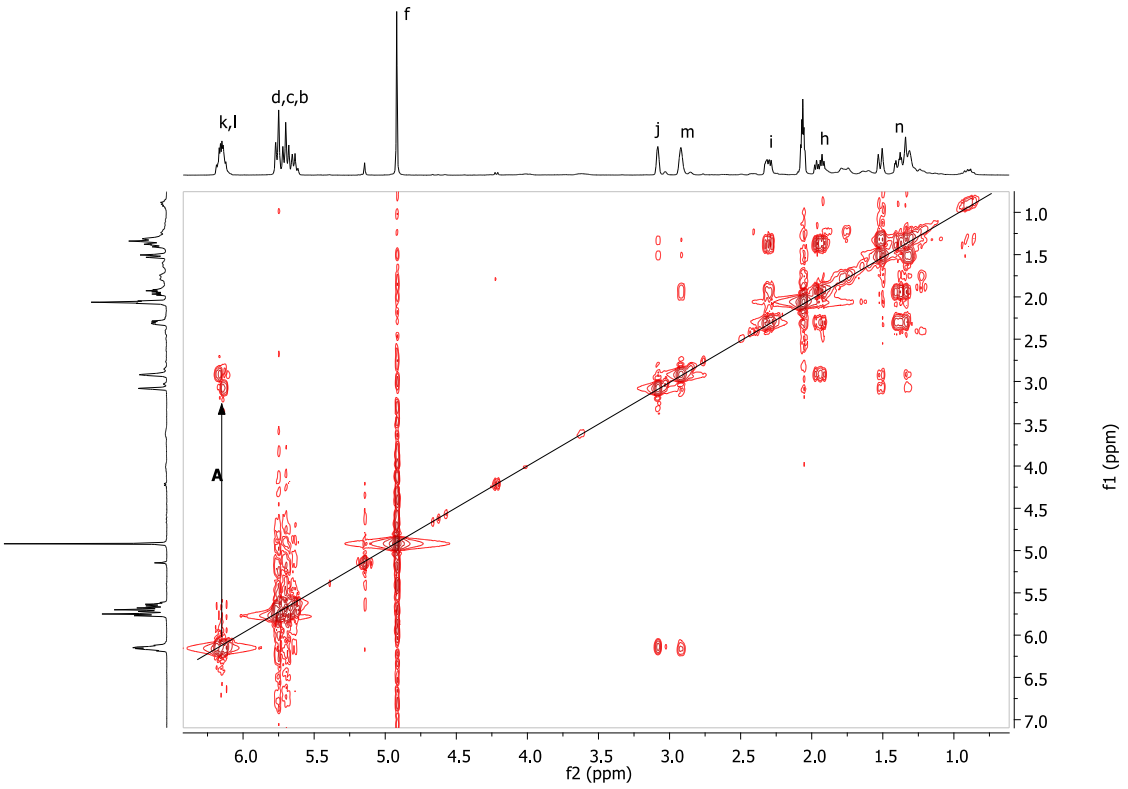

Figure 2.24: COSY NMR Spectrum of 2.18-*exo*.

The HSQC spectrum was subsequently used in order to assign carbon signals. The most notable correlations are between the benzylic protons (64.9 ppm, label A Figure 2.25), the metal bound aromatics (94.4, 94.7, and 94.9 ppm, label B Figure 2.25), and the olefinic protons (136.5 and 138.9 ppm, label C Figure 2.25). It was also determined that the aromatic carbon lacking a proton appeared at 107.8 ppm, due to its lack of a correlation to the ^{1}H NMR.

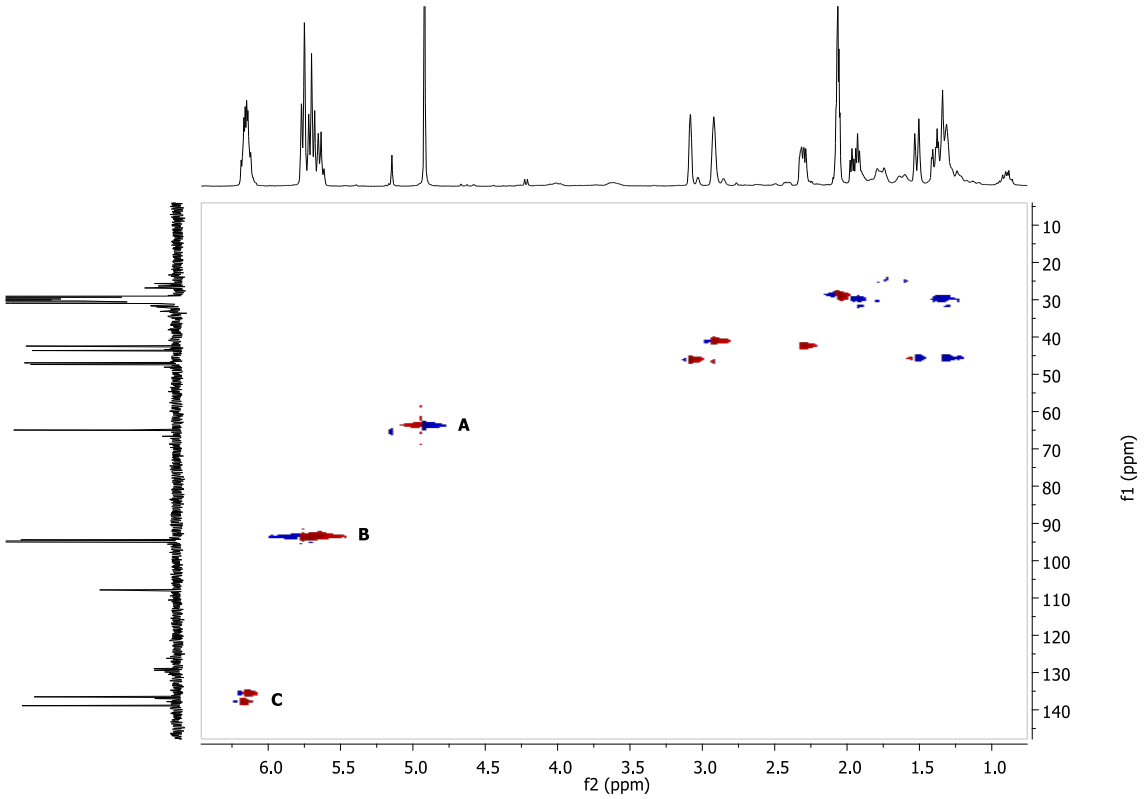

Figure 2.25: HSQC NMR Spectrum of 2.18-*exo*.

Polymerization of 2.18 was again performed using a 20:1 ratio of monomer to catalyst in dry, degassed THF under an atmosphere of N_2.

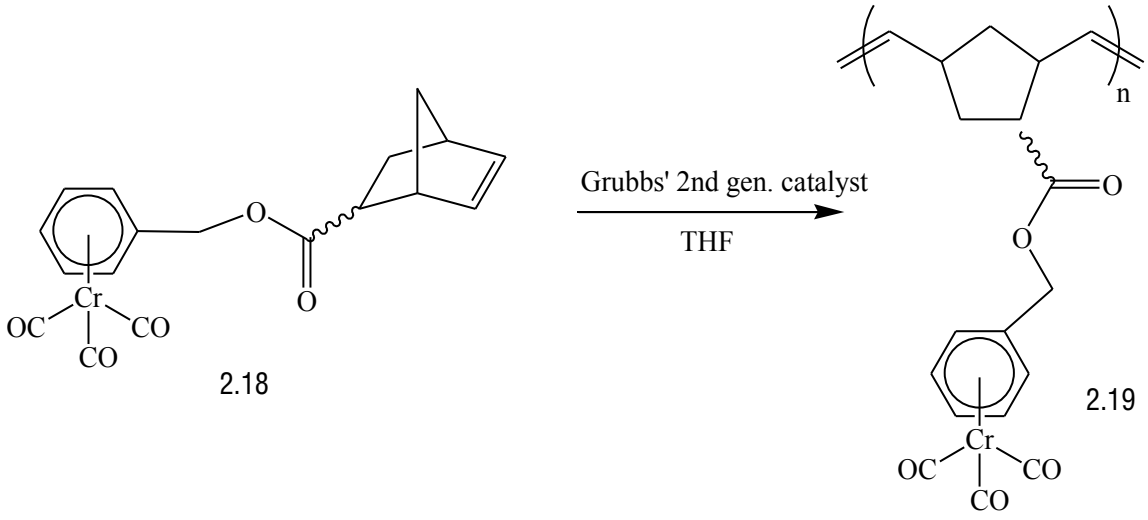

Scheme 2.10: Polymerization of 2.18 to form polymer 2.19.

After adding ethyl vinyl ether to end-cap the polymers and to kill the catalyst, the solvent was removed and polymer 2.19 was isolated as a yellow-green rubber like material. As with 2.14, the polymers proved insoluble in any lab solvents, so solution NMR was not performed. However, like polymer 2.14, it was possible to perform solid state NMR. As seen in Figure 2.26, the ^{13}C NMR shows that there is most likely some metal-free arenes now present, based on the large signal at 132.5 ppm, which is in the standard range for aromatics. There is also evidence for remaining metal-bound aromatics, as a peak at 92.9 ppm remains, which would correspond to the signals found between 90 and 95 ppm of compound 2.18 (Figure 2.19). Whether or not the loss of the metal is a result of the catalytic conditions or the post-polymerization exposure to air is not possible to determine, though it is likely the latter, due to the mild air sensitivity shown by 2.18.

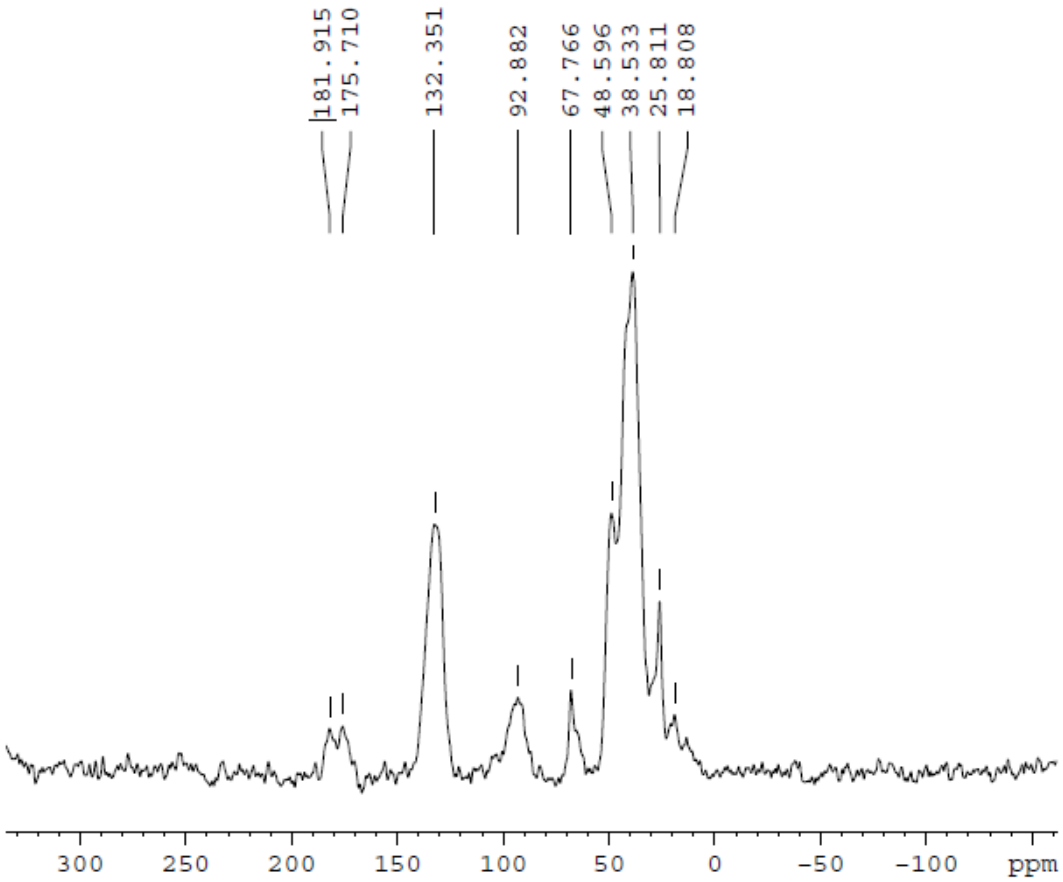

Figure 2.26: Solid state ^{13}C NMR spectrum of 2.19.

Again, the samples were examined by SEM. Unlike polymer 2.8, 2.19 was very smooth along the surface.

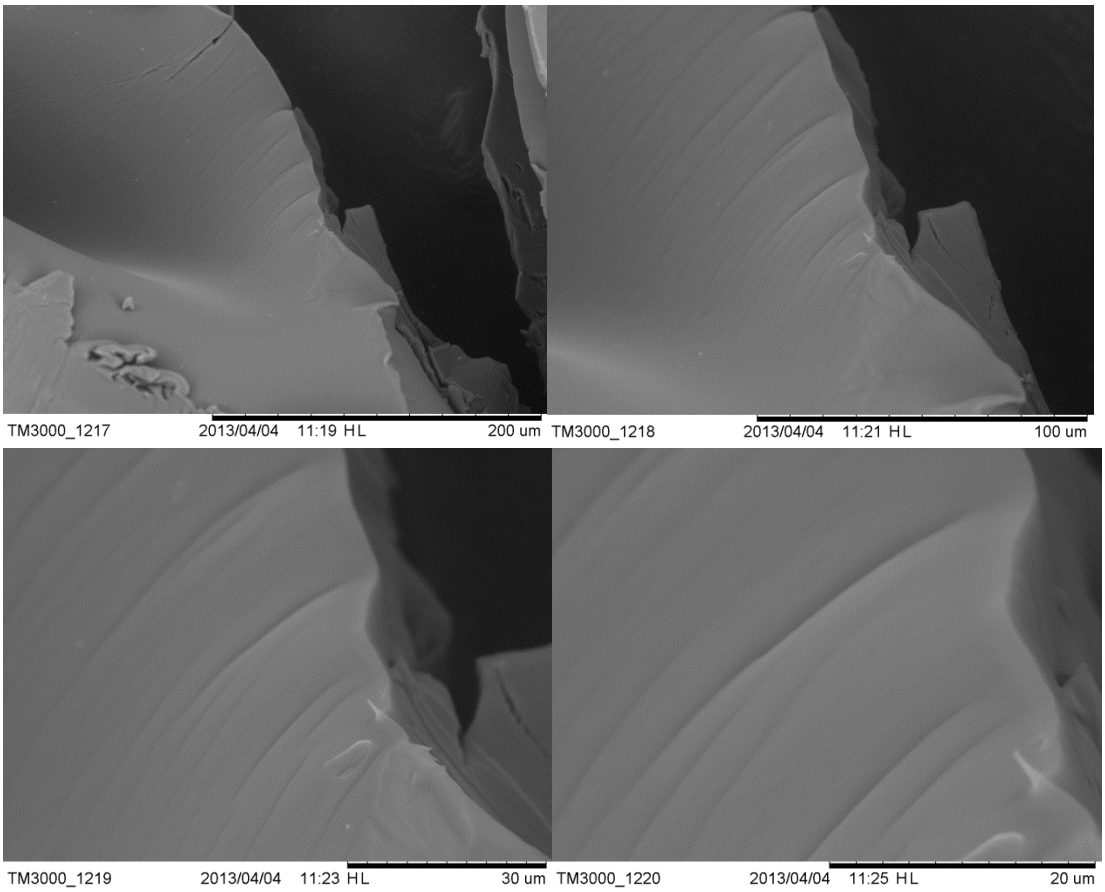

Figure 2.27: SEM images of polymer 2.19 at 500 x (top left), 1000 x (top right), 2000 x (bottom left), and 4000 x magnification (bottom right).

2.4 Thermal analysis

For polymer 2.8, the first decomposition step begins at 217 °C and corresponds to the breakdown of the Cp moiety[97]. The next degenerative step is the breakdown of the esters, followed by the gradual breaking down of the polymer backbone. As expected, polymer 2.14 shows the highest thermal stability of the three monometallic polynorbornenes. This is due to the stability of the ferrocene moiety, which begins to degrade at 356 °C. Again, degradation of the esters and the polymer backbone followed,

with decomposition being significantly more rapid than 2.8. Polymer 2.19 was the least thermally stable of the polymers, showing initial degradation at 204 °C, which can be attributed to the loss of the chromium bound carbonyl ligands. Similar to 2.14, polymer 2.19 underwent extremely rapid decomposition of greater than 50% of the mass of the sample at 368 °C. This much more rapid decomposition of the majority of polymers 2.14 and 2.19 when compared to 2.8 can be attributed to the smaller amount of carbon within the compounds.

Table 2.3: Thermogravimetric analysis of monometallic polynorbornenes, performed under standard atmosphere (All temperatures reported in °C).

Polymer	Step 1	Step 2	Step 3	Step 4
2.8	217, 17%	364, 33%	445, 31%	-
2.14	84, 7%	356, 19%	395, 8%	433, 40%
2.19	90, 18%	204, 13%	368, 55%	-

Table 2.4: Polymer remaining after completion of TGA.

Polymer	Air	Nitrogen	M%	M_nO_m%
2.8	4.4%	23.0%	9.5%	12.2%
2.14	25.5%	31.1%	16.6%	21.4%
2.19	14.1%	23.5%	11.2%	14.6/32.7%

Comparison of the degradations of each of the polymers when run under air versus nitrogen showed nearly identical decomposition patterns. However, there was more material left over upon the completion of heating when the samples were run under

nitrogen, which can be attributed to incomplete formation of oxides due to the lack of oxygen surrounding the sample. As seen in Table 2.4, polymers 2.14 and 2.19 degrade completely to the most common oxides for the metals present, with a small amount of other carbon decompositions also present. This is not the case for polymer 2.8, as it is possible the degradation of the cationic iron moiety resulted in the formation of ferrocene, which can sublime and will not remain in the TGA pan for the duration of the experiment. There would also be partial conversion into iron(II) oxide, as well as carbon based decompositions present.

Differential scanning calorimetry of the polymers showed that they each exhibited a glass transition temperature between 60 and 80 °C, with the cationic iron based 2.7 being the highest.

Table 2.5: Differential scanning calorimetry of monometallic polynorbornenes.

Polymer	T_g (°C)
2.8	81
2.14	71
2.19	83

2.5 Summary

Three different monometallic polynorbornenes were synthesized by functionalizing a metal arene and combining it with a substituted norbornene through a Steglich esterification. These compounds were then polymerized using Grubbs' 2nd Generation Catalyst. Only the polymer containing η^6-arene-η^5-cyclopentadienyl iron(II) showed any

solubility, allowing it to be characterized using solution NMR. The other two polymers were characterized using solid state NMR. SEM images of the polymers were collected in order to observe the surface morphology, with the cationic iron appearing globular along the surface, compared to smooth surfaces on the other two polymers. The thermal properties were analyzed using TGA and DSC. Each polymer showed clear decompositions of its individual components, while the glass transition temperatures were between 59 and 70 °C.

2.6 Experimental

Any NMR experiments performed but not directly referenced in Chapter Two can be found in appendix section A.1. All compounds containing the η^6-arene-η^5-cyclopentadienyl iron(II) moiety are kept in the dark at all times to avoid decomposition. All compounds containing the η^6-arene-chromium tricarbonyl moiety were stored under N_2 in order to prevent decomposition due to O_2 exposure. Any NMR experiments on these compounds were run with the samples being prepared in the glove box to prevent decomposition over the life of the experiment. These compounds can safely be handled in the presence of air during work up but should be limited in their exposure time. Compounds 2.3, 2.10, and 2.11 were synthesized according to previously published methods[6].

Benzyl alcohol substituted cationic iron complex 2.5

Compound 2.3 (1.5202 g, 4.0 mmol), 4-hydroxy benzyl alcohol (1.0400 g, 8.0 mmol) (2.4), K_2CO_3 (2.76 g, 20.0 mmol) were dissolved in 25.0 mL of DMF. The reaction mixture was heated to 50 °C and stirred for 36 hours. 0.6543 g of ammonium hexafluorphosphate (4.0 mmol) was dissolved in 100 mL of 2.6 M HCl and the reaction mixture was added to it. The aqueous solution was extracted with DCM, the organic layer dried using $MgSO_4$, and the solvent removed *in vacuo*. The resulting solution was dissolved in a minimal amount of acetone and poured into 400 mL od diethyl ether. After being cooled at -19 °C for 2 hours, the ether was decanted and compound 2.5 was isolated as a yellow oil. (1.8306 g, 97.6%)

Cationic iron norborene 2.7

Compound 2.5 (1.8306 g, 3.92 mmol), bicyclo[2.2.1]hept-5-ene-2-carboxylic acid, mixture of *endo* and *exo* (1.10 mL, 8.0 mmol) (2.6), DCC (0.8786 g, 4.1 mmol), and DMAP (0.5253 g, 4.1 mmol) were dissolved in a solution of DCM (25.0 mL) and DMF (5.0 mL). The reaction was stirred under N_2 for 16 hours and was then cooled to -19 °C for 2 hours. A white precipitate was removed via filtration and the filtrant was diluted with DCM, prior to subsequent washes using 2.6 M HCl and DI water. The organic solution was then dried using $MgSO_4$, and the solvent removed *in vacuo*. The resulting solution was dissolved in a minimal amount of acetone and then poured into 400 mL of diethyl ether. After being cooled to 19 °C for 2 hours, the ether was decanted and compound 2.7 was isolated as a yellow oil. (2.2590 g, 97.9 %)

^{1}H NMR (300 MHz, acetone-δ_6) δ 7.62 (t, *J* = 8.4, 2H), 7.40 (d, *J* = 8.5, 2H), 7.14 (d, *J* = 7.6 Hz, 1H), 7.03 (t, *J* = 8.1z, 1H), 6.51 (t, J = 6.4, 2H), 6.41 (d, *J* = 6.4, 2H), 6.33 (t, *J* =

5.9, 1H), 6.20 (m, 1H), 6.19 (m, 4H), 5.98 (m, 1H), 5.95 (dd, *J* = 5.6, 2.8 Hz, 2H), 5.88 (dd, *J* = 5.6, 2.8 Hz, 1H), 5.33 – 5.26 (s, 7H), 5.22 (s, 1H), 5.14 (s, 2H), 3.53 – 3.30 (m), 3.19 – 3.05 (m), 3.05 – 2.94 (m), 2.87 (s), 2.00 – 1.80 (m), 1.55 – 1.46 (m), 1.46 – 1.24 (m).

^{13}C NMR (75 MHz, acetone-δ_6) δ = 174.96, 161.38, 137.61, 132.84, 130.71, 130.31, 121.23, 94.06, 87.40, 85.43, 77.67, 77.47, 64.97, 49.67, 46.30, 45.99, 45.75, 42.91, 42.75, 30.84.

Cationic iron norbornene 2.7-*exo*

^{1}H NMR (300 MHz, acetone-d_6) δ = 7.62 (d, *J* = 8.2, 2H), 7.39 (d, *J* = 8.3, 2H), 6.49 (t, *J* = 5.9 Hz, 2H), 6.40 (d, *J* = 6.5 Hz, 2H), 6.32 (d, *J* = 5.5 Hz, 1H), 6.17 – 6.13 (m, 2H), 5.27 (s, 5H), 5.21 (s, 2H), 3.35 (s, 1H), 3.05 (s, 1H), 2.86 (s, 2H), 2.29 (dd, *J* = 8.9, 4.5 Hz, 1H), 1.94 (dt, *J* = 11.5, 3.9 Hz, 1H), 1.50 (t, *J* = 7.7 Hz, 1H), 1.42 – 1.28 (m, 2H).

^{13}C NMR (75 MHz, acetone-d_6) δ = 176.11, 153.93, 138.90, 136.51, 136.22, 134.43, 131.38, 130.87, 129.63, 121.84, 88.03, 86.06, 78.29, 78.10, 65.92, 47.42, 46.91, 43.77, 42.43, 30.99.

Polymer 2.8

Grubb's 2nd Generation catalyst (0.0552 g, 0.065 mmol) was dissolved in 3 mL of dry, degassed THF under an atmosphere of N_2. Compound 2.7 (1.1740 g, 2.0 mmol) was dissolved in 6 mL of dry, degassed THF and added to the catalyst solution. The reaction

was stirred for 30 minutes, during which a brown-red gel formed. 5 mL of ethyl vinyl ether was added to end cap the polymers and deactivate the catalyst. The reaction was then stirred for an additional 30 minutes before being exposed to air and the solvent removed *in vacuo*. The gel like material was washed with acetone and allowed to dry under vacuum for 2 hours. Polymer 2.8 formed as a brown solid (0.8748 g, 74.5%).

Ferrocene norbornene 2.13

Carboxylic acid ferrocene (2.11) (0.8919 g, 3.92 mmol), bicyclo[2.2.1]hept-5-ene-2-methanol, mixture of *endo* and *exo* (0.65 mL, 5.08 mmol) (2.12), DCC (1.0016 g, 4.5 mmol), and DMAP (0.5416 g, 4.5 mmol) were dissolved in a solution of DCM (35 mL) and DMF (5 mL). The reaction was stirred under N_2 for 16 hours and then cooled to -19 °C for 2 hours. A white precipitate was removed via filtration and the filtrant was washed subsequently with 2.6 M HCl and DI water. The organic solution was then dried using $MgSO_4$ and the solvent removed *in vacuo*. The resulting red liquid was purified via column chromatography, using silica as the stationary phase and a 3:2 mixture of diethyl ether:hexanes as the mobile phase. (1.0758 g, 82.1%)

^{1}H NMR (300 MHz, acetone-d_6) δ = 6.22 (dd, J = 5.7, 3.0 , 1H), 6.14 (dt, J = 8.5, 5.7 , 1H), 6.04 (dd, J = 5.6, 2.9 , 1H), 4.78 (dd, J = 3.6, 1.8 , 3H), 4.45 (dd, J = 4.1, 2.1 , 3H), 4.32 (dd, J = 10.9, 6.4 , 1H), 4.23 (d, J = 4.1 , 7H), 4.09 (dd, J = 10.9, 9.0 , 0H), 3.95 (dd, J = 10.7, 6.7 , 1H), 3.76 (dd, J = 10.7, 9.4 , 1H), 3.00 (s, 1H), 2.84 (s, 2H), 2.80 (s, 0H), 2.77 (d, J = 0.9 , 1H), 2.57 – 2.45 (m, 1H), 1.97 – 1.85 (m, 1H), 1.86 – 1.76 (m, 1H), 1.46 (dd, J = 13.0, 5.2 Hz, 2H), 1.39 – 1.27 (m, 3H), 0.64 (ddd, J = 11.6, 4.4, 2.5, 1H).

^{13}C NMR (75 MHz, acetone-d_6) δ = 138.36, 137.78, 137.19, 133.07, 72.10, 72.05, 70.87, 70.84, 70.51, 68.52, 67.95, 50.06, 45.67, 44.90, 44.70, 43.14, 42.54, 39.34, 38.96.

Ferrocene Polymer (2.14)

Compound 2.13 (0.4988 g, 1.4 mmol) was dissolved in 5.0 mL of dry, degassed THF and stirred under an atmosphere of N_2. Grubbs' 2nd generation catalyst (0.0577 g, 0.068 mmol) was dissolved in 3.0 mL of dry, degassed THF and injected into the reaction. After 30 min., 5.0 mL of ethyl vinyl ether was added, after which the reaction was stirred for an additional 30 min. The solvent was then removed *in vacuo* and polymer 2.14 was isolated as a red rubber-like material. (0 .5732 g, 125.4%)

η^6-(benzyl alcohol) chromium(0) tricarbonyl (2.17)

Chromium hexacarbonyl (1.1062 g, 5.0 mmol) (2.15) and benzyl alcohol (0.26 mL, 2.5 mmol) (2.16) were stirred under a continuous flow of N_2 for 15 minutes. 20 mL of dry dioxane and 5 mL of dry THF were injected into the reaction, which was then heated to reflux and stirred for 5 days. The solvent was then removed *in vacuo* and the resulting solid dissolved in diethyl ether. This solution was then filtered through celite. Compound 2.16 was then purified through column chromatography with silica as the solid phase and a 3:2 mixture of diethyl ether:hexanes as the mobile phase and collected as a green-yellow solid.

^{1}H NMR (300 MHz, acetone-d_6): δ = 5.66 (4H, m), 5.52 (1H, tt, j = 5.93, 1.64), 4.43 (2H, s).

^{13}C NMR (75.4 MHz, acetone-d_6): δ = 235.08, 115.35, 95.82, 93.93, 93.72, 62.63.

Chromium norbornene 2.18

Compound 2.17 (0.2120 g, 0.87 mmol), bicyclo[2.2.1]hept-5-ene-2-carboxylic acid, mixture of *endo* and *exo* (0.25 mL, 1.7 mmol) (2.6), DCC (0.2078 g, 1.0 mmol), DMAP (0.1211 g, 1.0 mmol), and 10 mL of DCM were stirred under a continuous flow of N_2 for 16 hours. The reaction mixture was then cooled to -15 °C for 1 hour, after which a fine white precipitate was removed through filtration. The solvent was removed *in vacuo* and compound 2.5 was purified through column chromatography with silica as the solid phase and a 3:2 mixture of diethyl ether and hexanes as the mobile phase and collected as a green gel (0.3018 g, 74.7%)

^{1}H NMR (300 MHz, $CDCl_3$) δ = 6.18 (dd, *J* = 5.6, 3.1 , 2H), 6.16 – 6.11 (m, 1H), 6.10 – 6.06 (m, 1H), 5.86 (dd, *J* = 5.6, 2.9 , 2H), 5.40 – 5.24 (m, 17H), 4.80 (s, 2H), 4.75 (s, 5H), 3.22 (s, 2H), 3.05 (s, 1H), 3.03 – 2.94 (m, 2H), 2.91 (s, 3H), 2.27 (dd, *J* = 10.4, 4.4 , 1H), 1.96 – 1.84 (m, 4H), 1.51 – 1.33 (m, 9H), 1.31 – 1.21 (m, 4H), 0.79 (s, 1H).

^{13}C NMR (75.4 MHz, acetone-d_6) δ = 234.17, 234.14, 175.88, 174.28, 139.04, 138.91, 138.55, 137.17, 137.00, 136.54, 134.33, 133.27, 130.48, 129.59, 108.00, 107.85, 94.94, 94.83, 94.79, 94.73, 94.71, 94.41, 94.31, 90.41, 69.22, 64.97, 64.67, 50.96, 50.20, 50.09, 48.19, 47.39, 46.96, 46.80, 46.55, 46.42, 43.82, 43.66, 43.55, 43.39, 43.31, 42.45.

Chromium norbornene 2.18-*exo*

^{1}H NMR (300 MHz, acetone-d_6) δ 6.14 (td, J = 8.3, 5.6 , 2H), 5.75 (d, J = 6.2 , 2H), 5.69 (t, J = 6.2 , 2H), 5.62 (t, J = 6.0 , 1H), 4.91 (s, 1H), 3.07 (s, 1H), 2.91 (s, 1H), 2.29 (dd, J = 4.9, 3.5 , 1H), 1.98 – 1.88 (m, 1H), 1.75 (d, J = 14.5 , 1H), 1.51 (d, J = 8.3 Hz, 1H), 1.43 – 1.23 (m, 2H), 0.89 (dt, J = 10.0, 6.9 , 1H).

^{13}C NMR (75.4 MHz, acetone-d_6) δ = 234.11, 175.84, 138.89, 136.51, 107.83, 94.92, 94.73, 94.40, 64.95, 47.37, 46.94, 43.63, 42.43, 30.97.

Chromium polymer 2.19

Grubb's 2nd Generation catalyst (0.0427 g, 0.055 mmol) was dissolved in 3 mL of dry, degassed THF under an atmosphere of N_2. Compound 2.16 (0.5119 g, 1.10 mmol) was dissolved in 6 mL of dry, degassed THF and added to the catalyst solution. After 30 minutes, 5 mL of ethyl vinyl ether was added to halt polymerization and endcap the polymers. The solution was allowed to stir for an additional 30 minutes. The solvent was removed *in vacuo* and the resulting polymer 2.17 was collected as a green-yellow rubber like material (0.7972 g, 155.7%).

Chapter Three: Synthesis and Characterization of Mulitmetallic Polynorbornenes

3.1 Cationic iron-chromium copolymers

After the completion of the monometallic polymers, development of several multi-metallic species was undertaken, in order to determine what effects the addition of more metals into the polymeric materials might have on their properties. This was first done through the copolymerization of two monomers: the η^6-arene-chromium tricarbonyl containing **2.18** and either the ferrocene based **2.13** or the cationic iron based **2.7**. This was done *via* two different mechanisms, either a random copolymerization or a sequential polymerization in order to create block copolymers.

The first multi-metallic polymer was created *via* the random polymerization of **2.7** and **2.18** (Scheme 3.1), which resulted in a green, rubber like material being formed upon removal of the solvent.

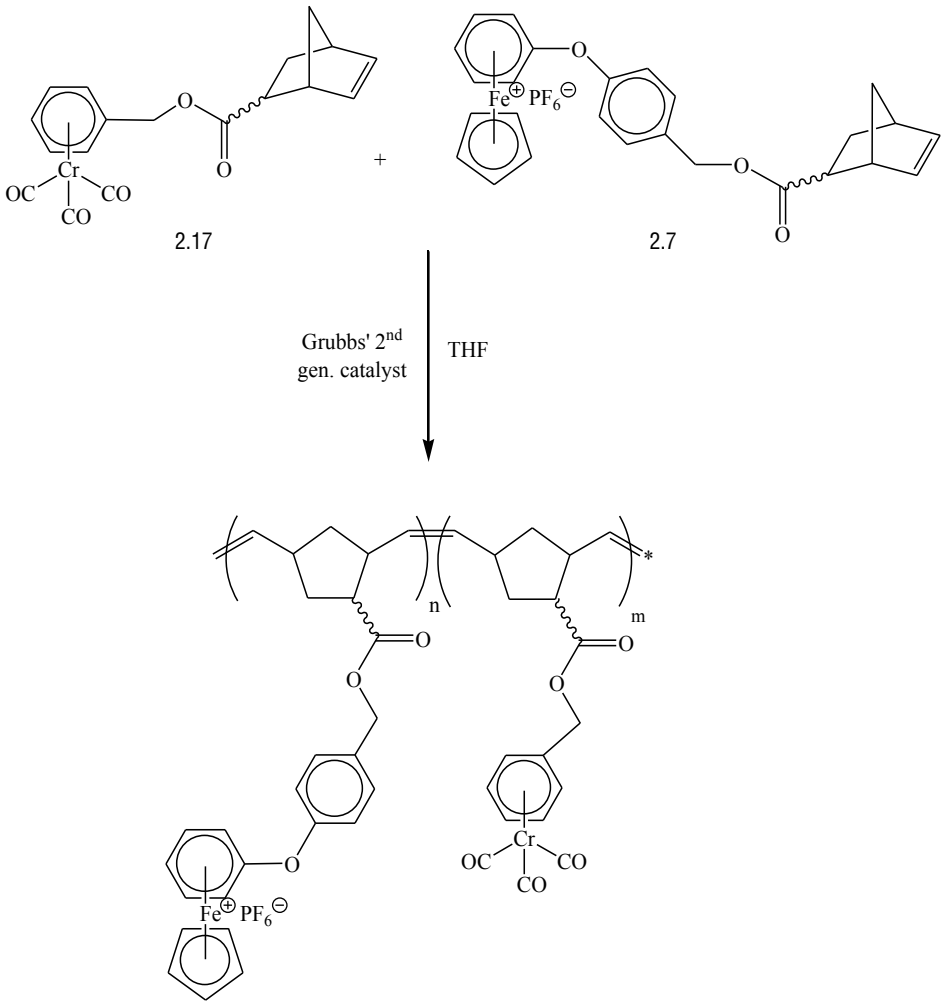

Scheme 3.1: Copolymerization of 2.7 and 2.17 to form random copolymer 3.1.

Despite repeated attempts and different solvents, it proved impossible to get polymer 3.1 into solution, which precluded solution NMR being performed for characterization. However, there was enough material generated that it was possible to perform solid state NMR on the compound (Figure 3.1). The most notable features are the peaks at 67.8 and 77.2 ppm, which correspond to the iron arene carbons, and the large peak at 132.3 ppm, which represents standard aromatics found in the cationic iron monomer.

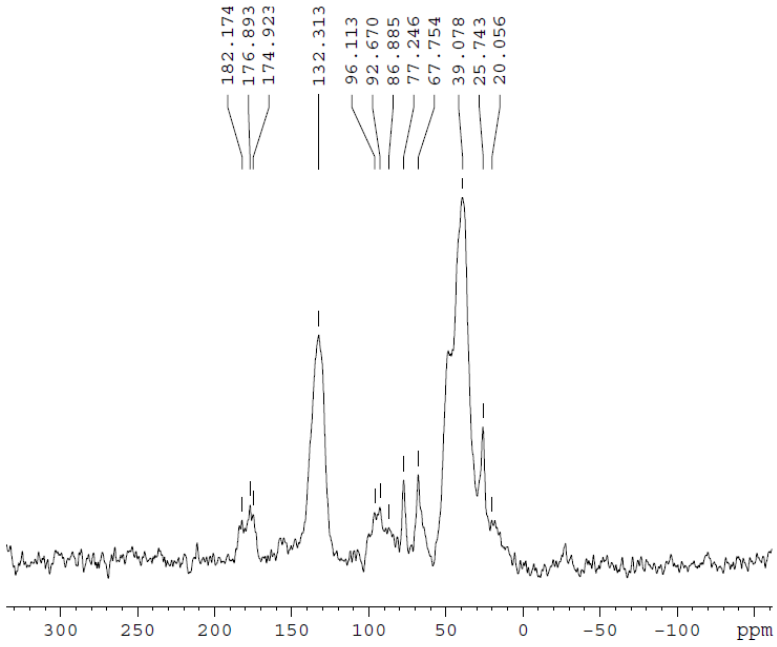

Figure 3.1: Solid state ^{13}C NMR spectrum of 3.1.

The polymer was then observed under an SEM in order to determine its surface morphology, which revealed a very smooth surface that was much more comparable to the chromium based polymer 2.19 than the globular surface of the cationic iron polymer 2.8.

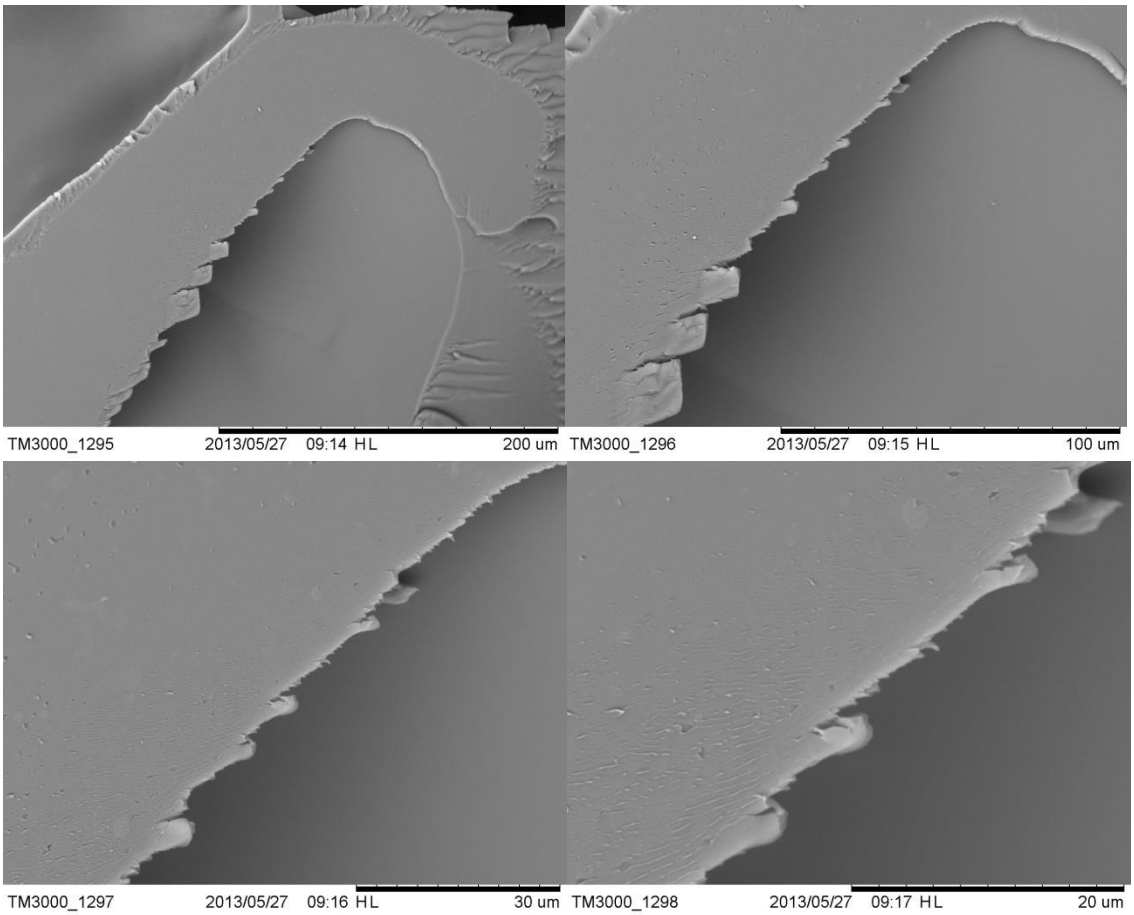

Figure 3.2: SEM images of copolymer 3.1 at 500 x (top left), 1000 x (top right), 2000 x (bottom left), and 4000 x magnification (bottom right).

The second polymerization mechanism was then undertaken, with the formation of the block copolymer 3.2 (Scheme 3.2). The monomers were added sequentially at 30 min. intervals, with the chromium monomer being added first, as the cationic iron polymer 2.8 fell out of solution during its formation, which would prevent the addition of a second monomer type.

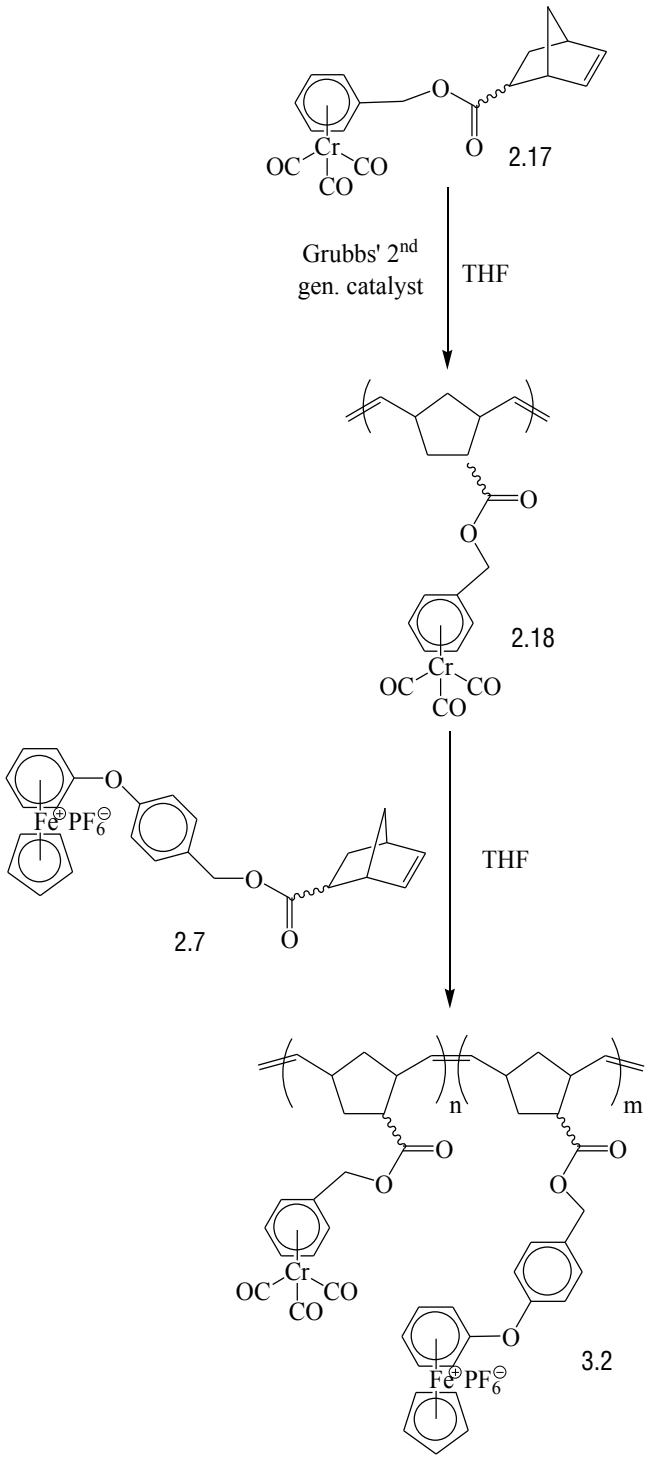

Scheme 3.2: Sequential polymerization of 2.17 and 2.7 to form block copolymer 3.2.

Again, 3.2 proved insoluble but did generate enough material for solid state NMR to be performed. The spectra was nearly identical to that of 3.1, but that is to be expected based on the type of experiment run (standard ^{13}C) and the similar makeup of the polymers.

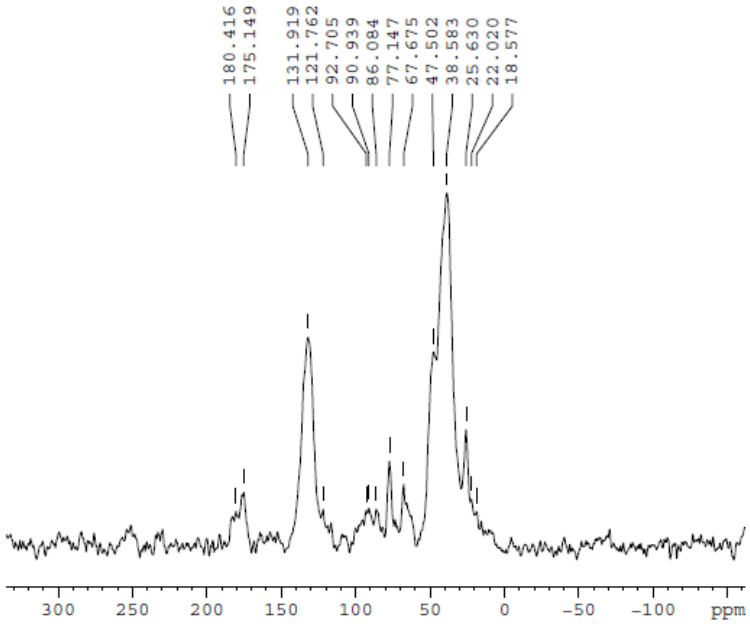

Figure 3.3: Solid state ^{13}C NMR spectrum of 3.2.

Examination of 3.2 under an SEM again revealed a very smooth surface morphology, similar to both the chromium polymer 2.19 and the random copolymer 3.1.

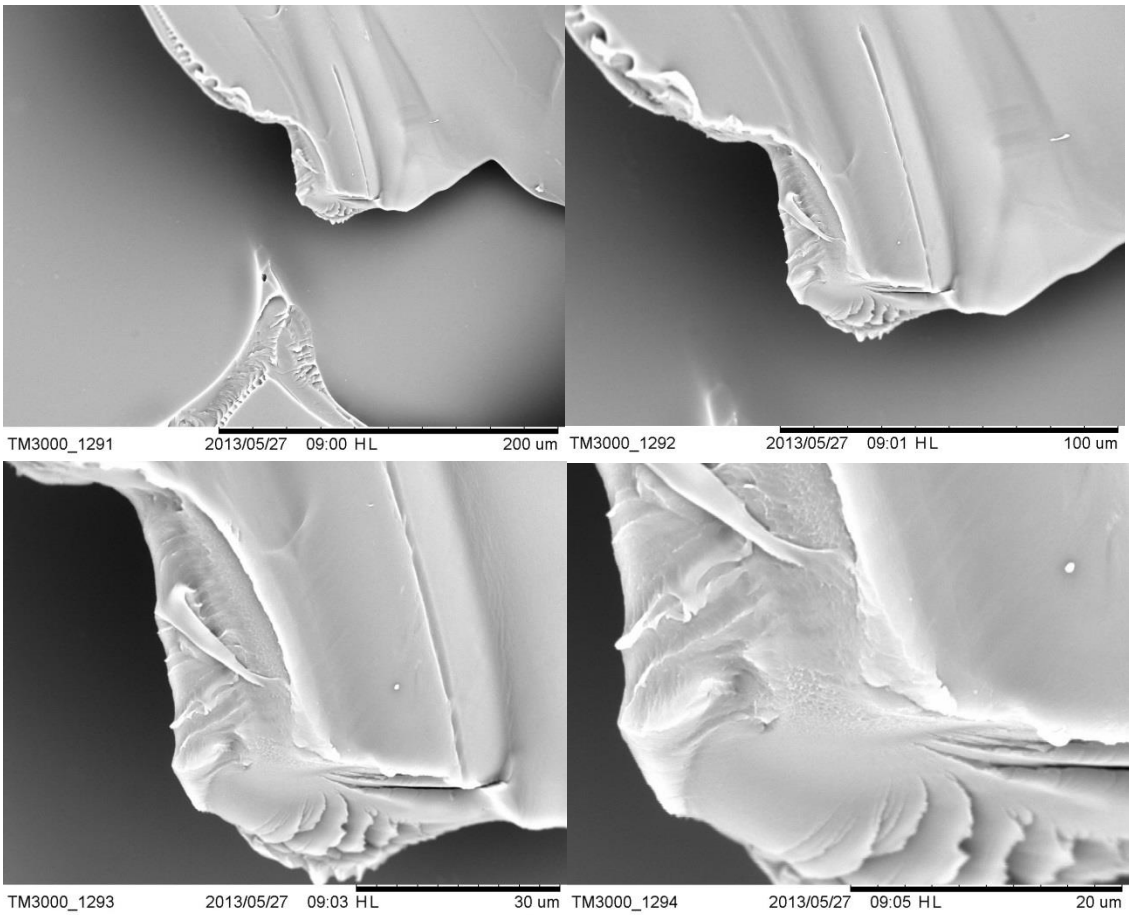

Figure 3.4: SEM images of block copolymer 3.2 at 500 x (top left), 1000 x (top right), 2000 x (bottom left), and 4000 x magnification (bottom right).

3.2 Ferrocene-chromium copolymers

Copolymerization was then performed using the neutral ferrocene based monomer 2.13 in addition to the chromium monomer. Again, this was initially performed using a random polymerization mechanism.

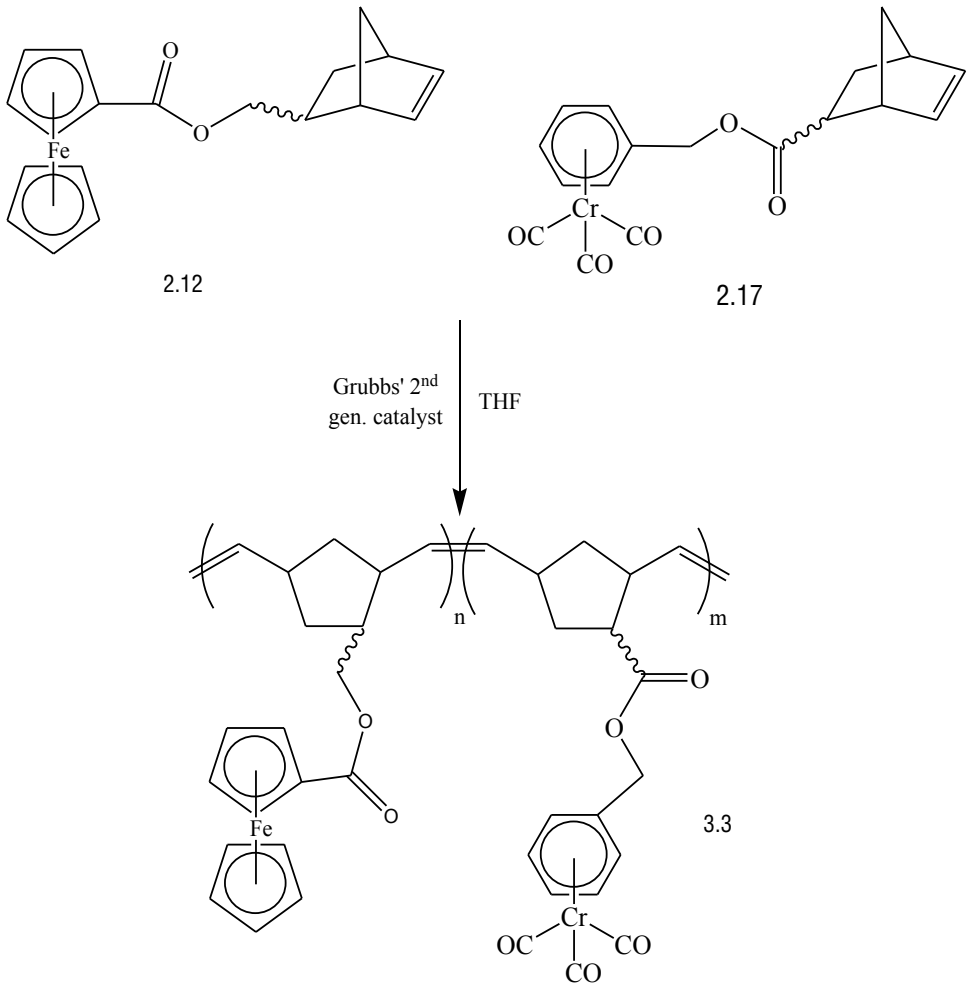

Scheme 3.3: Copolymerization of 2.12 and 2.17 to form random copolymer 3.3.

Unlike the previous two polymers, there was not enough material generated to perform solid state NMR, as the material was very fine crystalline powder. Confirmation of successful polymerization can be found in the materials insolubility, as it again proved impossible to get into solution. Observation under an SEM revealed a smooth surface morphology.

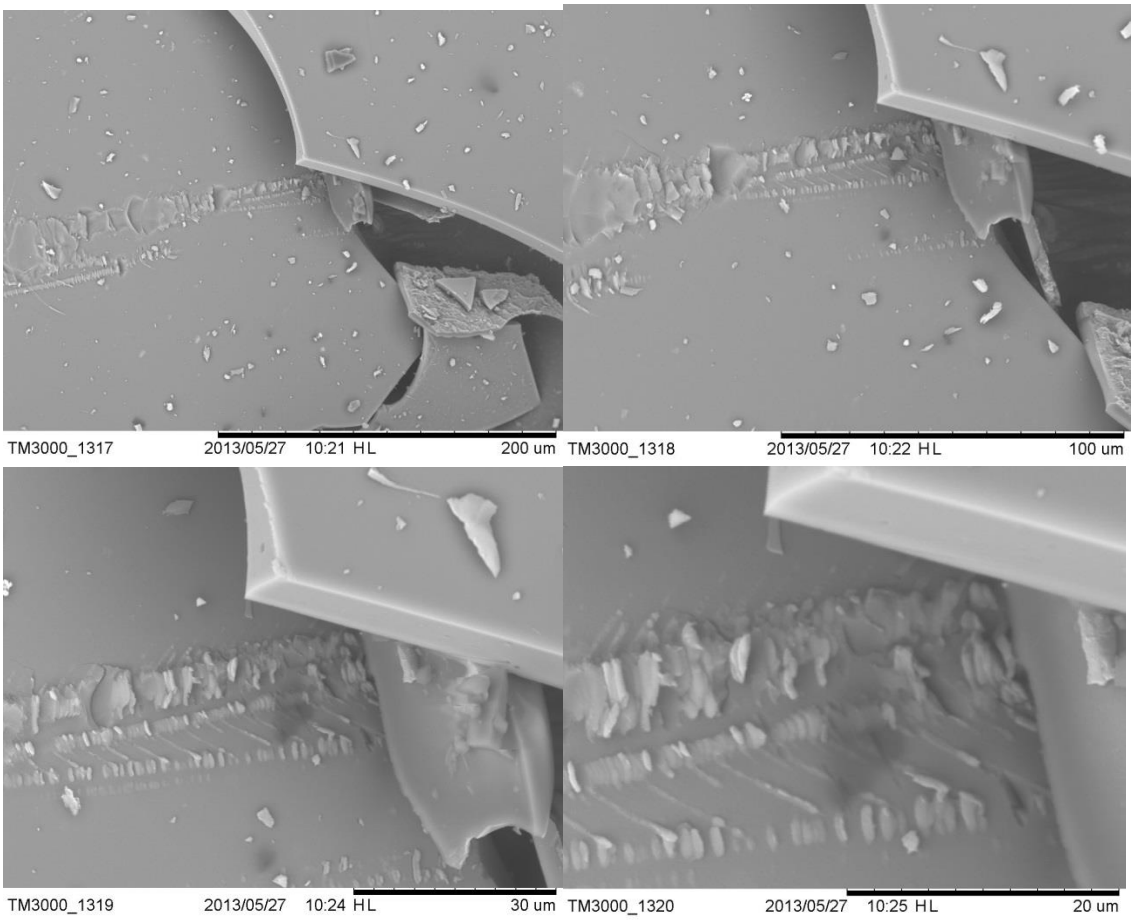

Figure 3.5: SEM images of copolymer 3.3 at 500 x (top left), 1000 x (top right), 2000 x (bottom left), and 4000 x magnification (bottom right).

Although there were no issues when generating the ferrocene polymer 2.14 with regards to the material becoming insoluble as it is formed, it was still added second in sequence after the polymerization of 2.18 (Scheme 3.4).

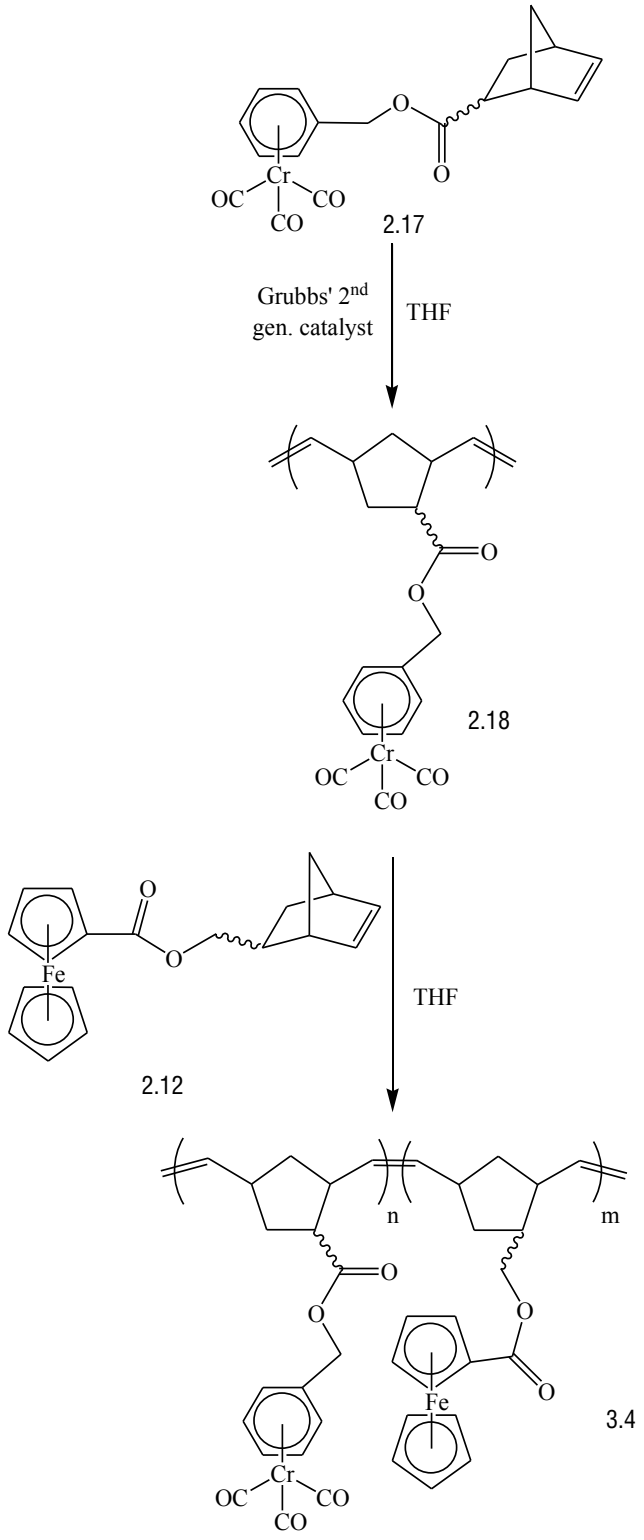

Scheme 3.4: Sequential polymerization of 2.17 and 2.12 to form block copolymer 3.4.

Examination of copolymer 3.4 revealed a very interesting surface morphology, one that differed from all of the other polymers synthesized. The outer surface of the compound was completely covered in very small crystals (Figure 3.6). Examination at 4000 x magnification reveals that the polymer possess the same smooth surface as the rest of the polymers, with the crystalline pieces most likely being the ends of the ferrocene block. This result was not seen in any of the other copolymers, as 3.4 was the only one synthesized *via* the addition of the ferrocene monomer 2.13 as the final synthetic step.

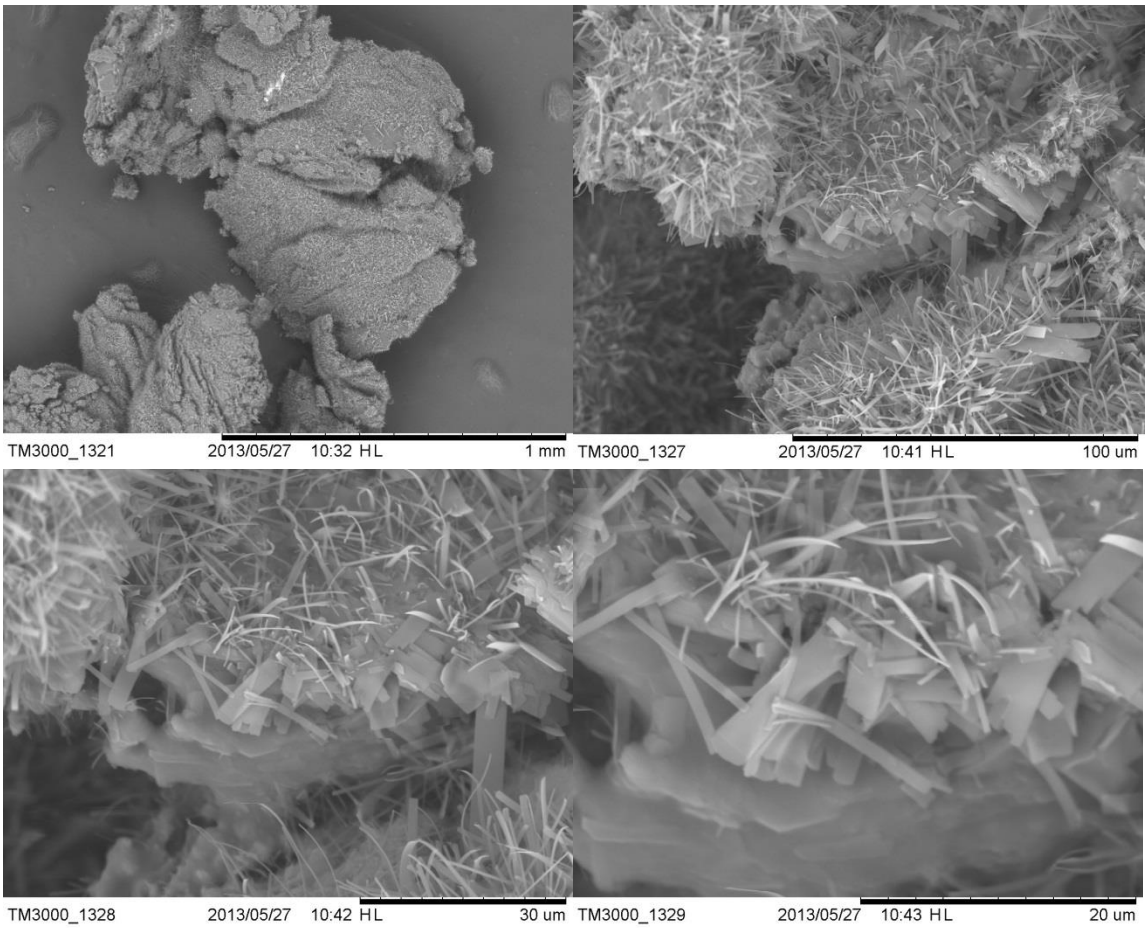

Figure 3.6: SEM images of block copolymer 3.4 at 100 x (top left), 1000 x (top right), 2000 x (bottom left), and 4000 x magnification (bottom right).

3.3 Cationic iron-chromium-ferrocene copolymers

After the completion of the copolymers containing two metal species, copolymerizations of all three of the unique monomers was undertaken, in order to create materials with the highest possible number of metals. As before, this was first done through a random polymerization (Scheme 3.5).

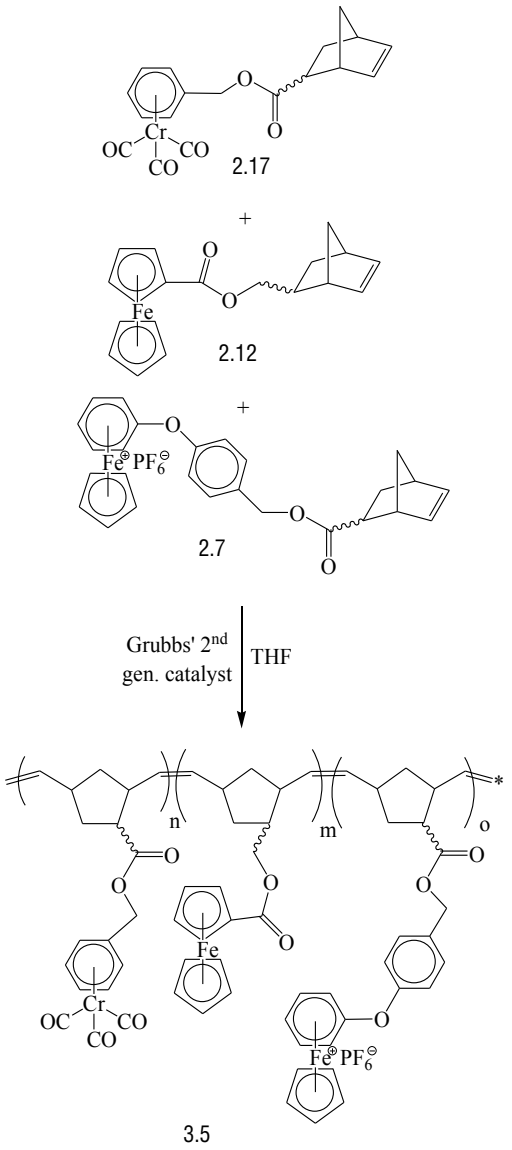

Scheme 3.5: Copolymerization of 2.7, 2.12, and 2.17 to form copolymer 3.5.

Once again, after the removal of all solvent, it proved impossible to get copolymer 3.5 to return into solution.

Examination of 3.5 under an SEM (Figure 3.7) revealed that the polymer exhibited the same smooth surface as seen previously. However, there did appear to be sections of the polymer that appeared rough and globular. This occurred in an area that revealed the interior of the polymer, making this polymer the best candidate for future conversion into nanotubes.

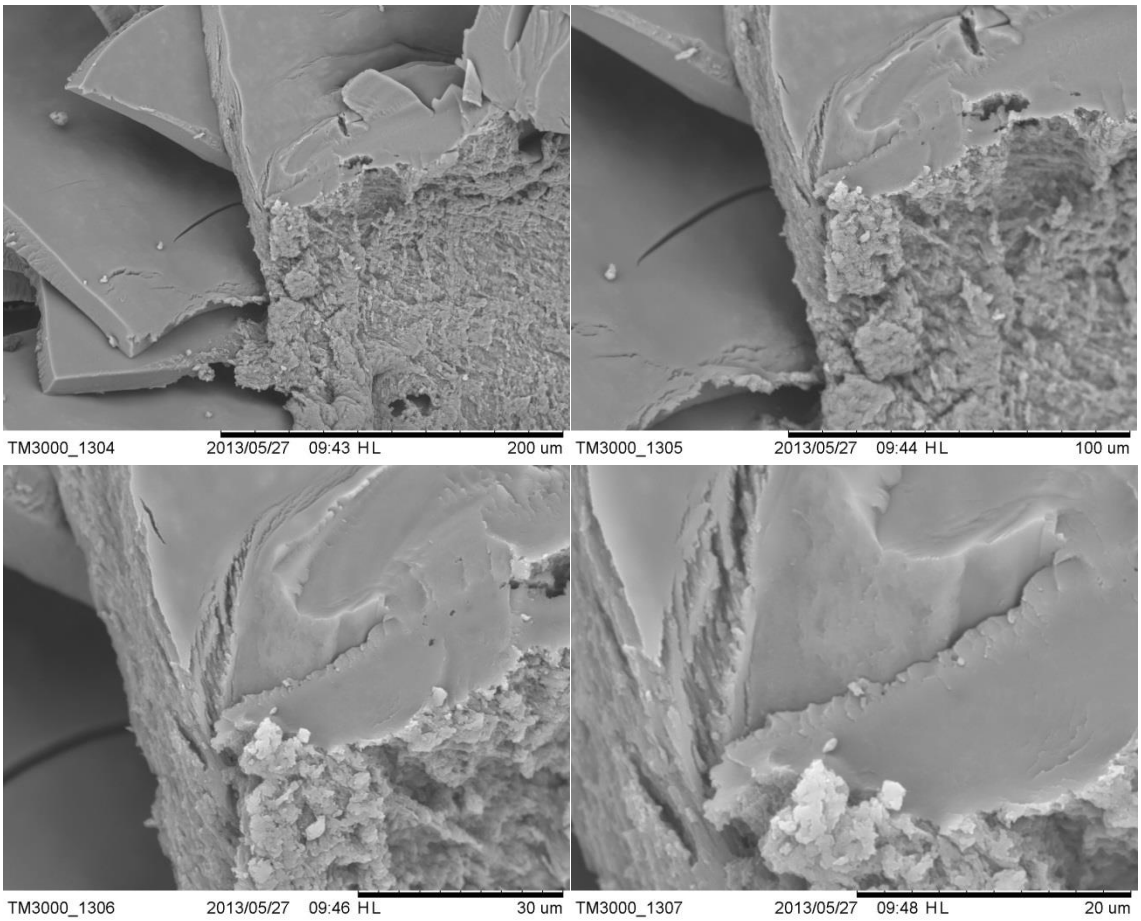

Figure 3.7: SEM images of copolymer 3.5 at 500 x (top left), 1000 x (top right), 2000 x (bottom left), and 4000 x magnification (bottom right).

The formation of a block copolymer containing each of the three monomers was performed via sequential addition of 2.18, 2.13, and 2.7 at 30 min. intervals, in order to allow for the formation of large blocks. The cationic iron monomer 2.7 was again added last in order to prevent any of the newly formed polymers from falling out of solution prior to completion.

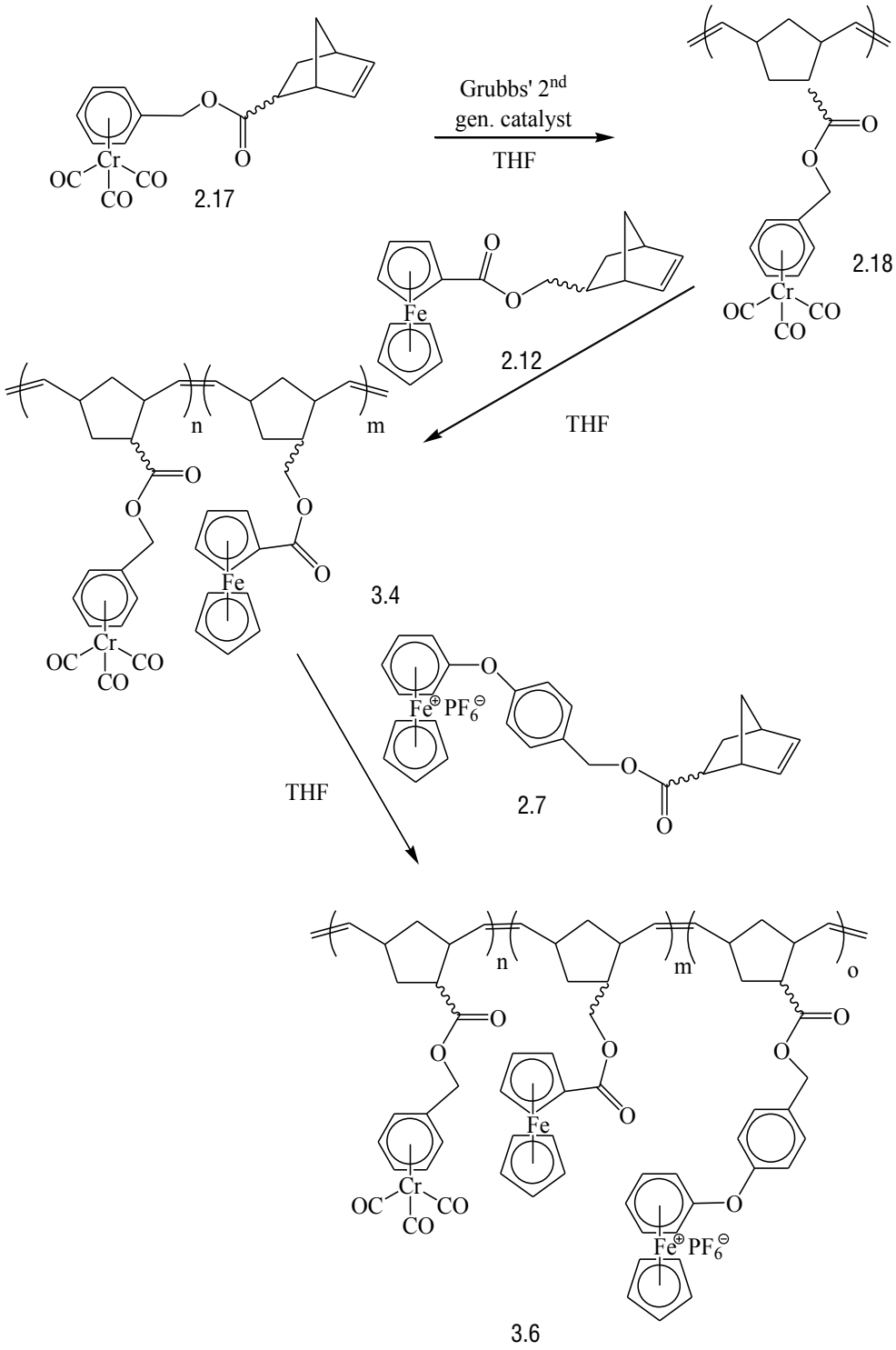

Scheme 3.6: Sequential polymerization of 2.17, 2.12, and 2.7 to form block copolymer 3.6.

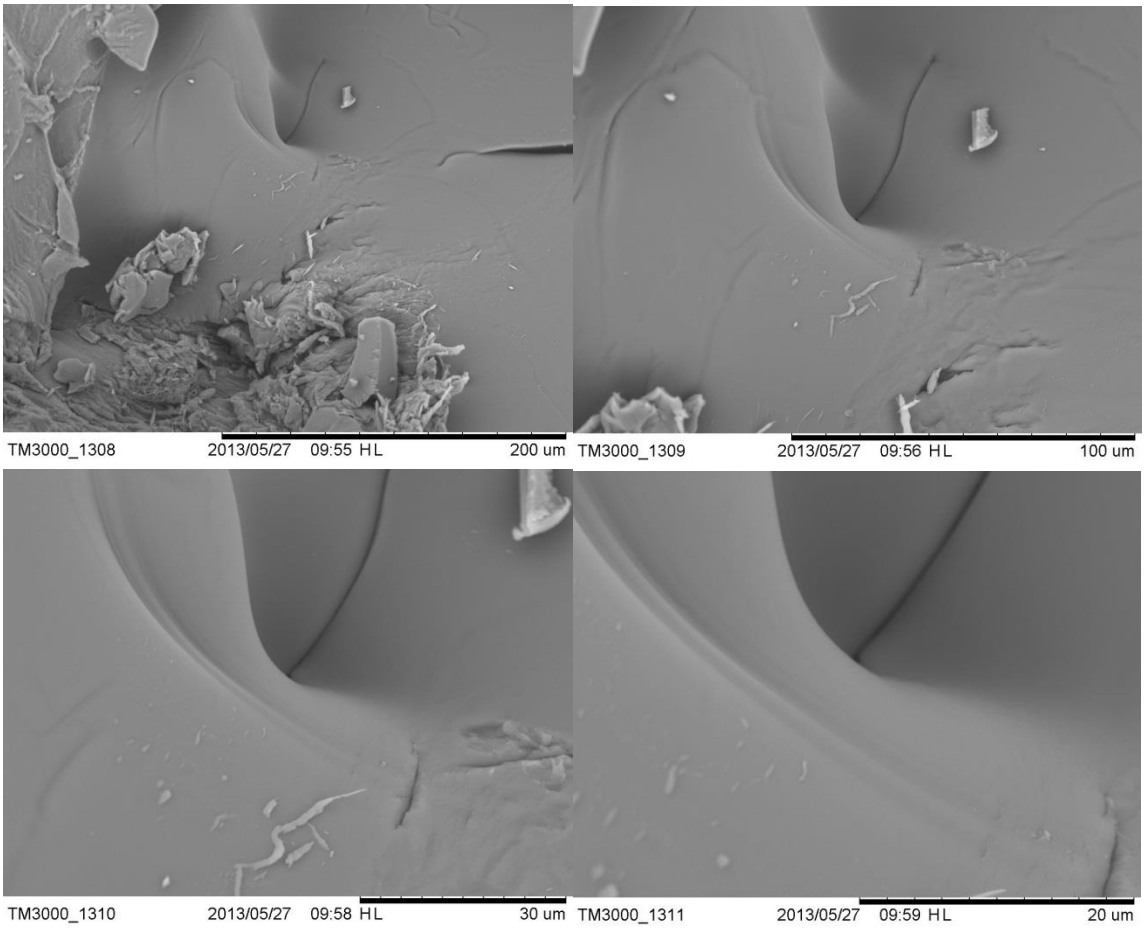

Figure 3.8: SEM images of block copolymer 3.6 at 500 x (top left), 1000 x (top right), 2000 x (bottom left), and 4000 x magnification (bottom right).

3.4 Thermal analysis

As with the polymers formed in Chapter Two, each of the copolymers began showed gradual thermal decomposition between 75 and 120 °C as a result of the release of solvent trapped within the polymers. However, unlike the single metal polymers, each of the copolymers showed very gradual thermal decomposition, most likely as a result of the loss of the chromium bound carbonyls until reaching a point of near instantaneous

decomposition of approximately 50% or greater of the total mass of the samples. Initial runs with larger samples showed clear indication of explosive decomposition at this point. However, when utilizing smaller sample sizes, this was avoided.

The copolymers containing only the cationic iron moiety (3.1 and 3.2) in addition to the chromium showed a higher degree of thermal stability, undergoing rapid decomposition at 403 and 413 °C, respectively. The introduction of the ferrocene component into the polymers resulted in a decrease in the temperature at which this occurs, as 3.3 and 3.4 decomposed rapidly at 330 and 376 °C, respectively. Additionally, it appears that the creation of a block copolymer results in the slight increase in the thermal stability of the materials.

Copolymers 3.5 and 3.6 showed near identical temperatures for this decomposition (approximately 375 °C), indicating that, unlike the copolymers containing only the two different metal types, creation of a block copolymer as opposed to a random mixture copolymer has no effect on the thermal decomposition.

TGA was also run on every sample under an atmosphere of nitrogen. These runs showed very similar decompositions, although they did not occur nearly as rapidly.

Table 3. 1: Thermogravimetric analysis of copolymers under air.

Polymer	Step 1	Step 2	Step 3	Step 4
3.1	101, 12%	216, 11%	296, 11%	404, 65%
3.2	119, 9%	225, 17%	414, 48%	472, 17%
3.3	, 11%	281, 14%	330, 75%	374, 23%
3.4	111, 10%	377, 53%	-	-
3.5	76, 10%	277, 11%	376, 61%	-
3.6	89, 17%	374, 62%	-	-

Examination of the material remaining after the completion of the TGA shows that approximately the appropriate amount of metal oxide residues remain. However, this is very imprecise due to the mixed nature of the polymers themselves.

Table 3.2: Polymer remaining after the completion of TGA.

Polymer	Air	Nitrogen	Cr%	Fe%	Cr_nO_m%	FeO%
3.1	0%	17.3%	5.1%	5.5%	6.7/14.9%	7.0%
3.2	8.5%	16.7%	5.1%	5.5%	6.7/14.9%	7.0%
3.3	0%	2.3%	6.5%	7.0%	8.5/19.0%	9.0%
3.4	36.4%	0%	6.5%	7.0%	8.5/19.0%	9.0%
3.5	17.6%	13.7%	3.7%	8.1%	4.9/11.0%	10.4%
3.6	21.0%	29.4%	3.7%	8.1%	4.9/11.0%	10.4%

Copolymers 3.1 and 3.2 also show a reduced T_g when compared to both the monometallic polymers, 2.8 and 2.13. The reverse is true for any of the compounds containing the ferrocene moiety, as all four polymers with this component showed an increased transition temperature when compared to the monometallic polymers.

Table 3.3: Differential scanning calorimetry of copolymers.

Polymer	T_g (°C)
3.1	64
3.2	47
3.3	76
3.4	83
3.5	88
3.6	76

From this data, it can be concluded that while the inclusion of the ferrocene moiety into the polymers results in a decrease in the thermal stability, it does result in a significant increase in the temperature at which the compounds undergo a glass transition.

3.5 Summary

A series of copolymers of iron and chromium were synthesized *via* olefin metathesis polymerization using Grubbs' 2nd generation catalyst. There were two different iron containing monomers used, one which was neutral ferrocene based and the other contained the cationic η^6-arene-η^5-cyclopentadienyl iron(II) species. These were copolymerized with an η^6-arene-chromium tricarbonyl containing compound. The copolymers containing cationic iron and chromium were characterized using solid state NMR and all polymers were observed under an SEM. The thermal properties were investigated, with the TGA revealing very rapid decompositions for all compounds and glass transition temperatures between 30 and 80 ° C.

3.6 Experimental

All compounds containing the η^6-arene-η^5-cyclopentadienyl iron(II) moiety were kept out of the light when not being directly worked with. All compounds were stored under an atmosphere of nitrogen to prevent decomposition of the η^6-arene-chromium tricarbonyl moiety.

Polymer 3.1

Compound 2.18 (0.1940 g, 0.40 mmol) was dissolved in 3.3 mL of dry THF and compound 2.7 (0.2459 g, 0.40 mmol) was dissolved in 5.0 mL of dry THF. The two solutions were combined under an atmosphere of N_2. Grubbs' 2nd generation catalyst (0.0342 g, 0.04 mmol) was dissolved in 2.0 mL of dry THF and injected into the reaction mixture and allowed to stir for 30 min., after which 5.0 mL of ethyl vinyl ether was added. After stirring for an additional 30 min., the solvent was removed *in vacuo* and polymer 3.1 was isolated as brown-yellow crystalline powder (0.5251 g, 110.8%)

Polymer 3.2

Compound 2.18 (0.1940 g, 0.40 mmol) was dissolved in 3.3 mL of dry THF and was stirred under an atmosphere of N_2. Grubbs' 2nd generation catalyst (0.0161 g, 0.02 mmol) was dissolved in 2.0 mL of dry THF and injected into the reaction mixture. After 30 min., compound 2.7 (0.2459 g, 0.40 mmol) was dissolved in 5.0 mL of dry THF and injected into the reaction mixture. After 30 min., 5.0 mL of ethyl vinyl ether was injected and the reaction allowed to stir for an additional 30 min. The solvent was then removed

in vacuo and polymer 3.2 was collected as a brown-yellow rubber like material (0.4963 g, 108.8%)

Polymer 3.3

Compound 2.18 (0.0307 g, 0.065 mmol) was dissolved in 3.0 mL of dry THF and compound 2.13 (0.0231 g, 0.065 mmol) was dissolved in 4.0 mL of dry THF. The two solutions were combined under an atmosphere of N_2. Grubbs' 2nd generation catalyst (0.0055 g, 0.0065 g) was dissolved in 2.0 mL of dry THF and injected into the reaction mixture. After 30 min., 3.0 mL of ethyl vinyl ether was injected. The reaction was stirred for an additional 30 min., after which the solvent was removed *in vacuo* and polymer 3.3 was isolated as a brown-yellow crystalline powder (0.0809 g, 136.4%)

Polymer 3.4

Compound 2.18 (0.0307 g, 0.065 mmol) was dissolved in 3.0 mL of dry THF and stirred under an atmosphere of N_2. Grubbs' 2nd generation catalyst (0.0055 g, 0.0065 mmol) was dissolved in 2.0 mL of dry THF and injected into the reaction. After stirring for 30 min., compound 2.13 (0.0231 g, 0.065 mmol) was dissolved in 4.0 mL of dry THF and injected. After another 30 min., 3.0 mL of ethyl vinyl ether was injected and allowed to stir for an additional 30 min. The solvent was then removed *in vacuo* and polymer 3.4 was isolated as a brown-yellow crystalline powder (0.0791 g, 133.4%).

Polymer 3.5

Compound 2.18 (0.0307 g, 0.065 mmol) was dissolved in 3.0 mL of dry THF, compound 2.13 (0.0221 g, 0.065 mmol) was dissolved in 4.0 mL of dry THF, and compound 2.7 (0.0382 g, 0.065 mmol) was dissolved in 2.0 mL of dry THF. The three solutions were combined under an atmosphere of N_2 and Grubbs' 2nd generation catalyst (0.0085 g, 0.195 mmol) dissolved in 2.0 mL of dry THF was injected. After 30 min., 3.0 mL of ethyl vinyl ether was injected. The reaction mixture was allowed to stir for an additional 30 min. before the solvent was removed *in vacuo*. Polymer 3.5 was isolated as a brown crystalline powder (0.0101 g, 10.2%).

Polymer 3.6

Compound 2.18 (0.0307 g, 0.065 mmol) was dissolved in 3.0 mL of dry THF and stirred under an atmosphere of N_2. Grubbs' 2nd generation catalyst (0.0028 g, 0.0030 mmol) was dissolved in 2.0 mL of dry THF and injected. At 30 min. intervals, compound 2.13 (0.0240 g, 0.065 mmol) dissolved in 4.0 mL of THF, compound 2.7 (0.0382 g, 0.065 mmol) dissolved in 2.0 mL of dry THF, and 3.0 mL of ethyl vinyl ether were injected. After stirring for an additional 30 min. after the final injection, the solvent was removed *in vacuo* and polymer 3.6 was isolated as a dark brown crystalline powder (0.1220 g, 127.5%).

4.1 Ferrocene-chromium bimetallic test compound

As previously mentioned in Chapter One, ferrocene and chromium containing compounds have previously been reported[55]. However, none of these were produced in significant yields (<20%) and none contained an ester functional group within the compound. Therefore, a simple test compound was developed in order to aid in developing the strongest possible synthetic route. As stated in Chapter Two, the addition of multiple substituents onto the arene can play a significant role in its ability bind chromium. So, prior to working with the necessary substituted compounds required for full polymer synthesis, the simplest arene possible that could be coordinated while still being bound to ferrocene, benzyl alcohol (2.16), was selected. However, unlike in Chapter Two, the chromium coordination will be performed after the Steglich esterification, as repeated attempts were made to improve the yields of the chromium coordination.

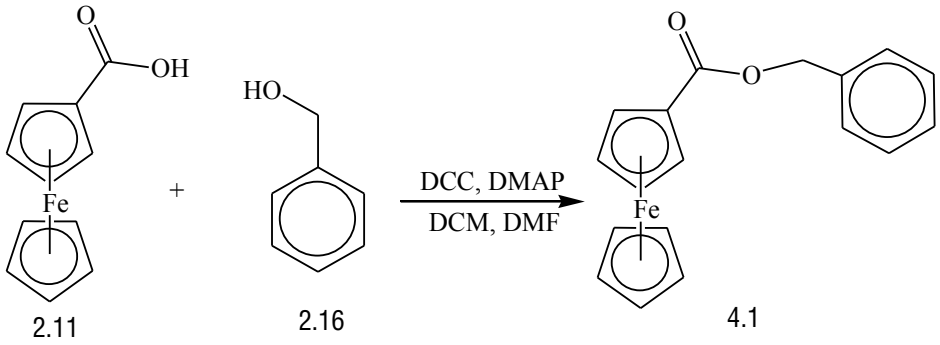

Scheme 4.1: Synthesis of 4.1 via Steglich Esterification.

It was found that the optimal conditions for the production of 4.2 involved refluxing compound 4.1 with chromium hexacarbonyl in 1,4-dioxane and THF (6:1 ratio), under a continuous flow of N_2 for 48 hours. Attempts to improve upon this synthesis using the *tris*-acetonitrile chromium tricarbonyl and the η^6-naphthalene chromium tricarbonyl regents proved unsuccessful, as did the use other high boiling ethers as the solvent.

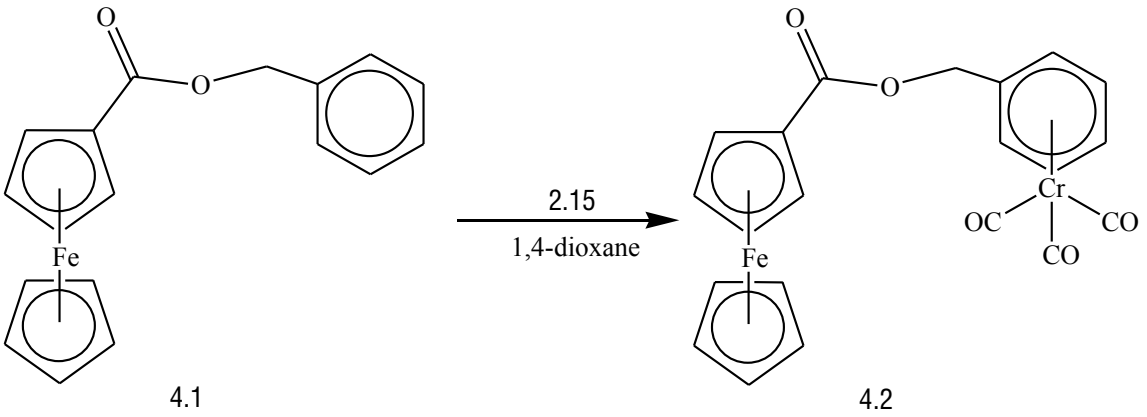

4.1 4.2

Scheme 4.2: Coordination of chromium hexacarbonyl to form compound 4.2.

Upon purification, the ^{1}H NMR spectrum of 4.2 showed a significant change in the aromatic resonances due to the complexation of the chromium tricarbonyl. As seen in Figure 4.1 (label A), these peaks had an upfield shift from 7.51, 7.44, and 7.38 ppm to 5.84, 5.74, and 5.65 ppm.

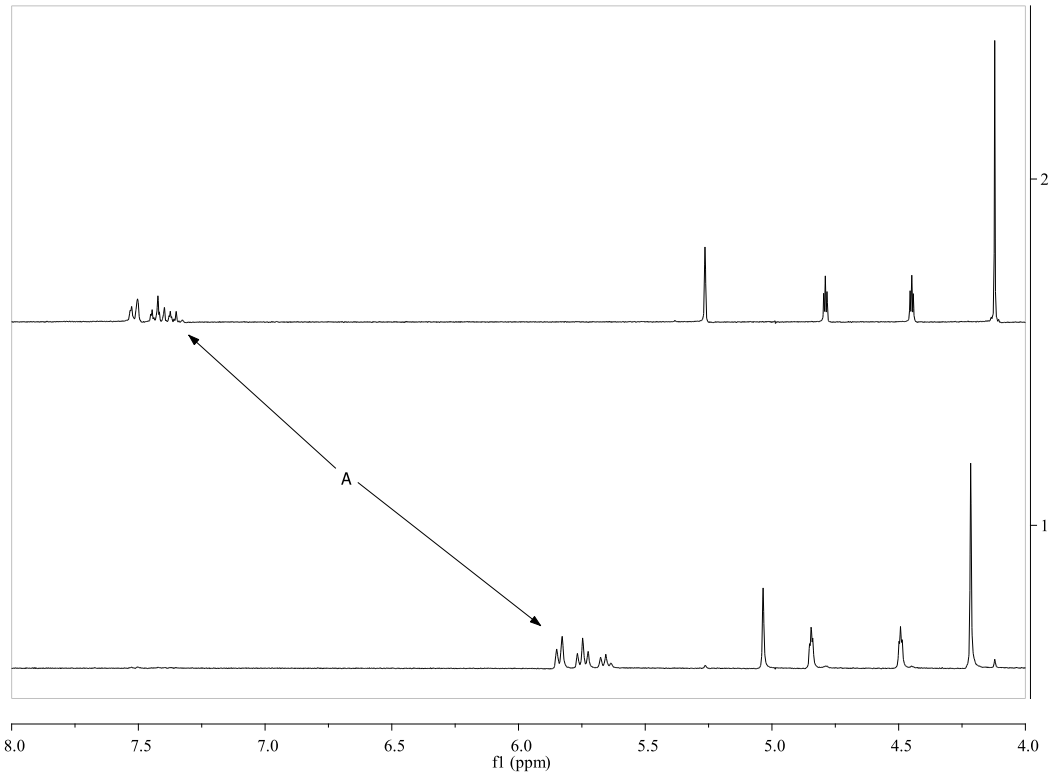

Figure 4.1: A section of the ^{1}H NMR spectra of 4.1 (top) and 4.2 (bottom), illustrating the effects of chromium coordination.

Comparison of the ^{13}C NMR spectra of 4.1 and 4.2 also clearly shows the effects of the inclusion of chromium into the compound. As seen in Figure 4.2, the carbon signal due to the chromium bound carbonyl ligand appears at 234.2 ppm (label A), as well as the resulting upfield shift of the aromatic carbons (label B), from 128.8, 128.6, and 128.4 ppm to 94.9, 94.9, and 94.4 ppm.

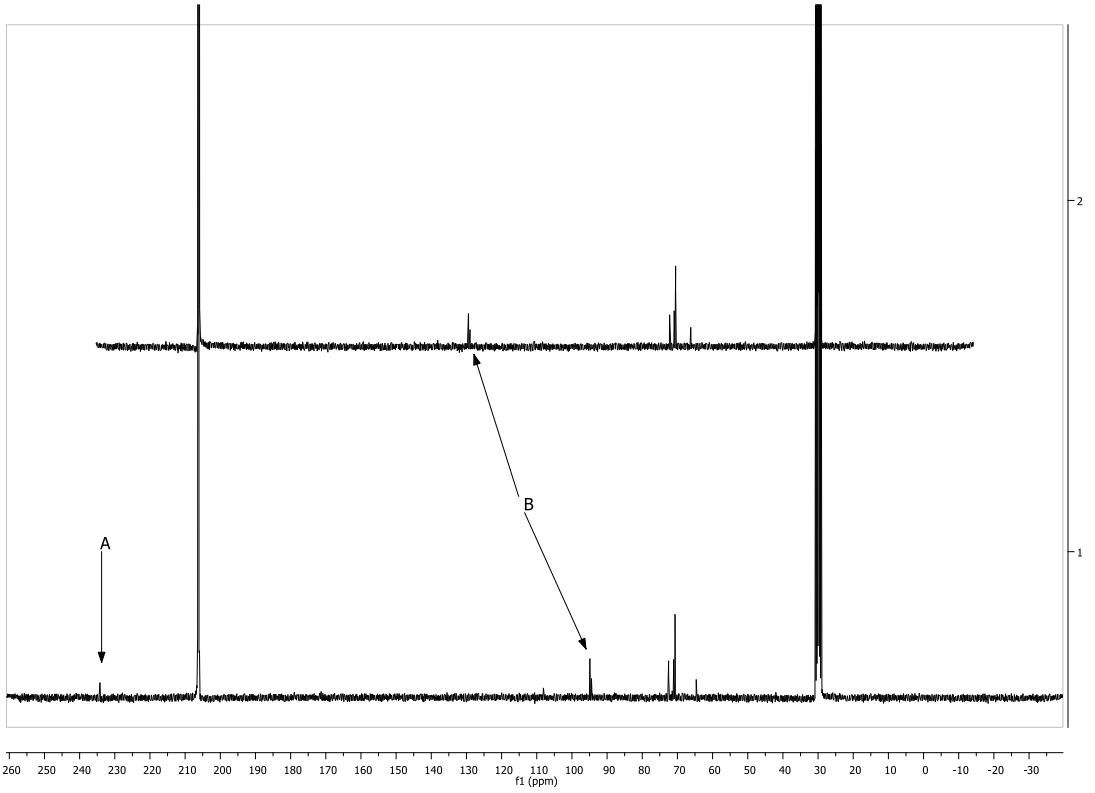

Figure 4.2: ^{13}C NMR spectra of 4.1 (top) and 4.2 (bottom), illustrating the effects of chromium coordination.

In order to confirm that the resulting change in the aromatic protons was a result of the η^6 coordination of the chromium, crystals of 4.2 were successfully grown and analyzed using X-ray crystallography.

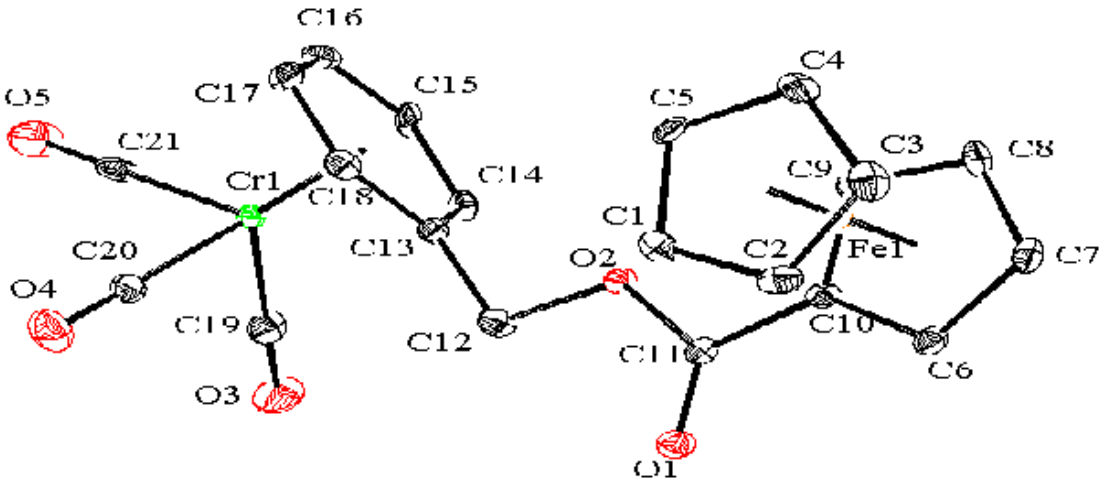

Figure 4.3: ORTEP diagram of 4.2.

Table 4.1: Comparison of bond lengths and angles between Compounds 4.1 and 4.2. All lengths are reported in Å and angles are reported in degrees.

Selected Bond Lengths	**4.1**[97]	**4.2**
Arene ring C-C avg.	1.389	1.406
C12-C13	1.503	1.505
O2-C12	1.471	1.443
C11-O1	1.211	1.201
Fe1-C1-5 plane	1.653	1.642
Fe1-C6-10 plane	1.643	1.634
Cr1-C13-18 plane	-	1.706
Cr1-C19	-	1.840
Cr1-C20	-	1.857
Cr1-C21	-	1.846
C19-O3	-	1.160
C20-O4	-	1.134
C21-O5	-	1.136
C1-5/C13-18 angle	88.06	88.36
C6-10/C13-18 angle	88.48	89.23

Comparison of the bond lengths of 4.2 to the literature structure of the chromium free 4.1 shows very little change in the geometric structure as a result of the binding of the chromium to the free arene[97].

4.3 Synthesis of a ferrocene-chromium bimetallic norbornene

After successfully synthesizing compound 4.2, the focus turned to creating functionalized versions of the compound, in order to be able to incorporate the norbornene functional group necessary to carry out the desired polymerizations. This was done by replacing benzyl alcohol (2.16) in Scheme 4.1 with 1,4-benzenedimethanol (4.3).

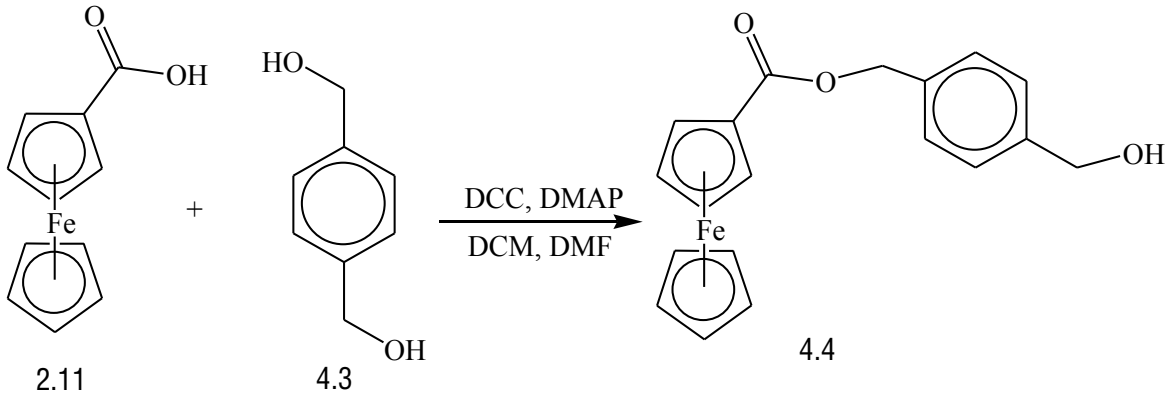

2.11 4.3 4.4

Scheme 4.3: Synthesis of Compound 4.4.

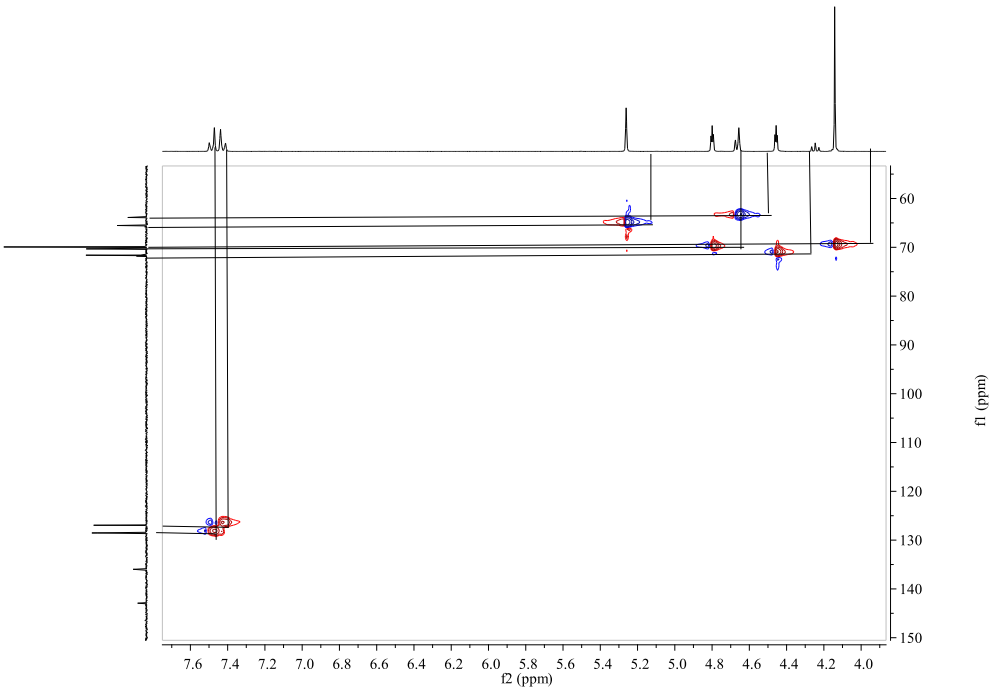

Figure 4.4: Portion of the HSQC NMR spectrum of 4.4, showing all relevant signals.

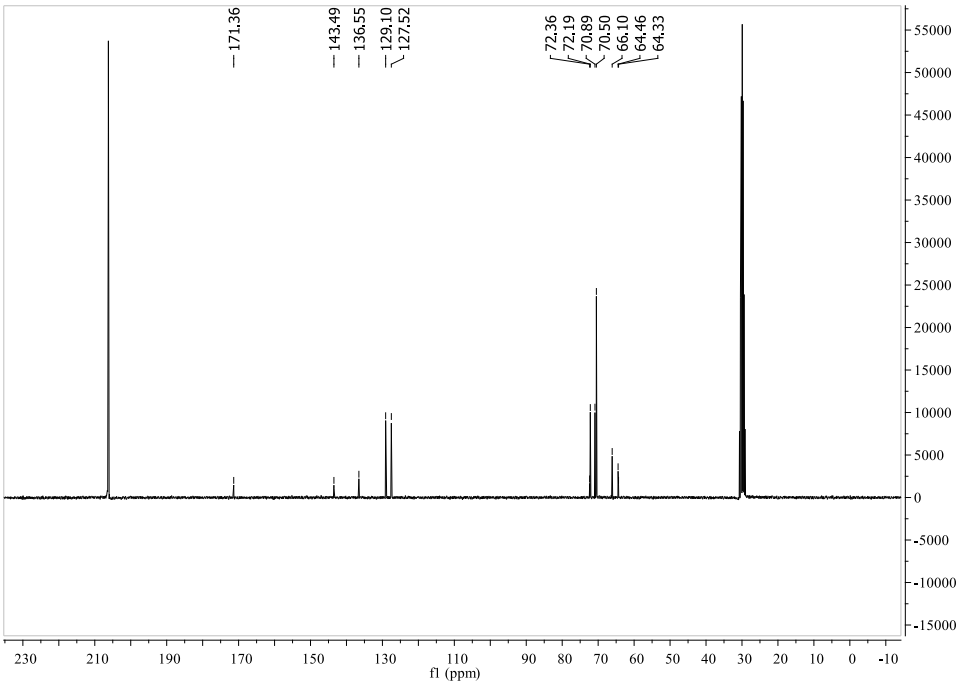

Figure 4.5: ^{13}C NMR spectrum of 4.4.

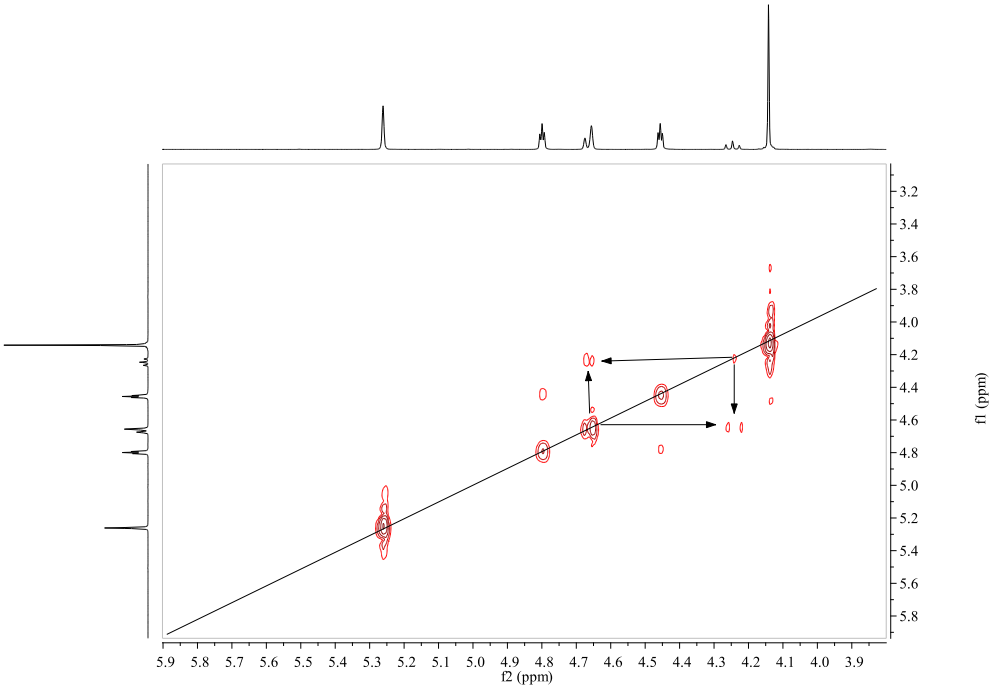

Figure 4.6: Section of the COSY NMR of 4.4, highlighting correlations between the free alcohol and the benzylic CH_2, labelled B in Figure 4.7.

Using the HSQC NMR (Figure 4.4), COSY NMR (Figure 4.6), and the ^{13}C NMR (Figure 4.5) spectra, a full assignment of signals for 4.4 was performed (Figure 4.7).

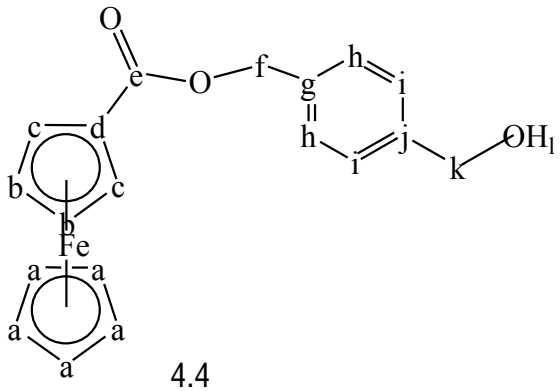

4.4

Figure 4.7: Atom labels for 4.4.

Table 4.2: NMR signal assignments for 4.4.

Signal	^{1}H NMR δ	^{13}C NMR δ
a	4.13	70.50
b	4.44	70.89
c	4.79	72.19
d	-	72.36
e	-	171.36
f	5.25	66.10
g	-	143.49
h	7.47	129.10
i	7.41	127.52
j	-	136.55
k	4.65	64.46
l	4.23	-

Compound 4.4 now has a free alcohol to which norbornene can attach. Due to the success of incorporating chromium into compounds prior to this synthetic step (Scheme 2. 9), 4.4 was reacted with chromium hexacarbonyl (2.15) by refluxing in 1,4-dioxane and THF for 5 days.

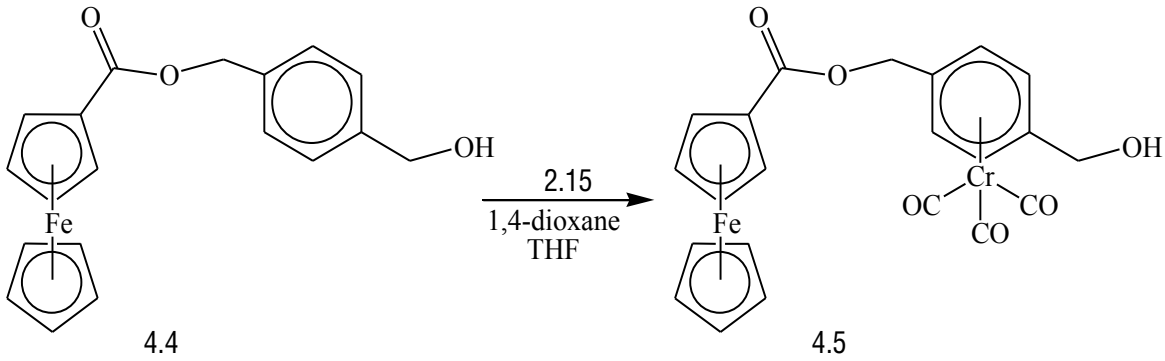

4.4 4.5

Scheme 4.4: Chromium coordination to form compound 4.5.

As seen with 4.2, the incorporation of the chromium results in a significant upfield shift of the aromatic protons, specifically from 7.47 and 7.41 ppm to 5.90 and 5.76 ppm

(Figure 4.8, label A), as well as the upfield shift of the aromatic carbons from 143.5, 136.6, 129.1, and 127.5 ppm to 114.4, 106.5, 95.2, and 92.9 ppm (Figure 4.8 label B). The inclusion of the chromium is also clearly shown by the appearance of the chromium bound carbonyl signal at 234.2 ppm (Figure 4.9 label A).

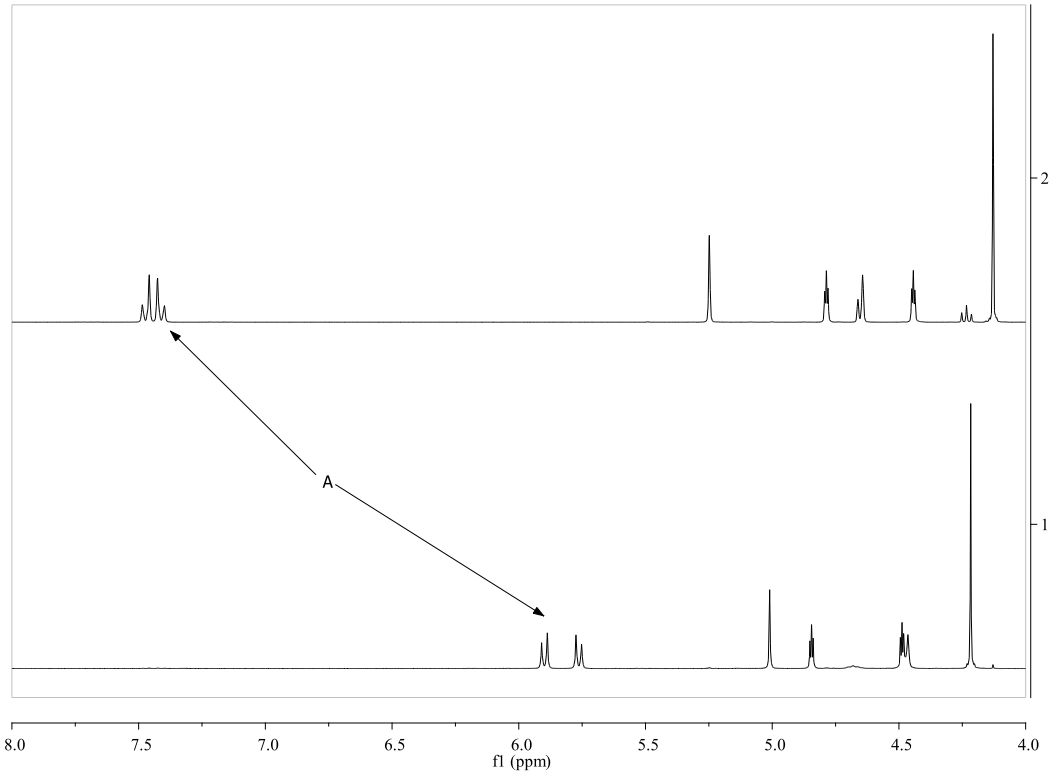

Figure 4.8: A section of the ^{1}H NMR of 4.4 (top) and 4.5 (bottom), illustrating the effects of chromium coordination.

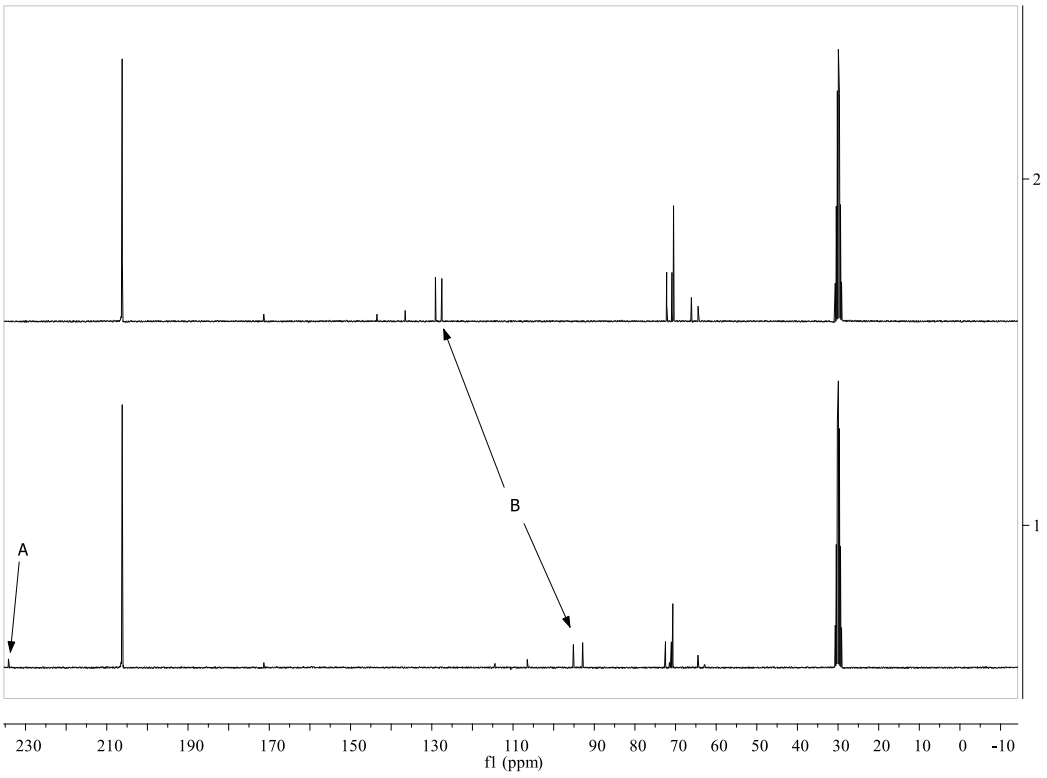

Figure 4.9: ^{13}C NMR spectra of 4.4 (top) and 4.5 (bottom), illustrating the effects of chromium coordination.

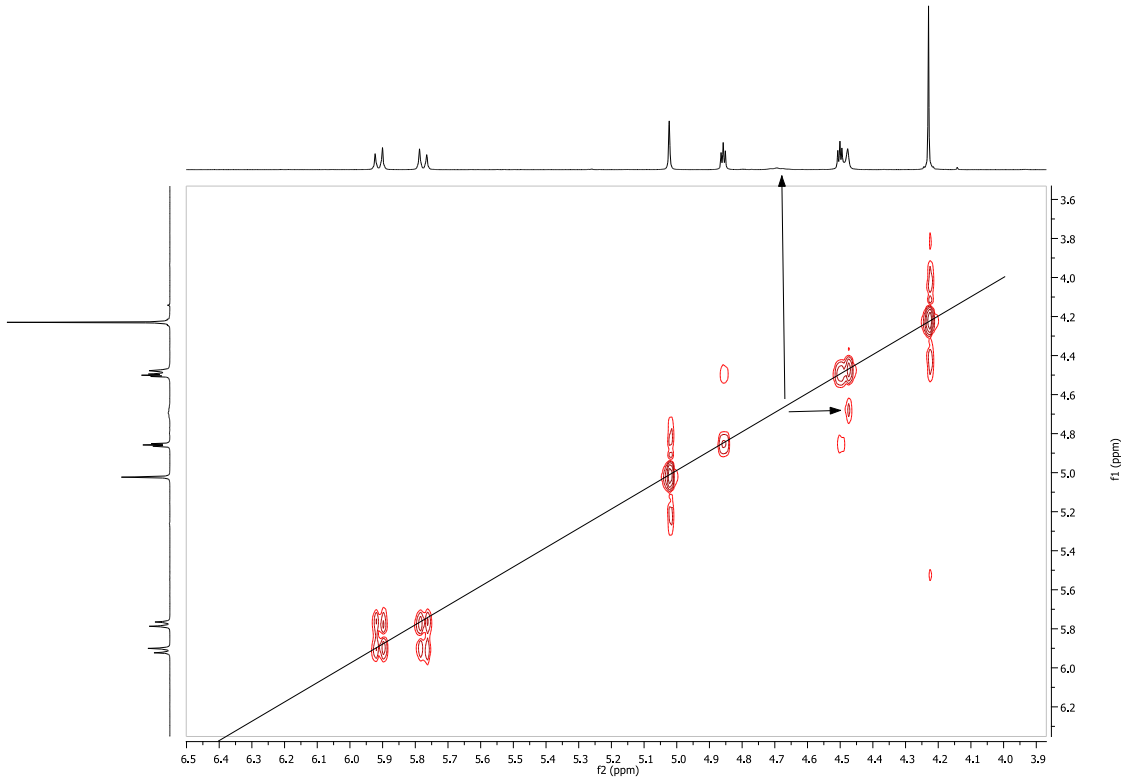

Figure 4.10: Section of the COSY NMR spectrum of 4.5 showing the structural signals.

As shown in Figure 4.10, there is again a correlation between the free alcohol and the benzylic position signal, although it is significantly weaker than previously seen with compound 4.4 (Figure 4.6). The bottom spectrum of Figure 4.8 also highlights the disappearance of this signal. This is most likely due to the electron withdrawing effects of the bound chromium. The binding of the chromium also results in better separation of the aromatic signals, allowing for clearer determination of correlation.

From 4.5, it is necessary to include the norbornene functional group in order to make a polymerizable compound. This was performed using the standard Steglich esterification reagents under N_2.

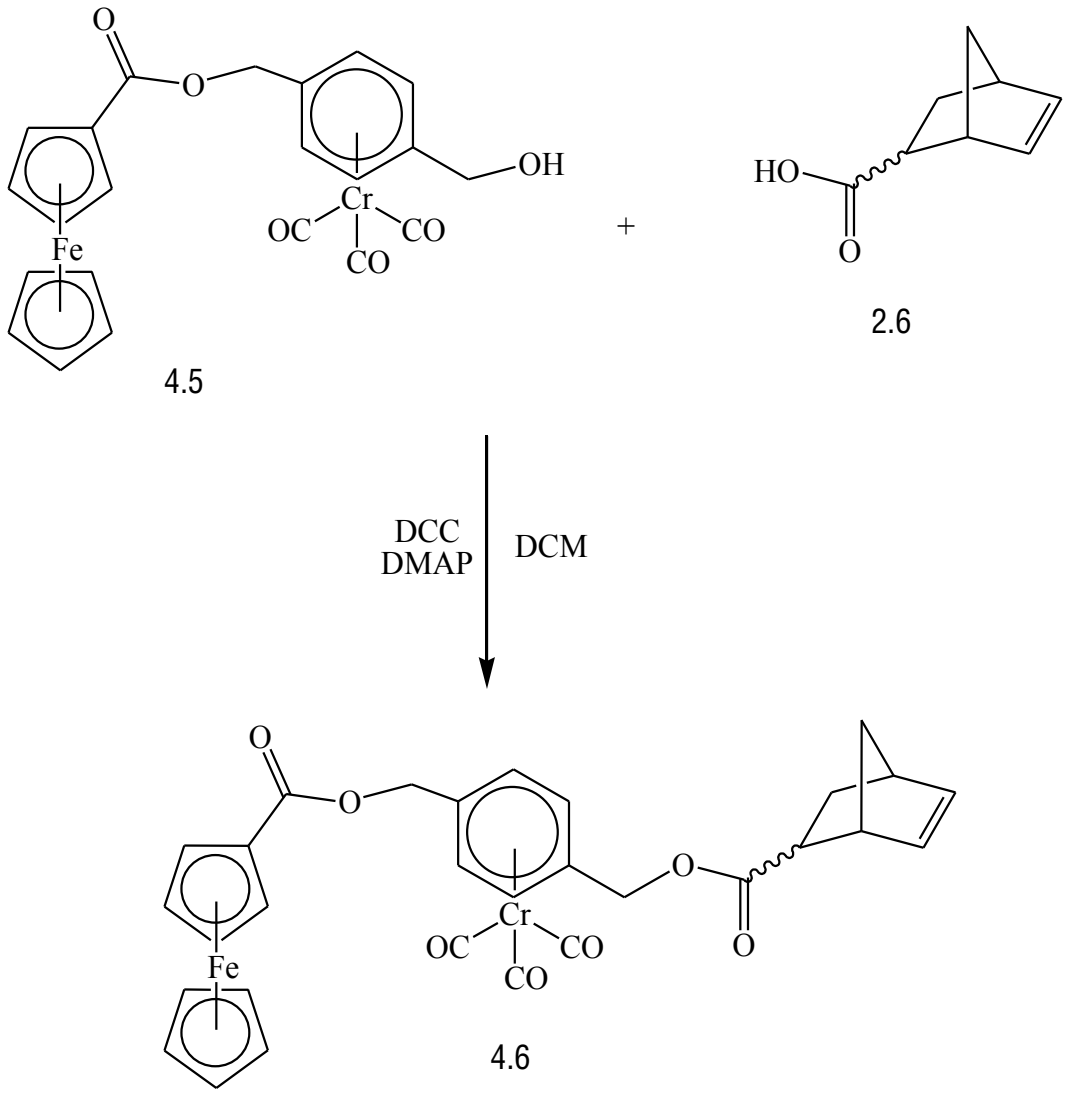

Scheme 4.5: Steglich esterification to form 4.6.

The incorporation of the norbornene can clearly be seen by the appearance of the signals resulting from the olefinic protons between 6.1 and 6.2 ppm in the ^{1}H NMR spectra (Figure 4.11). These peaks also appear in the ^{13} NMR spectra at 138.88, 138.55, 136.53, and 133.30 ppm (Figure 4.12). Additionally, there is a downfield shift of the benzylic protons in the α-position to the newly formed ester (from 4.65 ppm to 4.86 or 4.92 ppm)

in the ^{1}H NMR spectra. Integration of the signals due to the unsubstituted ferrocene Cp rings shows that there is approximately 5:3 ratio of *endo* to *exo* isomers present.

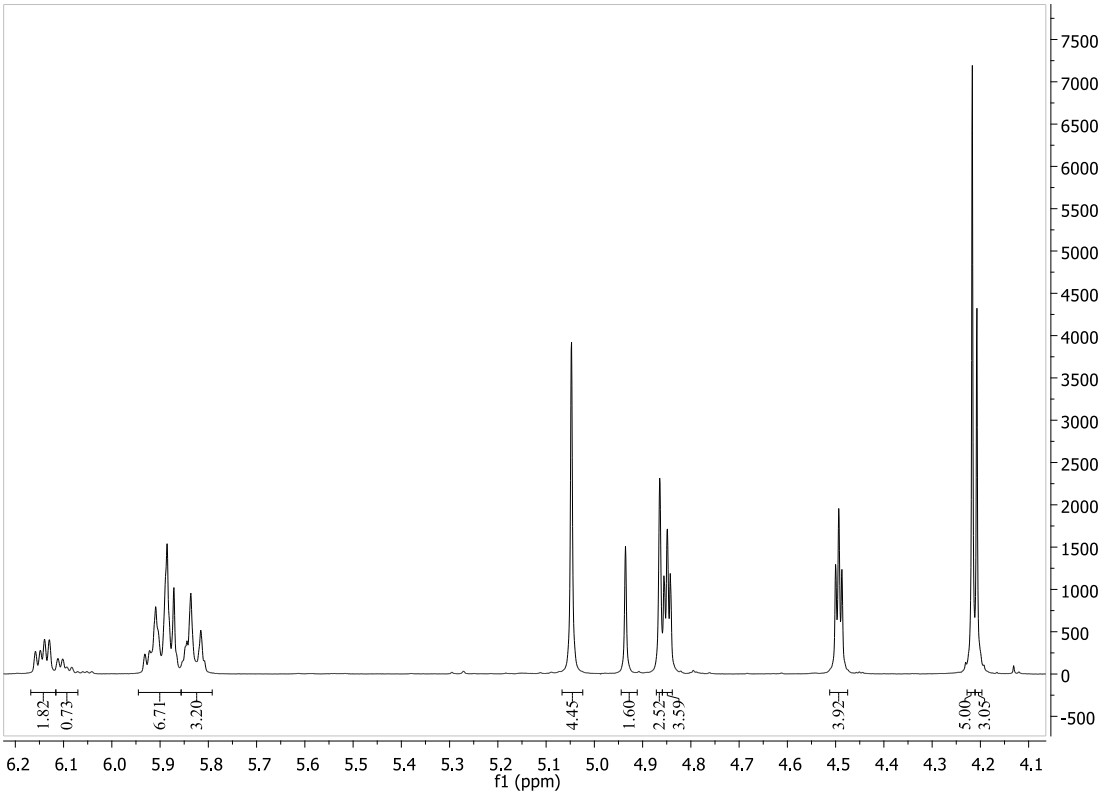

Figure 4.11: Section of the ^{1}H NMR spectra of 4.6, showing all non-aliphatic signals.

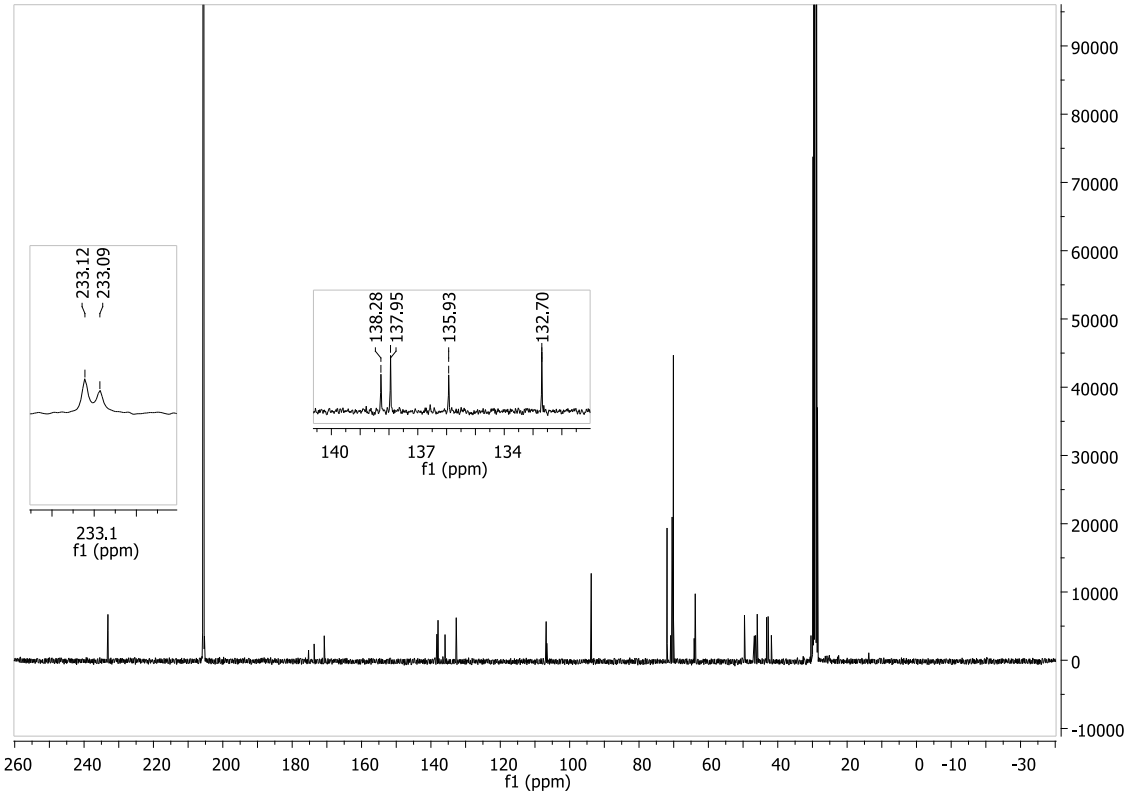

Figure 4.12: ^{13}C NMR spectrum of 4.6, with insets showing the metal bound carbonyls (left) and the olefinic carbons (middle).

As previously mentioned in Chapter Two, the presence of the two isomers of norbornene makes interpretation of the NMR spectra more difficult. To aid this process, a single isomer of 2.6 was used to form 4.6-*exo*.

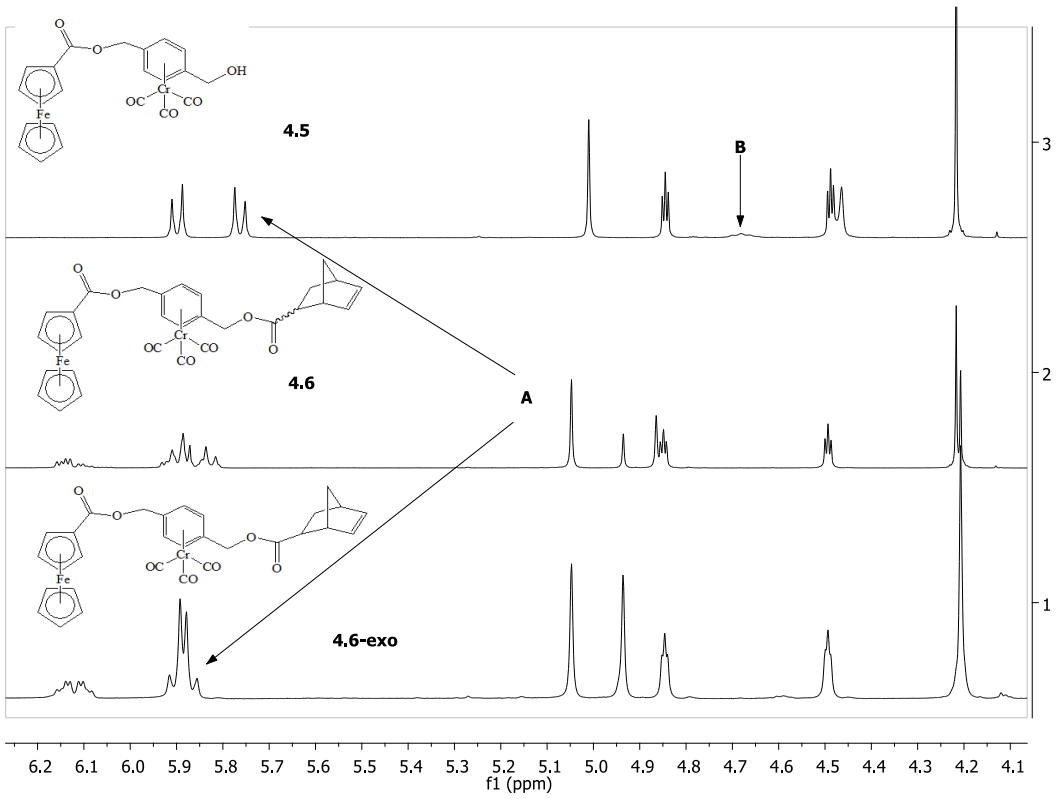

Figure 4.13: Comparison of the ^{1}H NMR spectra of 4.5, 4.6 and 4.6-*exo*.

As can be seen in Figure 4.13, the formation of the new ester results in the chromium bound aromatic proton signals shifting closer together (Label A), as well as the disappearance of the signal due to the free alcohol in 4.5 (Label B).

The isolation of the single form of 4.6 allowed for the full characterization of the compound through NMR.

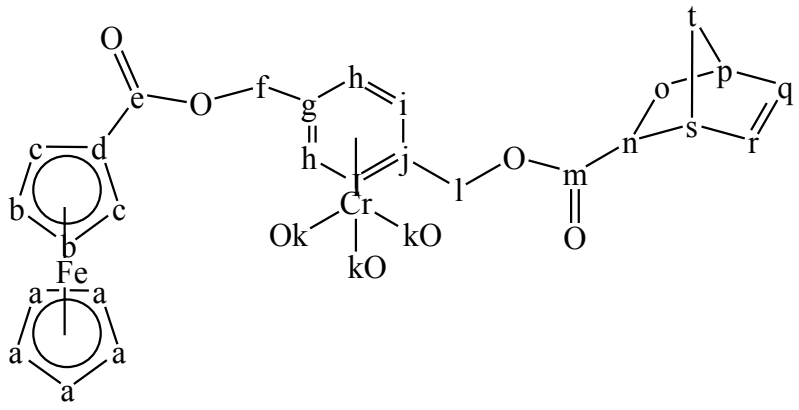

Figure 4.14: Atom labels for 4.6-*exo*.

Table 4.3: NMR assignments for 4.6-*exo*.

Signal	^{1}H NMR δ (ppm)	^{13}C NMR δ (ppm)
a	4.21	70.7
b	4.49	71.0
c	4.85	72.5
d	-	71.5
e	-	171.3
f	5.05	64.4
g	-	107.2
h	5.85-5.88	94.3
i	5.89-5.92	94.7
j	-	107.5
k	-	233.7
l	4.94	64.7
m	-	175.9
n	1.91	31.0
o	2.26	43.6
p	3.04	47.4
q	6.11	136.5
r	6.14	138.9
s	2.88	42.4
t	1.25-1.5	47.0

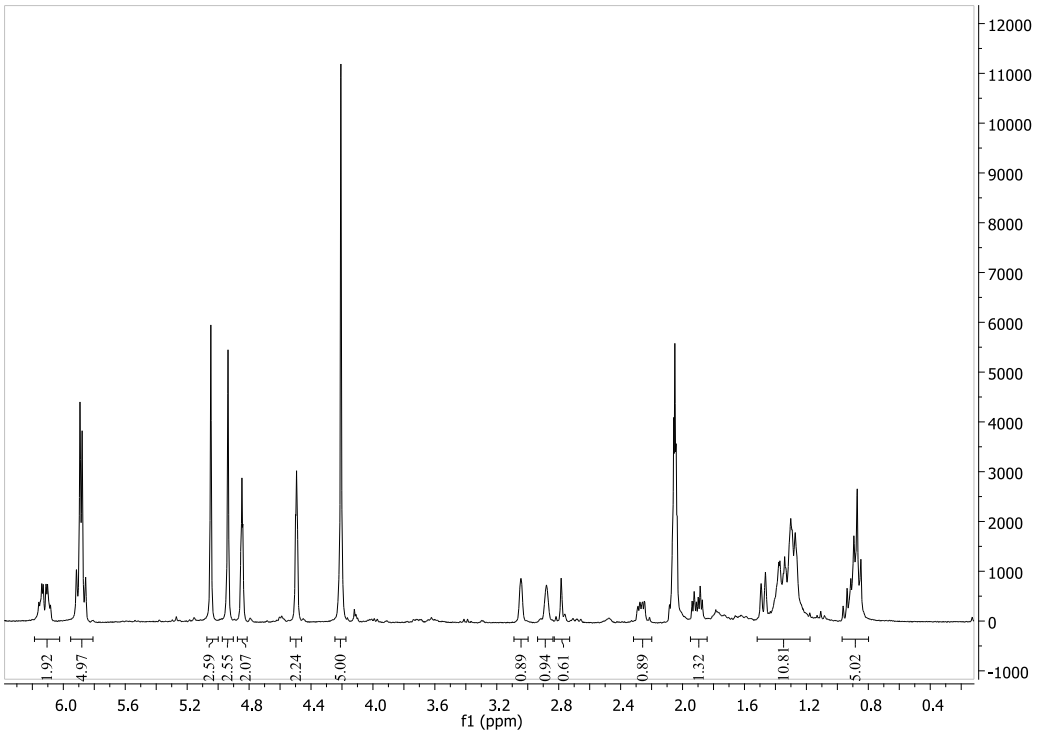

Figure 4.15: ^{1}H NMR spectrum of 4.6-*exo*.

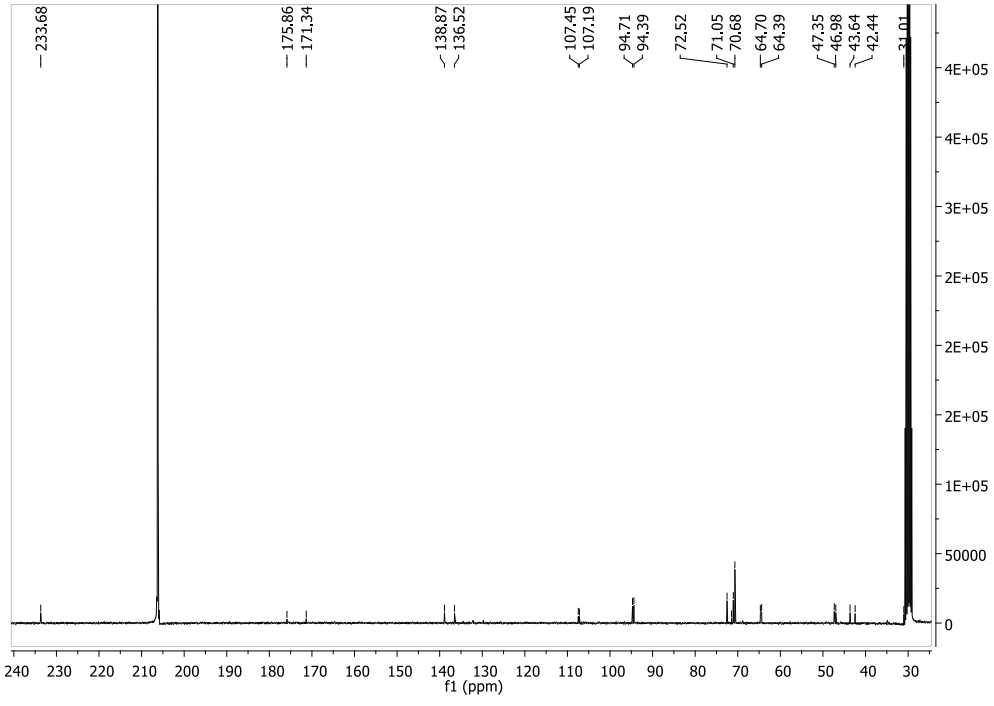

Figure 4.16: ^{13}C NMR spectrum of 4.6-*exo*.

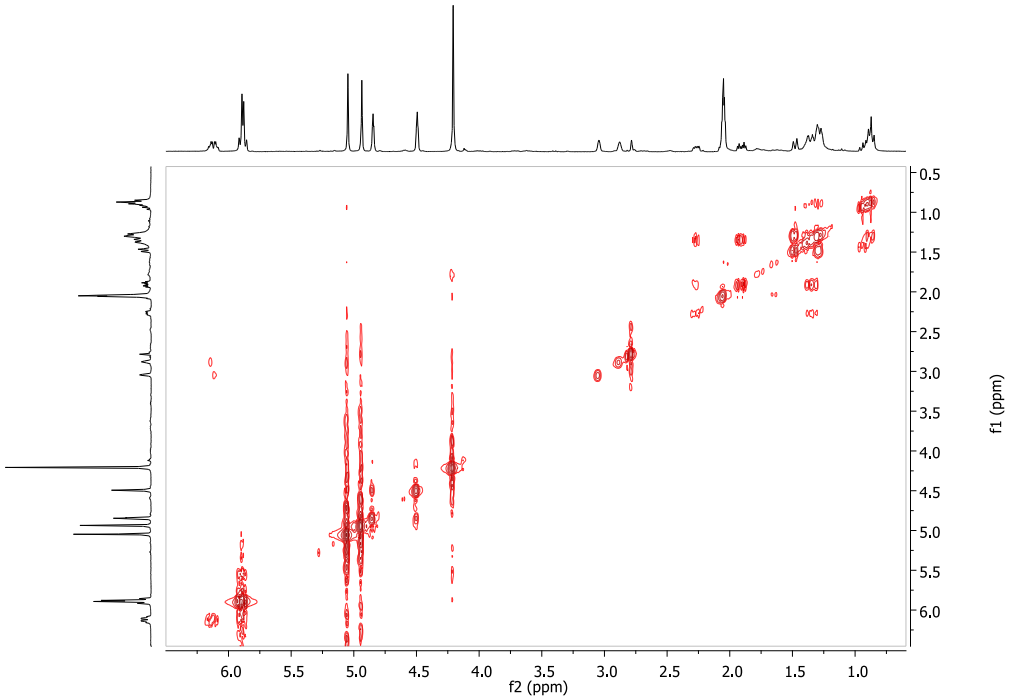

Figure 4.17: COSY NMR spectrum of 4.6-*exo*.

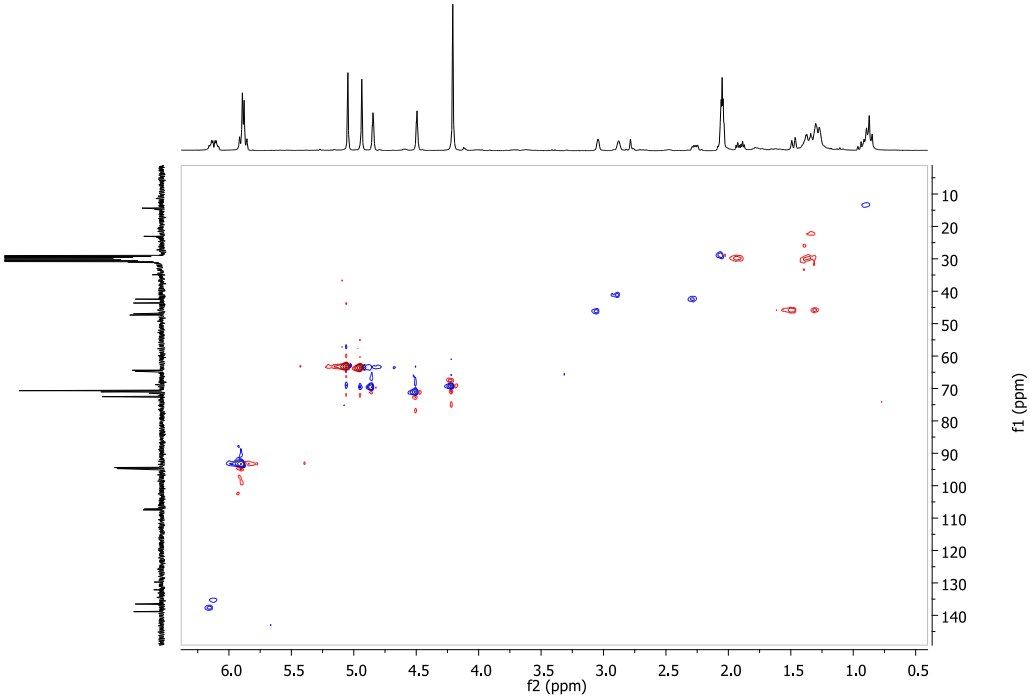

Figure 4.18: HSQC NMR spectrum of 4.6-*exo*.

4.4 Polymerization

As with each of the previously synthesized polymers, compound **4.6** was polymerized utilizing a 20:1 ratio of catalyst to monomer in dry THF under an atmosphere of N_2. Unlike the majority of the previous polymers, **4.7** was partially soluble in acetone, allowing for solution NMR to be performed.

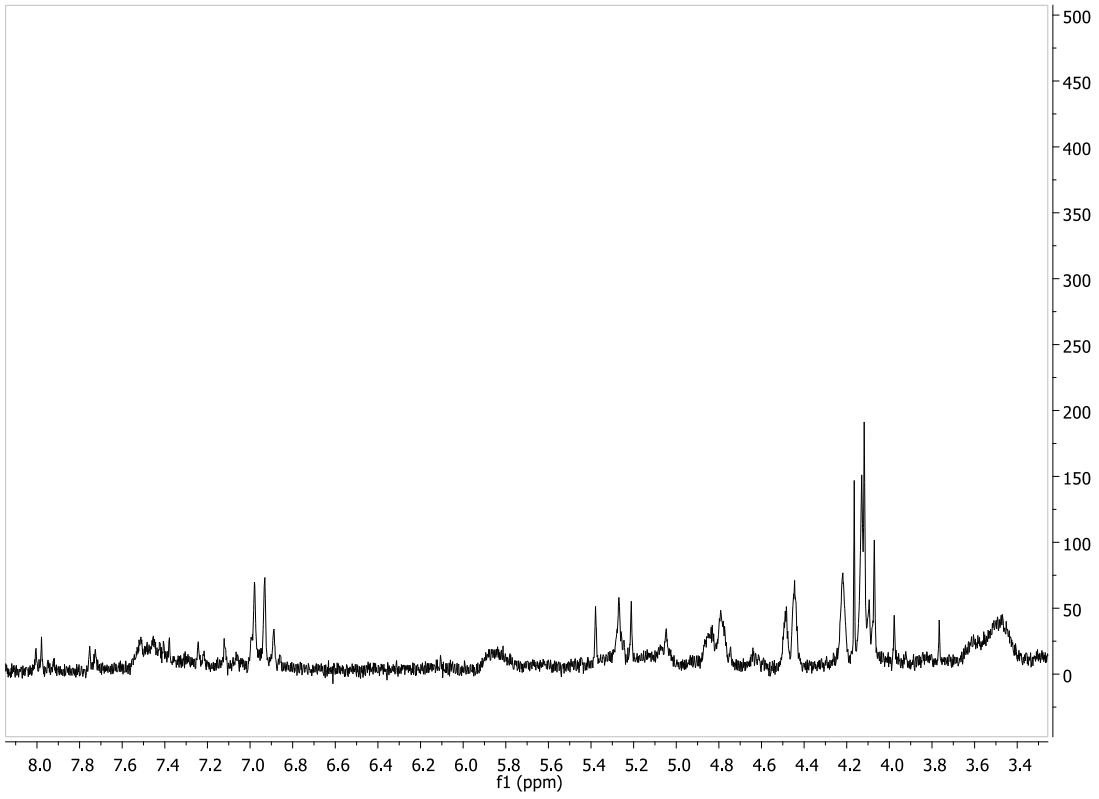

Figure 4.19: Portion of the ^{1}H NMR spectrum of polymer **4.7**.

As can be seen in Figure 4.19, there is some broadening of peaks that is characteristic of polymer formation. However, there are still a large number of well-defined peaks, particularly around 4.1 ppm. These are a representative of the protons of the unsubstituted Cp ring of the ferrocene moiety. The large number of these indicates the

formation of oligomers, which would still show sharp signals. It is likely that the only portions of 4.7 that were soluble were the lowest molecular weight units, with the larger polymers remaining insoluble. Additionally, there is the appearance of several signals in the standard aromatic region, which indicates that not all of the chromium remained bound throughout the entire polymerization process.

Due to the partial solubility of the polymer, it was possible to determine the molecular weight using gel permeation chromatography (GPC), with the with the weight average molecular weight being 22,454 Daltons and a polydispersity index (PDI) of 1.77. While this number is lower than previously synthesized compounds of a similar nature[34], this can be attributed to the largest molecular weight polymers being insoluble, which would also reduce the PDI as well.

Observation of the polymer under a SEM revealed that the polymer surface was very smooth. Portions of the sample did show cracking and a rough surface (left side of the top images in Figure 4.20), however, this is most likely due to damage to the polymer during recovery of the sample.

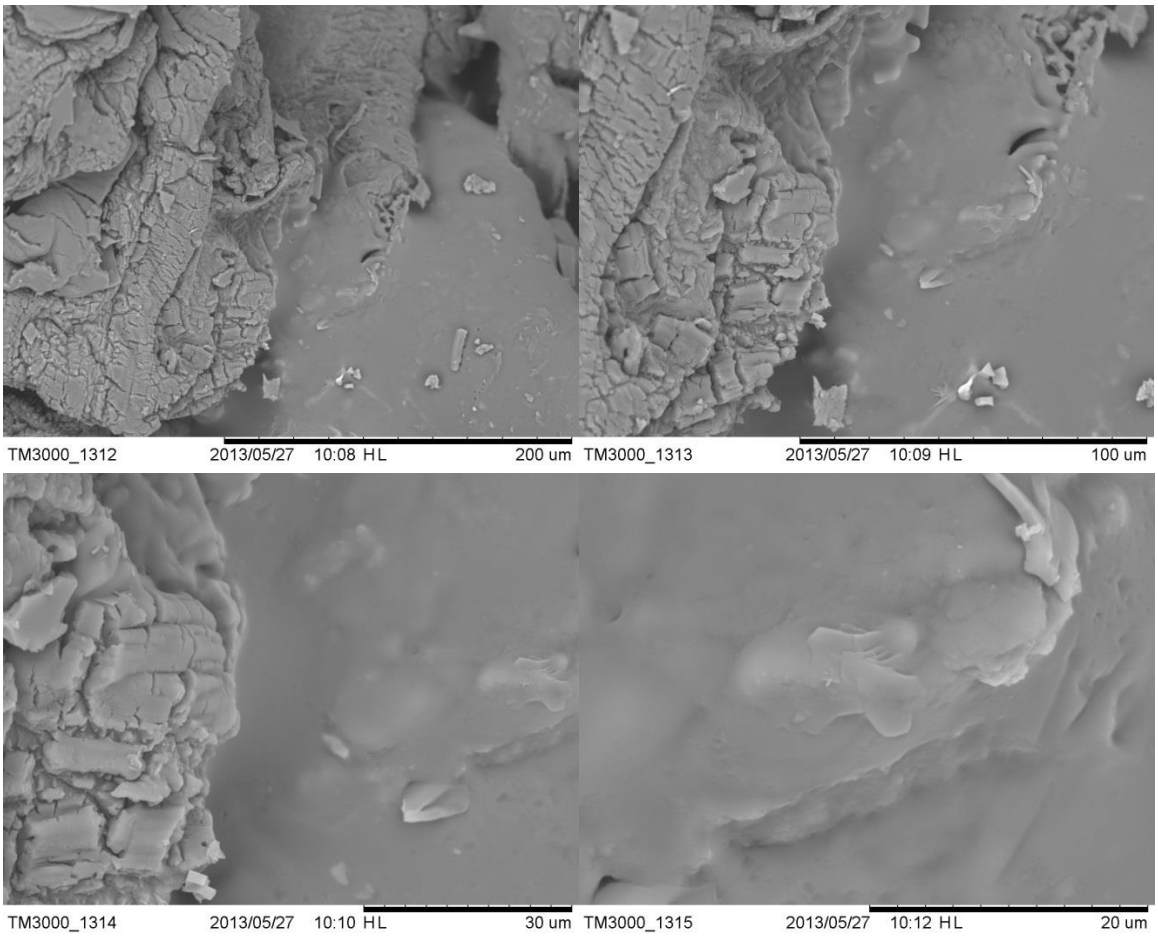

Figure 4.20: SEM images of polymer 4.7 at 500 x (top left), 1000 x (top right), 2000 x (bottom left), and 4000 x magnification (bottom right).

4.5 Thermal analysis

As with all previously synthesized polymers, 4.7 showed an initial decomposition at around 80 °C, which indicates that the material is trapping some of the solvent from the polymerization. The next thermal degradation, which occurs as a result of the loss of the metal bound carbonyls, begins lower than for the monometallic metal species 2.19, initiating at 195 °C. This can be attributed to the different electronic environment of the metal-bound arene ring as a result of the *para* substitution pattern. As with the previous

polymers, there is a greater than 50% decomposition of the total mass, occurring for 4.7 at 366 °C. Previous thermal data has been included in Table 4.4 for comparisons sake.

Table 4.4: Thermogravimetric analysis of polymer 4.7, the ferrocene monometallic polymer 2.14, the chromium monometallic polymer 2.19, and the ferrocene-chromium copolymers 3.3 and 3.4.

Polymer	Step 1	Step 2	Step 3	Step 4
4.7	80, 4%	195, 5%	242, 7%	357, 57%
2.14	84, 7%	356, 19%	395, 8%	433, 40%
2.19	90, 18%	204, 13%	368, 55%	-
3.3	, 11%	281, 14%	330, 75%	374, 23%
3.4	111, 10%	377, 53%	-	-

Comparison of the TGA run under nitrogen to that run under air revealed very similar decompositions. However, under nitrogen these occurred much more gradually than the extreme weight loss observed under air.

Examination of the material remaining after the conclusion of the TGA revealed that the material remaining corresponds to the expected amounts of metal oxides.

Table 4.5: Polymer remaining after the completion of TGA.

Polymer	Air	Nitrogen	Cr%	Fe%	Cr_nO_m%	FeO%
4.7	27.0%	34.7%	8.6%	9.2%	11.2/25.0%	11.9%

DSC of polymer 4.7 revealed a glass transition temperature of 72.1 °C, higher than both the ferrocene based monometallic polymer 2.14 and the chromium based monometallic polymer 2.19. The T_g of polymer 4.7 most closely resembles that of the random chromium-ferrocene copolymer 3.3, with only a 4 °C difference between the two.

Table 4.6: Differential scanning calorimetry of polymer 4.7, the ferrocene monometallic polymer 2.14, the chromium monometallic polymer 2.19, and the ferrocene-chromium copolymers 3.3 and 3.4.

Polymer	T_g (°C)
4.7	72
2.14	71
2.19	83
3.3	76
3.4	83

4.6 Summary

After successfully synthesizing a ferrocene-chromium test compound, a functionalized version of this compound was developed, and norbornene successfully attached. This bimetallic compound was then polymerized using Grubbs' 2nd generation catalyst. The molecular weight of this compound was determined through GPC and the thermal properties were analyzed using TGA and DSC, showing similar thermal properties to the analogous ferrocene-chromium copolymers described in Chapter Three.

4.7 Experimental

Any NMR spectra that were collected but not included in Chapter 4 can be found in section A.4 of the appendix. Full X-Ray Crystallography data for Compound 4.2 can be found in section A.4 of the appendix. All compounds containing the η^6-arene-chromium tricarbonyl moiety were stored under N_2 in order to prevent decomposition due to O_2 exposure. Any NMR experiments on these compounds were run with the samples being prepared in the glove box to prevent decomposition over the life of the experiment. These compounds can safely be handled in the presence of air during work up but should be limited in their exposure time.

Ferrocene test compound 4.1

Carboxylic acid ferrocene (1.1745 g, 5.1 mmol) (2.11), benzyl alcohol (2.19 mL, 20.3 mmol) (2.16), DCC (1.1677 g, 5.6 mmol), and DMAP (0.7031 g, 5.6 mmol) were dissolved in a solution of DCM (25 mL) and DMF (5 mL) under an atmosphere of N_2 for 16 hours. The mixture was then cooled to -15 °C for 2 hours and a white precipitate filtered off. The filtrant was diluted with DCM and washed subsequently with 2.6 M HCl and DI water. The organic solution was dried with $MgSO_4$ and the solvent removed *in vacuo*. Compound 4.1 was purified using column chromatography with silica gel as the solid phase and a 3:2 mixture of diethyl ether:hexanes as the mobile phase and isolated as a yellow powder. (1.3041 g, 78.3%)

^{1}H NMR (300 MHz, acetone-d_6) δ = 7.51 (dd, J = 5.61, 3.87, 2H), 7.44 (m, 2H), 7.38 (m, 1H), 5.26 (s, 2H), 4.79 (t, J = 1.93, 2H), 4.45 (t, J = 2.01, 2H), 4.12 (s, 5H).

^{13}C NMR (75.4 MHz, acetone- d_6) δ = 128.81, 128.61, 128.36, 81.84, 71.61, 70.31, 69.90, 65.59.

Ferrocene-chromium test compound 4.2

Compound 4.1 (0.1421g, 0.44 mmol) and chromium hexacarbonyl (1.1257, 5.0 mmol) (2.13) were stirred under a continuous flow of nitrogen for 15 min. 30 mL of dry, degassed 1,4-dioxane and 5 mL of dry, degassed THF were injected and the reaction refluxed for 24 hours. The solvent was then removed *in vacuo* and the reaction mixture dissolved in diethyl ether and filtered through Celite. Compound 4.2 was then purified *via* column chromatography, using silica gel as the solid phase and a 3:2 mixture of diethyl ether:hexanes as the mobile phase, and collected as an orange solid (0.0218 g, 22.0%). Crystals suitable for x-ray crystallography were grown from a cold solution of diethyl ether and hexanes.

^{1}H NMR (300 MHz, acetone-d_6) δ = 5.84 (d, J = 6.26, 2H), 5.74 (t, J = 6.38, 2H), 5.65 (t, J = 6.26, 1H), 5.04 (s, 2H), 4.85 (t, J = 1.83, 2H), 4.49 (t, J = 1.93, 2H), 4.22 (s, 5H).

^{13}C NMR (75.4 MHz, acetone- d_6) δ = 234.22, 108.11, 94.93, 94.89, 94.44, 72.50, 71.04, 70.68, 64.66.

Ferrocene benzenedimethanol compound 4.4

Carboxylic acid ferrocene (1.1650 g, 5.0 mmol) (2.11), 1,4-benzenedimethanol (1.3900 g, 10 mmol) (4.3), DCC (1.1446 g, 5.5 mmol), and DMAP (0.6767 g, 5.5 mmol) were

dissolved in a solution of DCM (25 mL) and DMF (5 mL) and stirred under N_2 for 16 hours. The reaction mixture was then cooled to -19 °C for 2 hours, after which a white precipitate was removed via filtration. The solvent was removed *in vacuo* and the resulting mixture was purified through column chromatography, using silica gel as the stationary phase and a 3:2 mixture of diethyl ether:hexanes as the mobile phase. Compound **4.4** was isolated as a pale yellow solid. (1.1465 g, 64.0%)

^{1}H NMR (300 MHz, acetone-d_6) δ = 7.47 (d, J = 8.18, 2H), 7.41 (d, J = 8.18, 2H), 5.25 (s, 2H), 4.79 (t, J = 1.92, 2H), 4.65 (d, J = 5.66, 2H), 4.44 (t, J = 1.91, 2H), 4.23 (t, J = 5.80, 1H), 4.13 (s, 5H).

^{13}C NMR (75.4 MHz, acetone-d_6) δ = 171.36, 143.49, 136.55, 129.10, 127.52, 72.36, 72.19, 70.89, 70.50, 66.10, 64.46, 64.33.

Chromium-iron compound **4.5**

Compound **4.4** (1.1465 g, 3.2 mmol) and chromium hexacarbonyl (1.5700 g, 7.1 mmol) (**2.13**) were stirred under a continuous flow of N_2 for 15 minutes. 30 mL of dry, degassed 1,4-dioxane and 10 mL of dry, degassed, THF injected into the reaction, which was then refluxed for 5 days. The solvent was then removed *in vacuo* and the reaction mixture dissolved in diethyl ether and filtered through celite. Compound **4.5** was then purified vi column chromatography, using silica gel as the solid phase and a 3:2 mixture of diethyl ether: hexanes as the mobile phase, and collected as a dark red oil. (0.4365 g, 28.0%)

^{1}H NMR (300 MHz, acetone-d_6) δ = 5.90 (d, J = 6.74, 2H), 5.76 (d, J = 6.72, 2H), 5.01 (s, 2H), 4.84 (m, 2H), 4.68 (m, 1H) 4.49 (m, 2H), 4.46 (br. s, 2H), 4.22 (s, 5H).

^{13}C NMR (75.4 MHz, acetone-d_6) δ = 234.20, 171.35, 114.43, 106.51, 95.15, 92.87, 72.48, 71.51, 71.03, 70.67, 64.49, 62.82.

Bimetallic monomer 4.6

Compound 4.5 (0.4356 g, 0.90 mmol), bicyclo[2.2.1]hept-5-ene-2-carboxylic acid, mixture of *endo* and *exo* (0.25 mL, 1.80 mmol) (2.6), DCC (0.2173 g, 1.0 mmol), and DMAP (0.1292 g, 1.0 mmol) were dissolved in 30 mL of DCM and stirred under N_2 for 16 hours. The reaction mixture was then cooled to -19 °C for 2 hours and a white precipitate was removed via filtration. The solvent was then removed *in vacuo* and the mixture purified via column chromatography using silica gel as the solid phase and a 3:2 mixture of diethyl ether:hexanes as the mobile phase. Compound 4.6 was isolated as an orange powder (0.4345 g, 80.0%).

^{1}H NMR (300 MHz, acetone-d_6) δ = 6.14 (dd, J = 5.6, 3.0, 2H), 6.12 – 6.07 (m, 1H), 5.94 – 5.85 (m, 5H), 5.83 (t, J = 4.3, 2H), 5.05 (s, 4H), 4.92 (s, 1H), 4.86 (s, 2H), 4.85 (t, J = 1.9, 4H), 4.49 (t, J = 1.9, 4H), 4.22 (s, 5H), 4.21 (s, 3H), 2.30 – 2.23 (m, 1H), 1.97 – 1.86 (m, 2H), 1.51 – 1.23 (m, 7H), 0.92 – 0.84 (m, 1H).

^{13}C NMR (75 MHz, acetone-d_6) δ = 233.72, 233.69, 175.87, 174.27, 171.36, 138.88, 138.55, 136.53, 133.30, 107.44, 107.38, 107.37, 107.19, 94.70, 94.43, 94.38, 72.52, 71.48, 71.06, 70.69, 64.70, 64.41, 64.39, 50.20, 47.35, 46.99, 46.52, 43.84, 43.65, 43.38, 42.44, 31.02.

4.6-*exo*

^{1}H NMR (300 MHz, acetone-d_6) δ = 6.14 (dd, J = 5.7, 25.6, 1H), 6.10 (dd, J = 5.7, 2.6 , 1H) 5.90 (d, J = 6.9, 2H), 5.87 (d, J = 6.9, 2H), 5.05 (s, 2H), 4.94 (s, 2H), 4.85 (t, J = 1.8, 2H), 4.49 (t, J = 1.8, 2H), 4.21 (s, 5H), 3.04 (s, 1H), 2.88 (s, 1H), 2.78 (s, 1H), 2.26 (dt, J = 13.3, 6.9, 1H), 1.91 (dt, J = 11.7, 4.0, 1H), 1.52 – 1.19 (m, 2), 0.90 (dt, J = 13.6, 7.4 Hz, 1H).

^{13}C NMR (75 MHz, acetone-d_6) δ = 233.7, 175.9, 171.3, 138.9, 136.5, 107.5, 107.2, 94.7, 94.39, 72.5, 71.5, 71.1, 70.7, 64.7, 64.4, 47.4, 47.0, 43.6, 42.4, 31.0.

Polymer 4.7

Compound 4.6 (0.1482 g, 0.20 mmol) was dissolved in 4 mL of dry, degassed THF under an atmosphere of N_2. Grubbs' 2nd Generation Catalyst (0.0099 g, 0.012 mmol) was dissolved in 2 mL of dry, degassed THF and injected into the reaction. After 30 min., 3 mL of ethyl vinyl ether was added. The reaction was allowed to stir for an additional 30 min. The solvent was subsequently removed *in vacuo* and polymer 4.7 was isolated as a red powder. (0.1206 g, 81.4%)

Chapter Five: Conclusion

Three norbornenes were developed, each containing a different metal species; a cationic η^6-arene-η^5-cyclopentadienyl iron(II), a neutral *bis*-η^5-cyclopentadienyl iron(II) (ferrocene), and a neutral η^6-arene chromium(0) tricarbonyl. These metal moieties were functionalized with either an alcohol or a carboxylic acid off of one of the arene ligands, allowing for the norbornene functional group to be incorporated *via* a Steglich esterification. These compounds were fully characterized using several NMR techniques. Polymerization of the norbornenes was performed using a 20:1 ratio of monomer to catalyst, which was the ruthenium based Grubbs' 2nd generation. The cationic iron polymer was isolated as a brown, rock-like material, the ferrocene polymer was isolated as a red, highly folded rubber-like material, and the chromium polymer was isolated as a green, rubber-like material. These compounds showed limited solubility, although the cationic iron polymer was able to be characterized using solution NMR in deuterated acetonitrile. The other two polymers were characterized using solid state NMR. The ferrocene polymer was soluble enough for GPC to be performed and had a M_w of 231 421 and a PDI of 1.72. The other two polymers were not soluble enough for M_w determination. The thermal properties of each of the polymers were studied, with the thermal degradations observed using TGA and the glass transition temperatures, which were 81, 70, and 60 °C, respectively, were determined through DSC.

Each of the previous monometallic norbornenes were then used to create a series of multi-metallic polymers through copolymerization. This was accomplished using two mechanisms; a random polymerization with all monomers present and a block

polymerization, where the monomers were added sequentially. The copolymers of cationic iron and chromium were able to be characterized by solid state NMR but the rest of polymers were not. All of the compounds were insoluble, precluding M_w determinations. The thermal properties were again determined through TGA and DSC.

Additionally, a bimetallic iron and chromium containing norbornene was developed. Initial experimentation was performed on a ferrocene test compound that contained a free arene. This was done in order to maximize the yield of chromium coordination to that arene through exploration of a number of different chromium reagents and solvent conditions. The chromium-iron test compound was successfully characterized using X-ray crystallography and compared to the chromium free analogue in order to determine the effects of chromium coordination on the structure. Once the synthetic process was optimized, a substituted arene was used to allow for incorporation of the norbornene after the coordination of the chromium. This compound was again polymerized using a 20:1 ratio of monomer to catalyst and produced a partially soluble red solid. This polymer was soluble enough to be characterized by both NMR and GPC, with the M_w being 22 454 and the PDI being 1.77. This would represent some of the smallest of the generated polymer chains, as the larger ones would remain insoluble. Thermal analysis was performed and the glass transition temperature was determined to be 72 °C.

Future work in this area would include a series of mechanical, conductive, and magnetic tests being performed on each of the polymers. The materials synthesized will also be converted into a ceramic material and it will be determined if similar properties exist.

Variation in the ratio of the metals within the copolymers will be performed in order to determine how this would affect the properties of the materials. Incorporation of several other metals into these materials, such as cobalt or manganese, will also be explored.

Chapter Six: References

1. Kealy, T. J.; Pauson, P. L. *Nature (London, U. K.)* 1951, *168*, 1039-1040.
2. Pauson, P. L. *Journal of Organometallic Chemistry* 2001, *637-639*, 3-6.
3. Wilkinson, G.; Rosenblum, M.; Whiting, M. C.; Woodward, R. B. *J. Am. Chem. Soc.* 1952, *74*, 2125-2126.
4. Rinehart, K. L.; Motz, K. L.; Moon, S. *J. Am. Chem. Soc.* 1957, *79*, 2749-2754.
5. Bublitz, D. E.; Rinehart, K. L.,Jr *Org. React.* 1969, *17*, 1-154.
6. Astruc, D. In *Organometallic chemistry and Catalysis;* Springer-Verlag: New York, 2007; pp 608.
7. Szafran, Z.; Pike, R. M.; Singh, M. M. In *Preparation and use of ferrocene;* Microscale inorganic chemistry: A complete laboratory experience; John Wiley & Sons, Inc.: NewYork, US, 1991; pp 302-313.
8. Arimoto, F. S.; Haven, A. C. *J. Am. Chem. Soc.* 1955, *77*, 6295-6297
9. Abd-El-Aziz, A. S.; Todd, E. K. *Coordination Chemistry Reviews,* 2003, *246*, 3-52.
10. Nguyen, P.; Gomez-Elipe, P.; Manners, I. *Chem. Rev.* 1999, *99*, 1515-1548.
11. Hudson, R. D. A. *J. Organomet. Chem.* 2001, *637-639*, 47-69.
12. Kalennikov, E. A.; Bochkov, G. I.; Kirilenko, Y. K.; Kaushanskii, D. A. *Fibre Chemistry,* 1974, *6*, 153-156.
13. Abd-El-Aziz, A. S.; Edel, A. L.; May, L. J.; Epp, K. M.; Hutton, H. M. *Can. J. Chem.* 1999, *77*, 1797-1809.
14. Abd-El-Aziz, A. S.; Edel, A. L.; Epp, K. M.; Hutton, H. M. *New J. Chem.* 1999, *23*, 569-571.

15. Abd-El-Aziz, A. S. *Coordination Chemistry Reviews,* 2002, *233-234*, 177-191.

16. Abd-El-Aziz, A. S.; Bernardin, S. *Coordination Chemistry Reviews,* 2000, *203*, 219-267.

17. Abd-El-Aziz, A. S.; May, L. J.; Hurd, J. A.; Okasha, R. M. *J. Polym. Sci. Part A: Polym. Chem.* 2001, *39*, 2716-2722.

18. Abd-El-Aziz, A. S.; Afifi, T. H.; Budakowski, W. R.; Friesen, K. J.; Todd, E. K. *Macromolecules* 2002, *35*, 8929-8932.

19. Abd-El-Aziz, A. S.; Carruthers, S. A.; Todd, E. K.; Afifi, T. H.; Gavina, J. M. A. *J. Polym. Sci. , Part A: Polym. Chem.* 2005, *43*, 1382-1396.

20. Abd-El-Aziz, A. S.; Carraher, C. E.; Pittman, C. U.; Zeldin, M., Eds.; In *Macromolecules containing metal and metal-like elements, Transition metal-containing polymers;* Wiley-Interscience: New Jersey, 2005; Vol. 6, pp 219.

21. Abd-El-Aziz, A. S.; Todd, E. K.; Ma, G.; DiMartino, J. *J. Inorg. Organomet. Polym.* 2000, *10*, 265-272.

22. Abd-El-Aziz, A. S.; Todd, E. K. *Macromol. Chem. Phys.* 2004, *205*, 418-429.

23. Abd-El-Aziz, A.S.; Okasha, R.M.; May, L.J.; Hurd, J. *J. Polym. Sci. Part A: Poly. Sci.* 2006, *44*, 3053, 3070.

24. Abd-El-Aziz, A. S.; Todd, E. K.; Ma, G.; DiMartino, J. *J. Inorg. Organomet. Polym.* 2000, *10*, 265-272.

25. Abd-El-Aziz, A. S.; Todd, E. K.; Okasha, R. M. *Macromol. Containing Met. Met. –Like Elem.* 2004, *2*, 233-273.

26. Abd-El-Aziz, A. S.; Shipman, P. O.; Neeland, E. G.; Corkery, T. C.; Mohammed, S.; Abd-El-Aziz, A. S.; Todd, E. K.; Ma, G.; DiMartino, J. *J. Inorg. Organomet. Polym.* 2000, *10*, 265-272.

27. Abd-El-Aziz, A. S.; de Denus, C. R.; Todd, E. K.; Bernardin, S. A. *Macromolecules* 2000, *33*, 5000-5005.

28. Abd-El-Aziz, A. S.; Todd, E. K.; Okasha, R. M.; Shipman, P. O.; Wood, T. E. *Macromolecules* 2005, *38*, 9411-9419.

29. Abd-El-Aziz, A. S. *Macromol. Rapid Commun.* 2002, *23*, 995-1031.

30. Abd-El-Aziz, A.; Todd, E.; Shipman, P. *Polymer News* 2005, *30*, 202-212.

31. Abd-El-Aziz, A. S.; Okasha, R. M.; Shipman, P. O.; Afifi, T. H. *Macromol. Rapid Commun.* 2004, *25*, 1497-1503.

32. Abd-El-Aziz, A. S.; Bernardin, S. A.; Khanh Tran *Tetrahedron Lett.* 1999, *40*, 1835.

33. Abd-El-Aziz, A.S.; Winram, D.J.; Shipma, P.O.; Bichler, L. *Macromol. Rapid Commun.* 2010, *31*, 1992-1997.

34. Abd-El-Aziz, A.S.; Winram, D.J.; Shipman, P.O.; Rock, C.L.; Vandel, M.S.; Patrick, B.O. *Macromol. Chem. Phys.* 2012, *213*, 2136-2156.

35. Nesmeyanov, A. N.; Vol'kenau, N. A.; Bolesova, I. N. *Tetrahedron Lett.* 1963, *4*, 1725-1729.

36. Litvak, V. V.; Filatova, L. S.; Khalikova, N. U.; Shteingarts, V. D. *Zh. Org. Khim.* 1980, *16*, 336-342.

37. Gomes, P. C. B.; Vichi, E. J. S.; Moran, P. J. S.; Federman Neto, A.; Maroso, M. L.; Miller, *J. Organometallics,* 1996, *15*, 3198-3203.

38. Winram, D. J. *Tailored Synthesis of Complexes and Polymers Containing Organoiron and Organocobalt.* 2009.

39. Nicholls, B.; Whiting, M.C. *Proc. Chem. Soc.*, 1958, 152;

40. Fischer, E.O.; Ofele, K.; Essler, H.; Frohlich, W.; Mortensen, J.P; Semmlinger, W. *Chem. Bm.*, 1958, *91*, 2763;

41. Natta, G.; Ercoli, R.; Calderazzo, F. *Chimica e Industria*, 1958, 40, 287.

42. Hannesschlager, P.; Brun, P. *Appl. Organomet. Chem.* 2000, *14*, 371.

43. Tate, D.P.; Knipple, W.R.; Augl, J.M. *Inorg. Chem.* 1962, *1*, 433.

44. Dembry, V.; Kiindig, E. P*. Helo. Chim. Acta* 1981, *64*, 1288-1297.

45. Deubzer, B.; Fischer, E. 0.; Fritz, H. P.; Kreiter, C. G.; Krie- bitzsch, N.; Simmons, H. D., Jr.; Willeford, B. R., Jr. Chem. Ber. 1967, 100, 3084-3096.

46. Gracey, D. E. F.; Jackson, W. R.; Jennings, W. B.; Mitchell, T. R. B. *J. Chem. Sc.* 1969, 1204.

47. Davies, S. G. ; Goodfellow, C. L. *J. Organomet. Chem.* 1988, *340*, 195.

48. Schmalz, H. G.; Millies, B.; Bats, J. W.; Dürner, G. *Angew. Chem. Int. Ed. Engl.* 1992, *21*, 631.

49. Mahaffy, C.A.L.; Hamilton, J. *Synth. React. Inorg. Met.-Org. Chem*. 1985, *17*, 849.

50. Mahaffy, C.A.L.; Pauson, P.L. *Inorg. Synth* 1990, *28*, 136.

51. Heppert, J.A.; Boyle, T.J.; Takusagawa, F. *Organometallics*, 1989, *8*, 461-467

52. Drehfahl, G.; Horhold, H.H.; Kuhne, K. *Chem. Berl*. 1965, *98*, 1826.

53. Alamiry, M.A.H.; Brennan, P.; Long, C.; Pryce, M.T. *J. Organomet. Chem*. 2008, *693*, 2907–2914.

54. Ceccon, A.; Gobbo, A.; Venzo, A. *J. Organomet. Chem.*, 1978, *162*, 311-321.

55. Janiak, C.; Lassahn, P. G. *Macromol. Rapid Commun.* 2001, *22*, 479-492.

56. Liu, W.; Nichols, P.; Smith, N. *Tetrahedron Lett.* 2009, *50,* 6103-6105.

57. Bielawski, C. W.; Grubbs, R. H. *Prog. Polym. Sci.* 2007, *32*, 1-29.

58. Toste, F. D.; Chatterjee, A. K.; Grubbs, R. H. *Pure Appl. Chem.* 2002, *74*, 7-10.

59. Li, H.; Tong, H.; Wang, C.; Song, L.; Zhang, W.; Zhu, X. *Lizi Jiaohuan Yu Xifu* 2005, *21*, 358-364.

60. Sutthasupa, S.; Sanda, F.; Masuda, T. *Macromolecules (Washington, DC, U. S.)* 2008, *41*, 305-311.

61. Malenfant, P. R. L.; Peters, A.; Wan, J. Patent Application Country: Application: US; Patent Country: US Patent 2008039589, 2008.

62. Katsumata, T.; Shiotsuki, M.; Sanda, F.; Masuda, T. *Polymer,* 2009, *50*, 1389-1394.

63. Stone, F.G.A.; Graham, W.A.G. In *Inorganic Polymers*, Academic Press, New York, 1962.

64. West, C.D. *Z. Kristallogr.* 1935, *90*, 555.

65. Arimoto, F.S.; Haven, Jr., A.C. *J. Am. Chem. Soc.* 1955, *77*, 6295.

66. George, M.; Hayes, G. *J. Polym. Sci. Chem. Ed.* 1975, *13*, 1049.

67. George, M.; Hayes, G. *J. Polym. Sci. Chem. Ed.* 1976, *14*, 475.

68. George, M.; Hayes, G. *Polymer*, 1974, *15*, 397.

69. Sasaki, Y.; Walker, L.L.; Hurst, E.L.; Pittmain, Jr., C.U. *J. Polym. Sci., Polym. Chem. Ed.* 1973, *11*, 1213.

70. Pittman, Jr., C.U.; Grube, P. *J. Polym. Sci: A1* 1971, *9*, 3175.

71. Pittman, Jr., C.U.; Marlin, G.V.; Rounsefell, T.D.; *Macromolecules,* 1973, *6*, 1.

72. Pittman, Jr., C.U.; Voges, R.L.; Elder, J. *Macromolecules,* 1971, *4*, 302.

73. Ayers, O.E.; McManus, S.P.; Pittman, Jr., C.U. *J. Polym. Sci. Chem. Ed.* 1973, *11*, 1201.

74. Pittman, Jr., C.U.; Lin, C.C.; Rounsefell, T.D. *Macromolecules*, 1978, *11*, 1022.

75. Pittman, Jr., C.U.; Priester, Jr., R.D.; Jayaraman, T.V. *J. Polym Sci. Chem. Ed.* 1981, *19*, 3351.

76. Pittman, Jr., C.U.; Rounsefell, T.D.; Lewis, E.A.; Sheats, J.E.; Edwards, B.H.; rausch, M.D.; Mintz, E.A. *Macromolecules* 1978, *11*, 560.

77. Macomber, D.W.; Rausch, M.D.; Jayaraman, T.V.; Priester, R.D.; Pittman, Jr., C.U. *J. Organomet. Chem.* 1981, *25*, 353.

78. Carraher, Jr., C.E.; Bajah, S. *Polymer*, 1974, *15*, 9.

79. Carraher, Jr., C.E.; Chapter 20. In *Interfacial Synthesis*. Millich, P.; Carraher, Jr., C.E.; eds. Marcel Dekker, New York, 1977. Vol. II.

80. Carraher, Jr., C.E.; Nordin, R.J. J. Appl. Polym. Sci 1974, 18, 53.

81. Carraher, Jr., C.E.; Bajah, S.T. *Br. Poly, J.* 1973, *14*, 42.

82. Carraher, Jr., C.E.; Nordin, R.J. *Makromol. Chem.* 1973, *164*, 42.

83. Carraher, Jr., C.E.; Piersma, J. *Makromol. Chem.* 1972, *153*, 49.

84. Carraher, Jr., C.E.; Riemer, J. *J. Polym. Sci. A1* 1972, *10*, 3367.

85. Carraher, Jr., C.E.; Sheats, J.E.; Pittman, Jr., C.U. eds. In *Organometallic Polymers*. Academic Press, New York, 1978. pp 79-85

86. Carraher, Jr., C.E.; Scott, W.J.; Schroeder, J.A.; Giron, D.J. *J. Macromol. Sci. Chem. Part A* 1981, *15* (4), 625.

87. Abd-El-Aziz, A. S.; Carraher, C. E.; Pittman, C. U.; Zeldin, M., Eds.; Introduction. In *Macromolecules containing metal and metal-like elements, A Half-Century of Metal-and Metalloid-Containing Polymers;* Wiley-Interscience: New Jersey, 2005; Vol. 1.

88. Manners, I., *Chem. Mater.* 1995, *7*, 2045-2053.

89. Manners, I. *J. Chem. Ed*. 1998, *75*(6), 766-768.

90. Manners, I. *Science*, 2001, *294,* 1664-1666.

91. Shi, J.; Tong, B.; Li, Z.; Shen, J.; Zhao, W.; Fu, H.; Zhi, J.; Dong, Y.; Häussler, M.; Lam, J.W.Y.; Tang, B.Z. *Macromolecules* 2007, *40*, 8195.

92. Neises, B.; Steglich, W. *Angew. Chem. Int. Ed.* 1978, *17*, 522–524.

93. Manning, D.D.; Strong, L.E.; Hu, X.; Beck, P.J.; Kiessling, L.L *Tetrahedron*, 1997, *53* (35), 11937-11952.

94. Albagli, D.; Bazan, G.C.; Schrock, R.R.; Wrighton, M.S. *J. Am. Chem. Soc.* 1992, *115*, 1328-1334.

95. Nicholls, B.; Whiting, M.C. *J. Chem. Soc.* 1959, 551.

96. Blagg, J.; Davies, S.G.; Goodfellow, C.L.; Sutton, K.H. *J. Chem. Soc. Perkin Trans.* 1990, *1*, 1133.

97. Abd-El-Aziz, A.S.; Lee, C.C.; Piorko, A.; Sutherland, R.G. *Synth. Commun.* 1988, *18*, 291-300.

98. Hür, D.; Ektin, S.F.; Dal, H. *J. Organomet. Chem.* 2010, *695* (7), 1031-1034.

Appendix

A.1 NMR data for Chapter Two

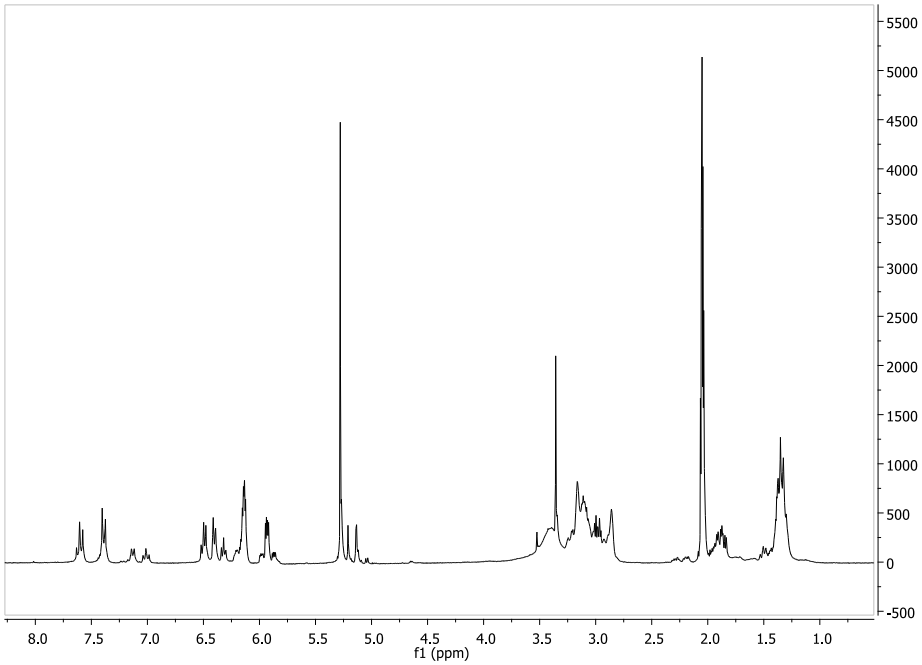

Figure A.1: ^{1}H NMR spectrum of 2.7.

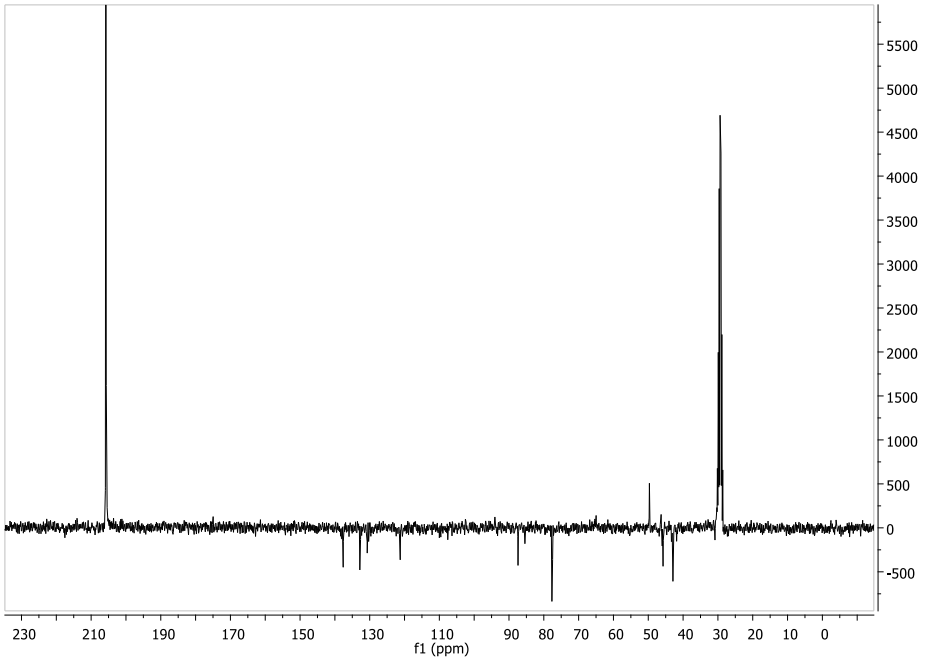

Figure A.2: DEPTQ135 ^{13}C NMR spectrum of 2.7.

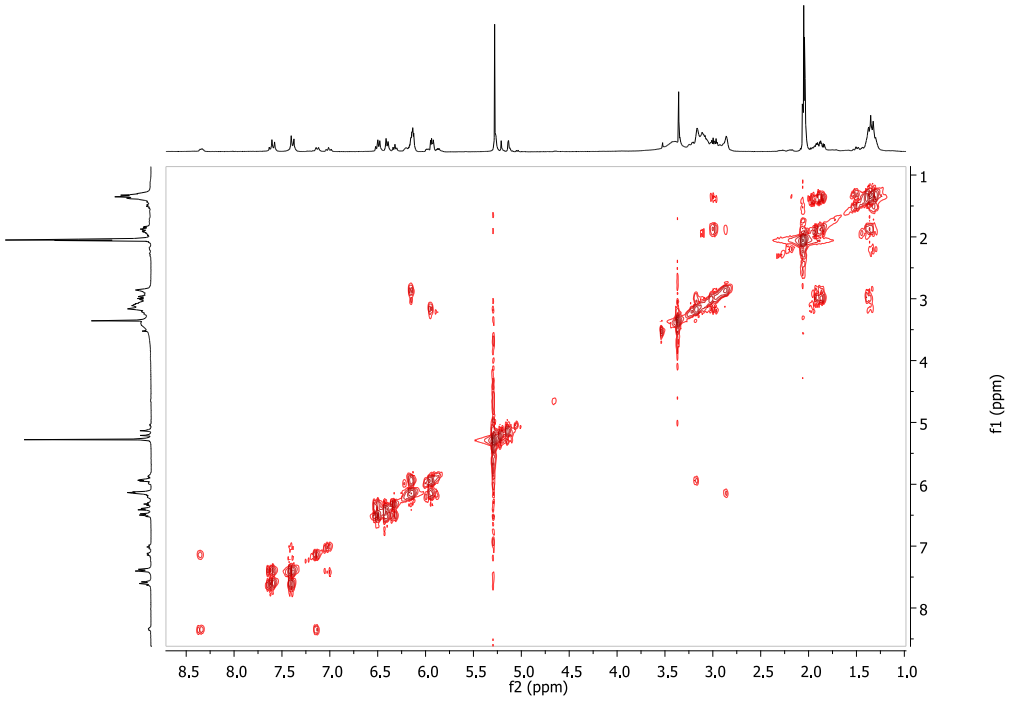

Figure A.3: COSY NMR spectrum of 2.7.

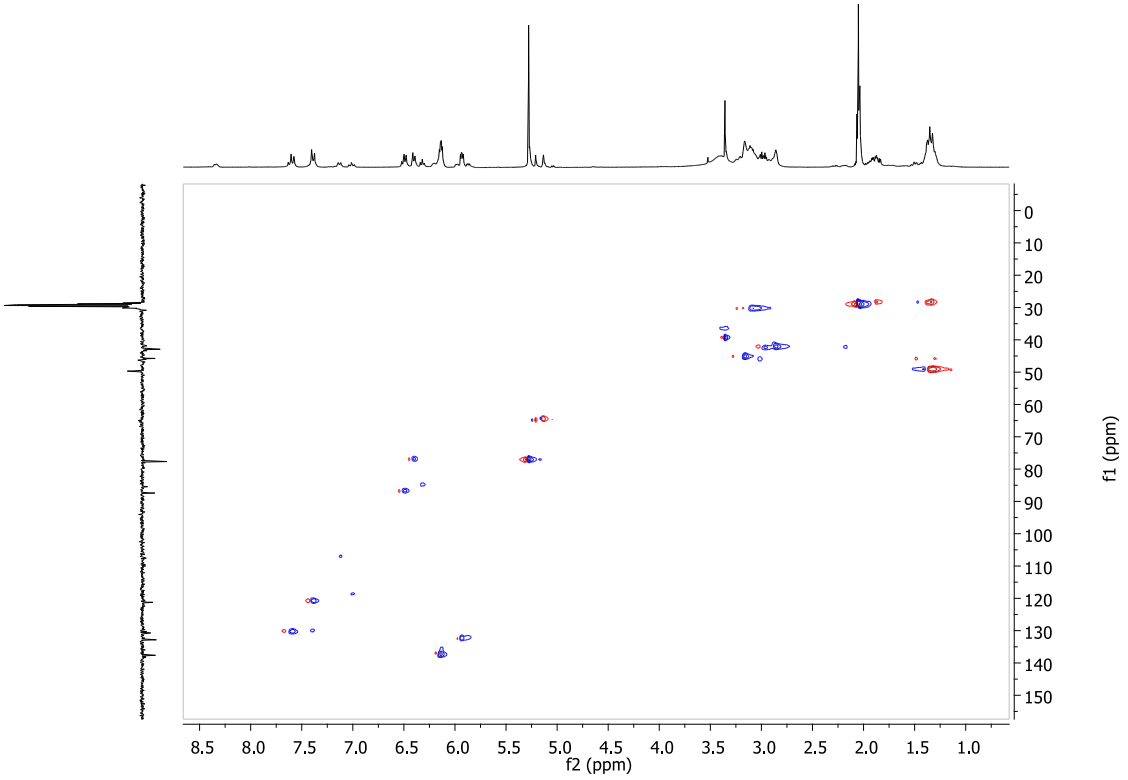

Figure A.4: HSQC NMR spectrum of 2.7.

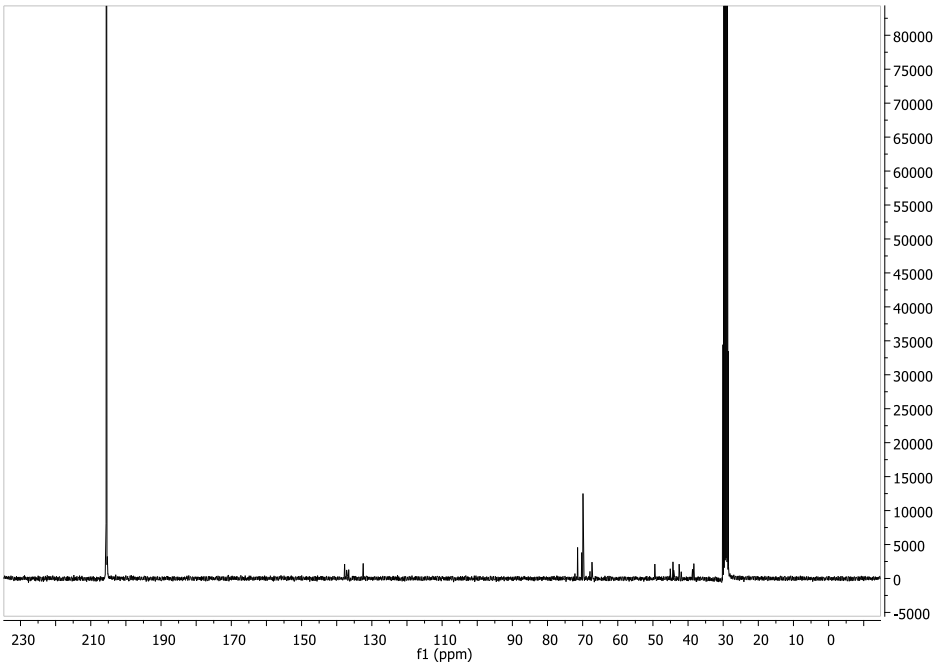

Figure A.5: ^{13}C NMR spectrum of 2.13.

A.2 Thermal data for Chapter Two

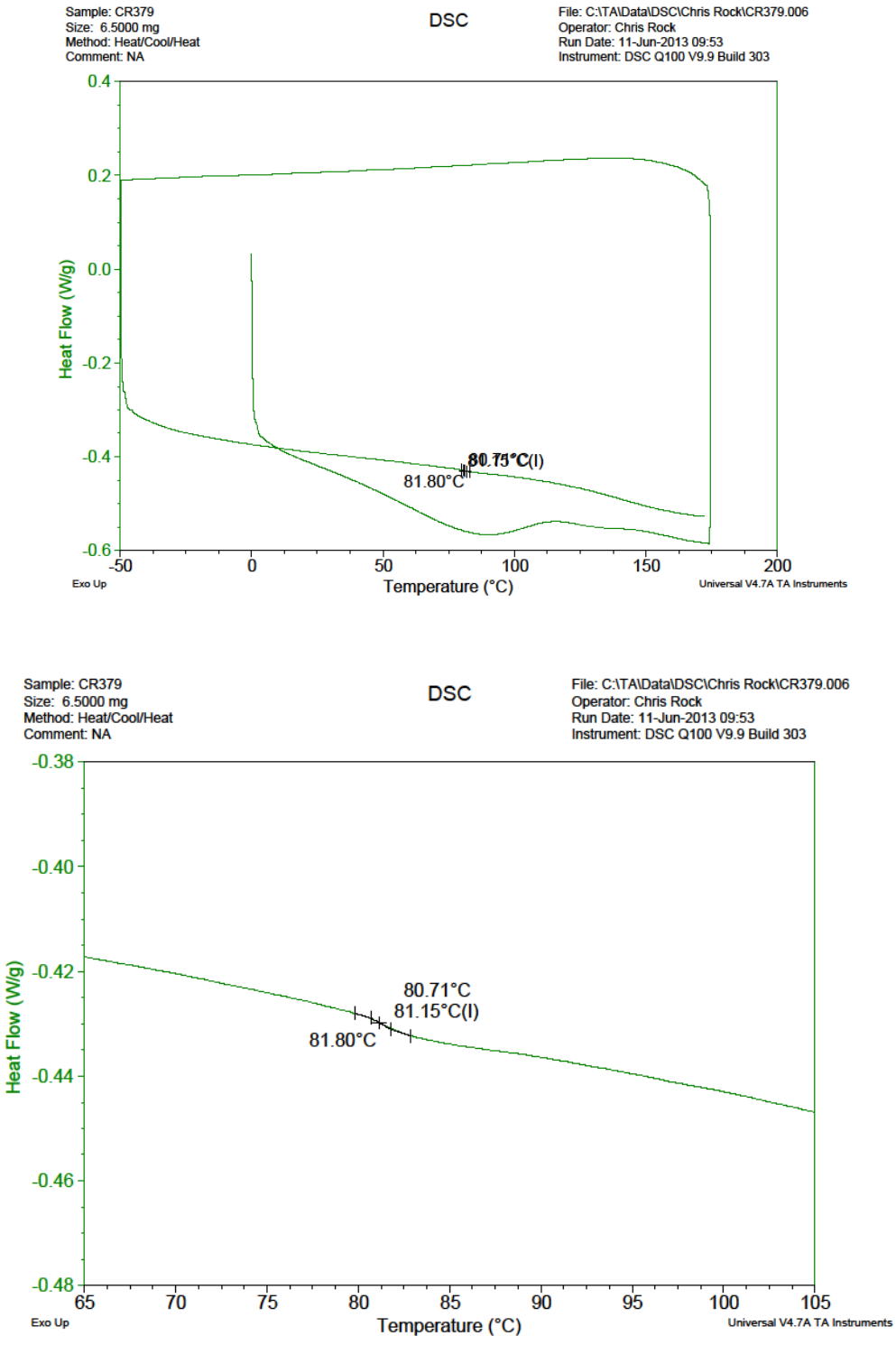

Figure A. 6: DSC for 2.8.

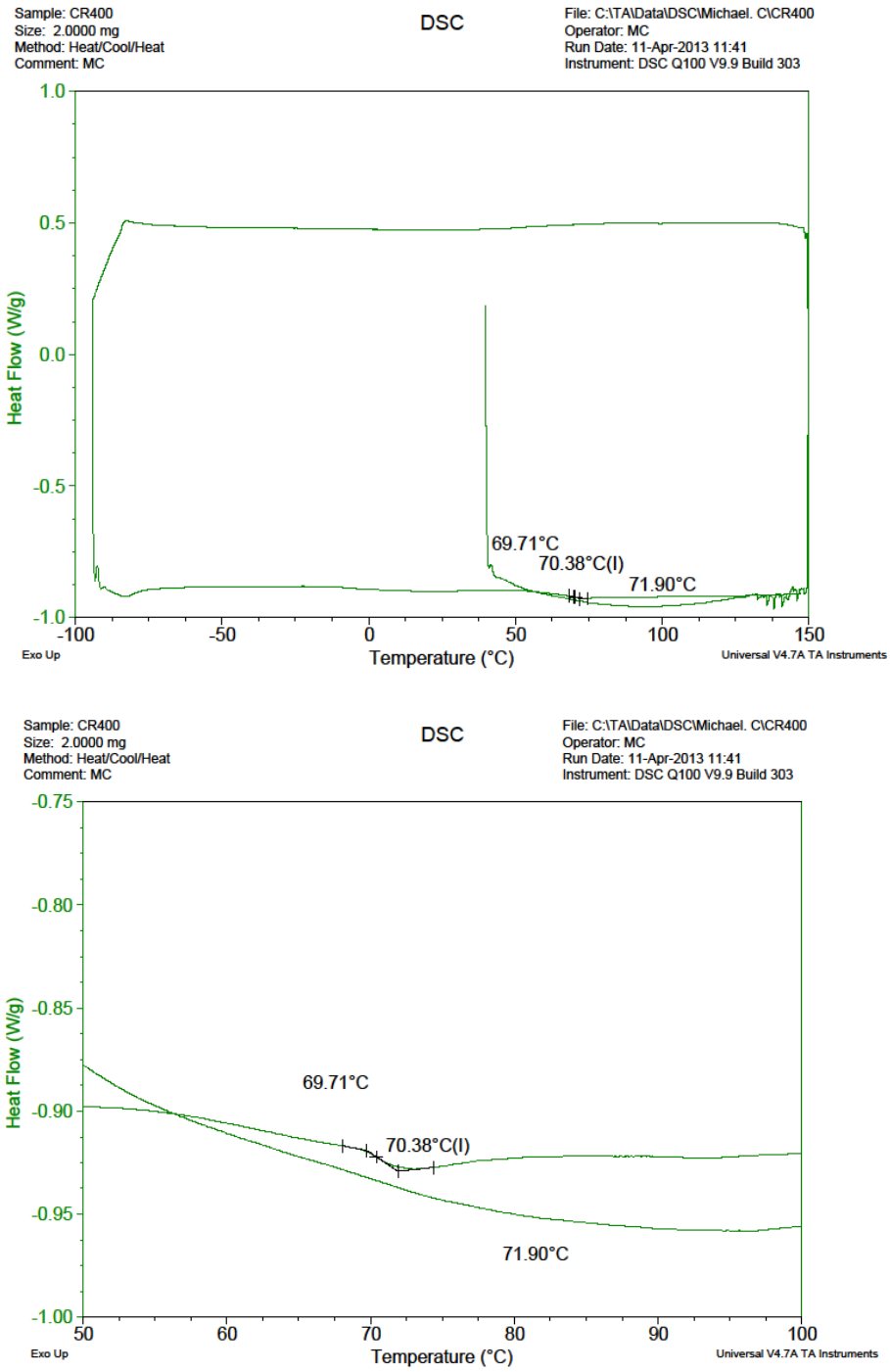

Figure A. 7: DSC for 2.12.

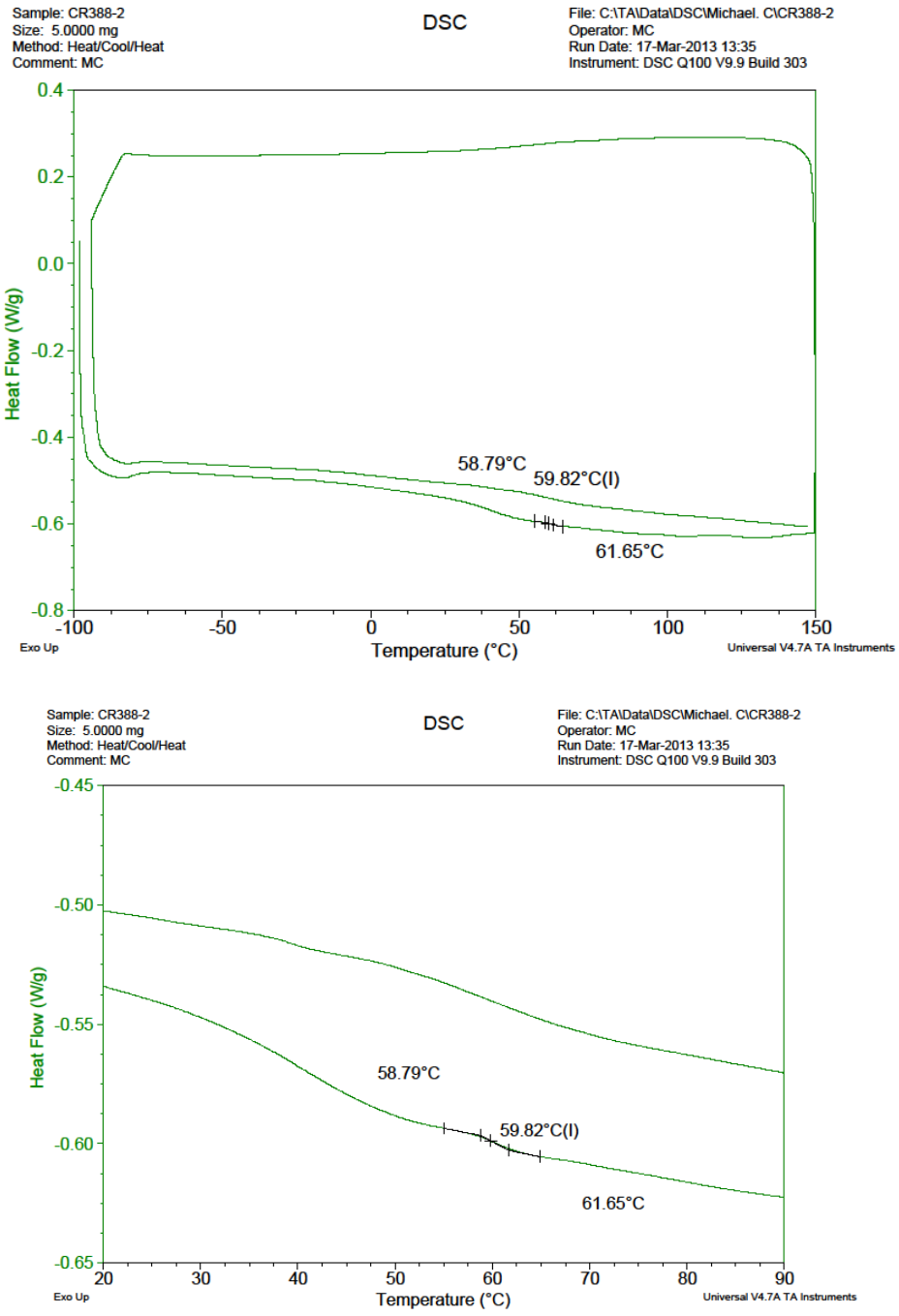

Figure A. 8: DSC for 2.17.

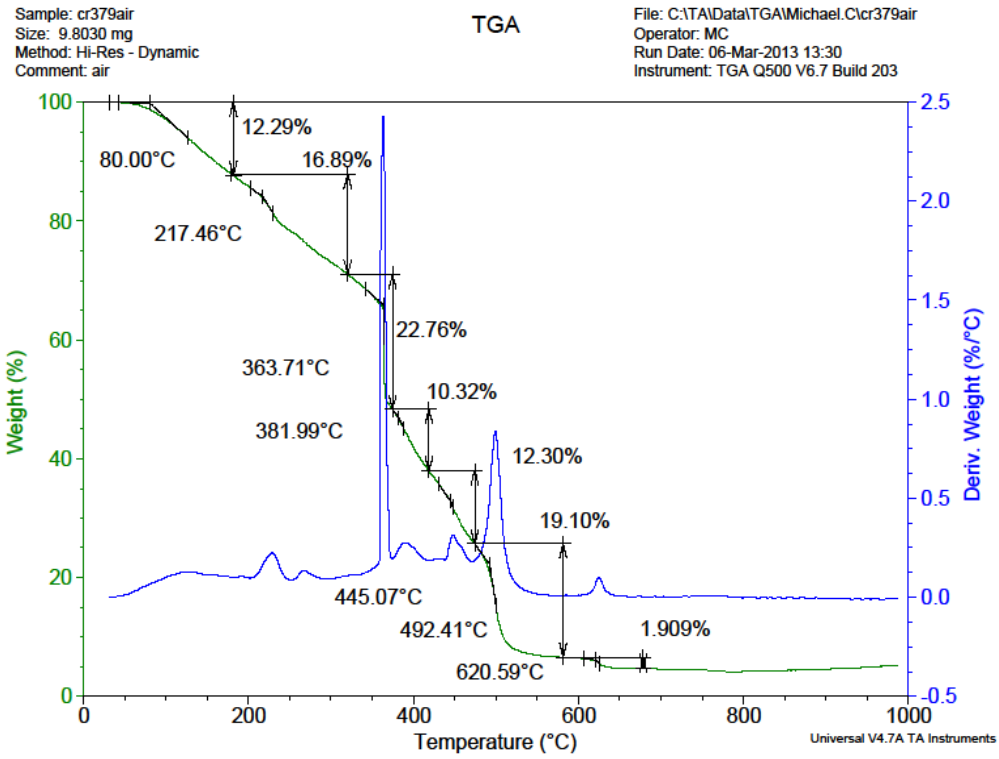

Figure A.9: TGA of 2.8 under air.

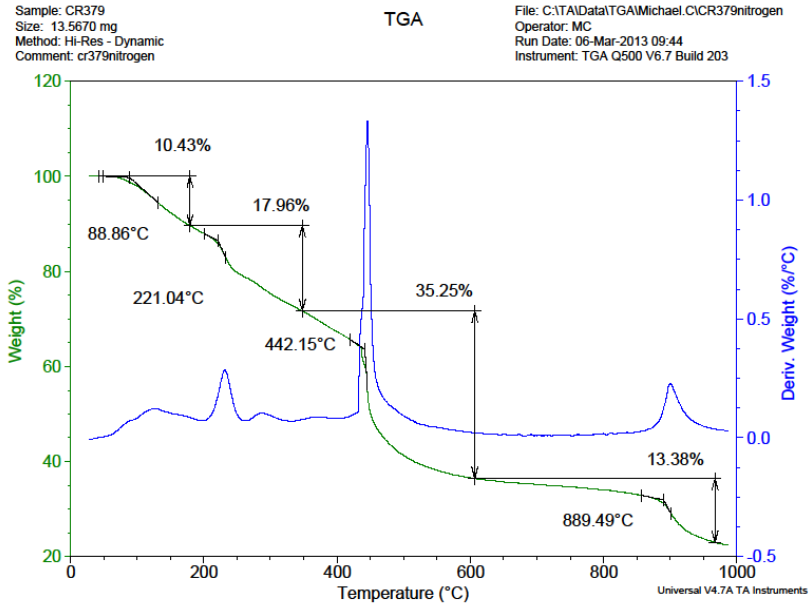

Figure A. 10: TGA of 2.8 under nitrogen.

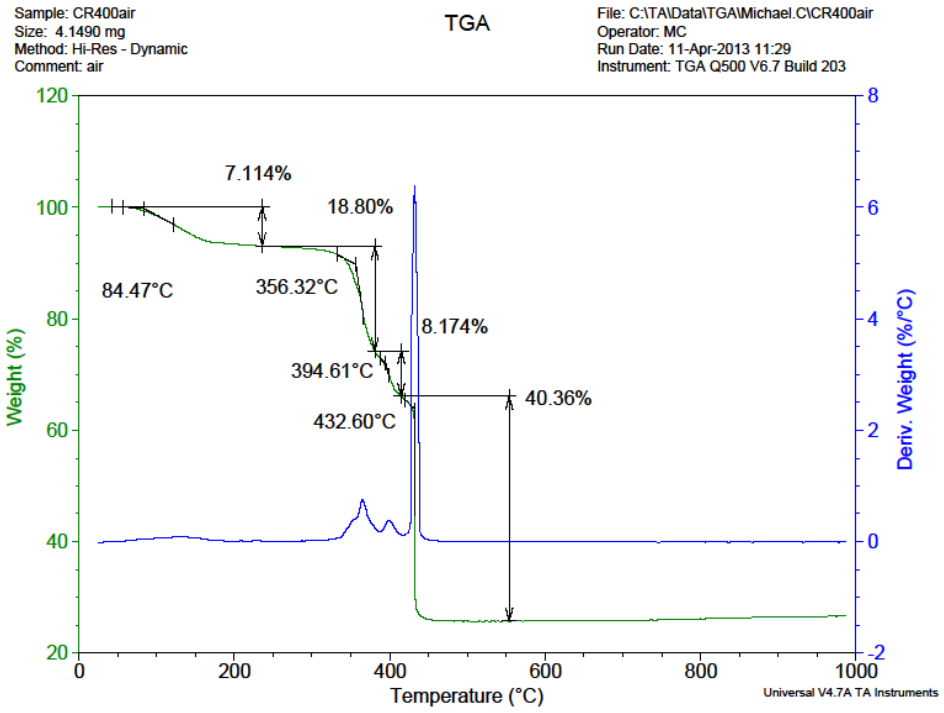

Figure A.11: TGA of 2.14 under air.

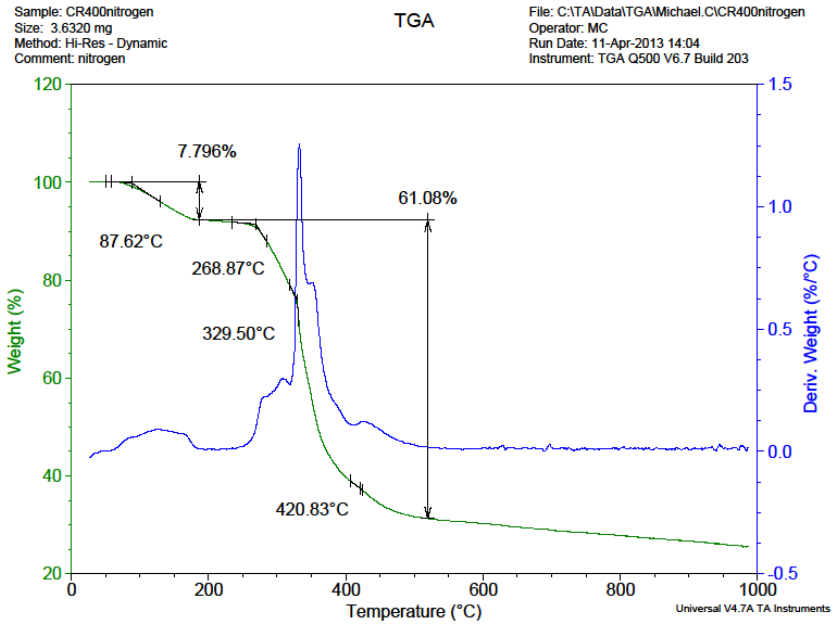

Figure A.12: TGA of 2.14 under nitrogen.

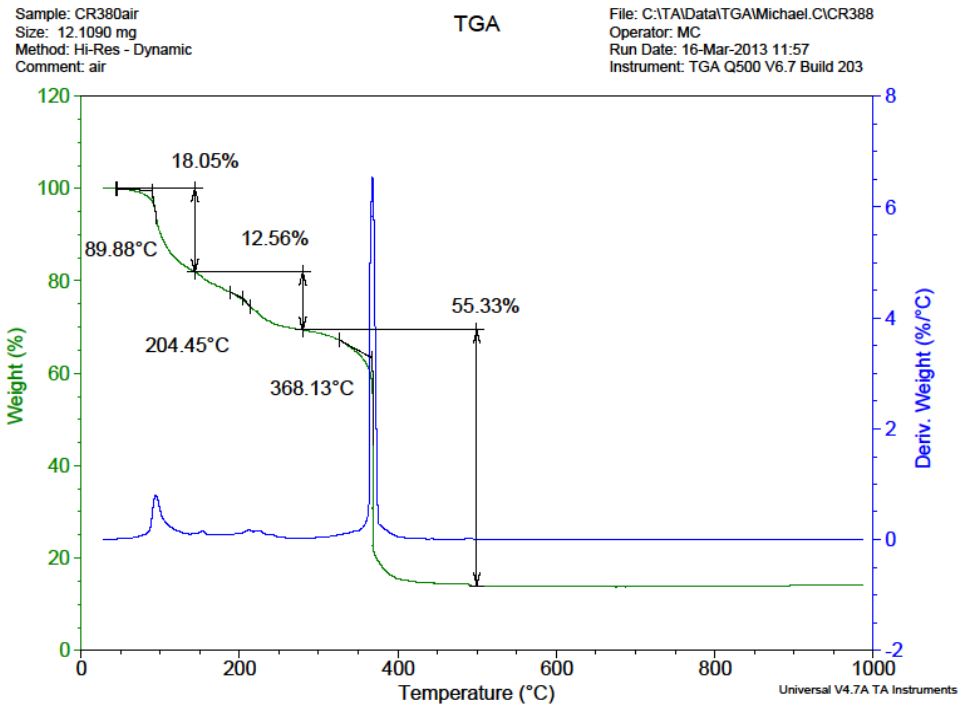

Figure A.13: TGA of 2.19 under air.

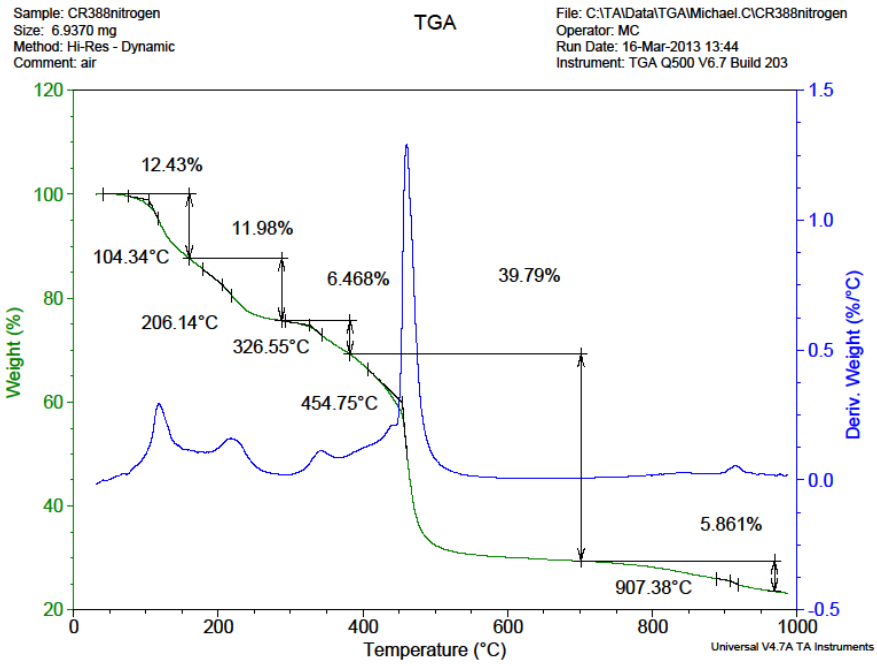

Figure A.14: TGA of 2.19 under nitrogen.

A.3 Thermal data for Chapter Three

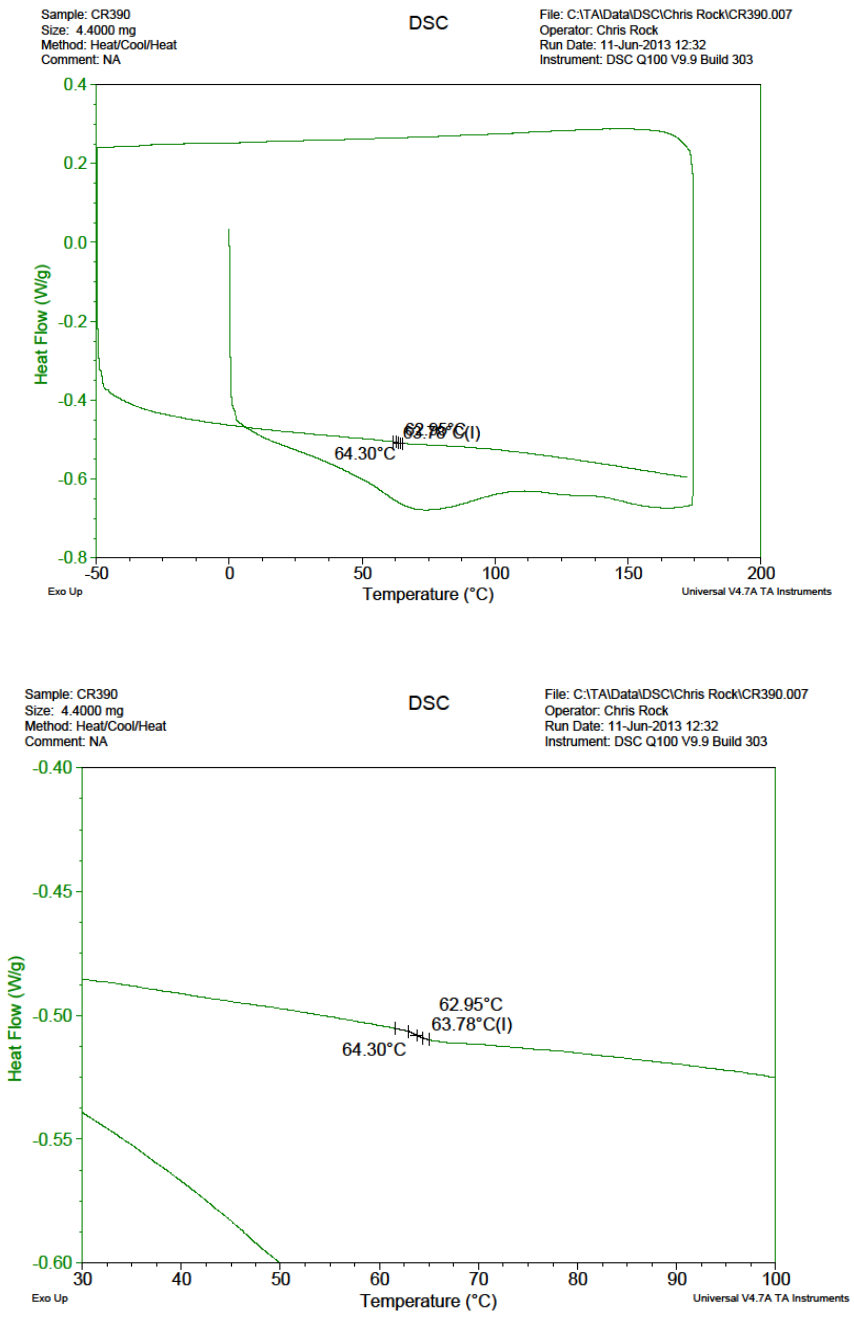

Figure A.15: DSC of 3.1.

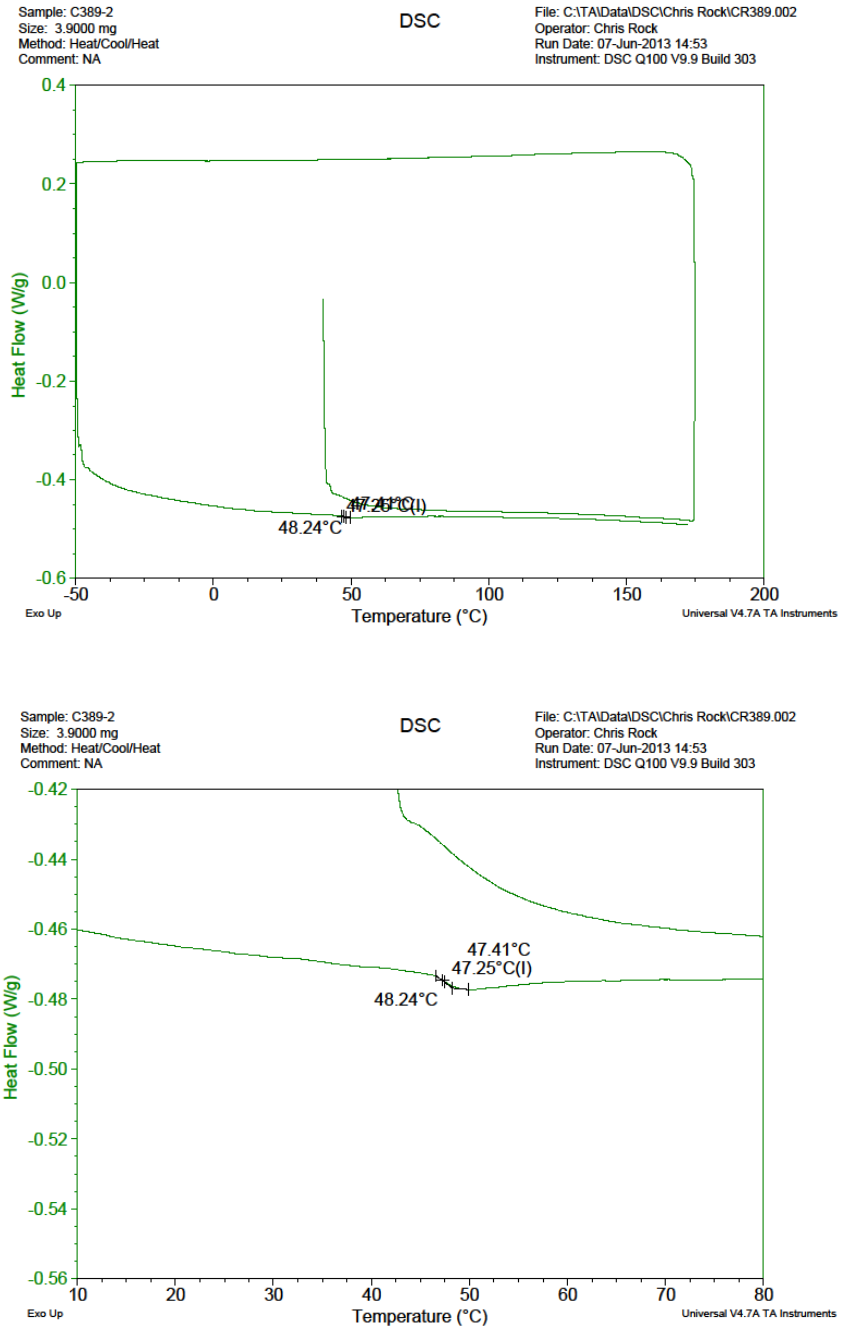

Figure A.16: DSC of 3.2.

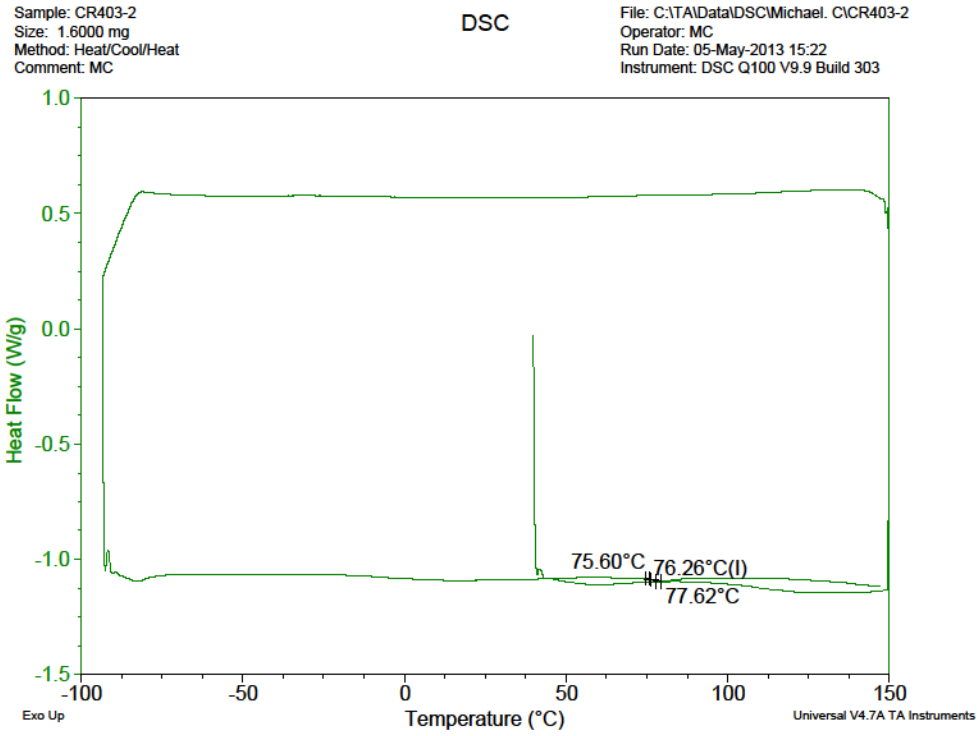

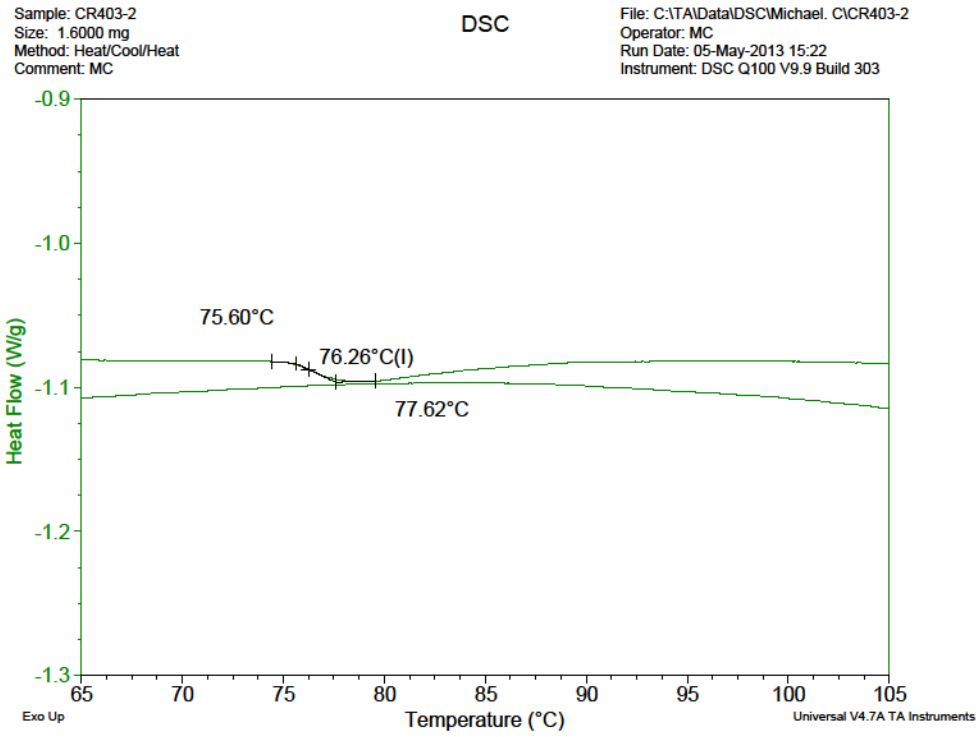

Figure A.17: DSC of 3.3.

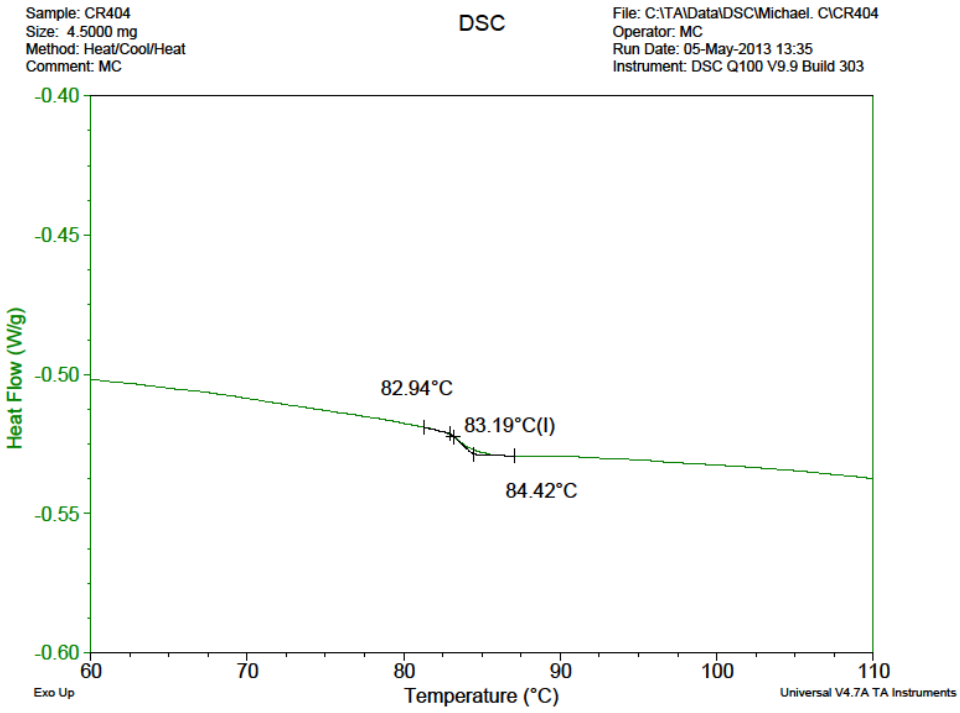

Figure A.18: DSC of 3.4.

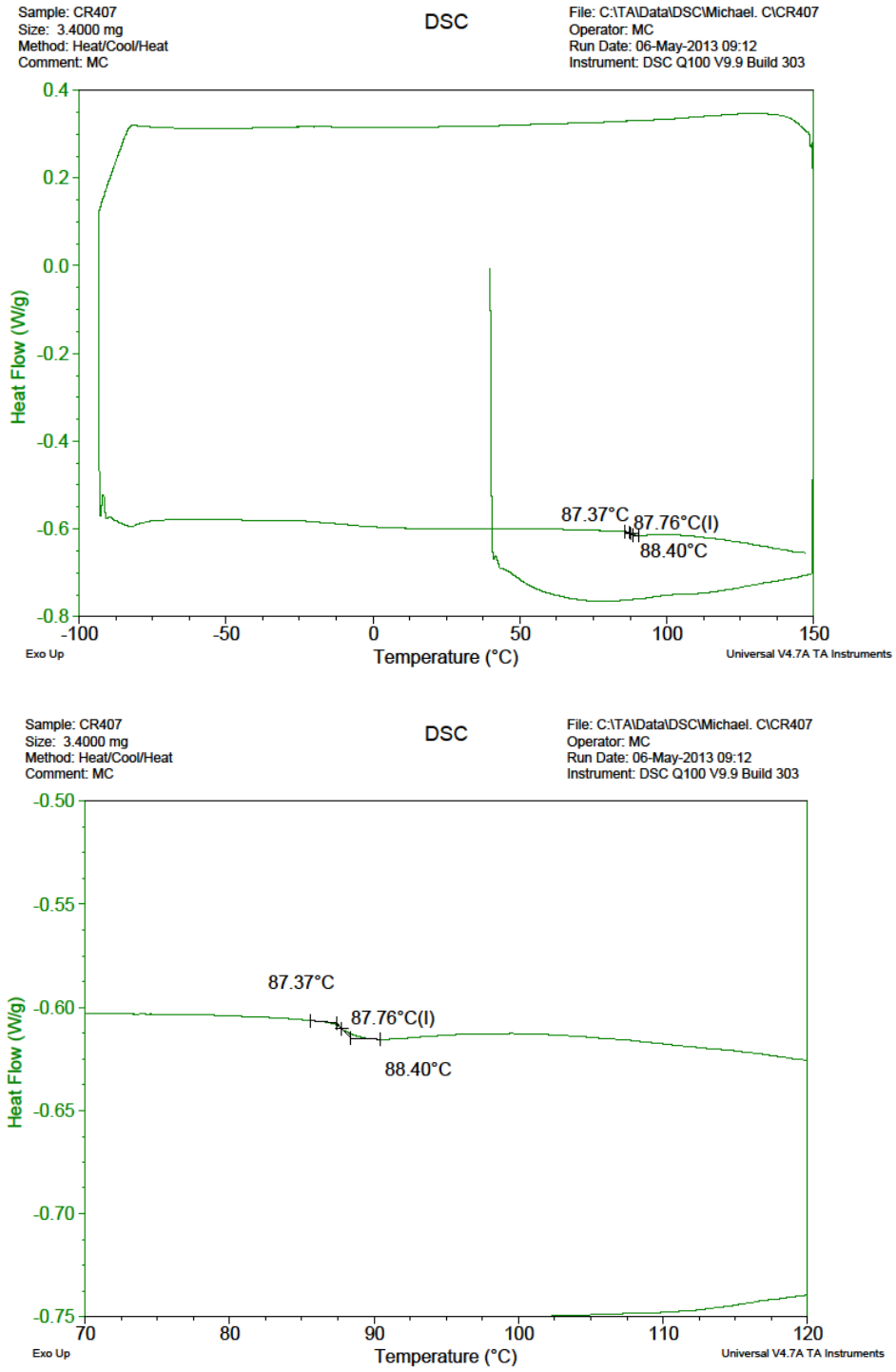

Figure A.19: DSC of 3.5.

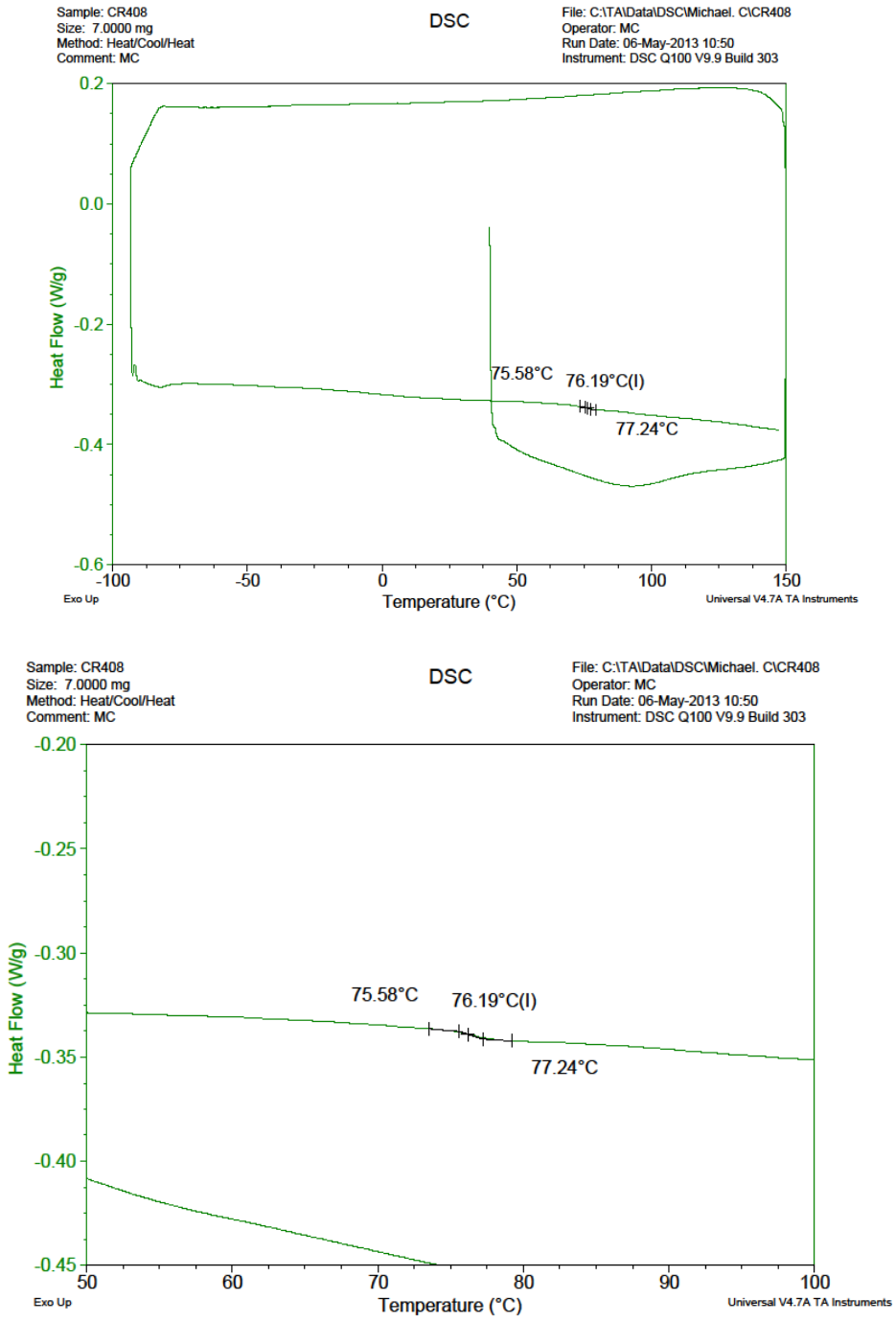

Figure A.20: DSC of 3.6.

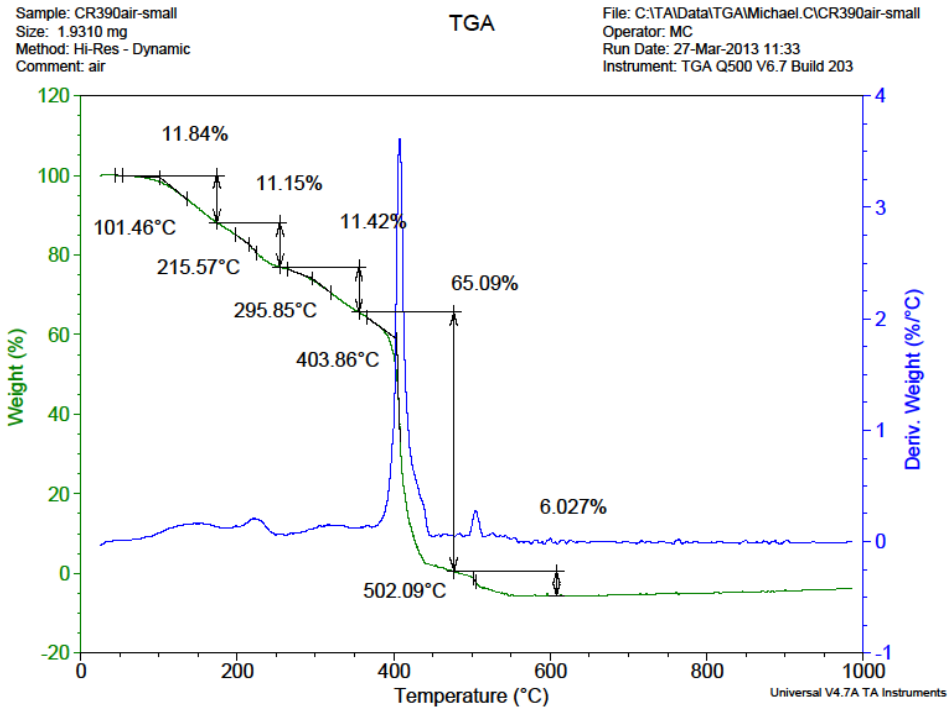

Figure A.21: TGA of 3.1 in air.

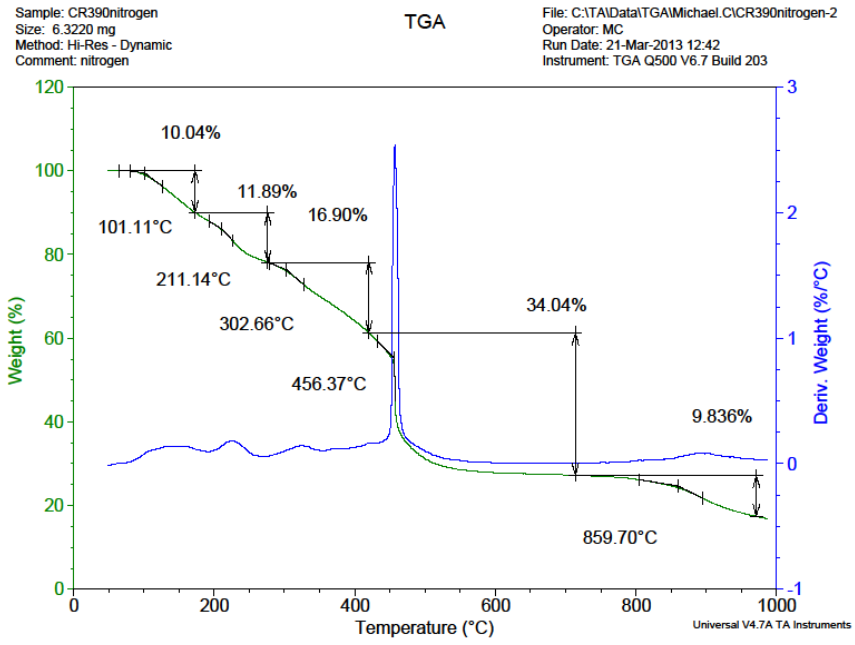

Figure A.22: TGA of 3.1 in nitrogen.

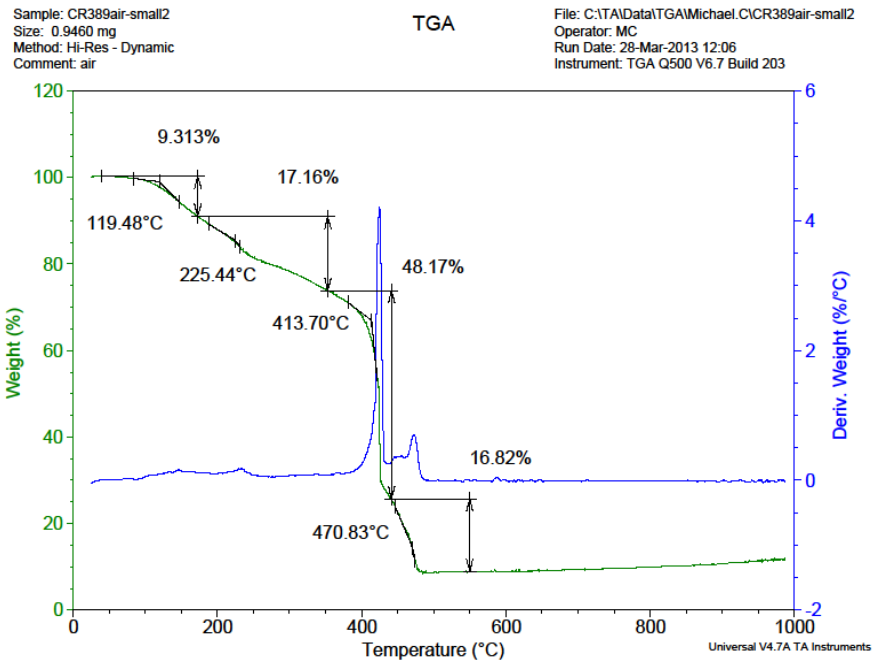

Figure A.23: TGA of 3.2 in air.

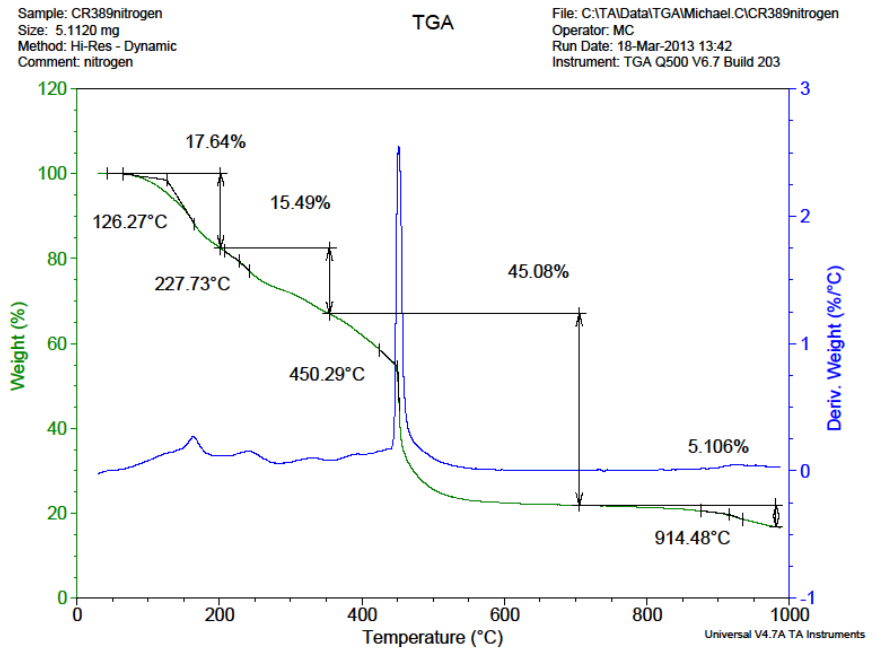

Figure A.24: TGA of 3.2 in nitrogen.

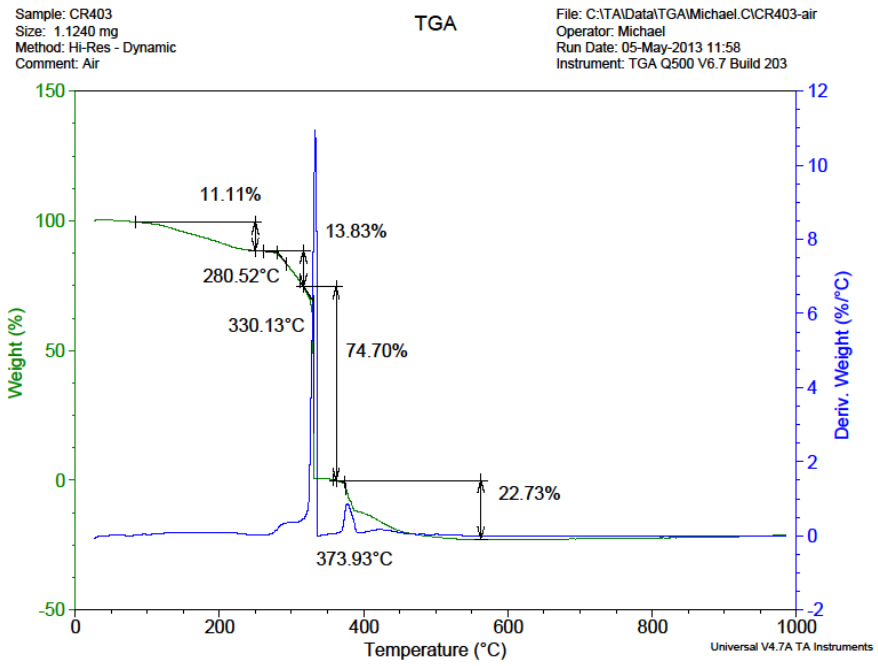

Figure A.25: TGA of 3.3 in air.

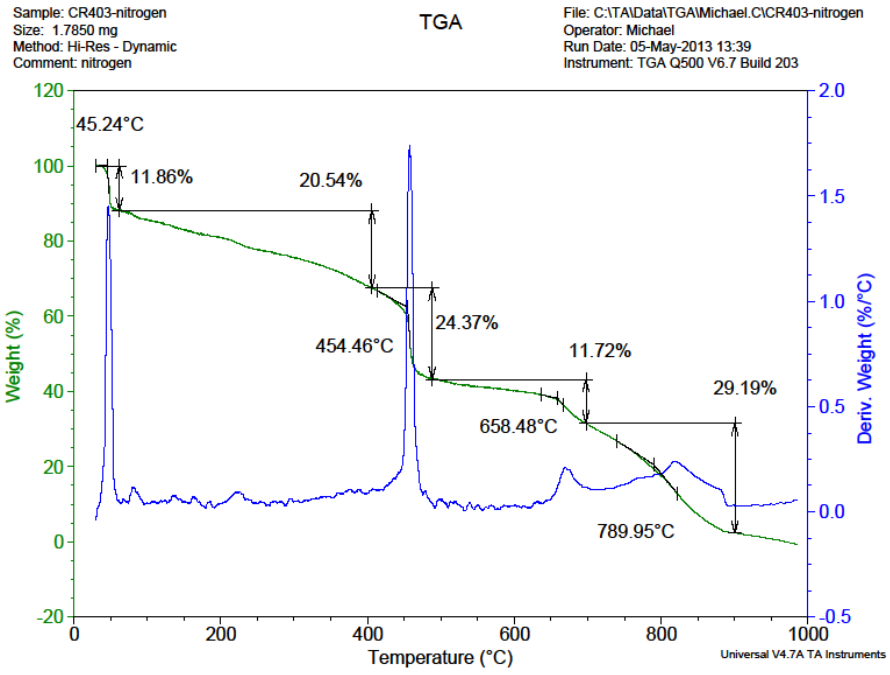

Figure A.26: TGA of 3.3 in nitrogen.

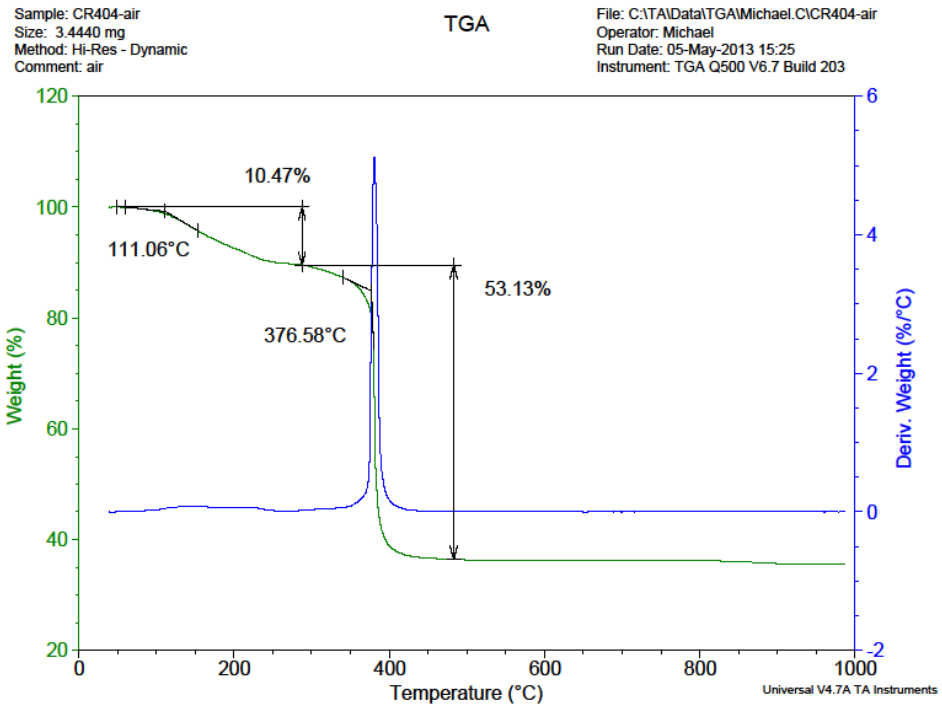

Figure A.27: TGA of 3.4 in air.

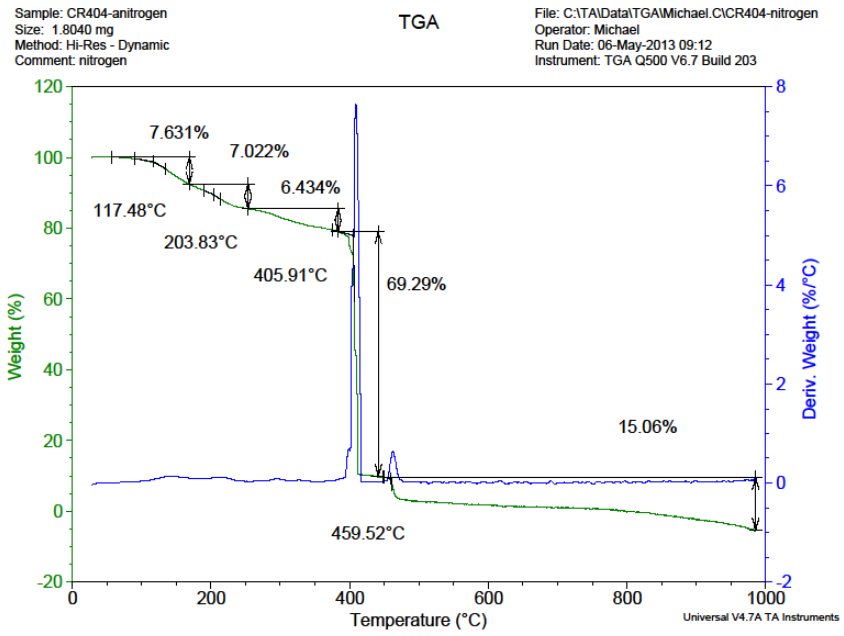

Figure A.28: TGA of 3.4 in nitrogen.

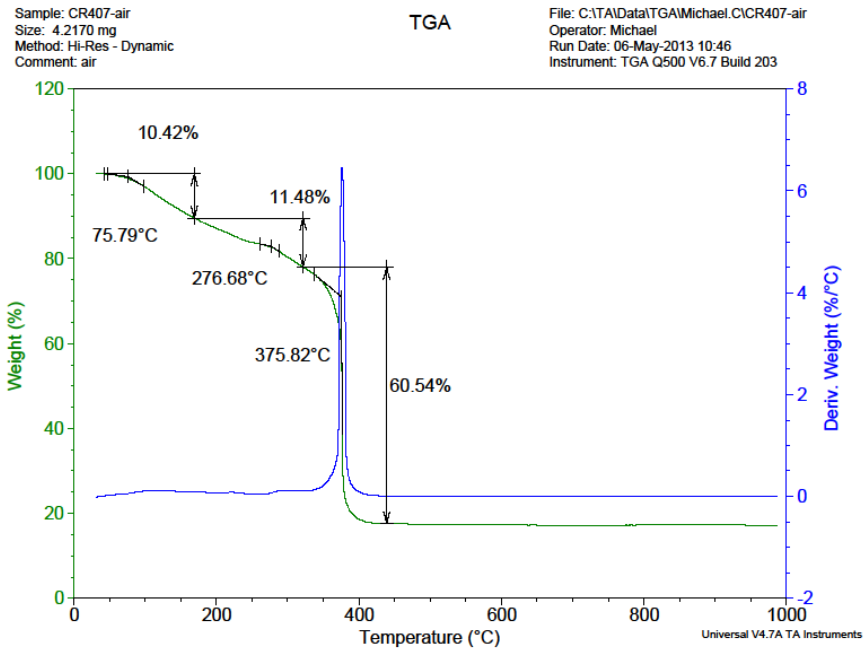

Figure A.29: TGA of 3.5 in air.

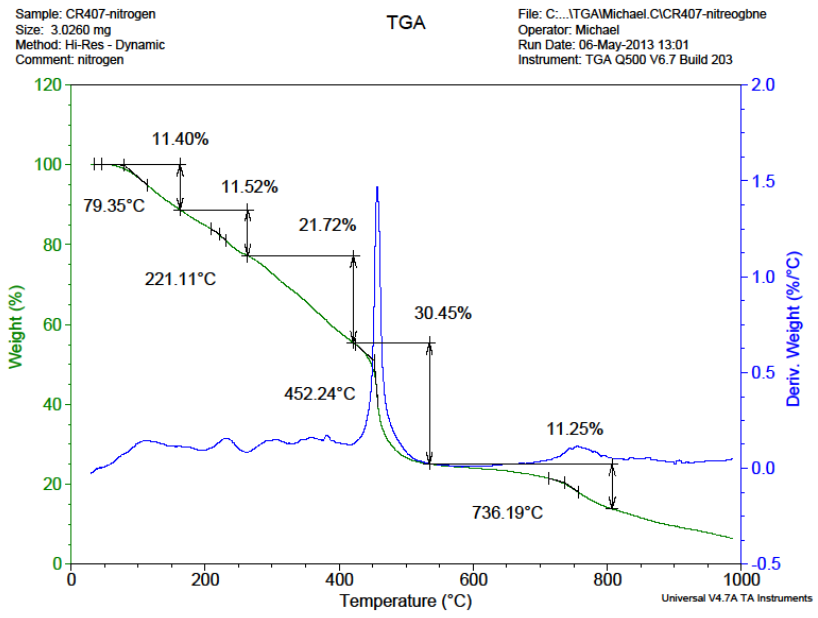

Figure A.30: TGA of 3.5 in nitrogen.

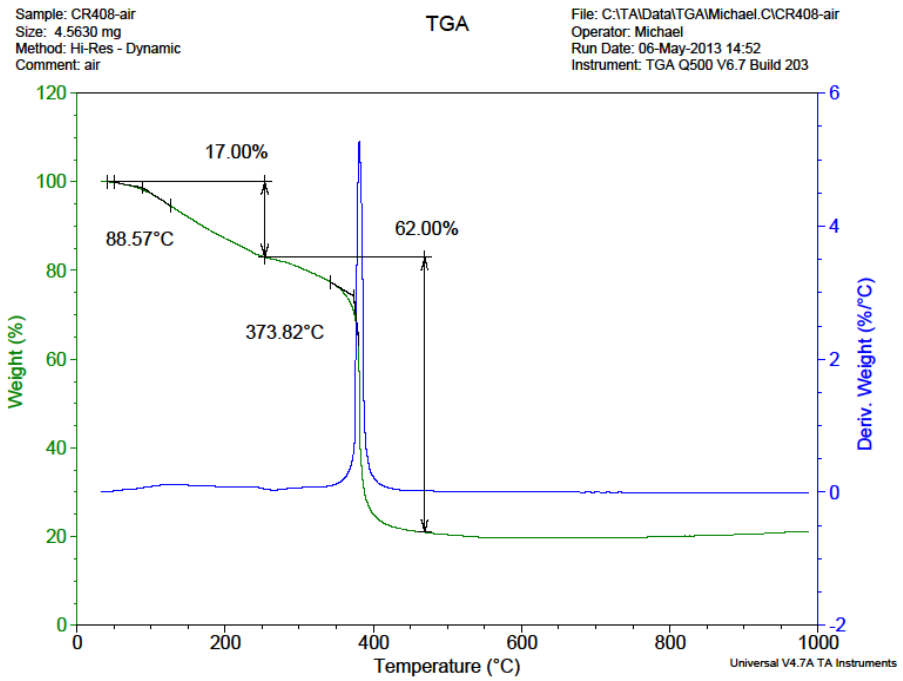

Figure A.31: TGA of 3.6 in air.

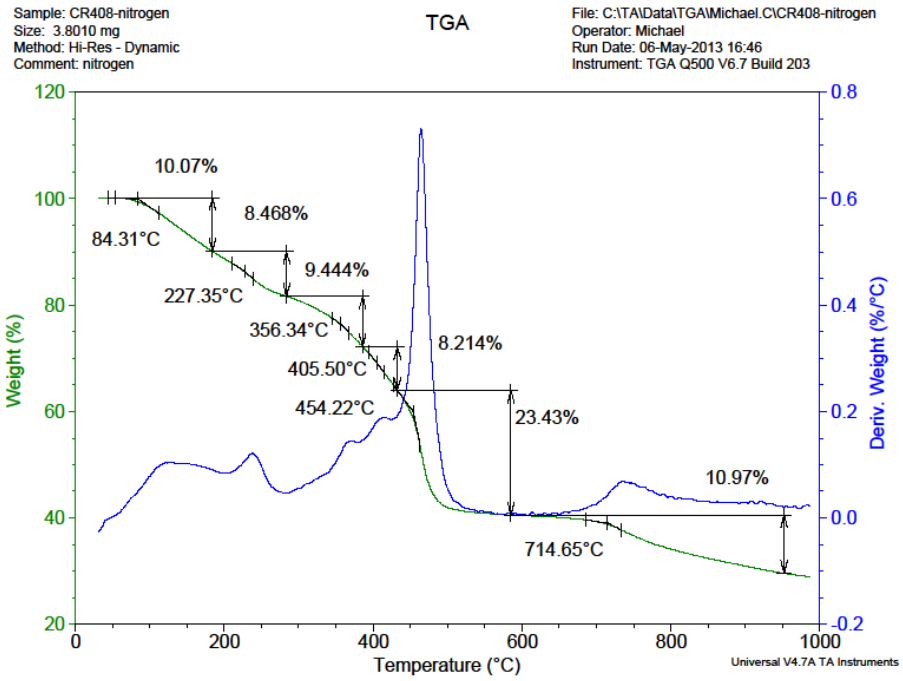

Figure A.32: TGA of 3.6 in nitrogen.

A.4 NMR data for Chapter Four

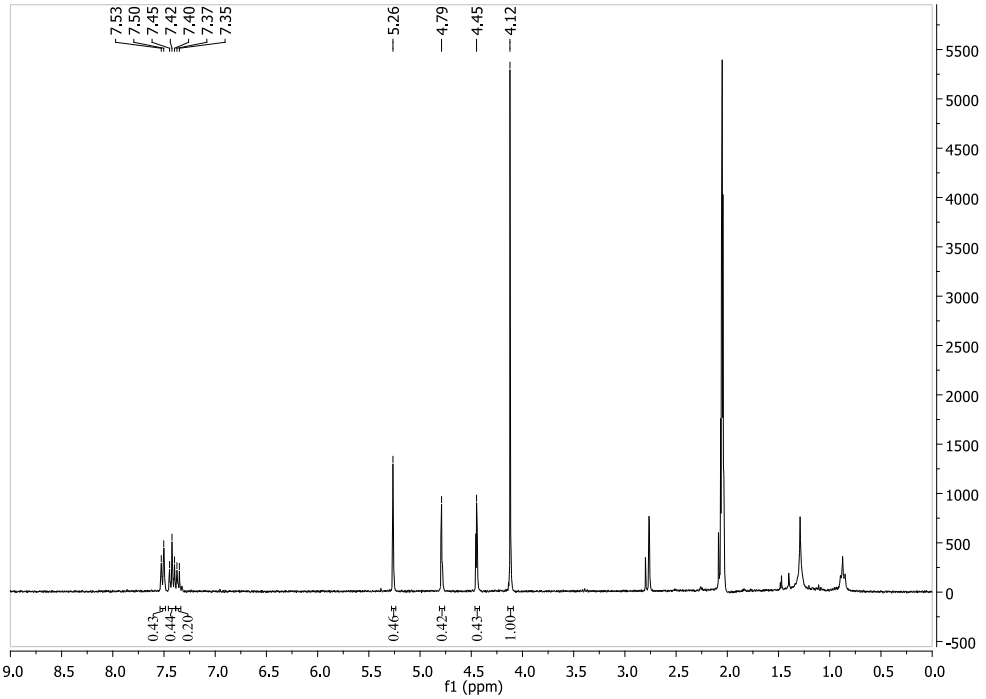

Figure A.33: Full ^{1}H NMR spectrum of 4.1.

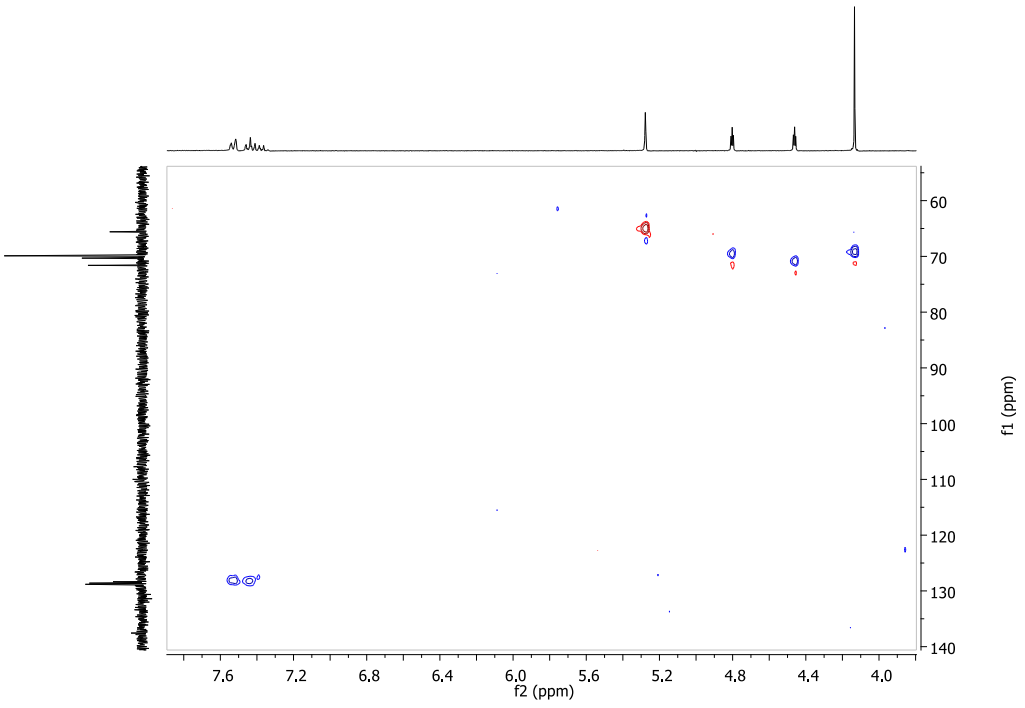

Figure A.34: Section of the HSQC NMR spectra of 4.1 showing structural signals.

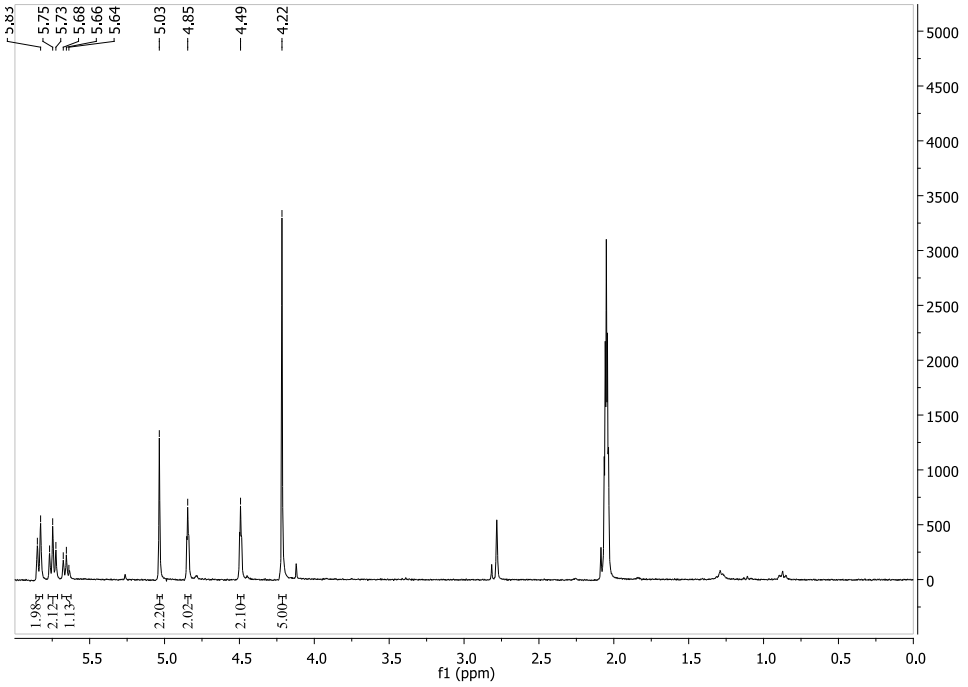

Figure A.35: ^{1}H NMR spectrum of 4.2.

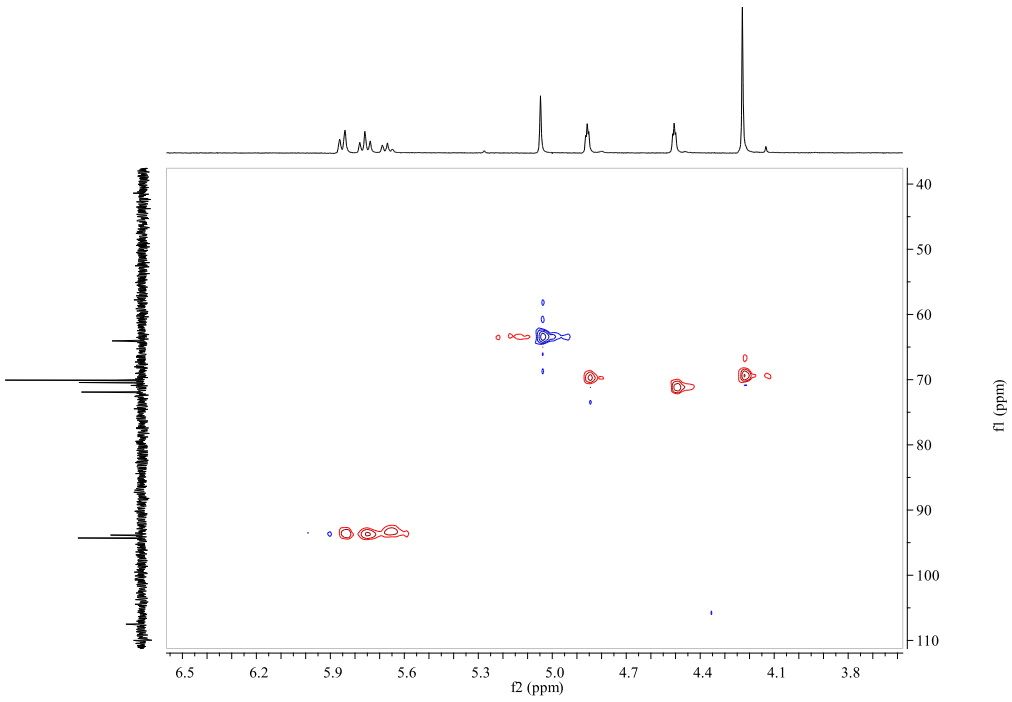

Figure A.36: Section of the HSQC NMR spectrum of 4.2 showing structural signals.

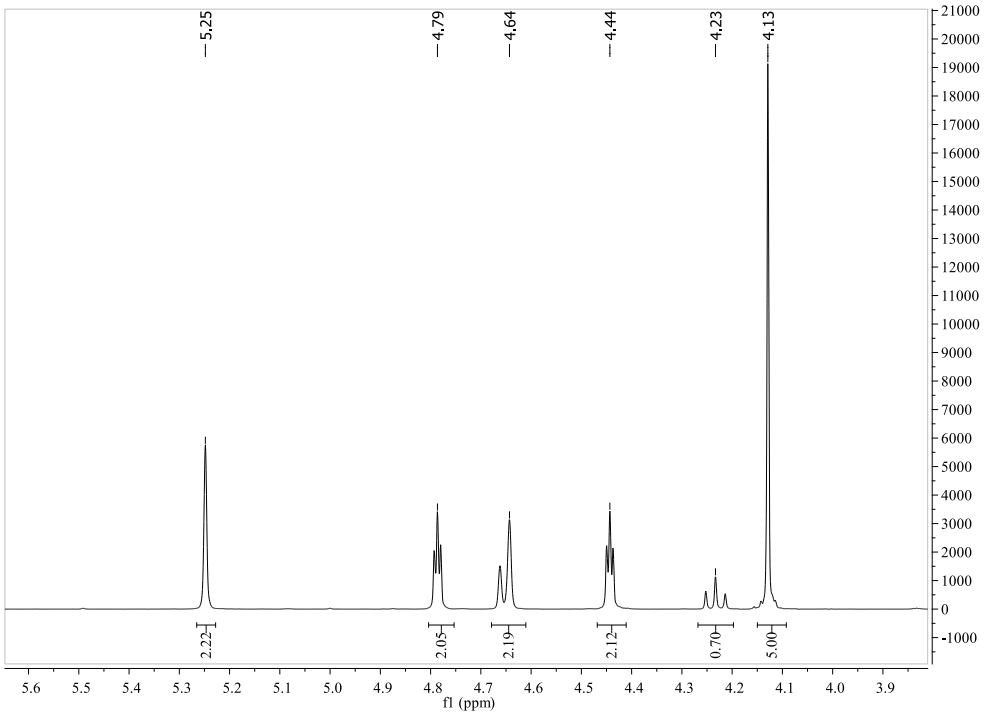

Figure A.37: ^{1}H NMR spectrum of 4.4.

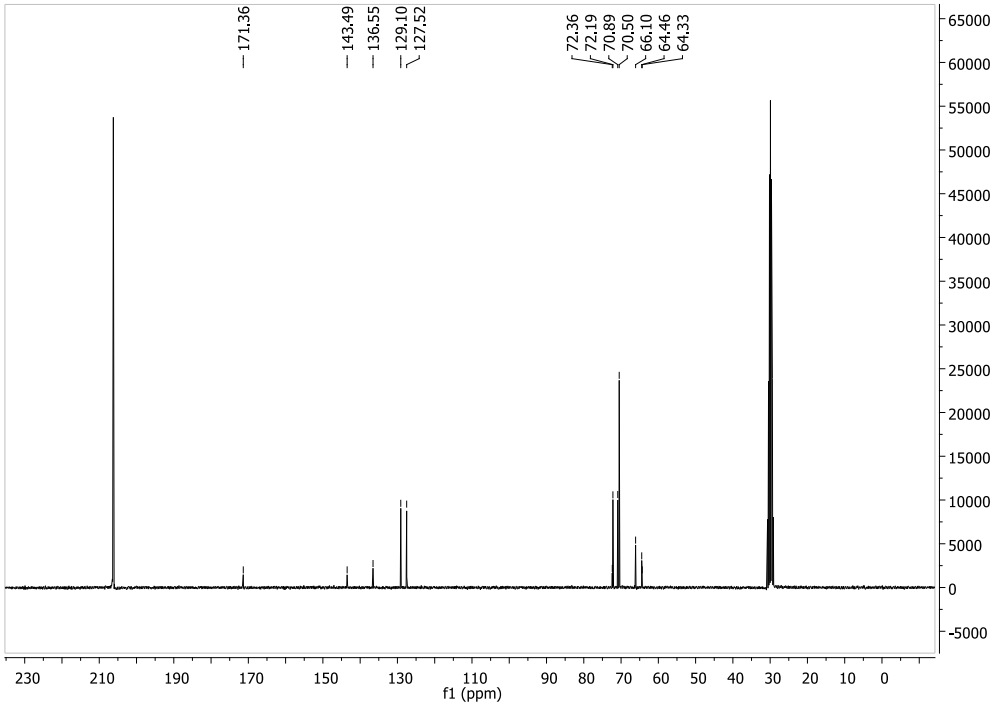

Figure A. 38: ^{13}C NMR spectrum of 4.4.

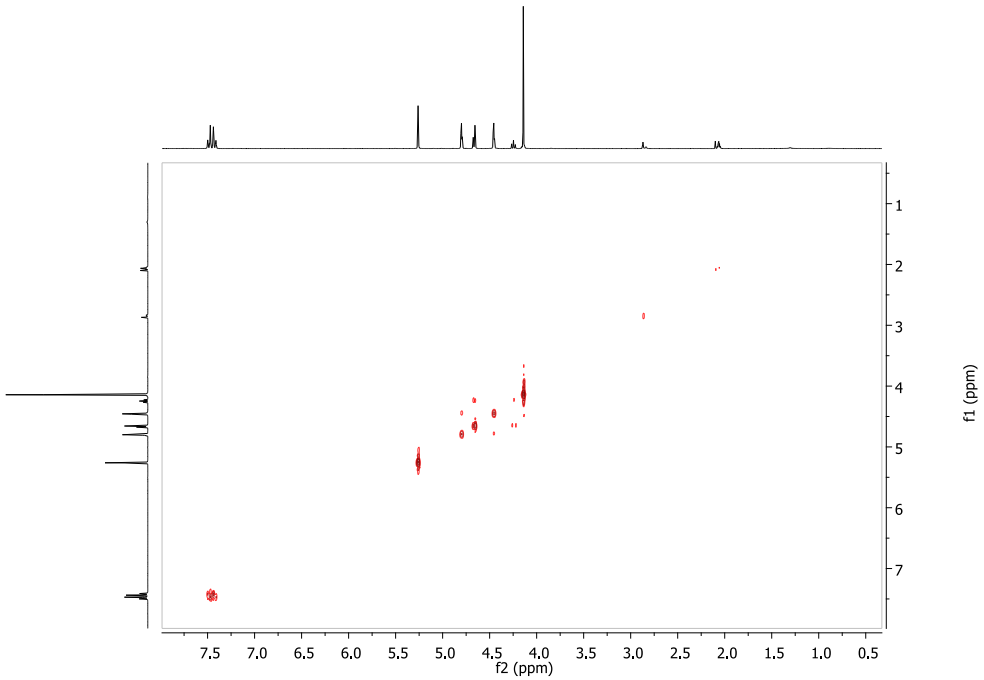

Figure A. 39: COSY NMR of 4.4.

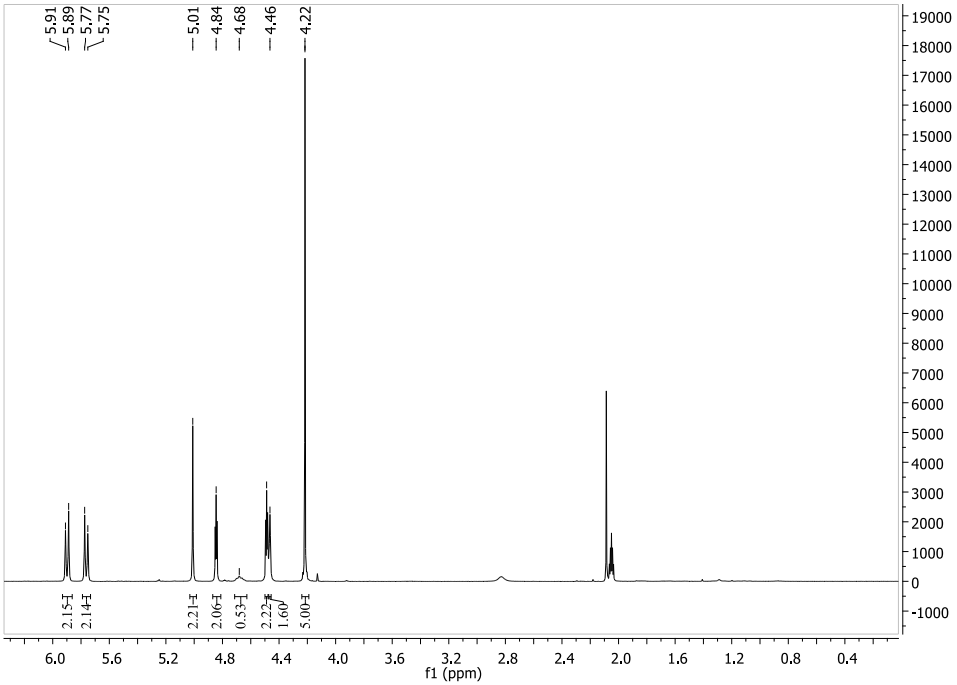

Figure A.40: ^{1}H NMR spectrum of 4.5.

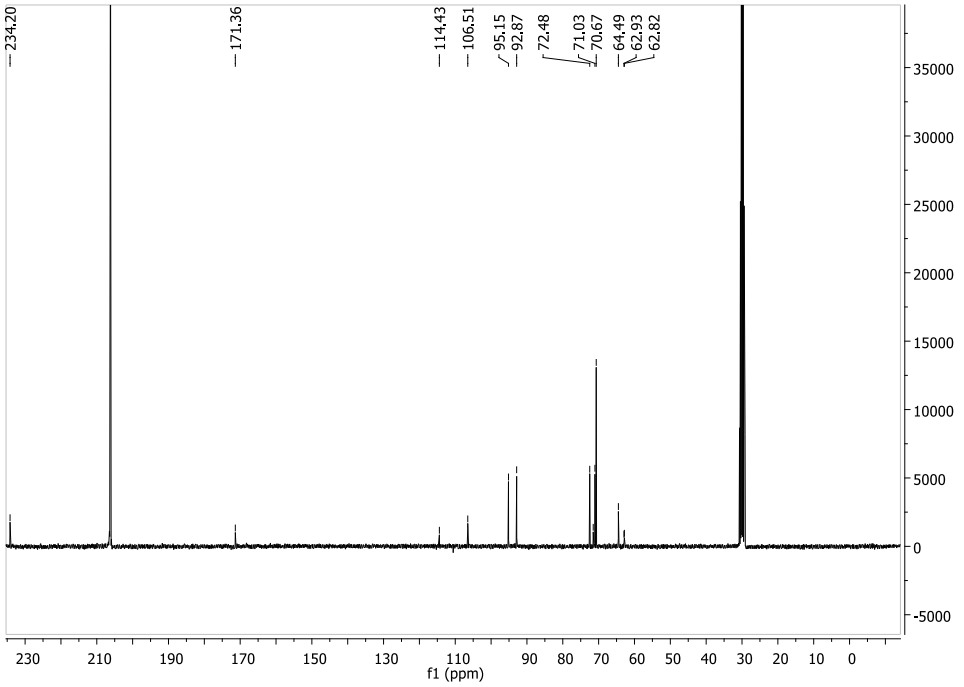

Figure A.41: ^{13}C NMR spectrum of 4.5.

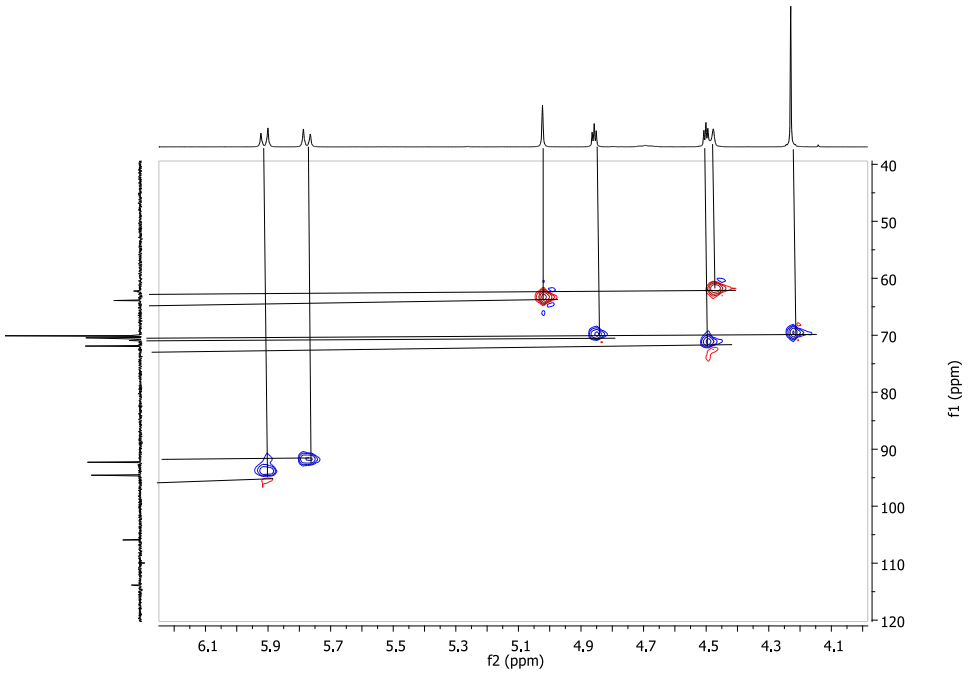

Figure A.42: Section of the HSQC NMR spectra of 4.5 showing structural signals.

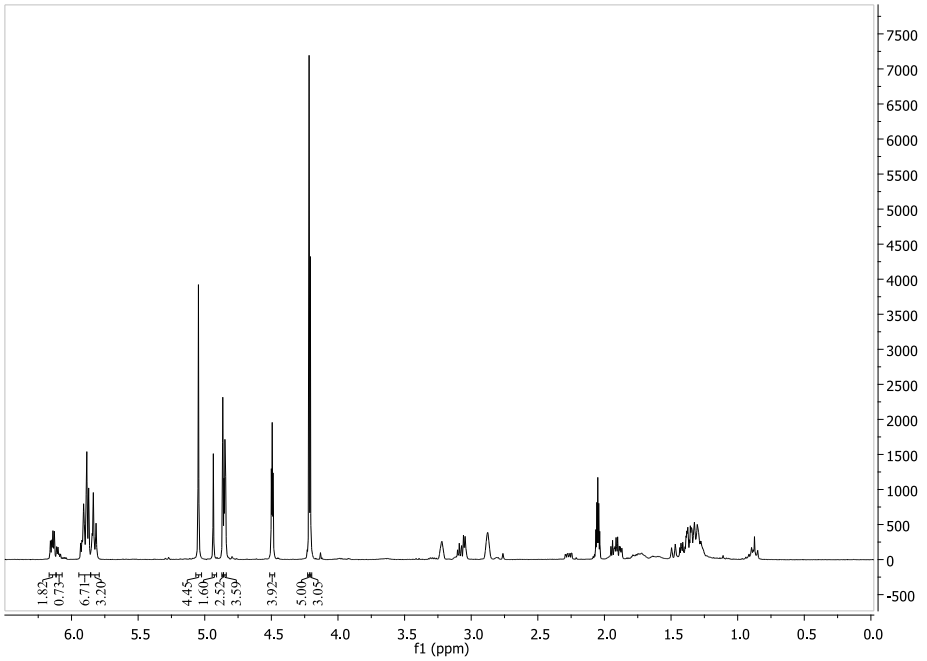

Figure A.43: Full ^{1}H NMR spectrum of 4.6.

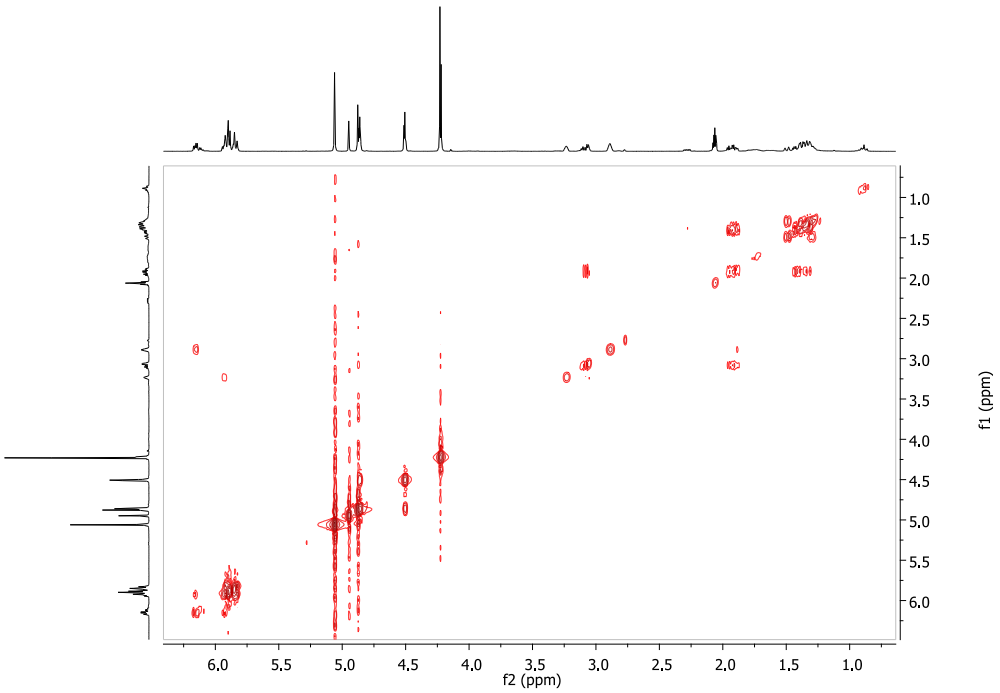

Figure A.44: COSY NMR spectrum of 4.6.

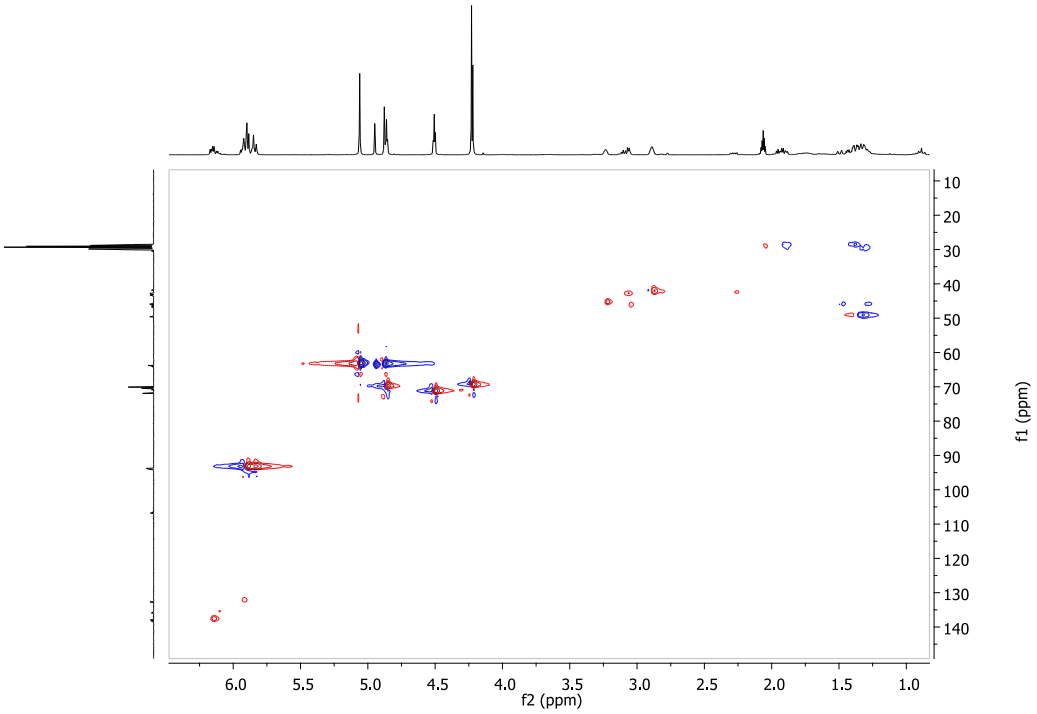

Figure A.45: HSQC NMR spectrum of 4.6.

A.5 Thermal data for Chapter Four

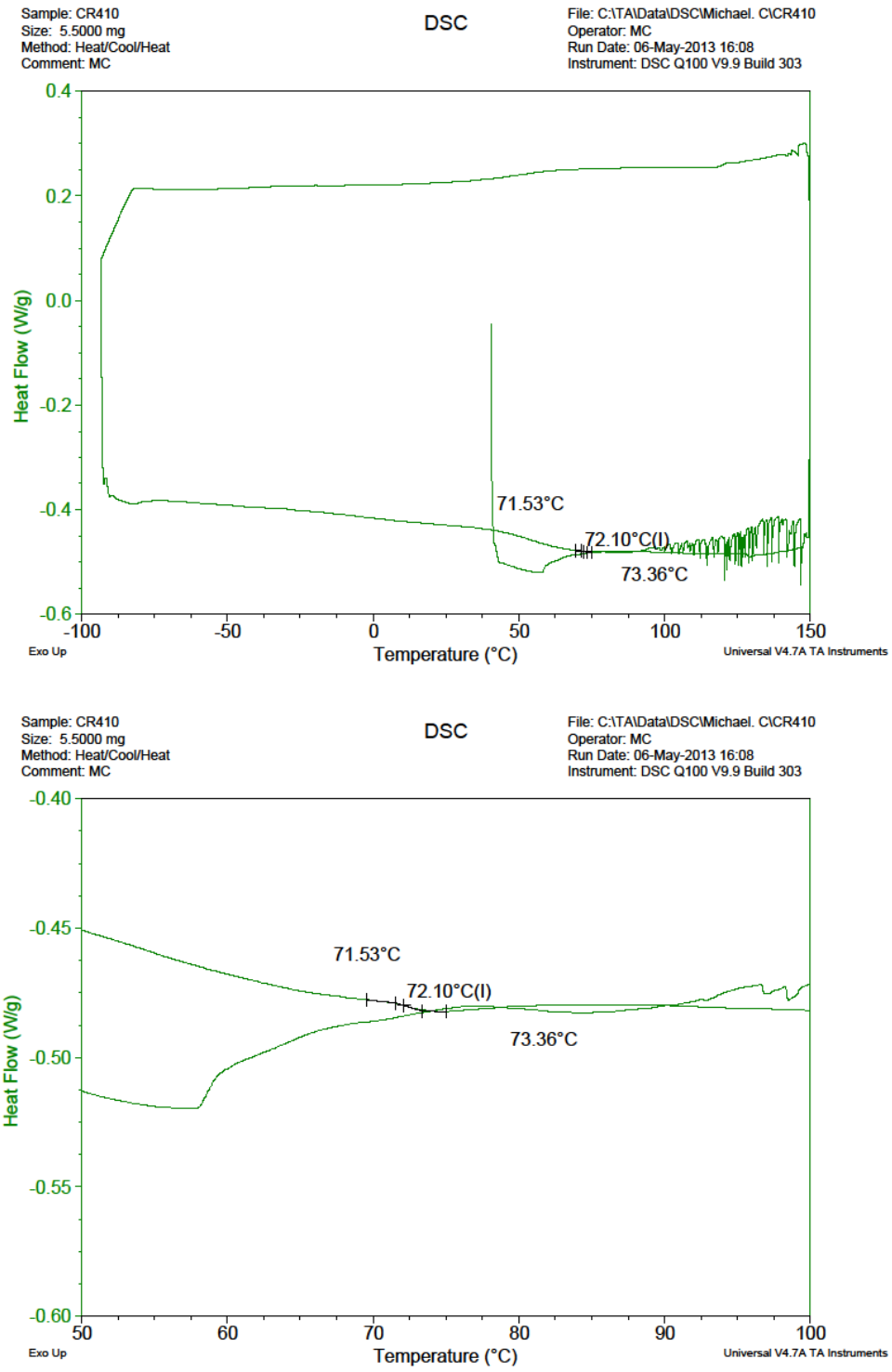

Figure A.46: DSC of 4.7.

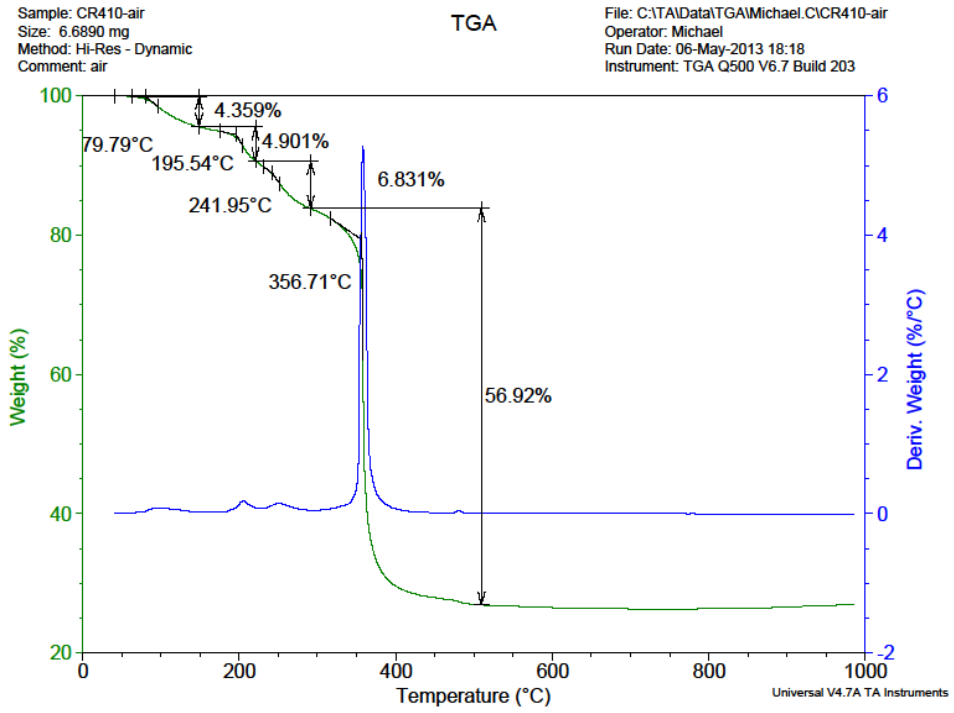

Figure A.47: TGA of 4.7 in air.

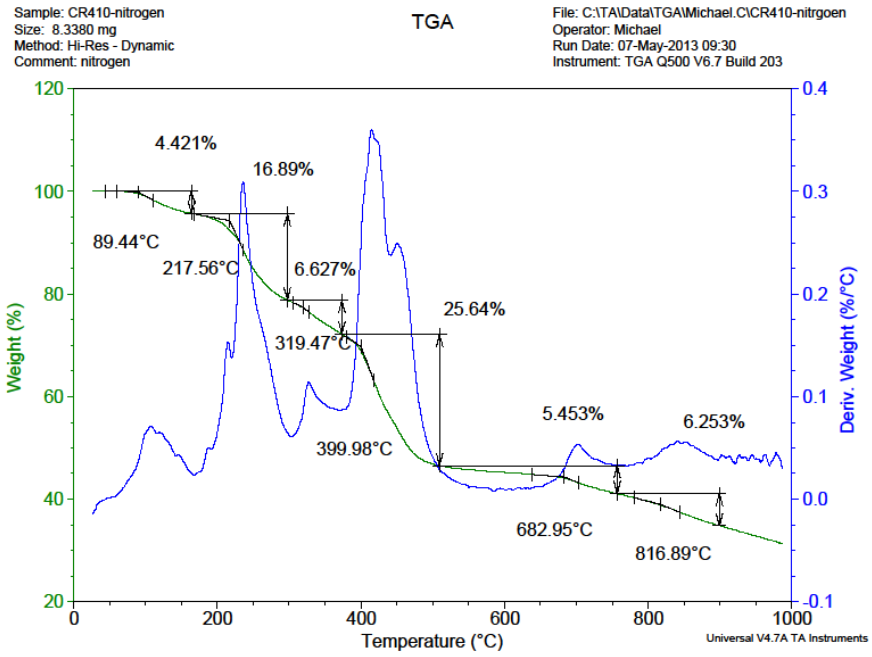

Figure A.48: TGA of 4.7 in nitrogen.

A.6 Solid state NMR experimental

Sample Description and Preparation

The samples were brilliantly colored films, some of them were very electrostati-cally charged during sample packing.

Experimental Conditions

The NMR experiments were carried out on a Bruker Advance NMR spectrometer with a 9.4 T magnet (400.24 MHz proton Larmor frequency, 100.64 MHz 13C Larmor frequency) using our probe head for rotors of 4 mm diameter. The ^{1}H NMR spectra were acquired with single pulse excitation and background suppression. Their spectral parameters are needed for the determination of the experimental parameters for the 13C NMR experiments. The ^{1}H NMR reference was calculated from the 13C reference using the IUPAC Recommendations 2001 [1]. The ^{1}H spin lattice relaxation times, T1, were determined by inversion-recovery sequences and were found to be on the order of 7 – 240 ms.

The parameters for the ^{13}C cross-polarization (CP)/ magic angle spinning (MAS) experiments with TPPM proton decoupling were optimized on glycine, whose carbonyl resonance also served as external, secondary chemical shift standard at 176.06 ppm. For the final ^{13}C CP/MAS NMR spectra between 80 to 1200 scans were accumulated using 2.6 ms CP contact time with repetition times of 2s, as dictated by the probe duty cycle.

The ^{13}C CP/MAS NMR spectra were measured at spinning speeds between 7 and 13 kHz. Since fast magic angle spinning suppresses the cross-polarization efficiency (1H - 13C dipole-dipole coupling) the slowest spinning speed, which prevented overlap of spinning sidebands with isotropic center bands, was chosen for the acquisition of the high quality spectra.

References

[1] R. K. Harris, E. D. Becker, S. M. Cabral De Menezes, R. Goodfellow, and P. Granger, *Pure. Appl. Chem.* 2001, *73* 1795-1818.

A.6 X-ray crystallography data for 4.4

Data Collection

An orange plate crystal of $C_{21}H_{16}CrFeO_5$ having approximate dimensions of 0.03 x 0.17 x 0.35 mm was mounted on a glass fiber. All measurements were made on a Bruker APEX DUO diffractometer with graphite monochromated Mo-Kα radiation..

The data were collected at a temperature of -183.0 $\pm$ 0.1°C to a maximum 2θ value of 60.2°. Data were collected in a series of ϕand ω scans in 0.5° oscillations using 10.0-second exposures. The crystal-to-detector distance was 60.00 mm.

Data Reduction

The material crystallizes as a two-component twinned crystal with the two components related by a 180º degrees about the (0 0 1) reciprocal axis. Data were integrated for both twin components, including both overlapped and non-overlapped reflections. In total 50244 reflections were integrated (4989 from component one only, 5001 from component two only, 40254 overlapped). Additionally, there are two crystallographically independent molecules in the asymmetric unit. Data were collected and integrated using the Bruker SAINT[1] software packages. The linear absorption coefficient, μ, for Mo-Kα radiation is 14.26 cm^{-1}. Data were corrected for absorption effects using the multi-scan technique (TWINABS[2]), with minimum and maximum transmission coefficients of 0.704 and 0.958, respectively. The data were corrected for Lorentz and polarization effects.

Structure Solution and Refinement

The structure was solved by direct methods[3] using non-overlapped data from the major twin component. Subsequent refinements were carried out using an HKLF 5 format data set containing complete data from component 1 and any overlapped reflections from component 2. The material crystallizes with two independent molecules in the asymmetric unit. All non-hydrogen atoms were refined anisotropically. All CH hydrogen atoms were placed in calculated positions. The batch scale refinement showed a roughly 55:45 ratio between the major and minor twin components. The final cycle of

full-matrix least-squares refinement[4] on F^2 was based on 10229 reflections and 506 variable parameters and converged (largest parameter shift was 0.00 times its esd) with unweighted and weighted agreement factors of:

$$R1 = \Sigma \, ||Fo| - |Fc|| \, / \, \Sigma \, |Fo| = 0.052$$

$$wR2 = [\, \Sigma \, (\, w \, (Fo^2 - Fc^2)^2 \,) / \, \Sigma \, w(Fo^2)^2]^{1/2} = 0.113$$

The standard deviation of an observation of unit weight[5] was 1.14. The weighting scheme was based on counting statistics. The maximum and minimum peaks on the final difference Fourier map corresponded to 0.61 and –1.40 $e^-/Å^3$, respectively.

Neutral atom scattering factors were taken from Cromer and Waber[6]. Anomalous dispersion effects were included in Fcalc[7]; the values for Δf' and Δf'' were those of Creagh and McAuley[8]. The values for the mass attenuation coefficients are those of Creagh and Hubbell[9]. All refinements were performed using the SHELXL-97[10] via the WinGX[11] interface.

References

(1) SAINT. Version 7.68A. Bruker AXS Inc., Madison, Wisconsin, USA. (1997-2010).

(2) TWINABS. Bruker AXS scaling for twinned crystals - V2008/4, Bruker AXS Inc., Madison, Wisconsin, USA (2008).

(3) SIR97 - Altomare A., Burla M.C., Camalli M., Cascarano G.L., Giacovazzo C. , Guagliardi A., Moliterni A.G.G., Polidori G.,Spagna R. (1999) J. Appl. Cryst. 32, 115-119.

(4) Least Squares function minimized:

$$\Sigma w(F_o^2-F_c^2)^2$$

(5) Standard deviation of an observation of unit weight:

$$[\Sigma w(F_o^2-F_c^2)^2/(N_o-N_v)]^{1/2}$$

where: N_o = number of observations

N_v = number of variables

(6) Cromer, D. T. & Waber, J. T.; "International Tables for X-ray Crystallography", Vol. IV, The Kynoch Press, Birmingham, England, Table 2.2 A (1974).

(7) Ibers, J. A. & Hamilton, W. C.; Acta Crystallogr., 17, 781 (1964).

(8) Creagh, D. C. & McAuley, W.J .; "International Tables for Crystallography", Vol C, (A.J.C. Wilson, ed.), Kluwer Academic Publishers, Boston, Table 4.2.6.8, pages 219-222 (1992).

(9) Creagh, D. C. & Hubbell, J.H..; "International Tables for Crystallography", Vol C, (A.J.C. Wilson, ed.), Kluwer Academic Publishers, Boston, Table 4.2.4.3, pages 200-206 (1992).

(10) SHELXTL Version 2008/4. Bruker AXS Inc., Madison, Wisconsin, USA. (2008).

(11) WinGX – V1.80.05 – Farrugia, L.J.; J. Appl. Cryst., 32, 837 (1999).

Experimental Details

A. Crystal Data

Empirical Formula	$C_{21}H_{16}CrFeO_5$
Formula Weight	456.19
Crystal Colour, Habit	orange, plate
Crystal Dimensions	0.03 X 0.17 X 0.35 mm
Crystal System	triclinic
Lattice Type	primitive
Lattice Parameters	a = 7.8586(16) Å
	b = 8.0242(15) Å
	c = 29.095(6) Å
	α = 88.092(4) ^{o}
	β = 88.215(4) ^{o}
	γ = 82.723(4) ^{o}
	V = 1818.2(6) Å^3
Space Group	*P* -1 (#2)
Z value	4
D_{calc}	1.666 g/cm^3
F_{000}	928.00
μ(Mo-Kα)	14.26 cm^{-1}

B. Intensity Measurements

Diffractometer	Bruker APEX DUO
Radiation	Mo-Kα (λ = 0.71073 Å)
Data Images	5741 exposures @ 10.0 seconds
Detector Position	60.00 mm
$2\theta_{max}$	60.2^{o}
No. of Reflections Measured	Total: 50244
	Unique: 10229 (R_{int} = 0.059)
Corrections	Absorption (T_{min} = 0.704, T_{max}= 0.958)
	Lorentz-polarization

C. Structure Solution and Refinement

Structure Solution	Direct Methods (SIR97)
Refinement	Full-matrix least-squares on F^2
Function Minimized	Σ w $(Fo^2 - Fc^2)^2$
Least Squares Weights	$w=1/(\sigma^2(Fo^2)+(0.0213P)^2+ 6.1194P)$
Anomalous Dispersion	All non-hydrogen atoms
No. Observations (I>0.00σ(I))	10229
No. Variables	506
Reflection/Parameter Ratio	20.22
Residuals (refined on F^2, all data): R1; wR2	0.052; 0.113
Goodness of Fit Indicator	1.14
No. Observations (I>2.00σ(I))	9421
Residuals (refined on F): R1; wR2	0.048; 0.111
Max Shift/Error in Final Cycle	0.00
Maximum peak in Final Diff. Map	0.61 $e^-/Å^3$
Minimum peak in Final Diff. Map	-1.40 $e^-/Å^3$

Table 2: Atomic coordinates (x 10^4) and equivalent isotropic displacement parameters (A^2 x 10^3) for 4.4.

U(eq) is defined as one third of the trace of the orthogonalized Uij tensor.

	x	y	z	U(eq)
C(1)	3501(6)	9176(5)	619(1)	14(1)
C(2)	3195(6)	8782(5)	1091(2)	15(1)
C(3)	4564(6)	7555(5)	1241(2)	17(1)
C(4)	5716(5)	7190(5)	856(2)	15(1)
C(5)	5053(5)	8201(5)	474(1)	13(1)
C(6)	934(5)	5921(5)	798(1)	13(1)
C(7)	2198(6)	4706(5)	1005(1)	15(1)
C(8)	3426(6)	4130(5)	652(1)	15(1)
C(9)	2942(5)	4982(5)	232(1)	10(1)
C(10)	1392(5)	6094(5)	321(1)	11(1)
C(11)	518(5)	7287(5)	-14(1)	10(1)
C(12)	718(5)	8330(5)	-787(1)	14(1)
C(13)	1953(5)	7955(5)	-1187(1)	11(1)
C(14)	1756(6)	6658(5)	-1486(1)	12(1)
C(15)	2950(6)	6260(5)	-1852(1)	15(1)
C(16)	4335(5)	7184(5)	-1916(2)	16(1)
C(17)	4566(6)	8471(6)	-1626(2)	16(1)
C(18)	3366(6)	8863(5)	-1258(1)	13(1)
C(19)	-278(6)	8867(6)	-2060(2)	18(1)
C(20)	1466(6)	11266(5)	-1825(1)	15(1)
C(21)	2516(6)	9422(6)	-2514(1)	17(1)
O(1)	-787(4)	8210(4)	53(1)	15(1)
O(2)	1406(4)	7208(4)	-422(1)	13(1)
O(3)	-1685(5)	8780(5)	-2156(1)	29(1)
O(4)	1203(5)	12671(4)	-1773(1)	25(1)
O(5)	2889(5)	9705(6)	-2886(1)	34(1)
Fe(1)	3301(1)	6675(1)	718(1)	9(1)
Cr(1)	1959(1)	8968(1)	-1905(1)	10(1)
C(22)	1689(6)	6044(6)	6103(2)	18(1)
C(23)	331(6)	7248(6)	6265(2)	19(1)
C(24)	-800(6)	7684(6)	5898(2)	19(1)
C(25)	-164(6)	6750(5)	5509(2)	17(1)
C(26)	1384(6)	5730(5)	5634(2)	17(1)
C(27)	3950(5)	9005(6)	5772(2)	15(1)
C(28)	2648(6)	10192(5)	5965(2)	18(1)
C(29)	1467(6)	10788(5)	5616(2)	16(1)
C(30)	2018(5)	9941(5)	5207(2)	14(1)
C(31)	3553(5)	8846(5)	5299(1)	12(1)
C(32)	4475(5)	7687(5)	4970(1)	13(1)
C(33)	4380(5)	6726(5)	4206(1)	13(1)
C(34)	3255(6)	7224(5)	3805(1)	13(1)

C(35)	1787(6)	6432(6)	3737(2)	16(1)
C(36)	692(6)	6958(6)	3374(2)	18(1)
C(37)	1076(6)	8249(6)	3067(2)	19(1)
C(38)	2529(7)	9077(6)	3132(2)	19(1)
C(39)	3616(6)	8537(5)	3497(1)	15(1)
C(40)	3735(6)	4045(6)	3194(2)	17(1)
C(41)	5609(6)	6312(6)	2910(2)	19(1)
C(42)	2772(6)	5924(6)	2498(2)	23(1)
O(6)	5797(4)	6769(4)	5038(1)	17(1)
O(7)	3632(4)	7788(4)	4572(1)	16(1)
O(8)	3992(5)	2599(4)	3260(1)	26(1)
O(9)	7030(5)	6288(5)	2800(1)	30(1)
O(10)	2405(5)	5698(6)	2128(1)	38(1)
Cr(2)	3333(1)	6327(1)	3091(1)	12(1)
Fe(2)	1604(1)	8218(1)	5716(1)	11(1)

Table 3: Bond lengths [A] and angles [deg] for 4.4.

C(1)-C(2)	1.418(6)
C(1)-C(5)	1.423(6)
C(1)-Fe(1)	2.043(4)
C(1)-H(1)	0.9500
C(2)-C(3)	1.432(6)
C(2)-Fe(1)	2.031(4)
C(2)-H(2)	0.9500
C(3)-C(4)	1.434(6)
C(3)-Fe(1)	2.036(4)
C(3)-H(3)	0.9500
C(4)-C(5)	1.424(6)
C(4)-Fe(1)	2.047(4)
C(4)-H(4)	0.9500
C(5)-Fe(1)	2.051(4)
C(5)-H(5)	0.9500
C(6)-C(10)	1.430(5)
C(6)-C(7)	1.433(6)
C(6)-Fe(1)	2.031(4)
C(6)-H(6)	0.9500
C(7)-C(8)	1.434(6)
C(7)-Fe(1)	2.039(4)
C(7)-H(7)	0.9500
C(8)-C(9)	1.418(5)
C(8)-Fe(1)	2.047(4)
C(8)-H(8)	0.9500
C(9)-C(10)	1.437(6)
C(9)-Fe(1)	2.041(4)
C(9)-H(9)	0.9500
C(10)-C(11)	1.466(5)
C(10)-Fe(1)	2.030(4)
C(11)-O(1)	1.202(5)
C(11)-O(2)	1.357(5)
C(12)-O(2)	1.443(5)
C(12)-C(13)	1.505(6)
C(12)-H(12A)	0.9900
C(12)-H(12B)	0.9900
C(13)-C(14)	1.406(5)
C(13)-C(18)	1.409(6)
C(13)-Cr(1)	2.217(4)
C(14)-C(15)	1.413(6)
C(14)-Cr(1)	2.205(4)
C(14)-H(14)	0.9500
C(15)-C(16)	1.397(6)
C(15)-Cr(1)	2.215(4)
C(15)-H(15)	0.9500
C(16)-C(17)	1.390(6)
C(16)-Cr(1)	2.204(4)
C(16)-H(16)	0.9500
C(17)-C(18)	1.421(6)
C(17)-Cr(1)	2.213(4)
C(17)-H(17)	0.9500
C(18)-Cr(1)	2.208(4)

C(18)-H(18)	0.9500
C(19)-O(3)	1.160(6)
C(19)-Cr(1)	1.840(5)
C(20)-O(4)	1.134(5)
C(20)-Cr(1)	1.857(4)
C(21)-O(5)	1.136(5)
C(21)-Cr(1)	1.847(4)
C(22)-C(23)	1.425(6)
C(22)-C(26)	1.430(6)
C(22)-Fe(2)	2.040(4)
C(22)-H(22)	0.9500
C(23)-C(24)	1.417(7)
C(23)-Fe(2)	2.042(4)
C(23)-H(23)	0.9500
C(24)-C(25)	1.421(6)
C(24)-Fe(2)	2.040(4)
C(24)-H(24)	0.9500
C(25)-C(26)	1.427(6)
C(25)-Fe(2)	2.048(4)
C(25)-H(25)	0.9500
C(26)-Fe(2)	2.048(4)
C(26)-H(26)	0.9500
C(27)-C(28)	1.422(6)
C(27)-C(31)	1.433(6)
C(27)-Fe(2)	2.036(4)
C(27)-H(27)	0.9500
C(28)-C(29)	1.426(6)
C(28)-Fe(2)	2.037(4)
C(28)-H(28)	0.9500
C(29)-C(30)	1.419(6)
C(29)-Fe(2)	2.063(4)
C(29)-H(29)	0.9500
C(30)-C(31)	1.426(6)
C(30)-Fe(2)	2.039(4)
C(30)-H(30)	0.9500
C(31)-C(32)	1.467(6)
C(31)-Fe(2)	2.028(4)
C(32)-O(6)	1.213(5)
C(32)-O(7)	1.346(5)
C(33)-O(7)	1.450(5)
C(33)-C(34)	1.500(6)
C(33)-H(33A)	0.9900
C(33)-H(33B)	0.9900
C(34)-C(35)	1.408(6)
C(34)-C(39)	1.410(6)
C(34)-Cr(2)	2.216(4)
C(35)-C(36)	1.404(6)
C(35)-Cr(2)	2.204(4)
C(35)-H(35)	0.9500
C(36)-C(37)	1.401(7)
C(36)-Cr(2)	2.212(5)
C(36)-H(36)	0.9500
C(37)-C(38)	1.413(7)
C(37)-Cr(2)	2.199(5)
C(37)-H(37)	0.9500
C(38)-C(39)	1.406(6)

C(38)-Cr(2)	2.223(5)
C(38)-H(38)	0.9500
C(39)-Cr(2)	2.200(4)
C(39)-H(39)	0.9500
C(40)-O(8)	1.163(6)
C(40)-Cr(2)	1.835(5)
C(41)-O(9)	1.149(6)
C(41)-Cr(2)	1.848(5)
C(42)-O(10)	1.152(6)
C(42)-Cr(2)	1.842(5)

C(2)-C(1)-C(5)	108.0(4)
C(2)-C(1)-Fe(1)	69.2(2)
C(5)-C(1)-Fe(1)	70.0(2)
C(2)-C(1)-H(1)	126.0
C(5)-C(1)-H(1)	126.0
Fe(1)-C(1)-H(1)	126.4
C(1)-C(2)-C(3)	108.2(4)
C(1)-C(2)-Fe(1)	70.1(2)
C(3)-C(2)-Fe(1)	69.6(2)
C(1)-C(2)-H(2)	125.9
C(3)-C(2)-H(2)	125.9
Fe(1)-C(2)-H(2)	126.0
C(2)-C(3)-C(4)	107.7(4)
C(2)-C(3)-Fe(1)	69.2(2)
C(4)-C(3)-Fe(1)	69.8(2)
C(2)-C(3)-H(3)	126.1
C(4)-C(3)-H(3)	126.1
Fe(1)-C(3)-H(3)	126.4
C(5)-C(4)-C(3)	107.5(4)
C(5)-C(4)-Fe(1)	69.8(2)
C(3)-C(4)-Fe(1)	69.0(2)
C(5)-C(4)-H(4)	126.2
C(3)-C(4)-H(4)	126.2
Fe(1)-C(4)-H(4)	126.5
C(1)-C(5)-C(4)	108.5(4)
C(1)-C(5)-Fe(1)	69.4(2)
C(4)-C(5)-Fe(1)	69.5(2)
C(1)-C(5)-H(5)	125.7
C(4)-C(5)-H(5)	125.7
Fe(1)-C(5)-H(5)	127.0
C(10)-C(6)-C(7)	107.9(4)
C(10)-C(6)-Fe(1)	69.3(2)
C(7)-C(6)-Fe(1)	69.7(2)
C(10)-C(6)-H(6)	126.1
C(7)-C(6)-H(6)	126.1
Fe(1)-C(6)-H(6)	126.5
C(6)-C(7)-C(8)	107.7(4)
C(6)-C(7)-Fe(1)	69.1(2)
C(8)-C(7)-Fe(1)	69.7(2)
C(6)-C(7)-H(7)	126.2
C(8)-C(7)-H(7)	126.2
Fe(1)-C(7)-H(7)	126.6
C(9)-C(8)-C(7)	108.6(4)
C(9)-C(8)-Fe(1)	69.5(2)
C(7)-C(8)-Fe(1)	69.2(2)

C(9)-C(8)-H(8)	125.7
C(7)-C(8)-H(8)	125.7
Fe(1)-C(8)-H(8)	127.2
C(8)-C(9)-C(10)	107.8(3)
C(8)-C(9)-Fe(1)	69.9(2)
C(10)-C(9)-Fe(1)	68.9(2)
C(8)-C(9)-H(9)	126.1
C(10)-C(9)-H(9)	126.1
Fe(1)-C(9)-H(9)	126.7
C(6)-C(10)-C(9)	108.1(3)
C(6)-C(10)-C(11)	126.2(4)
C(9)-C(10)-C(11)	125.6(4)
C(6)-C(10)-Fe(1)	69.4(2)
C(9)-C(10)-Fe(1)	69.8(2)
C(11)-C(10)-Fe(1)	122.9(3)
O(1)-C(11)-O(2)	123.7(4)
O(1)-C(11)-C(10)	126.4(4)
O(2)-C(11)-C(10)	109.8(3)
O(2)-C(12)-C(13)	104.3(3)
O(2)-C(12)-H(12A)	110.9
C(13)-C(12)-H(12A)	110.9
O(2)-C(12)-H(12B)	110.9
C(13)-C(12)-H(12B)	110.9
H(12A)-C(12)-H(12B)	108.9
C(14)-C(13)-C(18)	118.8(4)
C(14)-C(13)-C(12)	120.8(4)
C(18)-C(13)-C(12)	120.4(4)
C(14)-C(13)-Cr(1)	71.0(2)
C(18)-C(13)-Cr(1)	71.1(2)
C(12)-C(13)-Cr(1)	131.7(3)
C(13)-C(14)-C(15)	120.9(4)
C(13)-C(14)-Cr(1)	71.9(2)
C(15)-C(14)-Cr(1)	71.8(2)
C(13)-C(14)-H(14)	119.5
C(15)-C(14)-H(14)	119.5
Cr(1)-C(14)-H(14)	129.2
C(16)-C(15)-C(14)	119.2(4)
C(16)-C(15)-Cr(1)	71.1(2)
C(14)-C(15)-Cr(1)	70.9(2)
C(16)-C(15)-H(15)	120.4
C(14)-C(15)-H(15)	120.4
Cr(1)-C(15)-H(15)	130.0
C(17)-C(16)-C(15)	121.2(4)
C(17)-C(16)-Cr(1)	72.0(2)
C(15)-C(16)-Cr(1)	72.0(3)
C(17)-C(16)-H(16)	119.4
C(15)-C(16)-H(16)	119.4
Cr(1)-C(16)-H(16)	129.0
C(16)-C(17)-C(18)	119.4(4)
C(16)-C(17)-Cr(1)	71.3(3)
C(18)-C(17)-Cr(1)	71.1(2)
C(16)-C(17)-H(17)	120.3
C(18)-C(17)-H(17)	120.3
Cr(1)-C(17)-H(17)	129.7
C(13)-C(18)-C(17)	120.5(4)
C(13)-C(18)-Cr(1)	71.8(2)

C(17)-C(18)-Cr(1)	71.4(2)
C(13)-C(18)-H(18)	119.8
C(17)-C(18)-H(18)	119.8
Cr(1)-C(18)-H(18)	129.5
O(3)-C(19)-Cr(1)	179.1(5)
O(4)-C(20)-Cr(1)	178.4(4)
O(5)-C(21)-Cr(1)	178.7(4)
C(11)-O(2)-C(12)	116.6(3)
C(10)-Fe(1)-C(6)	41.23(15)
C(10)-Fe(1)-C(2)	124.97(17)
C(6)-Fe(1)-C(2)	105.17(17)
C(10)-Fe(1)-C(3)	161.80(18)
C(6)-Fe(1)-C(3)	123.21(18)
C(2)-Fe(1)-C(3)	41.23(17)
C(10)-Fe(1)-C(7)	69.32(17)
C(6)-Fe(1)-C(7)	41.22(17)
C(2)-Fe(1)-C(7)	117.36(17)
C(3)-Fe(1)-C(7)	104.71(17)
C(10)-Fe(1)-C(9)	41.35(16)
C(6)-Fe(1)-C(9)	69.48(16)
C(2)-Fe(1)-C(9)	164.03(17)
C(3)-Fe(1)-C(9)	154.25(18)
C(7)-Fe(1)-C(9)	69.16(16)
C(10)-Fe(1)-C(1)	108.20(17)
C(6)-Fe(1)-C(1)	119.11(17)
C(2)-Fe(1)-C(1)	40.74(17)
C(3)-Fe(1)-C(1)	68.93(17)
C(7)-Fe(1)-C(1)	153.12(18)
C(9)-Fe(1)-C(1)	127.66(16)
C(10)-Fe(1)-C(8)	68.94(17)
C(6)-Fe(1)-C(8)	69.16(18)
C(2)-Fe(1)-C(8)	153.09(17)
C(3)-Fe(1)-C(8)	118.55(17)
C(7)-Fe(1)-C(8)	41.10(17)
C(9)-Fe(1)-C(8)	40.59(16)
C(1)-Fe(1)-C(8)	164.94(17)
C(10)-Fe(1)-C(4)	156.17(17)
C(6)-Fe(1)-C(4)	161.47(17)
C(2)-Fe(1)-C(4)	69.15(18)
C(3)-Fe(1)-C(4)	41.12(18)
C(7)-Fe(1)-C(4)	124.41(17)
C(9)-Fe(1)-C(4)	120.60(17)
C(1)-Fe(1)-C(4)	68.80(17)
C(8)-Fe(1)-C(4)	107.48(18)
C(10)-Fe(1)-C(5)	121.65(16)
C(6)-Fe(1)-C(5)	155.31(17)
C(2)-Fe(1)-C(5)	68.53(17)
C(3)-Fe(1)-C(5)	68.66(17)
C(7)-Fe(1)-C(5)	163.18(18)
C(9)-Fe(1)-C(5)	109.70(16)
C(1)-Fe(1)-C(5)	40.66(17)
C(8)-Fe(1)-C(5)	127.25(18)
C(4)-Fe(1)-C(5)	40.67(17)
C(19)-Cr(1)-C(21)	90.0(2)
C(19)-Cr(1)-C(20)	90.3(2)
C(21)-Cr(1)-C(20)	88.48(19)

C(19)-Cr(1)-C(14)	86.38(18)
C(21)-Cr(1)-C(14)	134.72(18)
C(20)-Cr(1)-C(14)	136.59(17)
C(19)-Cr(1)-C(16)	134.74(19)
C(21)-Cr(1)-C(16)	85.18(17)
C(20)-Cr(1)-C(16)	134.40(18)
C(14)-Cr(1)-C(16)	66.71(16)
C(19)-Cr(1)-C(18)	135.52(18)
C(21)-Cr(1)-C(18)	134.23(19)
C(20)-Cr(1)-C(18)	86.94(17)
C(14)-Cr(1)-C(18)	66.61(15)
C(16)-Cr(1)-C(18)	66.73(16)
C(19)-Cr(1)-C(17)	165.25(18)
C(21)-Cr(1)-C(17)	99.65(18)
C(20)-Cr(1)-C(17)	101.07(18)
C(14)-Cr(1)-C(17)	78.90(16)
C(16)-Cr(1)-C(17)	36.67(16)
C(18)-Cr(1)-C(17)	37.50(16)
C(19)-Cr(1)-C(15)	100.97(19)
C(21)-Cr(1)-C(15)	100.16(17)
C(20)-Cr(1)-C(15)	165.76(18)
C(14)-Cr(1)-C(15)	37.30(15)
C(16)-Cr(1)-C(15)	36.85(17)
C(18)-Cr(1)-C(15)	78.91(16)
C(17)-Cr(1)-C(15)	66.49(18)
C(19)-Cr(1)-C(13)	101.20(17)
C(21)-Cr(1)-C(13)	164.36(18)
C(20)-Cr(1)-C(13)	102.24(17)
C(14)-Cr(1)-C(13)	37.07(14)
C(16)-Cr(1)-C(13)	79.18(16)
C(18)-Cr(1)-C(13)	37.14(15)
C(17)-Cr(1)-C(13)	67.37(16)
C(15)-Cr(1)-C(13)	67.19(15)
C(23)-C(22)-C(26)	108.0(4)
C(23)-C(22)-Fe(2)	69.6(2)
C(26)-C(22)-Fe(2)	69.8(2)
C(23)-C(22)-H(22)	126.0
C(26)-C(22)-H(22)	126.0
Fe(2)-C(22)-H(22)	126.1
C(24)-C(23)-C(22)	108.0(4)
C(24)-C(23)-Fe(2)	69.6(2)
C(22)-C(23)-Fe(2)	69.5(2)
C(24)-C(23)-H(23)	126.0
C(22)-C(23)-H(23)	126.0
Fe(2)-C(23)-H(23)	126.5
C(23)-C(24)-C(25)	108.4(4)
C(23)-C(24)-Fe(2)	69.8(3)
C(25)-C(24)-Fe(2)	70.0(3)
C(23)-C(24)-H(24)	125.8
C(25)-C(24)-H(24)	125.8
Fe(2)-C(24)-H(24)	126.0
C(24)-C(25)-C(26)	108.0(4)
C(24)-C(25)-Fe(2)	69.3(3)
C(26)-C(25)-Fe(2)	69.6(2)
C(24)-C(25)-H(25)	126.0
C(26)-C(25)-H(25)	126.0

Fe(2)-C(25)-H(25)	126.6
C(25)-C(26)-C(22)	107.6(4)
C(25)-C(26)-Fe(2)	69.6(3)
C(22)-C(26)-Fe(2)	69.2(2)
C(25)-C(26)-H(26)	126.2
C(22)-C(26)-H(26)	126.2
Fe(2)-C(26)-H(26)	126.5
C(28)-C(27)-C(31)	107.3(4)
C(28)-C(27)-Fe(2)	69.6(2)
C(31)-C(27)-Fe(2)	69.1(2)
C(28)-C(27)-H(27)	126.4
C(31)-C(27)-H(27)	126.4
Fe(2)-C(27)-H(27)	126.5
C(27)-C(28)-C(29)	108.8(4)
C(27)-C(28)-Fe(2)	69.5(2)
C(29)-C(28)-Fe(2)	70.6(2)
C(27)-C(28)-H(28)	125.6
C(29)-C(28)-H(28)	125.6
Fe(2)-C(28)-H(28)	125.9
C(30)-C(29)-C(28)	107.6(4)
C(30)-C(29)-Fe(2)	68.9(2)
C(28)-C(29)-Fe(2)	68.7(2)
C(30)-C(29)-H(29)	126.2
C(28)-C(29)-H(29)	126.2
Fe(2)-C(29)-H(29)	127.8
C(29)-C(30)-C(31)	108.3(4)
C(29)-C(30)-Fe(2)	70.6(2)
C(31)-C(30)-Fe(2)	69.1(2)
C(29)-C(30)-H(30)	125.8
C(31)-C(30)-H(30)	125.8
Fe(2)-C(30)-H(30)	126.0
C(30)-C(31)-C(27)	108.0(4)
C(30)-C(31)-C(32)	125.1(4)
C(27)-C(31)-C(32)	126.8(4)
C(30)-C(31)-Fe(2)	69.9(2)
C(27)-C(31)-Fe(2)	69.6(2)
C(32)-C(31)-Fe(2)	122.9(3)
O(6)-C(32)-O(7)	124.2(4)
O(6)-C(32)-C(31)	126.1(4)
O(7)-C(32)-C(31)	109.7(4)
O(7)-C(33)-C(34)	104.3(3)
O(7)-C(33)-H(33A)	110.9
C(34)-C(33)-H(33A)	110.9
O(7)-C(33)-H(33B)	110.9
C(34)-C(33)-H(33B)	110.9
H(33A)-C(33)-H(33B)	108.9
C(35)-C(34)-C(39)	118.7(4)
C(35)-C(34)-C(33)	120.7(4)
C(39)-C(34)-C(33)	120.5(4)
C(35)-C(34)-Cr(2)	71.0(2)
C(39)-C(34)-Cr(2)	70.8(2)
C(33)-C(34)-Cr(2)	132.0(3)
C(36)-C(35)-C(34)	120.5(4)
C(36)-C(35)-Cr(2)	71.8(3)
C(34)-C(35)-Cr(2)	71.9(2)
C(36)-C(35)-H(35)	119.8

C(34)-C(35)-H(35)	119.8
Cr(2)-C(35)-H(35)	128.9
C(35)-C(36)-C(37)	120.2(4)
C(35)-C(36)-Cr(2)	71.2(3)
C(37)-C(36)-Cr(2)	71.0(3)
C(35)-C(36)-H(36)	119.9
C(37)-C(36)-H(36)	119.9
Cr(2)-C(36)-H(36)	130.6
C(36)-C(37)-C(38)	120.2(4)
C(36)-C(37)-Cr(2)	72.0(3)
C(38)-C(37)-Cr(2)	72.3(3)
C(36)-C(37)-H(37)	119.9
C(38)-C(37)-H(37)	119.9
Cr(2)-C(37)-H(37)	128.0
C(39)-C(38)-C(37)	118.9(4)
C(39)-C(38)-Cr(2)	70.6(2)
C(37)-C(38)-Cr(2)	70.4(3)
C(39)-C(38)-H(38)	120.5
C(37)-C(38)-H(38)	120.5
Cr(2)-C(38)-H(38)	131.0
C(38)-C(39)-C(34)	121.3(4)
C(38)-C(39)-Cr(2)	72.3(3)
C(34)-C(39)-Cr(2)	72.0(2)
C(38)-C(39)-H(39)	119.3
C(34)-C(39)-H(39)	119.3
Cr(2)-C(39)-H(39)	128.7
O(8)-C(40)-Cr(2)	179.9(5)
O(9)-C(41)-Cr(2)	179.2(5)
O(10)-C(42)-Cr(2)	178.9(4)
C(32)-O(7)-C(33)	116.9(3)
C(40)-Cr(2)-C(42)	88.2(2)
C(40)-Cr(2)-C(41)	89.0(2)
C(42)-Cr(2)-C(41)	90.5(2)
C(40)-Cr(2)-C(37)	136.6(2)
C(42)-Cr(2)-C(37)	84.32(19)
C(41)-Cr(2)-C(37)	133.6(2)
C(40)-Cr(2)-C(39)	134.78(19)
C(42)-Cr(2)-C(39)	136.86(19)
C(41)-Cr(2)-C(39)	87.39(19)
C(37)-Cr(2)-C(39)	66.99(17)
C(40)-Cr(2)-C(35)	87.11(19)
C(42)-Cr(2)-C(35)	131.2(2)
C(41)-Cr(2)-C(35)	137.93(19)
C(37)-Cr(2)-C(35)	67.05(18)
C(39)-Cr(2)-C(35)	66.81(16)
C(40)-Cr(2)-C(36)	102.67(19)
C(42)-Cr(2)-C(36)	97.7(2)
C(41)-Cr(2)-C(36)	165.85(19)
C(37)-Cr(2)-C(36)	37.03(18)
C(39)-Cr(2)-C(36)	78.73(17)
C(35)-Cr(2)-C(36)	37.08(17)
C(40)-Cr(2)-C(34)	100.93(18)
C(42)-Cr(2)-C(34)	163.40(19)
C(41)-Cr(2)-C(34)	103.38(18)
C(37)-Cr(2)-C(34)	79.51(17)
C(39)-Cr(2)-C(34)	37.24(15)

C(35)-Cr(2)-C(34)	37.15(16)
C(36)-Cr(2)-C(34)	66.92(17)
C(40)-Cr(2)-C(38)	166.15(19)
C(42)-Cr(2)-C(38)	101.73(19)
C(41)-Cr(2)-C(38)	100.4(2)
C(37)-Cr(2)-C(38)	37.26(18)
C(39)-Cr(2)-C(38)	37.06(16)
C(35)-Cr(2)-C(38)	79.09(17)
C(36)-Cr(2)-C(38)	66.73(18)
C(34)-Cr(2)-C(38)	67.15(16)
C(31)-Fe(2)-C(27)	41.30(16)
C(31)-Fe(2)-C(28)	68.88(17)
C(27)-Fe(2)-C(28)	40.88(18)
C(31)-Fe(2)-C(30)	41.05(16)
C(27)-Fe(2)-C(30)	69.17(17)
C(28)-Fe(2)-C(30)	68.54(18)
C(31)-Fe(2)-C(24)	157.91(18)
C(27)-Fe(2)-C(24)	159.51(19)
C(28)-Fe(2)-C(24)	123.31(19)
C(30)-Fe(2)-C(24)	121.97(18)
C(31)-Fe(2)-C(22)	124.40(18)
C(27)-Fe(2)-C(22)	105.62(18)
C(28)-Fe(2)-C(22)	118.98(19)
C(30)-Fe(2)-C(22)	162.73(18)
C(24)-Fe(2)-C(22)	68.59(18)
C(31)-Fe(2)-C(23)	160.54(18)
C(27)-Fe(2)-C(23)	122.33(19)
C(28)-Fe(2)-C(23)	105.28(19)
C(30)-Fe(2)-C(23)	155.84(18)
C(24)-Fe(2)-C(23)	40.63(19)
C(22)-Fe(2)-C(23)	40.87(18)
C(31)-Fe(2)-C(26)	108.34(17)
C(27)-Fe(2)-C(26)	120.69(18)
C(28)-Fe(2)-C(26)	155.30(19)
C(30)-Fe(2)-C(26)	126.46(17)
C(24)-Fe(2)-C(26)	68.63(18)
C(22)-Fe(2)-C(26)	40.95(18)
C(23)-Fe(2)-C(26)	68.78(18)
C(31)-Fe(2)-C(25)	122.73(18)
C(27)-Fe(2)-C(25)	157.39(19)
C(28)-Fe(2)-C(25)	161.26(19)
C(30)-Fe(2)-C(25)	109.47(18)
C(24)-Fe(2)-C(25)	40.69(18)
C(22)-Fe(2)-C(25)	68.65(18)
C(23)-Fe(2)-C(25)	68.50(19)
C(26)-Fe(2)-C(25)	40.77(17)
C(31)-Fe(2)-C(29)	68.65(17)
C(27)-Fe(2)-C(29)	68.80(18)
C(28)-Fe(2)-C(29)	40.69(18)
C(30)-Fe(2)-C(29)	40.48(16)
C(24)-Fe(2)-C(29)	107.53(18)
C(22)-Fe(2)-C(29)	154.60(19)
C(23)-Fe(2)-C(29)	119.78(18)
C(26)-Fe(2)-C(29)	163.09(19)
C(25)-Fe(2)-C(29)	125.76(18)

Symmetry transformations used to generate equivalent atoms:

Table 4: Anisotropic displacement parameters (A^2 x 10^3) for 4.4.

The anisotropic displacement factor exponent takes the form:

-2 pi^2 [h^2 a*^2 U11 + ... + 2 h k a* b* U12]

	U11	U22	U33	U23	U13	U12
C(1)	14(2)	14(2)	15(2)	0(2)	-3(2)	0(2)
C(2)	12(2)	15(2)	18(2)	-5(1)	2(2)	-2(2)
C(3)	20(2)	18(2)	14(2)	1(2)	-6(2)	-5(2)
C(4)	10(2)	16(2)	22(2)	2(2)	-7(2)	-3(2)
C(5)	9(2)	17(2)	14(2)	2(1)	4(1)	-5(2)
C(6)	10(2)	17(2)	11(2)	2(1)	0(1)	-3(2)
C(7)	17(2)	15(2)	14(2)	4(1)	-1(2)	-7(2)
C(8)	21(2)	9(2)	15(2)	3(1)	-2(2)	-3(2)
C(9)	12(2)	14(2)	6(2)	-2(1)	0(1)	-3(1)
C(10)	8(2)	14(2)	11(2)	-1(1)	-2(1)	-2(1)
C(11)	11(2)	12(2)	8(2)	-2(1)	0(1)	-3(1)
C(12)	15(2)	16(2)	11(2)	-1(1)	-1(2)	2(2)
C(13)	12(2)	11(2)	9(2)	0(1)	-3(1)	0(1)
C(14)	17(2)	11(2)	9(2)	1(1)	-2(1)	-2(1)
C(15)	26(2)	14(2)	5(2)	2(1)	3(2)	-1(2)
C(16)	13(2)	21(2)	13(2)	2(2)	1(2)	5(2)
C(17)	11(2)	21(2)	17(2)	6(2)	0(2)	-3(2)
C(18)	15(2)	14(2)	11(2)	-1(1)	-2(2)	0(2)
C(19)	18(2)	24(2)	11(2)	3(2)	-2(2)	-3(2)
C(20)	16(2)	16(2)	12(2)	1(1)	2(2)	1(2)

C(21)	13(2)	25(2)	11(2)	2(2)	-2(2)	8(2)
O(1)	13(1)	18(1)	12(1)	0(1)	0(1)	0(1)
O(2)	13(1)	19(2)	4(1)	2(1)	2(1)	3(1)
O(3)	14(2)	45(2)	29(2)	8(2)	-6(1)	-7(2)
O(4)	34(2)	15(2)	25(2)	-1(1)	0(1)	1(1)
O(5)	30(2)	54(2)	13(2)	10(2)	4(1)	12(2)
Fe(1)	9(1)	11(1)	8(1)	1(1)	-1(1)	-2(1)
Cr(1)	10(1)	11(1)	7(1)	1(1)	0(1)	-1(1)
C(22)	16(2)	18(2)	20(2)	5(2)	0(2)	-3(2)
C(23)	24(2)	20(2)	14(2)	0(2)	6(2)	-6(2)
C(24)	11(2)	18(2)	26(2)	-1(2)	5(2)	-1(2)
C(25)	13(2)	16(2)	21(2)	2(2)	-3(2)	-3(2)
C(26)	14(2)	16(2)	20(2)	1(2)	0(2)	-4(2)
C(27)	10(2)	20(2)	15(2)	0(2)	-4(2)	-5(2)
C(28)	21(2)	18(2)	15(2)	-4(2)	-1(2)	-7(2)
C(29)	17(2)	13(2)	16(2)	0(2)	4(2)	-1(2)
C(30)	12(2)	12(2)	17(2)	-1(1)	-1(2)	-1(1)
C(31)	10(2)	14(2)	13(2)	0(1)	-2(1)	-4(1)
C(32)	13(2)	14(2)	13(2)	1(1)	0(2)	-4(2)
C(33)	13(2)	14(2)	11(2)	-3(1)	1(1)	-1(2)
C(34)	14(2)	15(2)	9(2)	-3(1)	2(1)	1(2)
C(35)	17(2)	17(2)	12(2)	-5(1)	5(2)	-2(2)
C(36)	14(2)	19(2)	22(2)	-8(2)	4(2)	1(2)
C(37)	20(2)	15(2)	22(2)	-4(2)	-6(2)	4(2)
C(38)	24(2)	9(2)	22(2)	1(2)	-3(2)	-1(2)
C(39)	21(2)	10(2)	15(2)	-2(1)	-1(2)	-5(2)
C(40)	16(2)	19(2)	15(2)	-4(2)	1(2)	1(2)
C(41)	20(2)	18(2)	18(2)	-5(2)	1(2)	1(2)

C(42)	23(2)	24(2)	20(2)	-5(2)	-2(2)	7(2)
O(6)	13(2)	17(1)	19(2)	0(1)	-1(1)	1(1)
O(7)	16(2)	20(2)	11(1)	-2(1)	-1(1)	4(1)
O(8)	35(2)	12(2)	31(2)	0(1)	4(2)	1(1)
O(9)	18(2)	42(2)	31(2)	-6(2)	5(1)	-5(2)
O(10)	36(2)	52(3)	23(2)	-14(2)	-11(2)	18(2)
Cr(2)	13(1)	11(1)	11(1)	-1(1)	0(1)	0(1)
Fe(2)	10(1)	13(1)	12(1)	0(1)	0(1)	-1(1)

Table 5: Hydrogen coordinates (x 10^4) and isotropic displacement parameters (A^2 x 10^3) for 4.4.

	x	y	z	U(eq)
H(1)	2794	9954	432	17
H(2)	2247	9252	1275	18
H(3)	4686	7069	1543	20
H(4)	6735	6414	854	18
H(5)	5562	8222	174	16
H(6)	-36	6509	951	15
H(7)	2218	4346	1320	18
H(8)	4401	3314	693	18
H(9)	3537	4843	-56	12
H(12A)	669	9517	-700	17
H(12B)	-450	8105	-863	17
H(14)	807	6039	-1442	15
H(15)	2813	5376	-2051	18
H(16)	5132	6928	-2164	20
H(17)	5519	9083	-1672	20
H(18)	3517	9742	-1058	16
H(22)	2632	5538	6277	22
H(23)	207	7682	6565	23
H(24)	-1813	8467	5910	22
H(25)	-678	6797	5217	20
H(26)	2084	4979	5440	20
H(27)	4904	8425	5927	18
H(28)	2578	10533	6275	21
H(29)	489	11604	5652	19
H(30)	1459	10080	4921	17
H(33A)	4370	5523	4292	15
H(33B)	5577	6931	4134	15
H(35)	1534	5536	3939	19
H(36)	-312	6436	3336	22
H(37)	357	8569	2814	23
H(38)	2768	9985	2932	22
H(39)	4613	9067	3537	18

Table 6: Torsion angles [deg] for 4.4.

C(5)-C(1)-C(2)-C(3)	0.0(5)
Fe(1)-C(1)-C(2)-C(3)	59.4(3)
C(5)-C(1)-C(2)-Fe(1)	-59.4(3)
C(1)-C(2)-C(3)-C(4)	-0.2(5)
Fe(1)-C(2)-C(3)-C(4)	59.4(3)
C(1)-C(2)-C(3)-Fe(1)	-59.7(3)
C(2)-C(3)-C(4)-C(5)	0.4(5)
Fe(1)-C(3)-C(4)-C(5)	59.5(3)
C(2)-C(3)-C(4)-Fe(1)	-59.0(3)
C(2)-C(1)-C(5)-C(4)	0.3(5)
Fe(1)-C(1)-C(5)-C(4)	-58.6(3)
C(2)-C(1)-C(5)-Fe(1)	58.9(3)
C(3)-C(4)-C(5)-C(1)	-0.4(5)
Fe(1)-C(4)-C(5)-C(1)	58.5(3)
C(3)-C(4)-C(5)-Fe(1)	-59.0(3)
C(10)-C(6)-C(7)-C(8)	-0.3(5)
Fe(1)-C(6)-C(7)-C(8)	-59.3(3)
C(10)-C(6)-C(7)-Fe(1)	59.0(3)
C(6)-C(7)-C(8)-C(9)	0.4(5)
Fe(1)-C(7)-C(8)-C(9)	-58.5(3)
C(6)-C(7)-C(8)-Fe(1)	58.9(3)
C(7)-C(8)-C(9)-C(10)	-0.4(4)
Fe(1)-C(8)-C(9)-C(10)	-58.7(3)
C(7)-C(8)-C(9)-Fe(1)	58.3(3)
C(7)-C(6)-C(10)-C(9)	0.0(4)
Fe(1)-C(6)-C(10)-C(9)	59.3(3)
C(7)-C(6)-C(10)-C(11)	-175.6(4)
Fe(1)-C(6)-C(10)-C(11)	-116.4(4)
C(7)-C(6)-C(10)-Fe(1)	-59.2(3)
C(8)-C(9)-C(10)-C(6)	0.2(4)
Fe(1)-C(9)-C(10)-C(6)	-59.1(3)
C(8)-C(9)-C(10)-C(11)	175.9(4)
Fe(1)-C(9)-C(10)-C(11)	116.6(4)
C(8)-C(9)-C(10)-Fe(1)	59.3(3)
C(6)-C(10)-C(11)-O(1)	-6.1(7)
C(9)-C(10)-C(11)-O(1)	179.1(4)
Fe(1)-C(10)-C(11)-O(1)	-93.5(5)
C(6)-C(10)-C(11)-O(2)	174.0(4)
C(9)-C(10)-C(11)-O(2)	-0.9(5)
Fe(1)-C(10)-C(11)-O(2)	86.6(4)
O(2)-C(12)-C(13)-C(14)	86.6(4)
O(2)-C(12)-C(13)-C(18)	-91.0(4)
O(2)-C(12)-C(13)-Cr(1)	177.9(3)
C(18)-C(13)-C(14)-C(15)	0.1(6)
C(12)-C(13)-C(14)-C(15)	-177.6(4)
Cr(1)-C(13)-C(14)-C(15)	54.6(4)
C(18)-C(13)-C(14)-Cr(1)	-54.5(3)
C(12)-C(13)-C(14)-Cr(1)	127.8(4)
C(13)-C(14)-C(15)-C(16)	-0.5(6)
Cr(1)-C(14)-C(15)-C(16)	54.2(4)
C(13)-C(14)-C(15)-Cr(1)	-54.7(4)
C(14)-C(15)-C(16)-C(17)	0.7(6)

Cr(1)-C(15)-C(16)-C(17)	54.8(4)
C(14)-C(15)-C(16)-Cr(1)	-54.1(4)
C(15)-C(16)-C(17)-C(18)	-0.5(6)
Cr(1)-C(16)-C(17)-C(18)	54.3(4)
C(15)-C(16)-C(17)-Cr(1)	-54.8(4)
C(14)-C(13)-C(18)-C(17)	0.1(6)
C(12)-C(13)-C(18)-C(17)	177.8(4)
Cr(1)-C(13)-C(18)-C(17)	-54.4(4)
C(14)-C(13)-C(18)-Cr(1)	54.5(3)
C(12)-C(13)-C(18)-Cr(1)	-127.9(4)
C(16)-C(17)-C(18)-C(13)	0.1(6)
Cr(1)-C(17)-C(18)-C(13)	54.5(3)
C(16)-C(17)-C(18)-Cr(1)	-54.4(4)
O(1)-C(11)-O(2)-C(12)	0.8(6)
C(10)-C(11)-O(2)-C(12)	-179.2(3)
C(13)-C(12)-O(2)-C(11)	-179.9(3)
C(9)-C(10)-Fe(1)-C(6)	-119.4(3)
C(11)-C(10)-Fe(1)-C(6)	120.6(4)
C(6)-C(10)-Fe(1)-C(2)	-71.7(3)
C(9)-C(10)-Fe(1)-C(2)	168.8(2)
C(11)-C(10)-Fe(1)-C(2)	48.9(4)
C(6)-C(10)-Fe(1)-C(3)	-35.9(6)
C(9)-C(10)-Fe(1)-C(3)	-155.4(5)
C(11)-C(10)-Fe(1)-C(3)	84.7(6)
C(6)-C(10)-Fe(1)-C(7)	37.9(2)
C(9)-C(10)-Fe(1)-C(7)	-81.6(2)
C(11)-C(10)-Fe(1)-C(7)	158.5(4)
C(6)-C(10)-Fe(1)-C(9)	119.4(3)
C(11)-C(10)-Fe(1)-C(9)	-120.0(4)
C(6)-C(10)-Fe(1)-C(1)	-113.7(3)
C(9)-C(10)-Fe(1)-C(1)	126.9(2)
C(11)-C(10)-Fe(1)-C(1)	6.9(4)
C(6)-C(10)-Fe(1)-C(8)	82.0(3)
C(9)-C(10)-Fe(1)-C(8)	-37.4(2)
C(11)-C(10)-Fe(1)-C(8)	-157.4(4)
C(6)-C(10)-Fe(1)-C(4)	167.7(4)
C(9)-C(10)-Fe(1)-C(4)	48.3(5)
C(11)-C(10)-Fe(1)-C(4)	-71.7(6)
C(6)-C(10)-Fe(1)-C(5)	-156.3(2)
C(9)-C(10)-Fe(1)-C(5)	84.2(3)
C(11)-C(10)-Fe(1)-C(5)	-35.8(4)
C(7)-C(6)-Fe(1)-C(10)	119.3(3)
C(10)-C(6)-Fe(1)-C(2)	126.3(2)
C(7)-C(6)-Fe(1)-C(2)	-114.4(3)
C(10)-C(6)-Fe(1)-C(3)	167.3(2)
C(7)-C(6)-Fe(1)-C(3)	-73.3(3)
C(10)-C(6)-Fe(1)-C(7)	-119.3(3)
C(10)-C(6)-Fe(1)-C(9)	-37.9(2)
C(7)-C(6)-Fe(1)-C(9)	81.4(3)
C(10)-C(6)-Fe(1)-C(1)	84.7(3)
C(7)-C(6)-Fe(1)-C(1)	-156.0(2)
C(10)-C(6)-Fe(1)-C(8)	-81.4(3)
C(7)-C(6)-Fe(1)-C(8)	37.9(2)
C(10)-C(6)-Fe(1)-C(4)	-164.3(5)
C(7)-C(6)-Fe(1)-C(4)	-45.0(6)
C(10)-C(6)-Fe(1)-C(5)	54.8(5)

C(7)-C(6)-Fe(1)-C(5)	174.1(4)
C(1)-C(2)-Fe(1)-C(10)	-76.8(3)
C(3)-C(2)-Fe(1)-C(10)	163.9(2)
C(1)-C(2)-Fe(1)-C(6)	-117.2(3)
C(3)-C(2)-Fe(1)-C(6)	123.5(3)
C(1)-C(2)-Fe(1)-C(3)	119.3(4)
C(1)-C(2)-Fe(1)-C(7)	-159.7(3)
C(3)-C(2)-Fe(1)-C(7)	81.0(3)
C(1)-C(2)-Fe(1)-C(9)	-49.1(7)
C(3)-C(2)-Fe(1)-C(9)	-168.4(5)
C(3)-C(2)-Fe(1)-C(1)	-119.3(4)
C(1)-C(2)-Fe(1)-C(8)	169.0(4)
C(3)-C(2)-Fe(1)-C(8)	49.8(5)
C(1)-C(2)-Fe(1)-C(4)	81.3(3)
C(3)-C(2)-Fe(1)-C(4)	-37.9(3)
C(1)-C(2)-Fe(1)-C(5)	37.6(3)
C(3)-C(2)-Fe(1)-C(5)	-81.7(3)
C(2)-C(3)-Fe(1)-C(10)	-46.7(6)
C(4)-C(3)-Fe(1)-C(10)	-165.7(5)
C(2)-C(3)-Fe(1)-C(6)	-74.2(3)
C(4)-C(3)-Fe(1)-C(6)	166.7(2)
C(4)-C(3)-Fe(1)-C(2)	-119.1(4)
C(2)-C(3)-Fe(1)-C(7)	-114.9(3)
C(4)-C(3)-Fe(1)-C(7)	126.0(3)
C(2)-C(3)-Fe(1)-C(9)	172.7(3)
C(4)-C(3)-Fe(1)-C(9)	53.6(5)
C(2)-C(3)-Fe(1)-C(1)	37.6(2)
C(4)-C(3)-Fe(1)-C(1)	-81.5(3)
C(2)-C(3)-Fe(1)-C(8)	-156.8(3)
C(4)-C(3)-Fe(1)-C(8)	84.1(3)
C(2)-C(3)-Fe(1)-C(4)	119.1(4)
C(2)-C(3)-Fe(1)-C(5)	81.3(3)
C(4)-C(3)-Fe(1)-C(5)	-37.7(2)
C(6)-C(7)-Fe(1)-C(10)	-37.9(2)
C(8)-C(7)-Fe(1)-C(10)	81.3(3)
C(8)-C(7)-Fe(1)-C(6)	119.2(4)
C(6)-C(7)-Fe(1)-C(2)	81.7(3)
C(8)-C(7)-Fe(1)-C(2)	-159.1(3)
C(6)-C(7)-Fe(1)-C(3)	124.0(3)
C(8)-C(7)-Fe(1)-C(3)	-116.8(3)
C(6)-C(7)-Fe(1)-C(9)	-82.3(3)
C(8)-C(7)-Fe(1)-C(9)	36.9(2)
C(6)-C(7)-Fe(1)-C(1)	51.7(5)
C(8)-C(7)-Fe(1)-C(1)	170.9(3)
C(6)-C(7)-Fe(1)-C(8)	-119.2(4)
C(6)-C(7)-Fe(1)-C(4)	164.2(2)
C(8)-C(7)-Fe(1)-C(4)	-76.6(3)
C(6)-C(7)-Fe(1)-C(5)	-171.5(5)
C(8)-C(7)-Fe(1)-C(5)	-52.4(7)
C(8)-C(9)-Fe(1)-C(10)	-119.3(3)
C(8)-C(9)-Fe(1)-C(6)	-81.6(3)
C(10)-C(9)-Fe(1)-C(6)	37.8(2)
C(8)-C(9)-Fe(1)-C(2)	-154.5(6)
C(10)-C(9)-Fe(1)-C(2)	-35.2(7)
C(8)-C(9)-Fe(1)-C(3)	43.2(5)
C(10)-C(9)-Fe(1)-C(3)	162.6(4)

C(8)-C(9)-Fe(1)-C(7)	-37.3(3)
C(10)-C(9)-Fe(1)-C(7)	82.0(2)
C(8)-C(9)-Fe(1)-C(1)	166.9(3)
C(10)-C(9)-Fe(1)-C(1)	-73.8(3)
C(10)-C(9)-Fe(1)-C(8)	119.3(3)
C(8)-C(9)-Fe(1)-C(4)	81.2(3)
C(10)-C(9)-Fe(1)-C(4)	-159.5(2)
C(8)-C(9)-Fe(1)-C(5)	124.8(3)
C(10)-C(9)-Fe(1)-C(5)	-115.9(2)
C(2)-C(1)-Fe(1)-C(10)	122.9(3)
C(5)-C(1)-Fe(1)-C(10)	-117.7(3)
C(2)-C(1)-Fe(1)-C(6)	79.2(3)
C(5)-C(1)-Fe(1)-C(6)	-161.4(2)
C(5)-C(1)-Fe(1)-C(2)	119.4(4)
C(2)-C(1)-Fe(1)-C(3)	-38.0(3)
C(5)-C(1)-Fe(1)-C(3)	81.4(3)
C(2)-C(1)-Fe(1)-C(7)	42.9(5)
C(5)-C(1)-Fe(1)-C(7)	162.3(4)
C(2)-C(1)-Fe(1)-C(9)	164.8(2)
C(5)-C(1)-Fe(1)-C(9)	-75.8(3)
C(2)-C(1)-Fe(1)-C(8)	-160.7(6)
C(5)-C(1)-Fe(1)-C(8)	-41.3(8)
C(2)-C(1)-Fe(1)-C(4)	-82.3(3)
C(5)-C(1)-Fe(1)-C(4)	37.1(2)
C(2)-C(1)-Fe(1)-C(5)	-119.4(4)
C(9)-C(8)-Fe(1)-C(10)	38.1(2)
C(7)-C(8)-Fe(1)-C(10)	-82.3(3)
C(9)-C(8)-Fe(1)-C(6)	82.4(3)
C(7)-C(8)-Fe(1)-C(6)	-38.0(2)
C(9)-C(8)-Fe(1)-C(2)	164.9(3)
C(7)-C(8)-Fe(1)-C(2)	44.5(5)
C(9)-C(8)-Fe(1)-C(3)	-160.2(2)
C(7)-C(8)-Fe(1)-C(3)	79.4(3)
C(9)-C(8)-Fe(1)-C(7)	120.4(4)
C(7)-C(8)-Fe(1)-C(9)	-120.4(4)
C(9)-C(8)-Fe(1)-C(1)	-43.7(8)
C(7)-C(8)-Fe(1)-C(1)	-164.1(6)
C(9)-C(8)-Fe(1)-C(4)	-116.9(3)
C(7)-C(8)-Fe(1)-C(4)	122.7(3)
C(9)-C(8)-Fe(1)-C(5)	-76.3(3)
C(7)-C(8)-Fe(1)-C(5)	163.3(2)
C(5)-C(4)-Fe(1)-C(10)	50.1(5)
C(3)-C(4)-Fe(1)-C(10)	169.0(4)
C(5)-C(4)-Fe(1)-C(6)	-156.1(5)
C(3)-C(4)-Fe(1)-C(6)	-37.2(6)
C(5)-C(4)-Fe(1)-C(2)	-80.9(3)
C(3)-C(4)-Fe(1)-C(2)	38.0(2)
C(5)-C(4)-Fe(1)-C(3)	-119.0(4)
C(5)-C(4)-Fe(1)-C(7)	169.5(2)
C(3)-C(4)-Fe(1)-C(7)	-71.5(3)
C(5)-C(4)-Fe(1)-C(9)	85.0(3)
C(3)-C(4)-Fe(1)-C(9)	-156.0(2)
C(5)-C(4)-Fe(1)-C(1)	-37.1(2)
C(3)-C(4)-Fe(1)-C(1)	81.8(3)
C(5)-C(4)-Fe(1)-C(8)	127.4(3)
C(3)-C(4)-Fe(1)-C(8)	-113.6(3)

C(3)-C(4)-Fe(1)-C(5)	119.0(4)
C(1)-C(5)-Fe(1)-C(10)	81.1(3)
C(4)-C(5)-Fe(1)-C(10)	-158.7(3)
C(1)-C(5)-Fe(1)-C(6)	41.8(5)
C(4)-C(5)-Fe(1)-C(6)	162.1(4)
C(1)-C(5)-Fe(1)-C(2)	-37.7(2)
C(4)-C(5)-Fe(1)-C(2)	82.6(3)
C(1)-C(5)-Fe(1)-C(3)	-82.1(3)
C(4)-C(5)-Fe(1)-C(3)	38.1(3)
C(1)-C(5)-Fe(1)-C(7)	-151.6(5)
C(4)-C(5)-Fe(1)-C(7)	-31.4(7)
C(1)-C(5)-Fe(1)-C(9)	125.4(2)
C(4)-C(5)-Fe(1)-C(9)	-114.4(3)
C(4)-C(5)-Fe(1)-C(1)	120.2(4)
C(1)-C(5)-Fe(1)-C(8)	167.6(2)
C(4)-C(5)-Fe(1)-C(8)	-72.2(3)
C(1)-C(5)-Fe(1)-C(4)	-120.2(4)
O(3)-C(19)-Cr(1)-C(21)	112(25)
O(3)-C(19)-Cr(1)-C(20)	-160(100)
O(3)-C(19)-Cr(1)-C(14)	-23(25)
O(3)-C(19)-Cr(1)-C(16)	28(25)
O(3)-C(19)-Cr(1)-C(18)	-74(25)
O(3)-C(19)-Cr(1)-C(17)	-20(26)
O(3)-C(19)-Cr(1)-C(15)	11(25)
O(3)-C(19)-Cr(1)-C(13)	-57(25)
O(5)-C(21)-Cr(1)-C(19)	175(100)
O(5)-C(21)-Cr(1)-C(20)	85(20)
O(5)-C(21)-Cr(1)-C(14)	-100(20)
O(5)-C(21)-Cr(1)-C(16)	-50(20)
O(5)-C(21)-Cr(1)-C(18)	1(20)
O(5)-C(21)-Cr(1)-C(17)	-16(20)
O(5)-C(21)-Cr(1)-C(15)	-84(20)
O(5)-C(21)-Cr(1)-C(13)	-49(20)
O(4)-C(20)-Cr(1)-C(19)	179(100)
O(4)-C(20)-Cr(1)-C(21)	-91(15)
O(4)-C(20)-Cr(1)-C(14)	94(15)
O(4)-C(20)-Cr(1)-C(16)	-9(15)
O(4)-C(20)-Cr(1)-C(18)	44(15)
O(4)-C(20)-Cr(1)-C(17)	9(15)
O(4)-C(20)-Cr(1)-C(15)	37(15)
O(4)-C(20)-Cr(1)-C(13)	78(15)
C(13)-C(14)-Cr(1)-C(19)	-114.0(3)
C(15)-C(14)-Cr(1)-C(19)	113.4(3)
C(13)-C(14)-Cr(1)-C(21)	159.6(3)
C(15)-C(14)-Cr(1)-C(21)	27.1(4)
C(13)-C(14)-Cr(1)-C(20)	-27.5(4)
C(15)-C(14)-Cr(1)-C(20)	-160.0(3)
C(13)-C(14)-Cr(1)-C(16)	103.3(3)
C(15)-C(14)-Cr(1)-C(16)	-29.2(3)
C(13)-C(14)-Cr(1)-C(18)	29.7(2)
C(15)-C(14)-Cr(1)-C(18)	-102.8(3)
C(13)-C(14)-Cr(1)-C(17)	67.0(3)
C(15)-C(14)-Cr(1)-C(17)	-65.6(3)
C(13)-C(14)-Cr(1)-C(15)	132.6(4)
C(15)-C(14)-Cr(1)-C(13)	-132.6(4)
C(17)-C(16)-Cr(1)-C(19)	-161.6(3)

C(15)-C(16)-Cr(1)-C(19)	-28.9(4)
C(17)-C(16)-Cr(1)-C(21)	113.3(3)
C(15)-C(16)-Cr(1)-C(21)	-114.1(3)
C(17)-C(16)-Cr(1)-C(20)	30.1(4)
C(15)-C(16)-Cr(1)-C(20)	162.8(3)
C(17)-C(16)-Cr(1)-C(14)	-103.1(3)
C(15)-C(16)-Cr(1)-C(14)	29.6(2)
C(17)-C(16)-Cr(1)-C(18)	-29.7(2)
C(15)-C(16)-Cr(1)-C(18)	103.0(3)
C(15)-C(16)-Cr(1)-C(17)	132.7(4)
C(17)-C(16)-Cr(1)-C(15)	-132.7(4)
C(17)-C(16)-Cr(1)-C(13)	-66.5(3)
C(15)-C(16)-Cr(1)-C(13)	66.2(3)
C(13)-C(18)-Cr(1)-C(19)	27.7(4)
C(17)-C(18)-Cr(1)-C(19)	160.1(3)
C(13)-C(18)-Cr(1)-C(21)	-160.1(3)
C(17)-C(18)-Cr(1)-C(21)	-27.8(4)
C(13)-C(18)-Cr(1)-C(20)	115.0(3)
C(17)-C(18)-Cr(1)-C(20)	-112.7(3)
C(13)-C(18)-Cr(1)-C(14)	-29.7(2)
C(17)-C(18)-Cr(1)-C(14)	102.7(3)
C(13)-C(18)-Cr(1)-C(16)	-103.3(3)
C(17)-C(18)-Cr(1)-C(16)	29.1(3)
C(13)-C(18)-Cr(1)-C(17)	-132.4(4)
C(13)-C(18)-Cr(1)-C(15)	-66.7(3)
C(17)-C(18)-Cr(1)-C(15)	65.6(3)
C(17)-C(18)-Cr(1)-C(13)	132.4(4)
C(16)-C(17)-Cr(1)-C(19)	61.9(8)
C(18)-C(17)-Cr(1)-C(19)	-69.7(8)
C(16)-C(17)-Cr(1)-C(21)	-68.2(3)
C(18)-C(17)-Cr(1)-C(21)	160.2(3)
C(16)-C(17)-Cr(1)-C(20)	-158.6(3)
C(18)-C(17)-Cr(1)-C(20)	69.9(3)
C(16)-C(17)-Cr(1)-C(14)	65.7(3)
C(18)-C(17)-Cr(1)-C(14)	-65.9(3)
C(18)-C(17)-Cr(1)-C(16)	-131.6(4)
C(16)-C(17)-Cr(1)-C(18)	131.6(4)
C(16)-C(17)-Cr(1)-C(15)	28.7(3)
C(18)-C(17)-Cr(1)-C(15)	-102.9(3)
C(16)-C(17)-Cr(1)-C(13)	102.7(3)
C(18)-C(17)-Cr(1)-C(13)	-28.9(2)
C(16)-C(15)-Cr(1)-C(19)	159.5(3)
C(14)-C(15)-Cr(1)-C(19)	-68.9(3)
C(16)-C(15)-Cr(1)-C(21)	67.6(3)
C(14)-C(15)-Cr(1)-C(21)	-160.8(3)
C(16)-C(15)-Cr(1)-C(20)	-59.0(8)
C(14)-C(15)-Cr(1)-C(20)	72.6(8)
C(16)-C(15)-Cr(1)-C(14)	-131.6(4)
C(14)-C(15)-Cr(1)-C(16)	131.6(4)
C(16)-C(15)-Cr(1)-C(18)	-65.8(3)
C(14)-C(15)-Cr(1)-C(18)	65.8(3)
C(16)-C(15)-Cr(1)-C(17)	-28.6(3)
C(14)-C(15)-Cr(1)-C(17)	103.0(3)
C(16)-C(15)-Cr(1)-C(13)	-102.8(3)
C(14)-C(15)-Cr(1)-C(13)	28.8(2)
C(14)-C(13)-Cr(1)-C(19)	68.3(3)

C(18)-C(13)-Cr(1)-C(19)	-160.6(3)
C(12)-C(13)-Cr(1)-C(19)	-46.3(4)
C(14)-C(13)-Cr(1)-C(21)	-66.5(8)
C(18)-C(13)-Cr(1)-C(21)	64.5(8)
C(12)-C(13)-Cr(1)-C(21)	178.8(6)
C(14)-C(13)-Cr(1)-C(20)	161.1(3)
C(18)-C(13)-Cr(1)-C(20)	-67.9(3)
C(12)-C(13)-Cr(1)-C(20)	46.4(4)
C(18)-C(13)-Cr(1)-C(14)	131.1(4)
C(12)-C(13)-Cr(1)-C(14)	-114.7(5)
C(14)-C(13)-Cr(1)-C(16)	-65.5(3)
C(18)-C(13)-Cr(1)-C(16)	65.6(3)
C(12)-C(13)-Cr(1)-C(16)	179.8(4)
C(14)-C(13)-Cr(1)-C(18)	-131.1(4)
C(12)-C(13)-Cr(1)-C(18)	114.3(5)
C(14)-C(13)-Cr(1)-C(17)	-101.9(3)
C(18)-C(13)-Cr(1)-C(17)	29.2(2)
C(12)-C(13)-Cr(1)-C(17)	143.4(4)
C(14)-C(13)-Cr(1)-C(15)	-29.0(3)
C(18)-C(13)-Cr(1)-C(15)	102.1(3)
C(12)-C(13)-Cr(1)-C(15)	-143.6(4)
C(26)-C(22)-C(23)-C(24)	-0.3(5)
Fe(2)-C(22)-C(23)-C(24)	59.2(3)
C(26)-C(22)-C(23)-Fe(2)	-59.5(3)
C(22)-C(23)-C(24)-C(25)	0.4(5)
Fe(2)-C(23)-C(24)-C(25)	59.5(3)
C(22)-C(23)-C(24)-Fe(2)	-59.1(3)
C(23)-C(24)-C(25)-C(26)	-0.3(5)
Fe(2)-C(24)-C(25)-C(26)	59.1(3)
C(23)-C(24)-C(25)-Fe(2)	-59.4(3)
C(24)-C(25)-C(26)-C(22)	0.1(5)
Fe(2)-C(25)-C(26)-C(22)	59.0(3)
C(24)-C(25)-C(26)-Fe(2)	-58.9(3)
C(23)-C(22)-C(26)-C(25)	0.1(5)
Fe(2)-C(22)-C(26)-C(25)	-59.3(3)
C(23)-C(22)-C(26)-Fe(2)	59.4(3)
C(31)-C(27)-C(28)-C(29)	-0.9(5)
Fe(2)-C(27)-C(28)-C(29)	-59.9(3)
C(31)-C(27)-C(28)-Fe(2)	59.0(3)
C(27)-C(28)-C(29)-C(30)	1.2(5)
Fe(2)-C(28)-C(29)-C(30)	-58.0(3)
C(27)-C(28)-C(29)-Fe(2)	59.2(3)
C(28)-C(29)-C(30)-C(31)	-1.0(5)
Fe(2)-C(29)-C(30)-C(31)	-59.0(3)
C(28)-C(29)-C(30)-Fe(2)	57.9(3)
C(29)-C(30)-C(31)-C(27)	0.5(5)
Fe(2)-C(30)-C(31)-C(27)	-59.4(3)
C(29)-C(30)-C(31)-C(32)	176.7(4)
Fe(2)-C(30)-C(31)-C(32)	116.8(4)
C(29)-C(30)-C(31)-Fe(2)	60.0(3)
C(28)-C(27)-C(31)-C(30)	0.2(5)
Fe(2)-C(27)-C(31)-C(30)	59.6(3)
C(28)-C(27)-C(31)-C(32)	-175.9(4)
Fe(2)-C(27)-C(31)-C(32)	-116.5(4)
C(28)-C(27)-C(31)-Fe(2)	-59.4(3)
C(30)-C(31)-C(32)-O(6)	178.6(4)

C(27)-C(31)-C(32)-O(6)	-5.9(7)
Fe(2)-C(31)-C(32)-O(6)	-94.0(5)
C(30)-C(31)-C(32)-O(7)	-1.3(6)
C(27)-C(31)-C(32)-O(7)	174.2(4)
Fe(2)-C(31)-C(32)-O(7)	86.1(4)
O(7)-C(33)-C(34)-C(35)	-88.5(4)
O(7)-C(33)-C(34)-C(39)	89.2(4)
O(7)-C(33)-C(34)-Cr(2)	-179.8(3)
C(39)-C(34)-C(35)-C(36)	-0.8(6)
C(33)-C(34)-C(35)-C(36)	176.9(4)
Cr(2)-C(34)-C(35)-C(36)	-54.9(4)
C(39)-C(34)-C(35)-Cr(2)	54.1(3)
C(33)-C(34)-C(35)-Cr(2)	-128.1(4)
C(34)-C(35)-C(36)-C(37)	1.7(6)
Cr(2)-C(35)-C(36)-C(37)	-53.3(4)
C(34)-C(35)-C(36)-Cr(2)	55.0(4)
C(35)-C(36)-C(37)-C(38)	-2.6(7)
Cr(2)-C(36)-C(37)-C(38)	-56.0(4)
C(35)-C(36)-C(37)-Cr(2)	53.4(4)
C(36)-C(37)-C(38)-C(39)	2.7(7)
Cr(2)-C(37)-C(38)-C(39)	-53.2(4)
C(36)-C(37)-C(38)-Cr(2)	55.8(4)
C(37)-C(38)-C(39)-C(34)	-1.9(7)
Cr(2)-C(38)-C(39)-C(34)	-55.0(4)
C(37)-C(38)-C(39)-Cr(2)	53.1(4)
C(35)-C(34)-C(39)-C(38)	1.0(6)
C(33)-C(34)-C(39)-C(38)	-176.8(4)
Cr(2)-C(34)-C(39)-C(38)	55.2(4)
C(35)-C(34)-C(39)-Cr(2)	-54.2(3)
C(33)-C(34)-C(39)-Cr(2)	128.0(4)
O(6)-C(32)-O(7)-C(33)	-0.3(6)
C(31)-C(32)-O(7)-C(33)	179.6(3)
C(34)-C(33)-O(7)-C(32)	-175.3(3)
O(8)-C(40)-Cr(2)-C(42)	139(100)
O(8)-C(40)-Cr(2)-C(41)	48(100)
O(8)-C(40)-Cr(2)-C(37)	-141(100)
O(8)-C(40)-Cr(2)-C(39)	-37(100)
O(8)-C(40)-Cr(2)-C(35)	-90(100)
O(8)-C(40)-Cr(2)-C(36)	-124(100)
O(8)-C(40)-Cr(2)-C(34)	-55(100)
O(8)-C(40)-Cr(2)-C(38)	-85(100)
O(10)-C(42)-Cr(2)-C(40)	156(26)
O(10)-C(42)-Cr(2)-C(41)	-115(26)
O(10)-C(42)-Cr(2)-C(37)	19(26)
O(10)-C(42)-Cr(2)-C(39)	-28(26)
O(10)-C(42)-Cr(2)-C(35)	72(26)
O(10)-C(42)-Cr(2)-C(36)	54(26)
O(10)-C(42)-Cr(2)-C(34)	32(27)
O(10)-C(42)-Cr(2)-C(38)	-14(26)
O(9)-C(41)-Cr(2)-C(40)	-34(39)
O(9)-C(41)-Cr(2)-C(42)	-122(39)
O(9)-C(41)-Cr(2)-C(37)	155(100)
O(9)-C(41)-Cr(2)-C(39)	101(39)
O(9)-C(41)-Cr(2)-C(35)	51(39)
O(9)-C(41)-Cr(2)-C(36)	112(39)
O(9)-C(41)-Cr(2)-C(34)	67(39)

O(9)-C(41)-Cr(2)-C(38)	136(100)
C(36)-C(37)-Cr(2)-C(40)	29.5(4)
C(38)-C(37)-Cr(2)-C(40)	160.7(3)
C(36)-C(37)-Cr(2)-C(42)	110.8(3)
C(38)-C(37)-Cr(2)-C(42)	-117.9(3)
C(36)-C(37)-Cr(2)-C(41)	-163.9(3)
C(38)-C(37)-Cr(2)-C(41)	-32.7(4)
C(36)-C(37)-Cr(2)-C(39)	-102.1(3)
C(38)-C(37)-Cr(2)-C(39)	29.1(2)
C(36)-C(37)-Cr(2)-C(35)	-28.7(3)
C(38)-C(37)-Cr(2)-C(35)	102.5(3)
C(38)-C(37)-Cr(2)-C(36)	131.2(4)
C(36)-C(37)-Cr(2)-C(34)	-65.4(3)
C(38)-C(37)-Cr(2)-C(34)	65.9(3)
C(36)-C(37)-Cr(2)-C(38)	-131.2(4)
C(38)-C(39)-Cr(2)-C(40)	-162.9(3)
C(34)-C(39)-Cr(2)-C(40)	-30.2(4)
C(38)-C(39)-Cr(2)-C(42)	23.1(4)
C(34)-C(39)-Cr(2)-C(42)	155.8(3)
C(38)-C(39)-Cr(2)-C(41)	111.1(3)
C(34)-C(39)-Cr(2)-C(41)	-116.3(3)
C(38)-C(39)-Cr(2)-C(37)	-29.2(3)
C(34)-C(39)-Cr(2)-C(37)	103.4(3)
C(38)-C(39)-Cr(2)-C(35)	-103.0(3)
C(34)-C(39)-Cr(2)-C(35)	29.6(3)
C(38)-C(39)-Cr(2)-C(36)	-66.1(3)
C(34)-C(39)-Cr(2)-C(36)	66.5(3)
C(38)-C(39)-Cr(2)-C(34)	-132.7(4)
C(34)-C(39)-Cr(2)-C(38)	132.7(4)
C(36)-C(35)-Cr(2)-C(40)	-115.5(3)
C(34)-C(35)-Cr(2)-C(40)	112.4(3)
C(36)-C(35)-Cr(2)-C(42)	-30.5(4)
C(34)-C(35)-Cr(2)-C(42)	-162.5(3)
C(36)-C(35)-Cr(2)-C(41)	159.1(3)
C(34)-C(35)-Cr(2)-C(41)	27.1(4)
C(36)-C(35)-Cr(2)-C(37)	28.7(3)
C(34)-C(35)-Cr(2)-C(37)	-103.4(3)
C(36)-C(35)-Cr(2)-C(39)	102.4(3)
C(34)-C(35)-Cr(2)-C(39)	-29.7(3)
C(34)-C(35)-Cr(2)-C(36)	-132.1(4)
C(36)-C(35)-Cr(2)-C(34)	132.1(4)
C(36)-C(35)-Cr(2)-C(38)	65.7(3)
C(34)-C(35)-Cr(2)-C(38)	-66.4(3)
C(35)-C(36)-Cr(2)-C(40)	67.5(3)
C(37)-C(36)-Cr(2)-C(40)	-159.7(3)
C(35)-C(36)-Cr(2)-C(42)	157.4(3)
C(37)-C(36)-Cr(2)-C(42)	-69.8(3)
C(35)-C(36)-Cr(2)-C(41)	-77.7(8)
C(37)-C(36)-Cr(2)-C(41)	55.1(9)
C(35)-C(36)-Cr(2)-C(37)	-132.8(4)
C(35)-C(36)-Cr(2)-C(39)	-66.3(3)
C(37)-C(36)-Cr(2)-C(39)	66.6(3)
C(37)-C(36)-Cr(2)-C(35)	132.8(4)
C(35)-C(36)-Cr(2)-C(34)	-29.2(2)
C(37)-C(36)-Cr(2)-C(34)	103.7(3)
C(35)-C(36)-Cr(2)-C(38)	-103.1(3)

C(37)-C(36)-Cr(2)-C(38)	29.7(3)
C(35)-C(34)-Cr(2)-C(40)	-70.1(3)
C(39)-C(34)-Cr(2)-C(40)	158.7(3)
C(33)-C(34)-Cr(2)-C(40)	44.5(4)
C(35)-C(34)-Cr(2)-C(42)	52.3(8)
C(39)-C(34)-Cr(2)-C(42)	-78.9(7)
C(33)-C(34)-Cr(2)-C(42)	166.9(6)
C(35)-C(34)-Cr(2)-C(41)	-161.7(3)
C(39)-C(34)-Cr(2)-C(41)	67.0(3)
C(33)-C(34)-Cr(2)-C(41)	-47.2(4)
C(35)-C(34)-Cr(2)-C(37)	65.6(3)
C(39)-C(34)-Cr(2)-C(37)	-65.6(3)
C(33)-C(34)-Cr(2)-C(37)	-179.8(4)
C(35)-C(34)-Cr(2)-C(39)	131.2(4)
C(33)-C(34)-Cr(2)-C(39)	-114.2(5)
C(39)-C(34)-Cr(2)-C(35)	-131.2(4)
C(33)-C(34)-Cr(2)-C(35)	114.6(5)
C(35)-C(34)-Cr(2)-C(36)	29.1(3)
C(39)-C(34)-Cr(2)-C(36)	-102.1(3)
C(33)-C(34)-Cr(2)-C(36)	143.7(4)
C(35)-C(34)-Cr(2)-C(38)	102.5(3)
C(39)-C(34)-Cr(2)-C(38)	-28.7(3)
C(33)-C(34)-Cr(2)-C(38)	-143.0(4)
C(39)-C(38)-Cr(2)-C(40)	60.8(9)
C(37)-C(38)-Cr(2)-C(40)	-71.3(9)
C(39)-C(38)-Cr(2)-C(42)	-164.1(3)
C(37)-C(38)-Cr(2)-C(42)	63.9(3)
C(39)-C(38)-Cr(2)-C(41)	-71.4(3)
C(37)-C(38)-Cr(2)-C(41)	156.6(3)
C(39)-C(38)-Cr(2)-C(37)	132.0(4)
C(37)-C(38)-Cr(2)-C(39)	-132.0(4)
C(39)-C(38)-Cr(2)-C(35)	65.8(3)
C(37)-C(38)-Cr(2)-C(35)	-66.3(3)
C(39)-C(38)-Cr(2)-C(36)	102.5(3)
C(37)-C(38)-Cr(2)-C(36)	-29.5(3)
C(39)-C(38)-Cr(2)-C(34)	28.9(3)
C(37)-C(38)-Cr(2)-C(34)	-103.2(3)
C(30)-C(31)-Fe(2)-C(27)	-119.1(4)
C(32)-C(31)-Fe(2)-C(27)	121.4(4)
C(30)-C(31)-Fe(2)-C(28)	-81.2(3)
C(27)-C(31)-Fe(2)-C(28)	38.0(3)
C(32)-C(31)-Fe(2)-C(28)	159.3(4)
C(27)-C(31)-Fe(2)-C(30)	119.1(4)
C(32)-C(31)-Fe(2)-C(30)	-119.5(4)
C(30)-C(31)-Fe(2)-C(24)	46.7(6)
C(27)-C(31)-Fe(2)-C(24)	165.8(4)
C(32)-C(31)-Fe(2)-C(24)	-72.8(6)
C(30)-C(31)-Fe(2)-C(22)	167.4(3)
C(27)-C(31)-Fe(2)-C(22)	-73.5(3)
C(32)-C(31)-Fe(2)-C(22)	47.9(4)
C(30)-C(31)-Fe(2)-C(23)	-157.0(5)
C(27)-C(31)-Fe(2)-C(23)	-37.9(6)
C(32)-C(31)-Fe(2)-C(23)	83.5(6)
C(30)-C(31)-Fe(2)-C(26)	124.9(3)
C(27)-C(31)-Fe(2)-C(26)	-115.9(3)
C(32)-C(31)-Fe(2)-C(26)	5.4(4)

C(30)-C(31)-Fe(2)-C(25)	82.3(3)
C(27)-C(31)-Fe(2)-C(25)	-158.6(3)
C(32)-C(31)-Fe(2)-C(25)	-37.2(4)
C(30)-C(31)-Fe(2)-C(29)	-37.4(2)
C(27)-C(31)-Fe(2)-C(29)	81.8(3)
C(32)-C(31)-Fe(2)-C(29)	-156.9(4)
C(28)-C(27)-Fe(2)-C(31)	118.7(4)
C(31)-C(27)-Fe(2)-C(28)	-118.7(4)
C(28)-C(27)-Fe(2)-C(30)	80.9(3)
C(31)-C(27)-Fe(2)-C(30)	-37.9(2)
C(28)-C(27)-Fe(2)-C(24)	-46.0(6)
C(31)-C(27)-Fe(2)-C(24)	-164.8(5)
C(28)-C(27)-Fe(2)-C(22)	-116.5(3)
C(31)-C(27)-Fe(2)-C(22)	124.8(3)
C(28)-C(27)-Fe(2)-C(23)	-75.3(3)
C(31)-C(27)-Fe(2)-C(23)	166.0(2)
C(28)-C(27)-Fe(2)-C(26)	-158.2(3)
C(31)-C(27)-Fe(2)-C(26)	83.0(3)
C(28)-C(27)-Fe(2)-C(25)	171.7(4)
C(31)-C(27)-Fe(2)-C(25)	53.0(5)
C(28)-C(27)-Fe(2)-C(29)	37.4(3)
C(31)-C(27)-Fe(2)-C(29)	-81.4(3)
C(27)-C(28)-Fe(2)-C(31)	-38.3(2)
C(29)-C(28)-Fe(2)-C(31)	81.4(3)
C(29)-C(28)-Fe(2)-C(27)	119.8(4)
C(27)-C(28)-Fe(2)-C(30)	-82.6(3)
C(29)-C(28)-Fe(2)-C(30)	37.2(2)
C(27)-C(28)-Fe(2)-C(24)	162.5(3)
C(29)-C(28)-Fe(2)-C(24)	-77.8(3)
C(27)-C(28)-Fe(2)-C(22)	80.2(3)
C(29)-C(28)-Fe(2)-C(22)	-160.0(3)
C(27)-C(28)-Fe(2)-C(23)	122.1(3)
C(29)-C(28)-Fe(2)-C(23)	-118.2(3)
C(27)-C(28)-Fe(2)-C(26)	49.8(5)
C(29)-C(28)-Fe(2)-C(26)	169.5(4)
C(27)-C(28)-Fe(2)-C(25)	-170.1(5)
C(29)-C(28)-Fe(2)-C(25)	-50.3(7)
C(27)-C(28)-Fe(2)-C(29)	-119.8(4)
C(29)-C(30)-Fe(2)-C(31)	-119.4(4)
C(29)-C(30)-Fe(2)-C(27)	-81.4(3)
C(31)-C(30)-Fe(2)-C(27)	38.1(2)
C(29)-C(30)-Fe(2)-C(28)	-37.4(3)
C(31)-C(30)-Fe(2)-C(28)	82.1(3)
C(29)-C(30)-Fe(2)-C(24)	79.4(3)
C(31)-C(30)-Fe(2)-C(24)	-161.2(2)
C(29)-C(30)-Fe(2)-C(22)	-156.7(6)
C(31)-C(30)-Fe(2)-C(22)	-37.3(7)
C(29)-C(30)-Fe(2)-C(23)	42.0(5)
C(31)-C(30)-Fe(2)-C(23)	161.4(4)
C(29)-C(30)-Fe(2)-C(26)	165.2(3)
C(31)-C(30)-Fe(2)-C(26)	-75.4(3)
C(29)-C(30)-Fe(2)-C(25)	122.7(3)
C(31)-C(30)-Fe(2)-C(25)	-117.8(3)
C(31)-C(30)-Fe(2)-C(29)	119.4(4)
C(23)-C(24)-Fe(2)-C(31)	168.1(4)
C(25)-C(24)-Fe(2)-C(31)	48.6(6)

C(23)-C(24)-Fe(2)-C(27)	-39.3(6)
C(25)-C(24)-Fe(2)-C(27)	-158.8(5)
C(23)-C(24)-Fe(2)-C(28)	-73.6(3)
C(25)-C(24)-Fe(2)-C(28)	166.9(3)
C(23)-C(24)-Fe(2)-C(30)	-157.6(3)
C(25)-C(24)-Fe(2)-C(30)	82.9(3)
C(23)-C(24)-Fe(2)-C(22)	37.8(3)
C(25)-C(24)-Fe(2)-C(22)	-81.7(3)
C(25)-C(24)-Fe(2)-C(23)	-119.5(4)
C(23)-C(24)-Fe(2)-C(26)	81.9(3)
C(25)-C(24)-Fe(2)-C(26)	-37.6(3)
C(23)-C(24)-Fe(2)-C(25)	119.5(4)
C(23)-C(24)-Fe(2)-C(29)	-115.6(3)
C(25)-C(24)-Fe(2)-C(29)	124.9(3)
C(23)-C(22)-Fe(2)-C(31)	162.8(3)
C(26)-C(22)-Fe(2)-C(31)	-78.0(3)
C(23)-C(22)-Fe(2)-C(27)	121.7(3)
C(26)-C(22)-Fe(2)-C(27)	-119.1(3)
C(23)-C(22)-Fe(2)-C(28)	79.7(3)
C(26)-C(22)-Fe(2)-C(28)	-161.2(3)
C(23)-C(22)-Fe(2)-C(30)	-168.4(5)
C(26)-C(22)-Fe(2)-C(30)	-49.2(7)
C(23)-C(22)-Fe(2)-C(24)	-37.6(3)
C(26)-C(22)-Fe(2)-C(24)	81.6(3)
C(26)-C(22)-Fe(2)-C(23)	119.2(4)
C(23)-C(22)-Fe(2)-C(26)	-119.2(4)
C(23)-C(22)-Fe(2)-C(25)	-81.4(3)
C(26)-C(22)-Fe(2)-C(25)	37.8(3)
C(23)-C(22)-Fe(2)-C(29)	48.4(5)
C(26)-C(22)-Fe(2)-C(29)	167.5(4)
C(24)-C(23)-Fe(2)-C(31)	-166.6(5)
C(22)-C(23)-Fe(2)-C(31)	-47.2(6)
C(24)-C(23)-Fe(2)-C(27)	164.8(3)
C(22)-C(23)-Fe(2)-C(27)	-75.9(3)
C(24)-C(23)-Fe(2)-C(28)	123.8(3)
C(22)-C(23)-Fe(2)-C(28)	-116.9(3)
C(24)-C(23)-Fe(2)-C(30)	52.3(5)
C(22)-C(23)-Fe(2)-C(30)	171.6(4)
C(22)-C(23)-Fe(2)-C(24)	119.4(4)
C(24)-C(23)-Fe(2)-C(22)	-119.4(4)
C(24)-C(23)-Fe(2)-C(26)	-81.5(3)
C(22)-C(23)-Fe(2)-C(26)	37.9(3)
C(24)-C(23)-Fe(2)-C(25)	-37.6(3)
C(22)-C(23)-Fe(2)-C(25)	81.8(3)
C(24)-C(23)-Fe(2)-C(29)	82.3(3)
C(22)-C(23)-Fe(2)-C(29)	-158.3(3)
C(25)-C(26)-Fe(2)-C(31)	-119.2(3)
C(22)-C(26)-Fe(2)-C(31)	121.7(3)
C(25)-C(26)-Fe(2)-C(27)	-162.8(3)
C(22)-C(26)-Fe(2)-C(27)	78.1(3)
C(25)-C(26)-Fe(2)-C(28)	161.6(4)
C(22)-C(26)-Fe(2)-C(28)	42.6(6)
C(25)-C(26)-Fe(2)-C(30)	-77.2(3)
C(22)-C(26)-Fe(2)-C(30)	163.8(3)
C(25)-C(26)-Fe(2)-C(24)	37.5(3)
C(22)-C(26)-Fe(2)-C(24)	-81.5(3)

C(25)-C(26)-Fe(2)-C(22)	119.1(4)
C(25)-C(26)-Fe(2)-C(23)	81.3(3)
C(22)-C(26)-Fe(2)-C(23)	-37.8(3)
C(22)-C(26)-Fe(2)-C(25)	-119.1(4)
C(25)-C(26)-Fe(2)-C(29)	-42.4(7)
C(22)-C(26)-Fe(2)-C(29)	-161.5(6)
C(24)-C(25)-Fe(2)-C(31)	-160.4(3)
C(26)-C(25)-Fe(2)-C(31)	80.1(3)
C(24)-C(25)-Fe(2)-C(27)	160.8(4)
C(26)-C(25)-Fe(2)-C(27)	41.3(6)
C(24)-C(25)-Fe(2)-C(28)	-36.3(7)
C(26)-C(25)-Fe(2)-C(28)	-155.8(5)
C(24)-C(25)-Fe(2)-C(30)	-116.7(3)
C(26)-C(25)-Fe(2)-C(30)	123.7(3)
C(26)-C(25)-Fe(2)-C(24)	-119.5(4)
C(24)-C(25)-Fe(2)-C(22)	81.6(3)
C(26)-C(25)-Fe(2)-C(22)	-38.0(3)
C(24)-C(25)-Fe(2)-C(23)	37.5(3)
C(26)-C(25)-Fe(2)-C(23)	-82.0(3)
C(24)-C(25)-Fe(2)-C(26)	119.5(4)
C(24)-C(25)-Fe(2)-C(29)	-74.4(3)
C(26)-C(25)-Fe(2)-C(29)	166.0(3)
C(30)-C(29)-Fe(2)-C(31)	37.9(2)
C(28)-C(29)-Fe(2)-C(31)	-82.0(3)
C(30)-C(29)-Fe(2)-C(27)	82.4(3)
C(28)-C(29)-Fe(2)-C(27)	-37.5(3)
C(30)-C(29)-Fe(2)-C(28)	119.9(4)
C(28)-C(29)-Fe(2)-C(30)	-119.9(4)
C(30)-C(29)-Fe(2)-C(24)	-119.0(3)
C(28)-C(29)-Fe(2)-C(24)	121.1(3)
C(30)-C(29)-Fe(2)-C(22)	164.1(4)
C(28)-C(29)-Fe(2)-C(22)	44.2(5)
C(30)-C(29)-Fe(2)-C(23)	-161.6(3)
C(28)-C(29)-Fe(2)-C(23)	78.5(3)
C(30)-C(29)-Fe(2)-C(26)	-45.0(7)
C(28)-C(29)-Fe(2)-C(26)	-164.9(6)
C(30)-C(29)-Fe(2)-C(25)	-77.8(3)
C(28)-C(29)-Fe(2)-C(25)	162.3(3)